

# **Lipidic Implants for Pharmaceutical Proteins: Mechanisms of Release and Development of Extruded Devices**

**Dissertation**

zur Erlangung des Doktorgrades der  
Fakultät für Chemie und Pharmazie der  
Ludwig-Maximilians-Universität München

vorgelegt von  
**Sandra Herrmann**  
aus Bernburg

München 2007

## Erklärung

Diese Dissertation wurde im Sinne von § 13 Abs. 3 bzw. 4 der Promotionsordnung vom 29. Januar 1998 von Herrn Prof. Dr. G. Winter betreut.

## Ehrenwörtliche Versicherung

Diese Dissertation wurde selbständig, ohne unerlaubte Hilfe erarbeitet.

München, den 26.06.2007



.....  
Sandra Herrmann

Dissertation eingereicht am: 28.06.2007

1. Gutachter: Prof. Dr. G. Winter

2. Gutachter: Prof. Dr. J. Siepmann

Mündliche Prüfung am: 26.07.2007

## ACKNOWLEDGEMENTS

The present thesis was written at the Department of Pharmacy, Pharmaceutical Technology and Biopharmaceutics at the Ludwig-Maximilians-University in Munich under the supervision of Prof. Dr. Gerhard Winter.

First of all, I want to express my deepest appreciation to my supervisor Prof. Dr. Gerhard Winter for the possibility to join his research group. Especially, I would like to thank him for his professional guidance and his scientific support. I always felt inspired and encouraged. Furthermore, I am very grateful to him for the great opportunities to present my work at congresses all over the world and in particular I want to thank him for making possible my research stay in Lille.

I am also deeply grateful to Prof. Dr. Jürgen Siepmann for the excellent cooperation and the scientific input and advice concerning the mathematical analysis of the release data. Moreover, I want to express my gratitude to Dr. Florence Siepmann for performing the mathematical modelling. Thanks to the whole research team in Lille for the warm welcome and the very pleasant stay. I really enjoyed this collaboration and my time in Lille. For the financial support allowing this collaboration, I want to acknowledge the “Bayerisch-Französisches Hochschulzentrum (BFHZ)”.

Special thanks to Dr. Silke Mohl for introducing me to lipidic depot devices and for the guidance over the first year. Above all, I would like to thank Silke for her friendship. My thanks are extended to Dr. Friedrich Gruber for rendering every assistance and support.

Many thanks to all the colleagues from the research group of Prof. Dr. Winter and Prof. Dr. Frieß who shared the time in Munich with me for the cooperative and convenient atmosphere. I especially like to thank Stefan Gottschalk, Andrea Hawe, Tim Serno, Michael Wiggernhorn, Kathrin Mathis and Ahmed Youssef for all the support and the numerous discussions.

Furthermore, I would like to acknowledge Christian Minke, from the Department of Chemistry and Biochemistry, LMU Munich, Germany, for conducting the scanning

electron microscopy measurements. Wolfgang Wunschheim, also at Department of Chemistry and Biochemistry, is acknowledged for the practical introduction to wide angle X-ray scattering.

Thanks are extended to Roche Diagnostics GmbH, Penzberg, Germany for the donation of rh-interferon  $\alpha$ -2a as well as to Sasol GmbH, Witten, Germany for providing various lipids.

Thanks are also extended to Prof. Dr. F. Bracher, Prof. Dr. F. Paintner, Prof. Dr. W. Frieß, and Dr. C. Culmsee for serving as members of my thesis advisor committee.

I would also like to thank my parents, my sister Constanze, my brother Lutz, and my grandparents for their constant support. Marek, thanks a lot for your love and the encouragement you gave me over the last years.

Finally, I want to thank Dr. Friedrich Gruber and Tim Serno for the proof-reading of this thesis.

## TABLE OF CONTENTS

<b>Chapter I: General introduction.....</b>	<b>1</b>
<b>1. Overview on approved controlled release systems for pharmaceutical peptides .....</b>	<b>4</b>
<b>2. Concerns associated with the use of PLA/PLGA as matrix formers .....</b>	<b>6</b>
2.1. Protein instability during manufacturing of PLA/PLGA microparticles .....	6
2.1.1. Protein loading – emulsion technique .....	6
2.1.2. Protein loading – suspension technique.....	7
2.2. Protein instability during release from PLA/PLGA matrices .....	9
<b>3. Alternative matrix materials.....</b>	<b>11</b>
3.1. Controlled release systems based on hydrogels .....	11
3.2. Controlled release systems based on lipidic materials .....	11
3.2.1. Lipid microparticles.....	13
3.2.2. Subtypes of lipid based microparticles .....	14
3.2.3. Lipidic implants.....	15
3.3. Lipids as matrix material – advantages and concerns .....	18
3.3.1. Possible advantages of lipidic matrices.....	18
3.3.2. Possible problems associated with the use of lipids .....	20
<b>4. Implants – a closer look at alternative manufacturing possibilities .....</b>	<b>23</b>
4.1. Compression moulding .....	23
4.2. Solvent casting.....	23
4.3. Extrusion .....	24
4.3.1. Ram extrusion .....	24
4.3.2. Screw extruder .....	26
4.4. Stability issues during implant manufacturing.....	27
4.4.1. Elevated temperatures .....	28
4.4.2. Elevated pressures.....	29
<b>5. General mechanism of protein release and mathematical modelling .....</b>	<b>31</b>
5.1. Protein release from non-degradable matrices.....	31
5.2. Drug release from degradable matrices.....	33
5.3. Introduction to mathematical modelling .....	34
5.3.1. Diffusion controlled systems.....	35
5.3.2. Swelling controlled release.....	41
5.3.3. Erosion controlled release.....	43
<b>Chapter II: Aim of the thesis .....</b>	<b>47</b>

<b>Chapter III: Materials and methods .....</b>	<b>48</b>
<b>1. Materials .....</b>	<b>48</b>
1.1. Proteins.....	48
1.1.2. Recombinant interferon $\alpha$ -2a (IFN- $\alpha$ ) .....	48
1.1.3. Hen egg white lysozyme .....	48
1.2. Lipids.....	48
1.2.1. Triglycerides .....	48
1.2.2. Chemicals and reagents.....	50
<b>2. Methods .....</b>	<b>51</b>
2.1. Preparation of lipidic controlled release devices .....	51
2.1.1. Lyophilisation of IFN- $\alpha$ .....	51
2.1.2. Manufacturing of implants by compression .....	51
2.1.3. Manufacturing of implants by ram extrusion.....	52
2.1.4. Manufacturing of implants by twin screw extrusion .....	52
2.2. Mechanical stability of the lipidic implants .....	52
2.3. Extraction of protein from the lipid matrix.....	53
2.4. In-vitro release studies of IFN- $\alpha$ .....	53
2.4.1. Size exclusion chromatography of IFN- $\alpha$ .....	53
2.4.2. Concentration of HP- $\beta$ -CD .....	54
2.4.3. Concentration of PEG .....	54
2.5. Determination of porosity .....	54
2.6. Water uptake and erosion.....	55
2.7. In-vitro release studies of lysozyme .....	55
2.8. Solubility studies .....	566
2.9. Reverse phase chromatography of IFN- $\alpha$ .....	56
2.10. Sodium dodecyl sulphate polyacrylamide gel electrophoresis (SDS-PAGE).....	57
2.11. Fluorescence spectroscopy .....	57
2.12. Fourier transform infrared spectroscopy (FTIR).....	57
2.12.1. Transmission FTIR-spectra of dissolved IFN- $\alpha$ .....	57
2.12.2. Transmission FTIR-spectra of solid IFN- $\alpha$ .....	58
2.12.3. Thermal denaturation of IFN- $\alpha$ .....	58
2.13. Investigations on the lipid modification .....	59
2.13.1. Wide-angle x-ray scattering (WAXS).....	59
2.13.2. Differential scanning calorimetry (DSC) .....	59
2.14. Microcalorimetry .....	59
2.15. Scanning electron microscopy .....	59
2.16. Determination of the diffusion coefficients of IFN- $\alpha$ .....	60

2.17. “Macropore model” .....	60
2.18. Mathematical modelling .....	61

## **Chapter IV: Mechanisms controlling the release from lipid-based delivery systems ..... 63**

<b>1. Effect of PEG addition on release kinetics from tristearin implants.....</b>	<b>63</b>
1.1. Release mechanisms of IFN- $\alpha$ from tristearin implants .....	63
1.2. Determination of the diffusion coefficient of IFN- $\alpha$ .....	70
1.3. Release mechanisms of the incorporated excipients – HP- $\beta$ -CD and PEG .....	75
1.4. Summary and conclusion.....	80
<b>2. Solubility studies and investigations on the protein stability .....</b>	<b>83</b>
2.1. Protein stability after precipitation and redissolution .....	84
2.2. Summary and conclusion.....	89
<b>3. Polyethylene glycol acting as in-situ precipitation agent – proof of concept .....</b>	<b>92</b>
3.1. “Macropore model” .....	94
3.2. pH-dependence of solubility and release .....	96
3.3. Alternative porogen and alternative protein .....	99
3.3.1. Release of IFN- $\alpha$ from tristearin implants loaded with an alternative porogen.....	99
3.3.2. Release of lysozyme from tristearin implants.....	100
3.4. Importance of the precipitation mechanism for protein stability .....	103
3.5. Summary and conclusion.....	106
<b>4. Potential effect of HP-<math>\beta</math>-CD on IFN-<math>\alpha</math> release and stability .....</b>	<b>110</b>
4.1. Potential effects of HP- $\beta$ -CD on the release of IFN- $\alpha$ from tristearin implants.....	110
4.2. Potential effects of HP- $\beta$ -CD on the stability of IFN- $\alpha$ .....	115
4.3. Summary and conclusion.....	122

## **Chapter V: Development of improved lipid based delivery systems for pharmaceutical proteins ..... 123**

<b>1. Manufacturing of extrudates by ram extrusion .....</b>	<b>123</b>
1.1. Experimental setup .....	123
1.2. Influence of the manufacturing process on the lipid modification .....	125
1.3. Influence of the manufacturing process on protein stability .....	126
1.4. In-vitro release studies.....	127

1.5.	Mechanisms of protein release from extruded implants .....	132
1.6.	Formulation factors influencing protein release .....	138
1.6.1.	Influence of the used triglyceride.....	138
1.6.2.	Influence of particle size.....	140
1.6.3.	Excipients to modify the erosion behaviour.....	143
1.7.	Summary and conclusion.....	146
<b>2.</b>	<b>Manufacturing of extrudates by twin screw extrusion.....</b>	<b>148</b>
2.1.	Experimental setup .....	148
2.1.1.	Admixing of oils or semi-softened lipids .....	149
2.1.2.	Suspending the lipidic material in a highly concentrated PEG solution.....	150
2.1.3.	Dissolving the lipidic material in an organic solvent .....	151
2.1.4.	Admixing of low melting point lipids.....	152
2.2.	Influence of the manufacturing process on the lipid modification .....	154
2.2.1.	Extrudates based on a mixture of mono-acid triglycerides.....	155
2.2.2.	Extrudates based on a mixture of mono-acid and mixed-acid triglycerides .....	158
2.3.	Influence of the manufacturing process on the protein stability .....	162
2.3.1.	Characterisation of the secondary protein structure within the lipidic extrudate ..	163
2.4.	In-vitro release studies.....	169
2.4.1.	Lysozyme as model protein.....	172
2.5.	Influence of the manufacturing procedure on the in-vitro release kinetics of IFN- $\alpha$ ..	175
2.6.	Protein stability during release.....	179
2.7.	Summary and conclusion.....	181
<b>Chapter VI:</b>	<b>Final summary .....</b>	<b>184</b>
<b>Chapter VII:</b>	<b>References .....</b>	<b>189</b>

## List of Abbreviations

ATR	attenuated total reflection
CD	circular dichroism
DSC	differential scanning calorimetry
DSPC	distearoyl-phosphatidyl-choline
FTIR	Fourier transformed infrared spectroscopy
HP- $\beta$ -CD	hydroxypropyl- $\beta$ -cyclodextrin
IFN- $\alpha$	rh-interferon $\alpha$ -2a
PAGE	poly(acrylamide) gel electrophoreses
PBS	isotonic phosphate buffer
PEG	poly(ethylene glycol), all experiments were carried out with poly(ethylene glycol) 6000
PLA	poly(lactic acid)
PLGA	poly(lactic-co-glycolic acid)
RP-HPLC	reverse phase high performance liquid chromatography
rpm	rounds per minute
SD	standard deviation
SE-HPLC	size exclusion high performance liquid chromatography
SEM	scanning electron microscopy
WAXS	wide angle X-ray scattering



## CHAPTER I: GENERAL INTRODUCTION

As integral part of the body, proteins are involved in all important biological processes. Consequently, the understanding of their role in physiological and pathophysiological processes led to an enormous request to exploit the potential of proteins as therapeutic agents. However, the large scale production of proteins for pharmaceutical applications was not possible until the mid 1970s, when the advances of recombinant DNA technology marked the beginning of modern biotechnology era. The first recombinant protein (Humulin<sup>®</sup>; marketed by Genentech and Eli Lilly) was approved in 1982, and nowadays, only 25 years later, approximately 20 % of new drug applications involve a protein as active compound. Most of them are used for the treatment of serious, life-threatening, and chronic diseases such as cancer, rheumatoid arthritis, hepatitis and others [166, 244].

In comparison to low molecular weight drugs especially the high activity and selectivity of proteins often allow a better treatment of these diseases [231, 250]. However, due to their fragile, three-dimensional macromolecular structure proteins are susceptible to a variety of chemical and physical degradation pathways. Therefore, the development of suitable formulations in which the native structure and activity of proteins are maintained during preparation, delivery, shipping, and long-term storage has become one of the most challenging tasks [129, 143, 250].

Unfortunately, proteins generally require parenteral administration for systemic delivery. One reason why non-parenteral application pathways are often restricted is the high molecular mass in combination with the polar characteristics of proteins. Consequently, proteins reveal a low permeability through biological membranes. Furthermore, proteases ubiquitously present at administration sites as well as the inherent instability of proteins hamper a non-invasive administration [98, 231]. Nevertheless, research is focussed on the improvement of the bioavailability through alternative routes of administration. These attempts recently led to the approval of pulmonary-delivered insulin [1]. However, still concerns remained, such as potential local side effects or anti-insulin antibody formation [231, 244].

As the plasma half-lives of proteins are often very short, frequent injections or administration via infusions are required for maintaining therapeutic plasma levels. This is associated with poor patient compliance, side effects, or cost consuming hospitalisation [41, 73, 98, 231]. One way to overcome these restrictions is the optimisation of pharmacokinetic properties by mutagenesis or post-translational

engineering of therapeutical proteins, like the conjugation with poly(ethylene glycol) [245]. Apart from these options, the development of injectable, sustained release systems can be regarded as another promising strategy to improve protein delivery [41, 73, 98, 231].

Several systems, like microspheres, liposomes, as well as solid and in-situ forming implants, have been suggested as delivery technologies for proteins. Among the plethora of investigated synthetic and natural polymers, biodegradable poly( $\alpha$ -hydroxy esters) and in particular poly(lactic acid), PLA, and poly(lactic-co-glycolic acid), PLGA, found most widespread use. Their popularity mainly stems from the fact that these polymers provide an excellent safety and biocompatibility record [80, 198, 233].

However, despite the early success of peptide-loaded microspheres and implants, the delivery of proteins appears to be more difficult and still no controlled release system for the delivery of proteins is launched [212]. The only protein-releasing depot device that reached the market in 1998 (Genentech's Nutropin Depot<sup>®</sup>) was withdrawn 2004 [78].

The limited success of polymeric delivery systems for the controlled release of pharmaceutical proteins can be explained with some inherent shortcomings of PLA/PLGA. Several detrimental effects on protein stability during device manufacturing as well as during storage and release were identified [169, 199, 212, 233].

In order to overcome these restrictions lipids (e.g., triglycerides, monoglycerides, and fatty acids) have been proposed as alternative matrix formers for controlled protein delivery systems [127, 144]. Being natural, physiological materials, lipids feature a superb biocompatibility [85, 180]. Moreover, compared to PLA/PLGA lipid matrix materials exhibited several potential advantages that might facilitate the preservation of the native protein structure during manufacturing, storage, and during release. This superiority was recently confirmed by Mohl and Winter. They introduced a tristearin-based implant system for the continuous release of interferon  $\alpha$ -2a (IFN- $\alpha$ ) over 1 month [153]. Importantly, IFN- $\alpha$  was released almost exclusively in its monomeric form and co-lyophilisation with hydroxypropyl- $\beta$ -cyclodextrin (HP- $\beta$ -CD) provided long-term stability of these formulations [151, 152].

However, little is known about the mechanisms controlling the liberation of IFN- $\alpha$  from lipidic implant systems so far. Therefore, one of the central aims of the present

work was the establishment of an understanding about the underlying release determining mechanisms.

Furthermore, the developed lipidic device exceeded the size that would be commonly accepted for an implant administration. Consequently, different ways for the preparation of miniaturised lipidic implants were evaluated in the course of this thesis, too. All methods for the manufacturing of lipidic implant systems described in literature rely on the preparation with a self-made manufacturing apparatus which is operated manually and only in lab-scale. In order to overcome this limitation within the scope of this thesis, state of the art extrusion techniques were applied with respect to an ease of up-scaling.

## 1. OVERVIEW ON APPROVED CONTROLLED RELEASE SYSTEMS FOR PHARMACEUTICAL PEPTIDES

The approved controlled release systems for pharmaceutical peptides can be divided into microspheres, solid implants, and in-situ forming implants [45, 198, 212]. Microspheres have a diameter of 1-100  $\mu\text{m}$  and are suspended in an appropriate oily or aqueous liquid prior to injection. Solid implants commonly reveal a cylindrical geometry. Even if films and tablets have been realised experimentally, small cylindrical implants which offer the possibility to be deposited subcutaneously via a large gauge needle (trochar) are preferred. A small size of the device is further crucial to avoid irritations at the site of injection [198].

Compared to microparticles, two main disadvantages are noted for implant systems:

- (1) the administration is more complicated and might be painful for the patient and
- (2) the administered doses are more limited [45, 198].

Thus, countless publications are dealing with the development of polymeric microparticulate systems, whereas the literature describing implants for the delivery of proteins is sparse. On the other hand, implants inhere the possibility of a surgical removal, if adverse events necessitate an interruption of the therapy [41, 121]. Moreover, the versatility of implant shape and sizes permits the adjustment of drug release rates [102].

Nowadays, two solid implant systems based on PLGA for the sustained delivery of goserelin acetate and buserelin acetate are commercially available (Zoladex<sup>®</sup> and Profact<sup>®</sup> Depot) [121].

In order to facilitate the administration, in-situ forming implants have received attention. Eligard<sup>®</sup> based on the ATRIGEL<sup>®</sup> technology is a sustained release formulation for leuprolide acetate that is administered as liquid and forms a solid implant after s.c. or i.m. injection. In-situ forming is realised by dissolving the polymeric matrix material (e.g. PLA, PLGA) in a water-miscible, biocompatible solvent (e.g. dimethyl sulfoxide, N-methyl-2-pyrrolidone, or triacetin). Upon administration the polymer precipitates due to the displacement of the organic solvent upon contact to the tissue fluids. However, potential disadvantages of in-situ forming implants are (1) inconsistent shapes of the implant formed after injection into the body, (2) undesired burst effects, and (3) solvent toxicity [61].

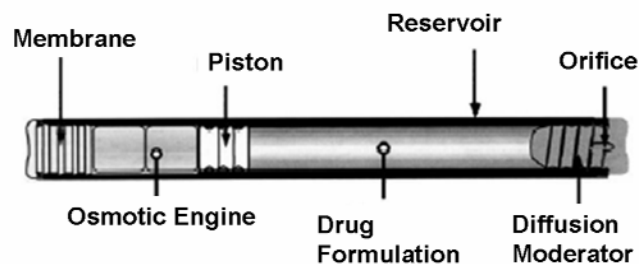


**Figure 1: Cross section of the DUROS® implant system [254].**

Apart from in-situ forming and solid implants based on PLGA osmotically driven implantable systems for peptides have been approved. Viadur™ is an adaptation of the DUROS® implant technology for the delivery of leuprolide acetate. The implant consists of a cylindrical titanium alloy reservoir capped at one end by a rate-controlling membrane and capped at the other end by a diffusion moderator. Within the diffusion moderator an orifice, through which the drug release occurs, is located (Figure 1). The osmotic engine, containing sodium chloride, expands as the device is imbedded into water. Consequently, the pressure applied by the piston forces the drug formulation through the orifice. Leuprolide is delivered in a constant manner over 1 year. The external dimension of the implant is 4 mm in diameter and 45 mm in length [254].

## 2. CONCERNS ASSOCIATED WITH THE USE OF PLA/PLGA AS MATRIX FORMERS

### 2.1. PROTEIN INSTABILITY DURING MANUFACTURING OF PLA/PLGA MICROPARTICLES

This chapter is focussed on potential sources for protein destabilisation during the preparation of controlled release devices. Detrimental conditions for the formulation of particulate drug delivery systems based on PLGA are discussed exemplarily. Nevertheless, the destabilising situations depicted below will threaten the protein stability in a similar way irrespective of the used matrix material and the kind of controlled release systems aimed to be produced.

**Table 1: Common techniques for the preparation of microparticles [258]**

chemical processes	physical processes
solvent evaporation and extraction	spray drying
phase separation	spray congealing
polyelectrolyte complexation	supercritical fluid precipitation
interfacial polymerisation	

The broad spectrum of physical and chemical techniques applied for the formation of microparticles is summarised in Table 1. All techniques require the loading of an organic polymer solution with the protein. A few attempts were made to dissolve the protein directly in the organic polymer solution [162, 176, 259]. In most cases the loading of the protein was realised by dispersing an aqueous protein solution (emulsion method) or the solid protein powder (suspension method) in the organic polymer phase. Therefore, in the following chapter denaturing stresses associated with the emulsion and the suspension loading will be outlined.

#### 2.1.1. PROTEIN LOADING – EMULSION TECHNIQUE

The most prominent technique to prepare microspheres is the double emulsion method which comprises the emulsifying of the aqueous protein solution in an organic solution of the polymer. This primary emulsion is then transferred into a second aqueous phase. The formation of a W/O/W emulsion is accomplished by intensive stirring, vortexing, or homogenisation. For particle hardening the polymer solvent needs to be removed which can be realised either by extraction with a water miscible solvent or by evaporation. Finally, the microparticles are washed and vacuum dried or lyophilised [258]. As alternatives to the double emulsion technique

the particle forming (after emulsification of the aqueous protein solution in the organic solvent) can be conducted, for example, by spray drying or by phase separation.

However, irrespective of the technique applied for particle shaping protein denaturation and aggregation may take place due to the presence of water/organic solvent interfaces. Because of their amphiphile character proteins tend to adsorb at such interfaces and as a result, protein unfolding followed by non-covalent aggregation occurs [16, 156, 189, 190, 234]. In addition, Pérez and Griebenow reported the formation of an alternative unfolded species ( $U^*$ ) for lysozyme after adsorption.  $U^*$  diffused from the interface back into the bulk solution which led to a continuous drop of the enzyme activity in the soluble fraction [168].

Furthermore, the organic solvent might diffuse to a certain extent into the aqueous protein phase resulting in (1) an alteration of the ionic strength and/or (2) in direct binding of the organic solvent to the protein [199].

Finally, proteins are exposed to large shear and cavitation stress during emulsification. In dependence on the applied homogenisation technique the mass transport to the surface and to water/organic interfaces increases. For instance, Morlock et al. reported that the formation of erythropoietin (EPO) aggregates was less pronounced when rotor/stator type homogenisers were used instead of ultrasound or vortex mixing [156]. The employment of sonication is particularly harmful since local temperature extremes as well as free radicals might be generated upon emulsifying [128].

Several attempts to stabilise the protein during emulsification have been proposed. For instance, the usage of higher protein concentrations or carrier proteins minimised the relative fraction of the therapeutically protein adsorbed at the interface [156, 188]. Furthermore, the protein could be stabilised by the addition of sugars, polyols etc. via preferential exclusion. In addition, co-encapsulation of cyclodextrins was shown to improve the stability of EPO [156], ovalbumin, and lysozyme [188].

### **2.1.2. PROTEIN LOADING – SUSPENSION TECHNIQUE**

This technique is based on the scientific knowledge that the conformational mobility of suspended proteins in aprotic, hydrophobic solvents is particularly restrictive [123]. Consequently, suspending the solid protein powder in the organic polymer solution causes less protein destabilisation than loading the protein as aqueous solution [43]. The particle forming can be performed with the methods mentioned in Table 1.

However, when water is required during the particle shaping step this will be associated with certain problems. In the case of the S/O/W method the solid protein is first suspended in the organic polymer solution. Afterwards, this suspension is emulsified in an outer aqueous phase for particle forming. Since proteins are hydrophilic they tend to leach from the polymer solution into the outer aqueous phase what accounts for low encapsulation efficiencies [169]. On the other hand, leakage of the outer aqueous phase into the organic solution will increase the flexibility of the protein. Consequently, the ability of unfolding is rising [148].

In order to obviate both obstacles, non-aqueous encapsulation procedures such as the S/O/O method were introduced [169]. Here, the suspension of the protein powder in an organic polymer solution is added to a coacervating fluid, which is miscible with the polymer solvent but does not dissolve the polymer (e.g. silicone oil, vegetable oil, or light liquid paraffin). Thus, the polymer solvent is slowly extracted, followed by the concentration of the polymer until coacervated drug loaded droplets are formed. The final hardening of the particles is accomplished by pouring them into a second non-solvent (e.g. aliphatic hydrocarbons) [212, 258].

However, serious practical concerns arise with the S/O/O technique. The obtained microparticles tend to aggregate and scale-up is hardly realisable [258]. Furthermore, multiple solvents are applied and their residual contents may restrict the approval by the authority. Moreover, the particle size of the protein powder must be sufficiently small to avoid contact to the microparticle surface, which in turn would result in a large burst release [169].

A non-aqueous, cryogenic methodology led to the unique protein-containing PLGA depot system (Nutropin Depot<sup>®</sup>) that reached commercialisation. The sustained release formulation of zinc-complexed rhGH in PLGA microspheres resulted in a one-month effect after one single injection [10, 109]. However, in 2004 Nutropin Depot<sup>®</sup> was withdrawn from market by Genentech, claiming “significant resources required ... to continue manufacturing and commercializing the product” as the main cause [78].

This short overview on techniques used to produce microspheres illustrates that there are several severe stability problems associated with the encapsulation of pharmaceutical proteins into microspheres. Unfortunately, methods that provide acceptable protein integrity, such as the anhydrous procedures, are often very complicated.

Apart from protein destabilisation during manufacture a further drawback is frequently reported for microspheres: high burst release due to low encapsulation efficiencies [119, 130]. High initial release rates may lead to drug concentrations near or above the toxic level in vivo. Also the drug released during burst might be metabolized and excreted without being effective. Thus, high burst release is mostly undesired [103].

## **2.2. PROTEIN INSTABILITY DURING RELEASE FROM PLA/PLGA MATRICES**

In addition to the destabilising effects identified during manufacturing several destructive conditions for proteins are generated within PLA or PLGA matrix systems during incubation [169, 198, 199, 212, 233].

During release, the degradation of the polymer backbone entails a mass loss. Generally, this material loss is referred to as erosion. For degradable polymers two mechanisms have been proposed: surface or heterogeneous erosion and bulk or homogeneous erosion. In the case of surface erosion the cleavage of the polymer chains mainly occurs at the outermost area of the matrix. The polymer degradation is faster than the intrusion of water into the matrix, thus the erosion only affects the surface and not the inner part of the matrix (heterogeneous). In contrast, bulk erosion occurs when the degradation of the polymer is slow compared to the water uptake. The matrix is completely wetted before scission of the polymer begins. Finally, the polymer chains are cleaved throughout the device (homogeneous process) [79, 80].

Obviously, the mechanism of degradation depends on the type of functional groups from which the polymer is built. Polymers comprising reactive functional groups such as polyanhydrides are predominantly subjected to surface erosion, whereas polymers containing less reactive groups for example poly( $\alpha$ -hydroxy esters) tend to bulk erosion [79, 80].

During the bulk erosion of PLA/PLGA matrices the generated degradation products are trapped within the matrices. Consequently, the incorporated proteins are faced to a completely altered microenvironment [169, 198, 199, 212, 233].

Due to the accumulation of degradation products within the matrix the following causes for protein unfolding, aggregation, and chemical degradation have been identified:

- (1) a significant pH drop [74],
- (2) an increase of the osmotic pressure [28],
- (3) accumulation of reactive species [140].

In order to overcome these stability problems the following attempts have been suggested:

- (1) neutralisation by the incorporation of basic salts (e.g.  $\text{Mg}(\text{OH})_2$ ) [261]
- (2) accelerated leaching out of degradation products due to an increase of the porosity of the matrix [169].

Another critical factor leading to potential deterioration of protein upon release is the hydration of the matrix. The presence of water increases the protein molecular mobility and consequently the occurrence of protein unfolding and irreversible aggregation. Typically, moisture induced aggregation is ascribed to a thiol-disulfide interchange [49, 50]. Furthermore, chemical reactions such as deamidation were reported as a result of water imbedding [131].

Finally, interactions between the PLA/PLGA matrix and the protein have been identified as further cause for incomplete protein release. Mainly the protein is adsorbed due to unspecific hydrophobic contacts and due to electrostatic interactions [70, 233].

### **3. ALTERNATIVE MATRIX MATERIALS**

Based on the multitude of reports describing the problems associated with the use of PLG/PLGA devices, current research is focussed on both the search for possibilities to stabilise the incorporated protein against the detrimental conditions and on the evaluation of alternative matrix formers. Among them, hydrogels and lipid-based formulations have achieved particular interest within the past few years [98, 111, 127, 144].

#### **3.1. CONTROLLED RELEASE SYSTEMS BASED ON HYDROGELS**

Hydrogels are cross-linked hydrophilic polymers assembled to a three-dimensional network, which can take up a large amount of water without losing structural properties. The obtained swollen and rubbery consistence is regarded to provoke minimal tissue irritations and less harmful conditions for incorporated proteins [121, 237]. The pool of investigated polymers is vast, including natural polymers (collagen, alginate, chitosan) as well as synthetic polymers poly(ethylene glycol), poly(vinyl alcohol), poly(hydroxyethylmethacrylate) [237].

Cross-linking can be accomplished either by the introduction of chemical linkers or by physical methods. However, chemical cross-linkers are often toxic and the proceeded chemical reaction might affect the entrapped protein. Thus, interest in physical cross-linking increased. During this procedure, non-permanent physical interactions between the polymer chains are initiated by an external trigger (e.g. pH, temperature, ionic strength) [92].

Hydrogels are either formulated as microspheres or as in situ forming implants. In spite of the interest especially on microspheres based on dextran hydrogel [91, 237], so far little research is dedicated to the physicochemical characterisation of the proteins within these hydrogel microparticles. For instance, the cross-linking or hardening procedure might be a concern with respect to protein stability [111].

#### **3.2. CONTROLLED RELEASE SYSTEMS BASED ON LIPIDIC MATERIALS**

Lipids have been referred to as “chemically heterogeneous group of substances, having in common the property of insolubility in water, but solubility in non-polar solvents”. More precisely the principal categories of lipids are: fatty acids, fatty acid salts, phospholipids, glycerides, waxes, glycolipids and sterols [220]. Due to this wide variety of compounds a diversity of lipid-based delivery platforms for peptides and proteins is described in literature. Based on the structural properties of the

predominant lipid, systems that rely on lipid bilayers and solid, matrix-like systems can be distinguished.

### Bilayer-based systems

When placing amphiphilic polar lipids in water lipid bilayers are formed spontaneously, which arrange to various geometric structures and shapes [200]. The obtained three-dimensional structures, like liposomes and cubic phase gels, have been utilised as drug delivery vehicles for the sustained release of peptides and proteins. Studies on the application of liposomes as microreservoir for the sustained release of proteins involve traditional liposomes, such as unilamellar and multilamellar vesicles [216], as well as newly developed multivesicular liposomes. The latter are based on the DepoFoam™ technology. Multilamellar liposomes are structurally distinct from lamellar liposomes and consist of aggregated, water-filled polyhedral compartments separated by lipid bilayers [257]. For instance, subcutaneous injection of DepoLeridistim (DepoFoam™ encapsulated Leridistim, a chimeric growth factor containing IL-3 and G-CSF receptor agonist) prolongates the biological effect for up to 10 days [134].

Alternatively, proteins have been incorporated into cubic phase gels. From these systems, release is regulated by diffusion through aqueous channels permeating the cubic phase. Incorporation into cubic phase provided protection of insulin against agitation induced aggregation. However, in-vivo delivery of insulin and desmopressin revealed limited liberation periods of 6-9 h [200]. Recently, the diameter of the channels was tailored to the hydrodynamic diameter of the incorporated drug. Nevertheless, protein delivery was still finished after approximately 12 days [46].

### Matrix-like systems

In spite of their advantages, the described liposomes and cubic phase gels have no matrix-type character which often leads to short release periods terminated within several hours to a few days. In contrast, relatively hydrophobic lipids have been used in the solid state to provide sustained release from solid lipid nanoparticles, microspheres, microcapsules, and implants.

Even though solid lipid nanoparticles (SLN) were suggested as delivery systems for proteins their hydrophobic nature and small sizes render high encapsulation yields very unlikely. For instance, only small quantities of lysozyme (50-500 µg protein/g lipid) were incorporated into SLNs comprising various lipids, even when a

special solubilisation technique was applied [4]. Rather than usage for prolonged release, SLN own potential for drug targeting after surface modification or as adjuvant for vaccines [195]

On the basis of their outstanding importance as protein delivery system lipidic microspheres and implants will be discussed in detail below.

### 3.2.1. LIPID MICROPARTICLES

Lipid microparticles can be produced by the use of similar methods as described for polymeric microparticles (see Chapter I.2.1). However, the manufacturing protocol itself threatens the protein stability irrespective of the applied matrix material. Consequently, applying the double emulsion method would also involve the creation of detrimental interfaces and shear forces. Therefore, several alternative techniques using the advantage that lipids can be manufactured as molten liquid were developed.

One of these microsphere preparation methods is the melt dispersion method. With this technique lipid microparticles were produced by emulsifying a drug loaded molten lipid into an aqueous, surfactant containing phase which is heated above the melting point of the lipid. Afterwards this emulsion is rapidly cooled down [18, 19, 48]. Using this technique Reithmeier et al. succeeded to encapsulate thymocartin, somatostatin, and insulin into glyceryl tripalmitate microparticles. The protein was loaded into the molten lipid either as aqueous solution (W/O/W) or as solid (S/O/W) [179, 180].

Another preparation technique was introduced by Del Curto [55]. Gonadotropin release hormone agonist (Antide<sup>®</sup>) was co-melted with glyceryl monobehenate (Compritol E ATO<sup>®</sup>) or glyceryl monostearate (Imwitor 900<sup>®</sup>). The obtained matrix was micronised in a milling aperture cooled with liquid nitrogen. The developed microparticles based on Compritol E ATO<sup>®</sup> revealed testosterone suppression up to 29 days in-vivo. However, the manufacturing procedure was limited by the solubility of the drug within the molten lipid. Due to the hydrophilic character of peptides and proteins monoglycerides were required as matrix material and still only low drug loadings of max. 2 % were realisable. Alternatively, the drug loading of the matrix was conducted by dissolving Antide<sup>®</sup> and the lipid in a benzyl-ethanol mixture. Afterwards, the solution was poured into petri dishes and the solvent was allowed to evaporate [55]. However, in this case the proposed method is restricted by the drug

solubility in the applied organic solvent. Thus, it remains questionable if this technique can be applied to other peptides and proteins.

Lipid microparticles can also be obtained by atomisation of the protein loaded lipid melt in a cold stream of air (spray congealing). For instance, with this technique bovine growth hormone was encapsulated into lipid microparticles. After application to dairy caddy the milk production could be enhanced over a time frame of 2 weeks [30]. More recently, Göpferich and co-workers reported the encapsulation of insulin by a spray congealing procedure [145].

A supercritical fluid process for the coating of protein particles with lipids was introduced in 2001 by the group of Benoit [184, 185, 224]. Protein particles were dispersed in a supercritical solution of the lipid. Then, the pressure was decreased to reduce the solubility of the lipid within the supercritical CO<sub>2</sub>, which induced a precipitation upon the insoluble protein particles [224]. In order to obtain a uniform coating layer, the usage of heterogeneous lipid mixtures was preferable. Compared to pure triglycerides such materials revealed a reduced tendency to form separate, distinct crystals on the protein particles. The supercritical procedure was shown to be suitable for the coating of bovine serum albumin (BSA) particles with Gelucire<sup>®</sup> 50-02 without affecting the protein structure. However, the obtained reservoir type microspheres delivered BSA within only 24 h [185] and were yet not capable for a sustained release .

### **3.2.2. SUBTYPES OF LIPID BASED MICROPARTICLES**

Domb et al. introduced a special kind of microparticles, called lipospheres that are defined as water-dispersible solid microparticles composed of a hydrophobic fat core coated by a monolayer of phospholipid molecules [59]. Despite the aforementioned definition some authors used the term liposphere and lipid microparticle interchangeably.

For the mucosal vaccination via the delivery of antibodies to the respiratory tract microparticles based on dipalmitoylphosphatidylcholin were prepared by spray drying. The developed microparticles exhibited a thin-walled porous morphology with a geometric diameter of around 7 µm [22, 23]. Thus, the developed system takes an intermediate position between microspheres and liposomes.

In spite of some progress obtained so far, thorough investigations on protein integrity within lipid microspheres are rare. Data on drug integrity are only provided in the case of peptide encapsulation. Thus, it remains unclear whether techniques such as

the melt dispersion method really offer the benefit to encapsulate proteins without affecting their three dimensional structure. In particular the creation of water-molten lipid interfaces might cause similar problems as the double emulsion process outlined in Chapter I.2.1.

But, considering the knowledge obtained with the preparation of polymeric microparticles it can be assumed that non-aqueous encapsulation approaches such as the spray congealing technique will display the potential of lipids as alternative matrix formers.

### 3.2.3. LIPIDIC IMPLANTS

#### 3.2.3.1. MANUFACTURING BY COMPRESSION

Lipidic implant systems are mostly prepared by compression of protein lipid blends. In contrast to polymeric implants (see Chapter I.4), the high compressibility of lipids allows the formation of solid matrices by traditional compression at mild conditions. Thus, several authors used this technique to demonstrate the suitability of lipids as carriers for pharmaceutical proteins. The first investigations rely on cholesterol as matrix material [115, 246]. Later on triglycerides, monoglycerides and fatty acids were applied, too [31, 214, 248]. In Table 2 an overview on implant systems prepared by compression is given.

**Table 2: Protein loaded lipid-based implant prepared by simple compression.**

author	matrix composition / protein	observation
Kent 1984 [115]	cholesterol, bovine growth hormone / insulin,	preparation of macromolecular-loaded lipidic implants is possible
Wang 1987 [247]	cholesterol / insulin	reduction of blood glucose levels over 24 days
Wang 1989 [246]	various fatty acids, fatty acid anhydrides, monoglycerides and triglycerides / insulin	reduction of blood glucose levels in-vivo over 43 days
Cady 1991 [31]	C <sub>10</sub> -C <sub>20</sub> fatty acid salts of growth hormone releasing heptapeptide	fatty acid chain length correlates with the daily release rate
Khan et al. 1991 [117]	cholesterol, lecithin / bovine serum albumin	release in-vitro over up to 1 month, in-vivo erosion of the implants within 40 days
Kaevichit and Tucker 1994 [112]	stearic acid / bovine serum albumin	prolonged release over 60 h
Steber 1995 [215]	triglycerides partially coated with methacrylate / somatotropin,	elevated blood levels of in-vivo for 1 month

Vogelhuber et al. 2003 [241]	trimyristin / TAMRA-BSA, hyaluronidase	release of bioactive hyaluronidase within 48 hours
Mohl and Winter [151-153]	tristearin / IFN- $\alpha$	sustained release of monomeric IFN- $\alpha$ over 1 month
Guse et al. 2006 [84]	various triglycerides / lysozyme	sustained release over 1 month
Koennings et al. 2006 [125]	tripalmitin / interleukin-16	sustained release over 18 days but integrity loss
Apple et al. 2006 [6]	tripalmitin / insulin	release of bioactive insulin
Koennings et al. 2007 [126]	tripalmitin / lysozyme, brain-derived neurotrophic factor (BDNF)	60 % intact BDNF were released over one month
Koennings et al. 2007 [124]	various triglycerides / lysozyme	increased wettability of the matrix accounted for accelerated release rates

All studies mentioned in Table 2 used compression to form the implant. However, the techniques applied to generate the lipid protein blend were quite different:

- (1) the solid protein was simply physically mixed with the lipid powder [112, 151-153, 241, 246],
- (2) the solid protein was physically mixed with precipitated lipid powder [117], or
- (3) the protein was co-precipitated with the lipid powder [6, 84, 115, 125].

Khan et al. [117] revealed that the loading techniques influenced the erosion rates and thus, the release behaviour. Before compression, the lipids, namely cholesterol and lecithin, were co-precipitated from organic solvents. After solvent evaporation the lipidic co-precipitates were pulverised and mixed with BSA. Finally, the lipid protein blend was compressed. When chloroform was used as precipitating agent the co-precipitates revealed reduced erosion and release rates compared to pellets prepared by physically mixing [117].

Recently, the group of Göpferich applied three alternative methods to co-precipitate protein and lipidic material: (1) the emulsion-compression method, (2) the suspension-compression method, and (3) the wetting-compression method.

When applying the emulsion-compression method the aqueous solution of the protein was emulsified into a solution of the lipid in methylene chloride by vortex mixing. This emulsion is subsequently freeze dried and the obtained dry powder comprising the lipid and the protein is compressed. Recently, Guse et al. used the emulsion-compression method to load various triglyceride matrices with lysozyme [84].

However, it has been shown extensively that the creation of water-organic solvent interfaces inheres several unfavourable conditions on protein stability. The protein denaturation and subsequent formation of higher order aggregates is claimed as one of the major cause for incomplete protein release from PLGA matrices (see Chapter I.2). Thus, it can be expected that the emulsification with an organic lipid solution might also affect the protein integrity. Indeed, Koennings et al. recently reported that the emulsion-compression method was unsuitable to maintain protein integrity. Protein aggregation was observed during the emulsifying of an aqueous lysozyme solution in an organic solution of tripalmitin [126].

Performing the suspension-compression method, the protein was suspended as solid powder in the organic lipid solution. This method was applied by Koennings et al. to encapsulate interleukin-18 (IL-18) into tripalmitin implants [125]. First, the protein had to be co-lyophilised with poly(ethylene glycol) 6000 (PEG) in order to obtain the solid IL-18 particles. After dispersing the protein powder in the lipid solution by ultrasonication, the suspension was frozen in liquid nitrogen, and the organic solvent was allowed to evaporate. Finally, the lipid-protein blend was ground in a mortar and compressed [125].

The authors suggested that this procedure resulted in a more homogenous distribution of the protein within the lipid matrix compared to the simple physical admixture before compression. However, only 30 % of IL-18 were delivered from these implants and also increasing the amount of the porogen PEG 6000 from 2 % to 7 % failed to improve the recovery rates. Furthermore, the fully bioactive IL-18 was only delivered within 24 hours; at later time points a progressive integrity loss was found. The protein stability after manufacturing was not investigated. Due to the progressive decrease of bioactivity during in-vitro incubation the authors concluded that the protein stability was compromised during release rather than during implant manufacture [125].

By applying the wetting-compression method insulin was encapsulated in tripalmitin implants. Here, the lipid powder was admixed with a solution of insulin. After drying, the lipid-insulin blend was compressed. The biological activity of the released protein was investigated in a long-term cartilage engineering culture. In a two-week trial, biological effects of the released insulin on the cartilage constructs could be proven, indicating the preservation of the protein activity [6].

An excellent protein stability of IFN- $\alpha$  delivered from HP- $\beta$ -CD was also reported by Mohl and Winter [151-153]. Importantly, the implants were prepared in a less complicated way by the compression of physically mixed lipid and protein powders. This manufacturing technique was demonstrated to maintain the integrity of IFN- $\alpha$ . The addition of PEG 6000 into the lipidic implant ensured a sustained delivery of monomeric protein over 1 month [151-153].

### 3.2.3.2. ALTERNATIVE MANUFACTURING TECHNIQUES FOR LIPIDIC IMPLANTS

Up to now, only two studies are available reporting protein-loaded lipidic implants that were not prepared by compression techniques. Pongjanyakul et al. filled polyethylene tubes (internal diameter 2.5 mm) with a suspension of lysozyme in molten glyceryl palmitostearate (Precirol ATO 5). The tubes were closed and cooled to 45 °C with a rate of 14 °C/min. Afterwards, the solidified lipid was pushed out of the tubing and cut into implants with a length of 4 mm. Compared to implants prepared by compression the obtained pellets revealed a smoother surface with only a few pores. Consequently, the amount of totally liberated protein was reduced [174].

Besides, Yamagata et al. suggested heat extrusion through a needle as manufacturing procedure for lipidic implants. In this report polyglycerol esters of fatty acids loaded with solid IFN- $\alpha$  powder were heated above their melting point and then forced through a stainless steel needle [255].

Apparently, all methods described above, are based on a manufacturing method in lab-scale with the help of self-made equipment. So far no attempts have been made to prepare lipid-based delivery systems for proteins with up-scalable techniques such as twin screw extrusion.

## 3.3. LIPIDS AS MATRIX MATERIAL – ADVANTAGES AND CONCERNS

### 3.3.1. POSSIBLE ADVANTAGES OF LIPIDIC MATRICES

Reithmeier et al. assessed the biocompatibility of lipid microparticles in comparison to PLGA microspheres by implanting both delivery forms subcutaneously into mice. After two days in both groups a weak proliferation combined with a slight infiltration of specific inflammatory cells was visible. The proliferation of the connective tissue was even more pronounced for PLGA microspheres. After 7 days the reaction of the connective tissue was finished in the lipid group, whereas the proliferation in the polymeric group still proceeded [179]. This excellent biocompatibility report for tripalmitin was confirmed several times later. For instance, after subcutaneous

implantation of cylindrical implants with a diameter of 2.0 mm no inflammatory reaction and only a slight encapsulation into connective tissue were observed [85]. Good biocompatibility was also demonstrated for implants based on alternative lipids, such as lecithin, cholesterol [243], and glyceryl monostearate (GMS) [3].

These studies indicate that an important prerequisite for the development of controlled release systems based on lipids is fulfilled: the biocompatibility has been shown to be comparable to that of approved polymeric systems.

As outlined above, lipids inhere some unique properties that allow the development of gentle manufacturing procedures. For instance, the preparation of lipidic implants by compression was shown to maintain protein stability during implant manufacturing, storage, and release [151-153]. Furthermore, due to the low melting temperatures of lipids the processing of the melt is feasible, and consequently the application of organic solvents becomes redundant. A fact of importance, since residue solvent levels in pharmaceutical products are well known as a potential toxic risk and might thus hamper the approval by authorities [253].

However, the outstanding benefit of lipids as matrix material might be that the protein is confronted to less detrimental conditions during the release period. As outlined in Chapter I.2, bulk erosion and the resulting accumulation of degradation products have been identified as a tremendous intrinsic problem of PLA/PLGA matrices comprising the protein stability during release. In contrast, matrices based on pure triglycerides revealed no swelling or erosion during in-vitro and in-vivo release [85, 241]. As a result, lipophilic matrices might provide a less challenging environment for the incorporated protein during release. Indeed, compressed tristearin implants comprising IFN- $\alpha$  co-lyophilised with HP- $\beta$ -CD revealed integrity of released INF- $\alpha$  and of INF- $\alpha$  trapped within the matrix [153]. In accordance with these findings the biological activity of hyaluronidase was maintained during the release period from triglyceride implants [241]. However, the incubation period of the latter example was very short (48 h). Moreover, Maschke et al. recently reported the formation of degradation products (desamidoinsulin and covalent insulin dimer) within tripalmitin microspheres during release [145]. In addition, the embedding of interleukin-18 into tripalmitin cylinders failed to conserve the biological activity [125]. In contrast to the implant system proposed for the delivery of IFN- $\alpha$  [153], both the described tripalmitin cylinders [125] and microspheres [145] did not contain an additional stabilising agent.

Consequently, it seems essential for the success of lipidic implants to include a protein stabiliser within the matrix.

### **3.3.2. POSSIBLE PROBLEMS ASSOCIATED WITH THE USE OF LIPIDS**

#### **3.3.2.1. POLYMORPHISM**

Almost all fats and fatty acids possess the ability to form different polymorphs. Dependent on the unit cell structures mono-acid saturated triglycerides are classified into three main crystallographic types. The least stable  $\alpha$ -modification is characterised by a loosely packing of the hydrocarbon chains in a hexagonal unit cell structure. The intermediate  $\beta'$ -modification reveals an orthorhombic unit cell structure and the most dense packing is achieved with the stable  $\beta$ -form by a triclinic packing [77, 192].

Thus, a polymorphic transformation might occur during the preparation of controlled release systems based on lipidic materials. Especially, when the manufacturing process comprises a melting or dissolution step, polymorphism needs to be considered since the crystallisation of lipids follows the so-called Ostwald step rule. Accordingly, the least stable  $\alpha$ -form nucleates first, followed by a transition to the intermediate  $\beta'$ -modification, and, finally, the optimal packing is accomplished by a rearrangement to the  $\beta$ -form [192]. Consequently, the presence of less stable  $\alpha$ - or  $\beta'$ -forms after manufacture will result in a polymorphic transformation to the more stable polymorphs upon storage. In the case of controlled release systems based on lipids such a rearrangement might account for changes in the release behaviour.

For example, the preparation of lipid microparticles by the melt dispersion technique or by spraying processes (such as spray congealing or spray drying) resulted in the formation of the unstable  $\alpha$ -form [64, 65, 179]. Since the transformation from the  $\beta'$ -form to the  $\beta$ -polymorph is often associated with swelling or blooming of saturated triglyceride [77], the rearrangement to the  $\beta$ -modification was responsible for changes in the appearance and the texture of the microparticles upon storage. After production, microparticles comprising the lipid in the  $\alpha$ -modification showed a smooth surface. In contrast, a grainy microstructure appeared after the rearrangement to the stable  $\beta$ -polymorph during storage [65].

It is highly conceivable that the visible change of the lipidic matrix structure will be reflected in a modification of the release characteristics upon storage. Such an effect is for example recognized when using Gelucire<sup>®</sup> as matrix material [39, 191, 218].

Gelucires are lipid-based excipients comprising a blend of mono-, di-, and triglycerides with mono- and diesters of fatty acids and poly(ethylene glycol). Due to the polymorphic transformation to a more stable form, large lipid crystals were generated disturbing the compact matrix and accounting for increased release rates [39].

Furthermore, with the rearrangement of the  $\alpha$ - to the  $\beta$ -modification the crystalline lattice becomes more perfect and the number of imperfections decreases. This may result in an expulsion of incorporated drug [158].

Due to the multitude of problems associated with delivery devices comprising less stable polymorphs a melting or dissolution step should be avoided. However, when it is not possible to circumvent the formation of instable modifications, various strategies are imaginable to overcome the above mentioned drawbacks.

By fluctuating the temperature around the melting point of the less stable modification the rearrangement to more stable forms could be accelerated. The application of a specific tempering process step might, furthermore, circumvent any blooming effects [77].

Another attempt to fasten the polymorphic transformation of lipid microparticles was introduced by Steber with the addition of liquid or semi-softened fats to the solid lipid matrix [213]. In preliminary studies - which are beyond the scope of the present thesis - it was shown that a Miglyol<sup>®</sup>812 content of 15 % ensured immediate crystallisation of tristearin material to the stable  $\beta$ -polymorph even when the melt was cooled down with liquid nitrogen [95].

Apart from these approaches aiming at an accelerated polymorphic rearrangement also the opposite, namely the stabilisation of the less stable modification can be found in literature. For example, some emulsifiers e.g. lecithin and monoglycerides serve as anti-blooming agents since they possess the ability to incorporate into the crystal lattice, preventing or delaying the transformation to the  $\beta$ -polymorph [77].

### 3.3.2.2. DEGRADATION

During in-vitro incubation [151, 240, 241] and after subcutaneous implantation [85, 241] implants based on pure triglycerides revealed no erosion. This means that such large lipidic devices need to be removed by a surgical intervention after completed release.

---

In contrast, implants based on lecithin and cholesterol [117] or glyceryl monostearate [3] revealed an erosion after implantation. Thus, the admixing of such “erosion modifiers” might improve the erosion behaviour of triglyceride implants. Promising results into this direction have been reported by the addition of phospholipids. The admixing of 10 % distearoyl-phosphatidyl-choline (DSPC) to a tripalmitin implant formulation led to visible signs of degradation after subcutaneous implantation into mice. As higher levels of phospholipids induced an inflammatory reaction the addition of 10 % might offer a balance between acceptable biocompatibility and bioerosion [85].

#### **4. IMPLANTS – A CLOSER LOOK AT ALTERNATIVE MANUFACTURING POSSIBILITIES**

Lipidic implantable controlled release devices have been mostly prepared by compression. So far, alternative manufacturing protocols have attracted only marginal attention (see Chapter I.3.2). In contrast, dozens of preparation techniques for polymeric implant systems are described in literature, since research has been focused on these materials for a long time. The following chapter will therefore briefly introduce to the manufacturing possibilities which were successfully applied for the preparation of polymeric implants.

##### **4.1. COMPRESSION MOULDING**

Compression moulding refers to the formation of implants by compression of a polymer/drug blend above its glass transition temperature. Due to the thermoplastic behaviour of most polymers a large variety of implant shapes can be realised. For instance, Liu et al. developed a method to prepare complex reservoir-type PLGA capsules for the treatment of osteomyelitis. The release system was loaded in two distinct manufacturing steps. First, an antibiotic/polymer blend was compression moulded to form a hollow cylinder with a cover. In order to fuse the polymer particles the device was sintered above the glass transition temperature at 55 °C. Afterwards, the core of the cylinder was loaded with aqueous solution of recombinant bone morphogenetic protein (rhBMP-2). The cylinder sealing was achieved by ultrasonic welding. Thereby, the applied mechanical vibrations induced intermolecular friction within the polymer, that generated heat, sufficient high enough to melt PLGA and to fusion bond the parts of the cylinder [139].

One potential advantage of the compression moulding technique is the avoidance of organic solvents. However, compared with other manufacturing processes this technique is more complicated and the potential of up-scaling remains questionable.

##### **4.2. SOLVENT CASTING**

Applying solvent casting, the matrix material is dissolved in an appropriate solvent. Afterwards the desired implant is formed by pouring the solution into moulds and evaporating the solvent. Therefore, the release rates do not only depend on the matrix formulation but also on the solvent characteristics, the mould material, and the solvent evaporation technique [263].

Protein encapsulation can be achieved by emulsifying the aqueous protein in the organic polymer solution and subsequent solvent casting. Alternatively, the protein

solution itself can be solvent casted by pouring the aqueous protein solution into moulds. After drying, the protein pellet is wetted with the organic polymer solution [68].

Since the solvent casting usually involves the dissolution of the carrier material in an organic solution, the protein drug has to incorporate either as aqueous solution or as lyophilisate. In particular the first scenario inheres several problems similar to that discussed for the preparation of microparticles (see Chapter I.2.1).

### **4.3. EXTRUSION**

Most polymeric implants are prepared by extrusion [121]. Generally, extrusion describes a process during which the raw material is forced through an orifice or a die. For that purpose at least two main components are necessary: (1) a transport system that may impart a mixing function and (2) a die system, which forms the material. The pressure required for extrusion depends on the design of the die, on the extrusion rate, and in particular on the rheological characteristics of the formulation. With respect to the method used to adapt the viscosity, extrusion can be classified into molten systems (hot-melt extrusion) and semisolid systems. Semisolid systems are generated by dispersing a high portion of solid material in a liquid phase [219]. This technique is widely used to prepare granules or pellets, whereas for the preparation of parenteral controlled release devices mostly the hot melt extrusion technique is applied [121].

Since PLA and PLGA fulfil the basic prerequisite of thermoplasticity, various peptides have been embedded into these matrices by hot melt extrusion. In order to enable the flow through the extruder die, the drug and the polymer have to be heated above the glass transition temperature. The obtained rods are cooled and cut to a specified length. Finally, sterilization of the implants can be accomplished by gamma-irradiation [121].

According to their design, various extruder types can be distinguished. Among them ram and screw extruders are particularly capable for the production of controlled release systems [219].

#### **4.3.1. RAM EXTRUSION**

The setup of a ram extruder is schematically illustrated in Figure 2. The extruder consists of a barrel that is pre-filled with the powder mixture. By means of a piston (or ram) the material is forced through the die at the bottom of the barrel [219].

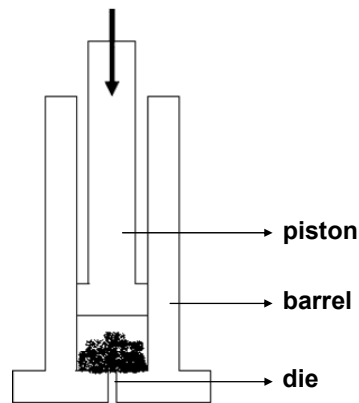


**Figure 2: Schematic setup of a ram extruder.**

The extrusion process can be divided into three phases: (1) compression, (2) steady state flow, and (3) forced flow. The first phase is characterised by a large displacement of the piston with little pressure increase leading to the compaction of the powder to a plug prior to extrusion. After the maximal density of the material is reached, the pressure increases until the material commences a continuous extrusion (steady state flow). Optimally, when the piston is very close to the die forced flow occurs (Figure 3) [219].

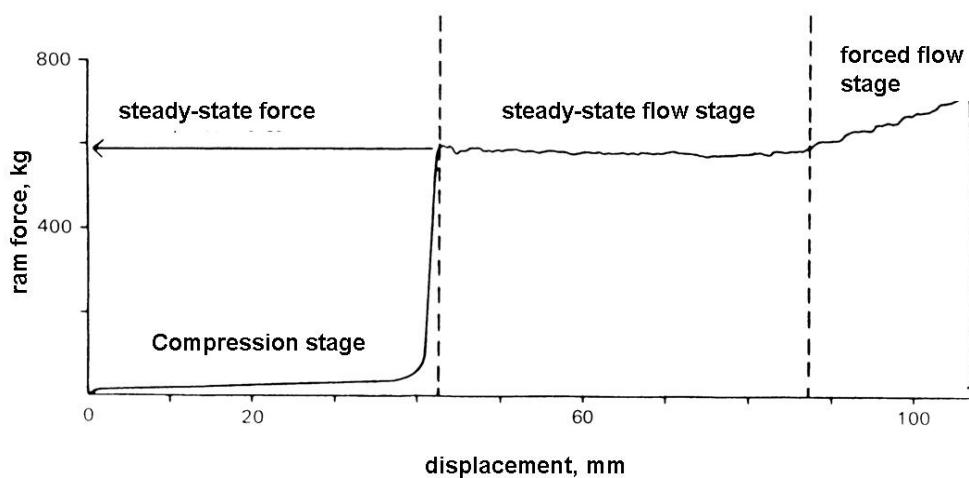


**Figure 3: Typical force displacement plot for a ram extrusion [219].**

The area under the steady state curve represents the work required for extrusion [219]. Pito et al., for instance, used this value to evaluate the extrudability of various saturated polyglycolysed glyceride formulations. It was shown that the melting temperature correlates well with the energy required to produce extrudates. Furthermore the applied force strongly depends on the die diameter, the length-to-radius-ratio, and the extrusion rate [171].

Compared to twin-screw extrusion, ram extrusion is a non-continuous procedure (unless more than one barrel is employed). Since only small amounts of substance are necessary, ram extrusion is mostly used in laboratory scale. In lab scale, also a very simple modification of the ram extrusion procedure is often applied – the extrusion through a needle.

Ram extrusion has been performed with semisolid systems as well as with molten materials. An example for the latter technique is the preparation of BSA-loaded rods based on poly(orthoester) [90, 187]. Zhu and Schwendeman developed an extrusion process without the employment of heat [262]. The semi-solid system of protein powder suspended in an acetone PLGA solution was extruded through a needle into a silicon tube. Afterwards, the solvent was evaporated first at room temperature and then by vacuum drying for 24 h. Semi-solid extrusion was further utilised for the preparation of collagen mini-rods. Fujioka et al., for instance, prepared co-lyophilisates of interferon and collagen, which were wetted with distilled water leading to a gel that could be forced through a nozzle [76].

Semisolid extrusion apparently offers the advantage that heat is generated only by friction. Consequently, the risk of temperature induced denaturation is reduced compared to hot-melt extrusion. However, the employment of an aqueous solution as wetting agent may result in a highly concentrated protein solution in which the carrier material is dispersed. Thus, the possibility of molecule collisions followed by aggregation may increase [250].

#### **4.3.2. SCREW EXTRUDER**

The screw type extruder consists of at least one rotating screw inside a stationary cylindrical barrel. At the end of the barrel a die is connected to shape the implant [219].

The extrusion channel can be divided into three distinct sections (Figure 4). Within the first zone, the feed zone, the extruder is loaded. After the feeding zone the transition zone follows. Within this zone the pressure increases due to the reduction of the thread pitch while maintaining a constant flight depth or due to the reduction flight depth while maintaining the thread pitch [25, 219]. Thus, a compression of the material takes place. Finally, the material arrives the metering zone as a homogeneous plastic melt suitable for extrusion. In this last section the pulsating flow is reduced and a uniform delivery rate through the die is achieved [219].

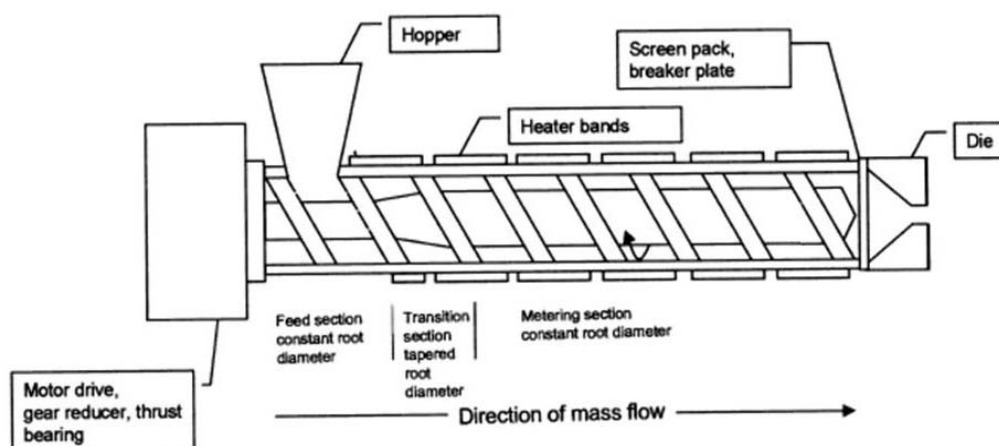


**Figure 4: Component parts of a single screw extruder [25].**

Because of the high extrusion rates that can be achieved with single- or twin-screw extruders, they are predominantly applied in the industrial manufacturing of implants [121].

Based on this technology two commercially available release systems, Implanon<sup>®</sup> and NuvaRing<sup>®</sup>, were developed. Implanon<sup>®</sup> is administered subcutaneously to deliver a progestagen for a period of three years. The vaginal ring NuvaRing<sup>®</sup> is designed for the liberation of both a progestagen and an estrogen for a period of 21 days. Since the carrier material polyethylene vinyl-acetate (EVA) is non-erodable, the implants need to be removed after the release period. In both systems the drug is delivered from a coaxial fibre. The fibre consists of a drug loaded core, which is enveloped with a thin polymer membrane. The steroids within the core polymer are either dispersed as solid crystals or molecularly dissolved. The co-axial fibres are prepared with the help of two single screw extruders that are connected with a spinning block. Core and membrane polymer are melted separately within one of the single screw extruders and delivered to a spinneret, where the coaxial fibre is formed [235, 236].

#### **4.4. STABILITY ISSUES DURING IMPLANT MANUFACTURING**

During implant manufacturing proteins might be exposed to various unfavourable conditions and thus the question arises whether the protein suffer physical or chemical destabilisation.

Protein destabilisation is highly expectable when the manufacturing procedure involves the creation of interfaces (see Chapter I.2.1).

Fortunately, various techniques such as compression and extrusion are feasible allowing the avoidance of water/organic solvent interfaces during production. Nevertheless, in the course of these methods the protein – dispersed as solid within the solid, molten, or dissolved matrix material – might be exposed to elevated temperatures and pressures. The approved implant systems (Zoladex<sup>®</sup> and Profact<sup>®</sup>Depot) comprise peptides. However, the sensibility of proteins against various stresses can be expected to be higher. Therefore, destabilisation that might occur during extrusion will be discussed in the following section.

#### 4.4.1. ELEVATED TEMPERATURES

The free energy of unfolding  $\Delta G_{\text{unfold}}$  of the native protein in aqueous solution typically shows a parabolic profile in dependence of the temperature. Consequently, most proteins are only stable in a certain temperature range and high or low temperatures out of this range may destabilise or denature a protein. Typically,  $\Delta G_{\text{unfold}}$  becomes negative at temperatures higher than 50-100 °C accounting for protein unfolding at elevated temperatures [38]. With increasing temperature interactions within the polypeptide backbone change: electrostatic interactions as well as hydrogen bonding are weakened, whereas hydrophobic interactions are strengthened [250]. The overall mobility of the polypeptide chain increases and thus the tendency for unfolding grows. The temperature at which 50 % of the protein is unfolded is defined as melting or transition temperature  $T_m$  [250]. For example, the  $T_m$  for IFN- $\alpha$  was denoted at around 60 °C when the protein was dissolved in acetate buffer (pH>4.0) [202].

In addition to physical instability, the rate constant of chemical reactions increases exponentially with temperature. Consequently, high temperatures also accelerate chemical degradation [38, 250].

In contrast to the rather low thermal stability of proteins in aqueous solution, proteins suspended as dry powder in non-aqueous media maintained their biological activity even at high temperatures. The melting temperature for bovine pancreatic ribonuclease, for instance, increased from 61 °C in aqueous solution up to 124°C when the protein was suspended in anhydrous nonane [242]. Generally, solid proteins transferred to anhydrous organic solvent systems retain their correct conformation. Furthermore, the minimal layer of water necessary to solvate folded proteins remains associated with the protein. Since an unfolding would require a greater number of water molecules, unfolding becomes unlikely in hydrophobic systems. Moreover, water is a pivotal participant for deleterious reactions such as

deamidation and hydrolysis. Thus, in addition to increased stability against unfolding, proteins can be expected to be more stable against chemical degradation pathways when they are suspended in organic solvents [66, 123].

Assuming parallelism between non-hydrous protein suspensions and the dispersion of dry protein powder within a hydrophobic molten carrier material an increased resistance of proteins against heat can be expected during implant manufacturing.

Indeed, a few authors reported such a scenario. Rothen-Weinhold investigated the thermal stability of the somatostatin analogue vapreotide within a PLGA matrix during ram extrusion. It was shown that a short exposure (10 min) to temperatures up to 120 °C did not lead to impurities, whereas a significant destruction of vapreotide was observed when the extrusion times exceeded 10 minutes. At lower temperatures (80-90 °C) no degradation of the peptide occurred even for a period of 1 h [186]. More recently, Maschke et al. developed a micronisation process for pharmaceutical peptides and proteins based on the high pressure homogenisation within oils or molten fats. After micronisation of insulin crystals in molten tripalmitin at a temperature of 75 °C and a pressure of 1000 bar HPLC-MS revealed no chemical degradation [146].

Beside these studies which comprised only peptides, IFN- $\alpha$  dispersed in molten polyglycerol esters of fatty acids (60 °C) maintained 95 % of its antiviral activity after incubation at 60 °C for 6 hours [255]. Furthermore, the biological activity of lysozyme dispersed in molten glyceryl palmitostearate (65 °C) was not affected [174]. In contrast, the addition of Gelucire 50/13 to the formulation led to an activity loss, indicating that not only the applied temperatures but also the characteristics of the formulation are of importance for the preservation of the protein stability [174].

#### **4.4.2. ELEVATED PRESSURES**

The effects of high pressure on the protein stability are quite complex. Pressure has long been recognized as potential source for protein denaturation and aggregation [21, 250]. On the other hand, high pressures are also applied for protein folding and aggregate dissociation [81].

Moreover, during implant manufacturing a stabilisation against pressure induced denaturation can be expected when the protein is dispersed as solid in the matrix material, since it is reported that pressure induced unfolding of proteins decreases with the water content of the system [161]. In accordance with this, Maschke et al.

---

showed that insulin crystals suspended in oily medium insulin maintained their biological activity even after exposure to high pressures (1500 bar) [146].

Compared to the high melting points of PLA/PLGA, triglycerides that will be employed within this thesis offer the benefit of rather low melting points (35-80 °C). Considering the aforementioned studies dealing with the effects of elevated temperatures on protein stability, the utilisation of the extrusion techniques is not generally prohibitive. This motivates to explore the possibilities of extrusion techniques to prepare lipid-based implantable delivery systems within the course of this project.

## **5. GENERAL MECHANISM OF PROTEIN RELEASE AND MATHEMATICAL MODELLING**

For the development and the optimisation of controlled release systems it is crucial to understand how drug release is controlled. One tool to get an insight into the underlying release mechanisms is the description of the release data with a mathematical model. Beside the so obtained knowledge, the correct choice of an existing mathematical model or the creation of a new one offers the practical benefit that the effects of various design parameters (e.g. the device geometry or the matrix composition) on the release can be predicted. As a result, the number of experiments required to achieve a certain desired drug release profile is minimised [8, 114, 207].

Therefore, the following chapter will first outline the fundamentals of protein release from matrix like systems. Then an introduction into the most important mathematical models will follow. Though the release systems described in the present thesis are non-degradable, a short overview on the drug release mechanism and the mathematical models for degradable matrices will also be given. This is enclosed not only for matters of comparison but also to illustrate potential improvements for mathematical models, since the models for non-degradable systems are usually more sophisticated.

### **5.1. PROTEIN RELEASE FROM NON-DEGRADABLE MATRICES**

During in-vitro incubation implants based on various triglycerides revealed no erosion or swelling [153, 240]. Consequently, an analogy to protein release from non-degradable polymeric matrices can be assumed.

Until the seventies it was commonly accepted that the development of effective controlled release systems for macromolecules is not realisable, since these molecules were simply considered being too large to penetrate through polymer chains [132, 205]. However, in 1974 Davis reported the sustained release of various proteins and peptides from cross-linked poly(acrylamide) and poly(vinylpyrrolidone) gels [53]. Two years later Langer and Folkman also published that proteins and other large molecules can be liberated from poly-(2-hydroxyethylmethacrylate) (Hydron<sup>®</sup>) and ethylene-vinyl-acetate copolymer (EVA) devices [133].

Detailed mechanistic studies on these systems revealed that protein release occurs via diffusion through a complex porous pathway within the inert matrix [132]. First of all water penetrates into the system and dissolves the incorporated polypeptide as well as hydrophilic excipients leading to the creation of the porous microstructure.

The subsequent leaching out of the protein and water soluble excipients further alters the matrix morphology. Pores and channels randomly distributed through the matrix are formed, enabling diffusion of the protein into the bulk fluid.

Due to the randomness of the particle position, the created pores are not straight but very sinuous. How twisted and turned the pores are, is described with the tortuosity factor [13, 150, 205]. The tortuosity directly relates to the effective distance the protein needs to transfer for diffusing out of the matrix. An increasing tortuosity is associated with an increase in the diffusion pathways and thus in a stronger retardation of the release. Therefore, the effective diffusivity  $D_e$  – that characterises the drug mobility within the matrix – is of magnitudes smaller than in aqueous media. Typically, for matrices comprising spherical particles rather low tortuosities between 1.5 and 3 are assumed [196]. Obviously, these values cannot completely explain why protein release is often sustained over months. Thus, Siegel and Langer suggested that beside the tortuosity the connection of the pores through narrow channels contributes to the retardation of the protein release. Since the protein is executing a random walk, it will need a certain time until the molecule finds its way from one pore to another (Figure 5) [205].

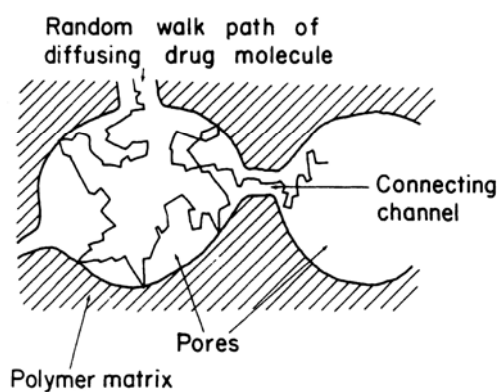


**Figure 5: Retardation of the protein release due to the narrowness of connecting channels.**

Due to the fact that the channel radius is much smaller than the pore radius, the passage from one pore to another is restricted [205].

Apart from the applied manufacturing procedure for a certain controlled release device, the pore morphology and thus the in-vitro release kinetics are influenced by two other important parameters: the initial drug loading and the particle size of the drug powder. As the protein is dispersed randomly within the matrix, the chance for two polypeptide particles to touch each other is very rare, when protein loadings are low. A certain amount of drug particles is then surrounded entirely by the matrix material and as this is impermeable for macromolecules the protein cannot be

released. Only at higher drug loadings the particles get in touch and upon dissolution a fully interconnected pore network is created, which ensures a complete protein liberation (Figure 6) [184].

Generally, protein release is reported to occur faster when larger drug particles are incorporated. The larger the drug particle size the more likely they will touch the implant surface. Moreover, the diameter of the created pores as well as the overall porosity increases with increasing particle size [13, 205].

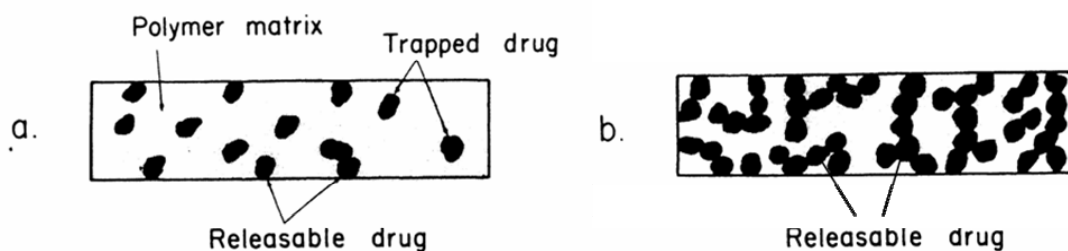


**Figure 6: Effect of drug loading on the creation of an interconnected network [205].**

For compressed fatty acid matrices Kaewwichit and Tucker confirmed that the release of BSA occurs similarly to non-erodible polymeric systems through an interconnected pore-network. Furthermore, the effects of particle size and drug loading on the rate of macromolecule release were comparable to that described above [112].

## 5.2. DRUG RELEASE FROM DEGRADABLE MATRICES

Based on the physical and chemical characteristics of a matrix polymer protein release from degradable matrices is governed by several mechanisms: (1) diffusion through a water-filled pore network, (2) degradation of the polymer, and/or (3) swelling of the system. The real conditions are often very complex and a combination of all three processes is mostly noted [80, 132, 172].

For example, protein release from PLGA-based microspheres is initially controlled by desorption of the protein from the surface. This phase is followed by the diffusion of protein through water filled pores, which in turn might be influenced by swelling. Finally, the polymer starts to degrade and a combination of diffusion and erosion phenomena governs drug release [41, 80, 212]. As a result, a pulsatile liberation profile is often observed: after a burst release of surface located and poorly encapsulated protein, a phase of lower release rates controlled by diffusion follows. Ultimately, increased diffusion rates corresponding to the polymer cleavage mark the third release period [58, 80, 100].

In addition to these rather complex, overlapping processes the physical state of the polymer can change during in-vitro release. For instance, Park et al. reported that hydration of PLGA matrices during in-vitro release lowered the glass transition temperature. Hence, the polymer changed from the glassy to the rubbery state, which accelerated polymer degradation and release rates [163]. Furthermore, osmotic effects as well as ionic interactions e.g. between polymer terminal carboxylic acid groups and basic polypeptides may be important for a full understanding of the protein release properties from polymeric depot systems [20, 162].

Finally, the impact of protein stability on the in-vitro release kinetics from both, degradable and non-degradable delivery devices, seems to be of importance. Several authors attributed a high burst followed by a non-release phase to protein aggregation within the device. As described above, protein aggregation may be induced during both, manufacture and release (see Chapter I.2). Because of their large size higher-order aggregates cannot diffuse through the restricted diameter of the pore network and hence are trapped within the matrix. In this context, Park and co-workers demonstrated that the addition of sodium dodecyl sulphate (SDS) or guanidine hydrochloride (GdnHCl) to the release media, increased the fraction of released protein, because both excipients enabled the dissociation of non-covalent aggregates formed within PLGA microspheres [52, 119]

### **5.3. INTRODUCTION TO MATHEMATICAL MODELLING**

The mathematical models described in literature can roughly be divided into mechanistic models and empirical models. Whereas mechanistic models take specific chemical and physical phenomena occurring during release into account, empirical models only describe the apparent release rates. Empirical models inherit the advantage that they are easier to handle. However, information about the underlying mass transport processes are obtained only with mechanistic models [207].

The practical benefit of such models is that they might facilitate the optimisation of the developed controlled release device. Due to the prediction of the effects of various design parameters (e.g. the device geometry or the matrix composition) on the release, the number of experiments required to achieve a desired drug release profile can be minimised [8, 114, 207].

Especially in the case of erodible matrices, the underlying drug liberation processes are very complex. Therefore, it is not reasonable to develop a mathematical model

that accounts for all processes, since such a model would be very complicated. It is rather crucial to identify and consider the dominant physical and chemical phenomena. Generally, for parallel processes the fastest and for sequential processes the slowest step is of prime interest [207]. Depending on the rate-controlling step release mechanisms can be classified into:

- (1) diffusion controlled,
- (2) swelling controlled, and
- (3) erosion controlled release [114].

This classification should just help to categorise and to understand the plethora of controlled drug delivery systems developed so far. Of course, the real processes are more sophisticated and, for instance, diffusion will be involved in all three cases.

### 5.3.1. DIFFUSION CONTROLLED SYSTEMS

#### 5.3.1.1. FUNDAMENTALS

Diffusion controlled systems can be categorised into reservoir and matrix systems depending on the region where the diffusion primarily takes place [8]. In reservoir systems the drug has to diffuse through a surrounding membrane with a constant thickness. After the saturation of the membrane the concentrations at both sites of the membrane are constant (provided that the initial drug load within the core is above the drug's solubility). At this time point steady state conditions are achieved and the concentration of the diffusing substance does not depend on time. In this special case the rate of release is governed by Fick's first law. In analogy to the transfer of heat by conduction, Fick recognised in 1855 that the transfer rate of a diffusing substance through a unit area is proportional to the concentration gradient:

$$J = -D \cdot \frac{\partial C}{\partial x} \quad \{1\} \quad \text{Steady state conditions: } \frac{dC}{dt} = 0$$

where J is the flux of drug being transferred per unit area, D is the diffusion coefficient and  $dc/dx$  is the concentration gradient [51, 107, 114].

In matrix systems non-steady state conditions have to be considered. This means, that the concentration of the diffusing substance within the matrix depends on position and time. The one-dimensional diffusion is described by the differential solution of {1}, generally referred as Fick's second law of diffusion [51]:

$$\frac{\partial C}{\partial t} = D \cdot \frac{\partial^2 C}{\partial x^2} \quad \{2\}$$

Considering diffusion along all three axes {2} can be rewritten as:

$$\frac{\partial C}{\partial t} = D \cdot \left( \frac{\partial^2 C}{\partial x^2} + \frac{\partial^2 C}{\partial y^2} + \frac{\partial^2 C}{\partial z^2} \right) \quad \{3\}$$

### 5.3.1.2. EMPIRICAL MODELS

The Higuchi equation, postulated 1961 [97] for the release of drugs from an ointment base, is probably the most frequently used model to describe the drug release from matrix systems [114, 207, 209]:

$$Q = \sqrt{D (2C_0 - C_s) C_s t} \quad \text{for } C_0 \gg C_s \quad \{4\}$$

Where Q is the amount of drug released at time t per unit area, D is the diffusion coefficient and  $C_0$  and  $C_s$  are the initial drug concentration and the solubility of the drug, respectively.

For application to porous matrices the Higuchi model must be modified and extended for the effective volume and path where diffusion occurs:

$$Q = \sqrt{D_B (2C_0 - \varepsilon C_s) C_s t} \quad \text{for } C_0 \gg C_s \quad \{5\}$$

As explained above, the diffusion of the drug from an inert, porous matrix is affected by the pore structure. Thus Higuchi related the bulk diffusion ( $D_B$ ) with the tortuosity ( $\tau$ ), the matrix porosity ( $\varepsilon$ ) and the diffusion coefficient in water ( $D_{aq}$ ) as following [96]:

$$D_B = \frac{D_{aq} \varepsilon}{\tau} \quad \{6\}$$

According to the Higuchi model the amount of drug released from the matrix is proportional to the square root of time. The proportionality constant depends on the drug load, the solubility, the diffusion coefficient, and the porosity.

The Higuchi model relies on the following assumptions: (1) diffusion is only one-dimensional (edge end effects must be negligible), (2) the diffusion coefficient remains constant during the entire release period, (3) perfect sink conditions are maintained, and (4) pseudo-steady state conditions are provided. The last point is the most important limitation of the Higuchi model, since pseudo-steady state circumstances are only achieved when the initial drug load is much higher than the

solubility of the drug ( $C_0 \gg C_s$ , monolithic dispersion). In Figure 7 the theoretical concentration profile under pseudo-steady-state conditions is illustrated. The solid line represents the concentration gradient after time  $t$  and the broken line the same after an additional time interval  $\Delta t$ . It is apparent, that the assumed situation is similar to the reservoir type systems: the core with the undissolved drug  $C_0$  is surrounded by a diffusing region. However, in contrast to the reservoir type system, the core incorporates not only the drug but also the matrix. Furthermore, as result of the ongoing release, the core region shrinks and the thickness of the diffusing region increases with time [8, 209].

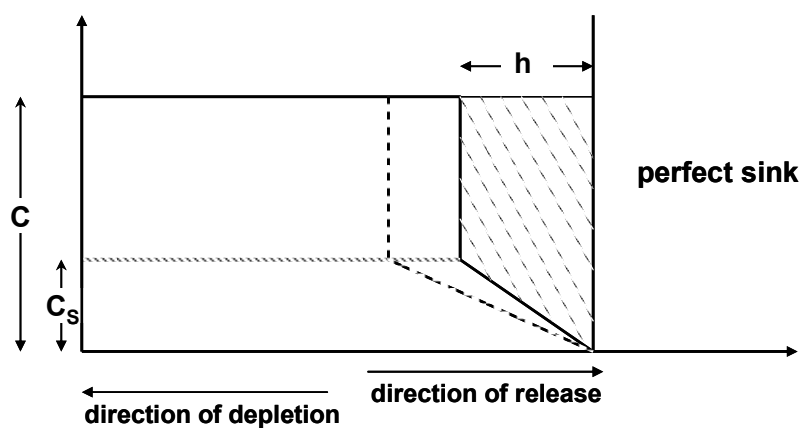


**Figure 7: Pseudo-steady state conditions considered in the Higuchi equation.**

Theoretical concentration profile assumed in an ointment containing suspended drug in contact with perfect sink conditions [97].

Due to its simplicity, the Higuchi equation is often fitted to experimental release data. For instance, it was used to describe the liberation of low molecular weight drugs from matrices comprising hydrogenated castor oil and polyethylene glycol monostearate. The calculated tortuosity values were orders of magnitude higher than expected. This effect was ascribed to the plastic behaviour of most lipids that allows these materials to flow around the drug particles [196, 197]. This unique behaviour of lipids will be utilised later for the preparation of sustained release matrices by simple compression.

The derivation of the exact analytical solution for the diffusion from a sphere under perfect sink conditions revealed that the approximate solution of Higuchi is valid, when the initial drug loading highly exceeds the drug solubility. In contrast, when  $C_0$  converges  $C_s$  and  $C_0/C_s$  becomes 1, the deviation to the exact solution increases [2, 8].

Furthermore, the original Higuchi model does not consider a boundary layer resistance of adjacent liquid layers. But even in-well agitated systems next to the

surface unstirred liquid boundary layers exist, that might lead to an additional mass transfer resistance [99]. Improvement was provided, for instance, by Wu and Zhou 1999 [8]. They developed an alternative numerical solution for slabs, cylinders, and spheres that includes an additional diffusion boundary layer at the surface of the matrix. Due to the introduction of the additional diffusion boundary layer, two diffusing zones are assumed. The thickness of the first zone changes over time, whereas the second zone, the diffusion boundary layer, revealed a constant thickness. Importantly, the obtained mathematical model describes the entire diffusional release process irrespective whether the dispersed drug has been dissolved or not. Moreover, the solution can be applied to predict the release kinetics under sink and under non-sink conditions. This is a fact of practical importance, since after administration the available liquid content and the absorption rates can be very low, so that under real conditions non-sink must be assumed [8].

It is clear from both Fick's law and the Higuchi model that the release rates decrease as the diffusion pathways increase with time. However, Langer and co-workers conducted a theoretical analysis for a hemisphere device, that allowed release only through a cavity in the flat surface (Figure 8) [102]. This study can be considered as a good example to illustrate how the understanding of the drug release mechanism and the subsequent mathematic analysis can facilitate the development of advanced controlled release systems.

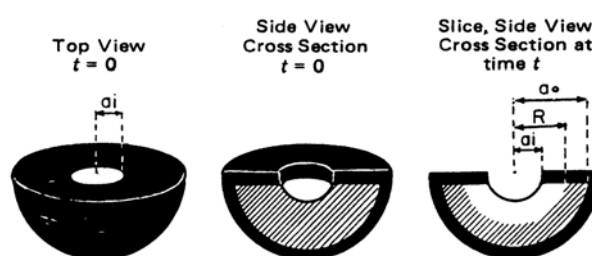


**Figure 8: Schematic picture of the hemisphere devices developed by [102].**

$A_i$  and  $A_o$  are the inner and the outer radius, respectively, and  $R$  is the distance between dissolved region (white) and dispersed zone (diagonal lines). The impermeable EVA coating layer is illustrated in black.

The developed hemisphere was produced by solvent casting a blend of drug and ethylene-vinyl acetate in a hemisphere mould at  $-80\text{ }^\circ\text{C}$ . Afterwards, the obtained hemisphere was coated with an impermeable polymer except of a small orifice in the centre of the circular face. For the delivery of BSA it was confirmed experimentally that the release follows a zero order kinetic over 60 days [102]. In order to elucidate

the role of the burst effect, later on an exact solution of Fick's second law of diffusion was derived for describing the zero-order release kinetics [160].

Especially the tortuosity factor in the Higuchi model for porous matrices is an empirical correction parameter that is derived from curve fittings without a physical meaning [88]. Alternatively, the percolation theory is postulated providing a simple mathematically derived model that predicts the transport properties from a porous matrix in dependence on the device morphology. A morphological description of the matrix is accomplished by subdividing the porous material into many small spaces (i.e. sites, clusters) [88, 137]. With respect to their location, these clusters can be classified either as conductive (water-filled pores within the matrix) or as non-conductive (matrix particles) (Figure 9).

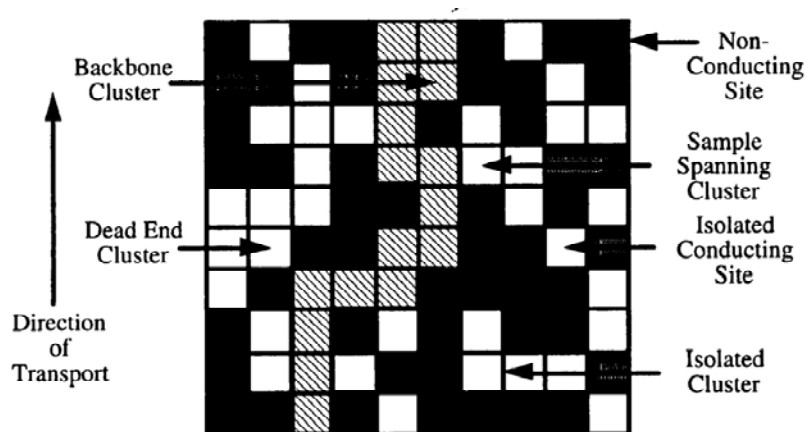


Figure 9: Schematic of diffusional transport according to the percolation model (from [89]).

In order to facilitate transport through the matrix, the conductive sites must form a sample spanning pathway. The critical drug load at which the sample spanning clusters first traverse the matrix is called critical percolation threshold ( $\phi_c$ ). Obviously, a non-erodible controlled release device must contain at least a loading of drug (and hydrophilic excipients) above  $\phi_c$  to allow transport through the matrix.

The diffusivity of the drug through the matrix is defined as [88, 89]:

$$D_B = \phi^E D_{aq} \quad \{7\}$$

where  $D_B$  is the diffusion coefficient within the matrix,  $D_{aq}$  the diffusion coefficient in aqueous media, and  $\phi^E$  is the relative diffusivity or effective volume fraction. The value for  $\phi^E$  can be between 0 and 1. If no sample spanning pathways exist  $\phi^E$  becomes zero and consequently there is no diffusion. The other extreme  $D_B = D_{aq}$  occurs under the assumption that the matrix is completely composed of drug.

Eliminating the tortuosity the Higuchi model can be modified in terms of the percolation concept to [88, 89]:

$$Q = \sqrt{D_B C_S (2\varnothing_D^A \rho - (\varnothing_D^A + \varepsilon) C_S)} t \quad \{8\}$$

where  $\varnothing_D^A$  is the drug load,  $\varepsilon$  is the initial, inherent porosity of the matrix,  $C_S$  is the solubility and  $\rho$  is the solid state density. Determining these parameters experimentally from the slope of a plot of  $Q$  versus the square root of time the bulk diffusion coefficient  $D_B$  can be obtained. From the value of  $D_B$  and the experimentally determined  $D_{aq}$  the percolation parameters can be evaluated.

Several authors applied this approach to relate the effects of formulation design parameters (drug load, particle sizes of the matrix material) to matrix morphology and to the obtained release kinetics [32, 137].

### 5.3.1.3. MECHANISTIC MODELS

Assuming that: (1) the drug dissolution is very fast compared to the drug diffusion, (2) no matrix swelling occurs, and (3) the diffusion coefficient is constant, the amount of drug release from slabs, cylinders or spheres with an initially uniform or a non-uniform drug distribution can be determined with the solutions of {2} described by Crank [82].

For instance, Siepmann et al. applied a solution of Fick's second law of diffusion for spheres to predict the release rates of diltiazem hydrochloride and theophylline from microspheres based on ethyl cellulose and Eudragit®RS 100. The diffusion coefficients of the drug within the polymers as well as the effects of various non-water soluble plasticizers were first evaluated by studying the release from the simple geometry of a film. The determined parameters of diffusion were then successfully transferred to the sphere geometry [208].

Fu and co-workers deduced an analytical solution of Fick's law for a cylindrical geometry considering mass transport in all three dimensions. The obtained model was verified for the release of hydrocortisone from polycaprolactone and ethylene-vinyl-acetate implants prepared by injection moulding. Furthermore, the model is applicable to cylindrical geometries ranging from flat disks (radius > thickness) to rods (radius < thickness) [72].

Another model was suggested by Vergnaud by using infinite series of exponential functions and considering the rotational symmetry around the z-axis as well as the

respective initial and boundary conditions (homogeneous drug distribution before exposure to the release medium and perfect sink conditions) [107]:

$$\frac{M_t}{M_\infty} = 1 - \frac{32}{\pi^2} \cdot \sum_{n=1}^{\infty} \frac{1}{q_n^2} \cdot \exp\left(-\frac{q_n^2}{R^2} \cdot D \cdot t\right) \cdot \sum_{p=0}^{\infty} \frac{1}{(2 \cdot p + 1)^2} \cdot \exp\left(-\frac{(2 \cdot p + 1)^2 \cdot \pi^2}{H^2} \cdot D \cdot t\right) \quad \{9\}$$

where  $M_t$  and  $M_\infty$  represent the absolute cumulative amounts of protein released at time  $t$  and infinite time, respectively;  $q_n$  are the roots of the Bessel function of the first kind of zero order [ $J_0(q_n)=0$ ], and  $R$  and  $H$  denote the radius and height of the cylinder [107].

Recently this solution of Fick's second law was applied to describe the release pattern of lysozyme from lipidic implants [84]. The authors showed, that Equation {9} was well suitable to describe the diffusion controlled release of lysozyme from compressed matrices based on various triglycerides. Moreover, the fact that the model has a mechanistic character rendered the solution derived by Vergnaud in particular interesting for the progress of the present thesis.

### 5.3.2. SWELLING CONTROLLED RELEASE

#### 5.3.2.1. EMPIRICAL MODELS

When the polymeric matrix revealed extensive swelling upon the imbedding of solvent molecules, the drug release cannot be described adequately by a concentration-dependent form of Fick's law with constant boundary conditions. The observed deviations from Fickian diffusion have been associated with the rearrangement of the polymer structures due to swelling [51, 114].

Based on the relative rates of diffusion and polymer relaxation three cases are distinguished. If the diffusion rate is lower compared to the relaxation, diffusion controlled release (Fickian diffusion, Case I transport) will be observed. The other extreme will occur in the so-called Case II diffusion if the drug release is governed by swelling. The intermediate Non-Fickian or anomalous diffusion is characterised by comparable diffusion and relaxation rates [51, 114].

In order to differentiate between Case I, Case II, and anomalous transport, the so-called power law equation developed by Korsmeyer can be applied [211]:

$$\frac{M_t}{M_\infty} = kt^n$$

where  $M_{\infty}$  is the amount of drug released after an infinite time,  $k$  is a constant describing the geometric characteristics, and the exponent  $n$  characterises the underlying release mechanism. If  $n$  is 0.5, 0.45 or 0.43, this will indicate a Fickian diffusion from a thin film, a cylinder, or a sphere. In contrast, if  $n$  is 1, 0.89 or 0.85, swelling controlled release (Case II) will occur from the same geometric matrices. A value in-between can be regarded as an indicator for the superposition of both phenomena [209].

#### 5.3.2.2. MECHANISTIC MODELS

Lee and Peppas mechanistically investigated polymer swelling. This process is accompanied not only by an increase of the device volume but also by a transformation of the polymer from the glassy to the rubbery state. A rubbery gel layer is created around the glassy core of the matrix. Consequently, two moving fronts – the rubbery-solvent front and the glassy-rubbery front – need to be considered. Initially, the rubbery-solvent front is moving outward, whereas the glassy-rubbery front is moving in the opposite direction. As soon as the polymer dissolution starts, the rubbery-solvent front is moving inwards until the glassy core disappears. At the final stage only the rubbery region is present [8].

Compared to the very low diffusion rates in the glassy core, the mobility in the fully swollen polymer layers is comparable to those in aqueous solutions [210]. Consequently, the mathematical modelling of the drug release from such systems can be realised with non-constant diffusion coefficients, that depend on the degree of polymer swelling [8, 209].

A more sophisticated solution was provided by Siepmann et al. with the development of the “sequential layer” model. A cylindrical device based on hydroxypropylcellulose was assumed to be built up on a certain amount of layers, simulated with a computational grid. The subsequent numerical analysis enabled to simulate non-homogeneous swelling in which the outermost layer swelled first followed by the neighbouring inner layers. Both the volume change and the increase in drug diffusivities in the swollen layer were reproduced well with the developed model [8]. However, since triglyceride implants revealed no swelling during in-vitro incubation [241] such complex processes can be neglected for the investigated pure tristearin matrices.

### 5.3.3. EROSION CONTROLLED RELEASE

#### 5.3.3.1. EMPIRICAL MODELS

Hopfenberger supposed that the rate of drug release from an erodible polymer is proportional to the surface area of the device and derived the following empirical model:

$$\frac{Mt}{M_{\infty}} = 1 - \left(1 - \frac{k_0 t}{C_0 a}\right)^n$$

where  $k_0$  is a rate constant,  $a$  is the radius of a cylinder or sphere, or the half thickness of a slab. According to the geometry of the device the shape factor  $n$  becomes  $n = 3$  for spheres,  $n = 2$  for cylinders or  $n = 1$  for slab geometry. Thus, according to the Hopfenberger model a zero-order release can be achieved with slab-shaped systems [114, 207].

#### 5.3.3.2. MECHANISTIC MODELS

Mechanistic models for degradable matrices either treat polymer erosion as a combined diffusion and chemical reaction process, or consider erosion as a random event by applying the Monte Carlo simulation [8, 207].

A model belonging to the first subclass was proposed by Heller and Baker. Here, based on the Higuchi equation, a mathematical solution for bulk eroding polymers was developed by considering that the permeability of the polymer matrix increases due to polymer cleavage. Relating the change of permeability to a function of the numbers of remaining bonds and assuming first order kinetics for the polymer degradation the following equation was established [207]:

$$\frac{dMt}{dt} = \frac{A}{2} \sqrt{\frac{2P_0 \exp(kt)C_0}{t}}$$

where  $P$  is initial permeability,  $A$  the surface area, and  $k$  the first order rate constant. Due to the increase in diffusion pathways the release rates first decrease with time. After a certain time point this is compensated by the exponential term, which represents the permeability of the progressively eroding polymer. Hence, the release rates increase when erosion takes place [207].

Several other models were developed that apply the equations of diffusion with a time-dependent increase in the diffusion coefficients. The diffusion coefficients are thereby calculated based on the molecular weight loss of the polymer matrix [8, 114,

207]. However, these approaches neglect the acceleration of the drug release due to the evolving pore network concomitant to the erosion process [8].

Especially in our case of macromolecule delivery, the microporous structure of the matrix is of outstanding importance since the release will be restricted to the diffusion through water filled pores.

In order to study the release of a model macromolecule (FITC-dextran) from porous PLGA microspheres Ehtezazi and Washington introduced an alternative attempt to obtain the effective diffusivity within the matrix. Here, based on the percolation theory (see Chapter I.5.3.1) the diffusivity within the polymeric matrix was assumed. This data allowed the subsequent calculation of the released fraction with a derivation of Crank's solution for diffusion in spheres [63].

Langer and co-workers developed another model for the release of proteins from PLA and PLGA microspheres that took into account alteration of the microstructure [12]. The structural change of the matrix was thereby related to the mass and molecular weight loss of the polymer during erosion. The following assumptions were made to describe the release process: after microsphere preparation with the double emulsion technique the protein is localised in occlusions that are entirely embedded within the polymer matrix. Consequently, the observed initial burst release was ascribed only to the desorption of protein from the exterior microsphere surface or from the surface of pre-existing mesopores. The concomitant hydration gives rise to polymer erosion. As a result, micropores grow up and coalesce to mesopores. Since the large size of the protein restricted the release until a sufficient number of mesopores was created, there was an "induction phase" with low or no protein release, followed by a second burst.

While the developed model predicted well the release of a glycoprotein, it failed for tetanus toxoid. The release of the latter did not show biphasic release behaviour. The authors assumed that in this case, the desorption was either very slow or the hydration was very fast and thus both phenomena were overlapped [12].

A subclass of mechanistic models simulates the polymer degradation as a random event using the Monte Carlo technique. This attempt was introduced in the late 1980's by Zygourakis to describe the drug release from surface eroding polymers. The complexity of simultaneous polymer and drug dissolution, which in turn changes continuously the morphology of the erosion front, is solved by generating a two-dimensional grid that simulates the microstructure within the device (Figure 10). Each

cell/pixel represents one of the device elements: drug, solvent, polymer, or pore void, respectively. In order to model the drug or polymer dissolution for each cell a lifetime is defined. According to this lifetime expectance the cellular grid is updated after distinct time-intervals. For example, if a drug cell is adjacent to one or more solvent cells, then its lifetime will end and the cell may change to a solvent cell at the next time interval [264]. However, the diffusional resistance to the transport of the drug to the bulk fluid is neglected and the drug release rate is thought to be determined only by the detachment of the molecule from the matrix surface. Furthermore, the model does not consider other mass transport processes, such as diffusion of water or polymer degradation products [207].

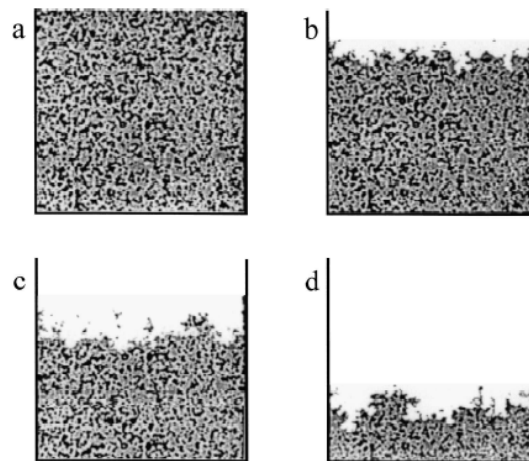


**Figure 10: Zygourakis' model for the simulation of drug release from surface eroding polymers.** The pictures depict the configuration of the cellular array modelling the cross section of the controlled release device. The two-dimensional grid is shown at four different stages of release: (a) initial situation, (b) 25 % released, (c) 50 % released, (d) 75 % released drug. Four types of pixels are distinguished: polymer, drug, filler, and solvent [264].

More sophisticated models were developed by Göpferich and co-workers by taking into account Monte Carlo simulation based polymer degradation and diffusional mass transport phenomena. These models are not limited to surface eroding polymers and can also be applied to bulk eroding matrices. Due to the fact that polymer degradation is affected by porosity, device geometry, and crystallinity these parameters were also taken into account [207].

While these models were developed for cylindrical implants, Siepmann et al. proposed a model based on Monte Carlo simulation for the release kinetics from PLGA microspheres. According to the symmetry conditions of an idealised sphere the mathematical analysis could be reduced to one quarter of the sphere (Figure 11). That way the computation time for numerical analysis was minimised. Importantly,

the proposed model covers well complex triphasic drug release kinetics with an initial burst, followed by zero-order release, and a second burst. Due to the continuous update of the grid it was possible to take into account the time dependent changes of the microsphere morphology. As outlined above especially in the second release period a superposition of drug dissolution, diffusion, and polymer erosion occurs. Since the matrix porosity increases, the drug diffusivity within the matrix is enhanced. Consequently, the time- and direction-dependent porosities within the microparticle were calculated for any grid point. Based on this information the time-, position-, and direction-dependent diffusivities were calculated. Furthermore, the schematic representation of the microsphere by a two dimensional pixel grid allows elucidating the influence of drug dissolution on the resulting release kinetics. At each time interval the concentration of drug and water of each grid are calculated and only the amount of soluble drug is considered to be available for diffusion [211].

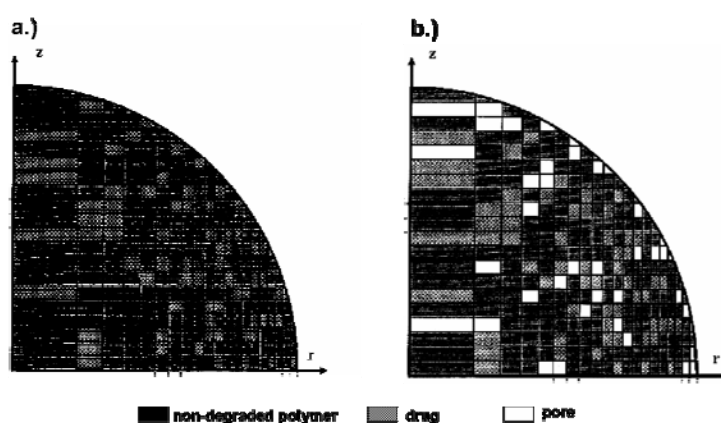


**Figure 11: Monte Carlo-based attempt to simulate polymer degradation and diffusional drug release from PLGA microspheres.**

The schematic structure of the system is illustrated before exposure to the release medium (a) and during release (b).

Recently, a Monte-Carlo scheme was developed to simulate the diffusion and the release of proteins from cross-linked dextran microspheres. Importantly, with the obtained scaling relations it was possible to predict the release curves of various proteins [239].

The apparent advantage of Monte Carlo-based models is that they provide a very realistic comprehension of the drug release mechanism. In contrast to simple analytic solution, these models take into account the complexity of several overlapping physical and chemical phenomena which influence the drug release kinetics. However, no explicit mathematic model is derived, hence it is difficult to get an idea of the effects of certain device design parameters on the drug release [8, 209].

## CHAPTER II: AIM OF THE THESIS

Controlled delivery systems for proteins based on degradable polymers, in particular on polyesters of lactic and/or glycolic acid, inhere several substantial sources for protein degradation during manufacturing, release, and storage [169, 199, 212, 233]. These restrictions led to the evaluation of alternative matrix materials, wherein lipids emerged as promising candidates [127, 144, 180].

Recently, it was demonstrated that IFN- $\alpha$  can be delivered over an one-month period from lipidic implants comprising tristearin as matrix material [153]. In contrast to several other studies [40, 108, 138, 174], the admixing of poly(ethylene glycol) 6000 (PEG) to the implant formulation resulted in a more sustained protein delivery compared to PEG-free delivery devices [153]. Therefore, the first major aim of the present work was to disclose the mechanism by which PEG affects the liberation of IFN- $\alpha$  from these tristearin-based implants.

Importantly, incorporated IFN- $\alpha$  was delivered from the developed implant completely and in its monomeric form [151]. Moreover, an excellent storage stability regarding both reproducibility of protein release kinetics as well as maintenance of protein integrity was proven [151]. However, despite these successes the implant system must be considered too large for a convenient way of administration. Furthermore, to our knowledge the manufacturing of lipidic implant systems has so far only been realised by self-made tools which were operated manually and only in lab-scale. Consequently, the second part of this thesis was focused on the development of new, improved lipidic implants.

In brief, the goals were:

- (1) Experimental and mathematical analysis of the in-vitro release behaviour of IFN- $\alpha$ , HP- $\beta$ -CD, and PEG from tristearin implants prepared by compression.
- (2) Elucidation of the mechanism by which PEG affects protein release.
- (3) Elucidation of the effects that the lyoprotectant HP- $\beta$ -CD has on protein release and stability.
- (4) Development of new, lipidic implant systems permitting subcutaneous injection in a patient-friendly way and allowing feasible up-scaling of manufacture.

## CHAPTER III: MATERIALS AND METHODS

### 1. MATERIALS

#### 1.1. PROTEINS

##### 1.1.1. RECOMBINANT INTERFERON $\alpha$ -2A (IFN- $\alpha$ )

Three classes of interferons are distinguished: interferon- $\alpha$ , interferon- $\beta$ , and interferon- $\gamma$ . Each of these classes can be further subdivided. In contrast to natural interferon- $\alpha$ , rh-interferon  $\alpha$ -2a (IFN- $\alpha$ ) is non-glycosylated [57]. IFN- $\alpha$  (Mw = 19.237 Da) was provided as a gift by Roche Diagnostics (Penzberg, Germany). The protein is formulated with a concentration of either 1.7 mg/mL or 4.9 mg/mL in 25 mM acetate buffer pH 5.0, containing 120 mM sodium chloride.

IFN- $\alpha$  contains four cysteins and two disulfide linkages one from position 1 to 98 and one from position 29 to 138 [57]. The three-dimensional structure of IFN- $\alpha$  determined by NMR revealed that IFN- $\alpha$  is an all-helical protein containing five  $\alpha$ -helices [122].

Due to its antitumour and antiviral efficacy, recombinant IFN- $\alpha$  (Roferon<sup>®</sup> A) is approved for the treatment of hair cell leukaemia, AIDS related Kaposi's sarcoma, and chronic hepatitis B and C [57].

##### 1.1.2. HEN EGG WHITE LYSOZYME

Lysozyme from hen egg white was purchased from Sigma Aldrich (Lot 114K7054, Steinheim, Germany). Historically, lysozyme was first described by Alexander Fleming in 1922 as remarkable bacteriolytic element found in tissues and secretions. Lysozyme hydrolyses  $\beta$  (1-4) linkages between N-acetylmuramic acid and N-acetyl-D-glucosamine residues in bacterial peptidoglycan [110].

Lysozyme is a 129 amino acid protein with a molecular weight of 14.7 kDa. The secondary structure of lysozyme comprises three helical regions and two regions of  $\beta$ -sheets [178]. An overall  $\alpha$ -helical content of 42 % was estimated by x-ray 2Å resolution, this means that 55 of the 129 amino acids are included into these helical structures [17].

### 1.2. LIPIDS

#### 1.2.1. TRIGLYCERIDES

##### 1.2.1.1. MONO-ACID TRIGLYCERIDES

Mono-acid triglycerides (Dynasan<sup>®</sup>) in the stable  $\beta$ -modification were received from Sasol GmbH (Witten, Germany). The used triglycerides and their characteristics are summarised in Table 3.

**Table 3: Characterisation of used Dynasan<sup>®</sup> triglycerides.**

	Dynasan <sup>®</sup> D112	Dynasan <sup>®</sup> D114	Dynasan <sup>®</sup> D118	Dynasan <sup>®</sup> D120
Chemical structure	trilaurin	trimyristin	tristearin	triarachidin
Acid value (mg KOH/g)	max. 3	max. 3	max.3	max. 0.7
Hydroxyl number (mg KOH/g)	not indicated	max.10	max.10	not indicated
Saponification no. (mg KOH/g)	256-268	229-238	186-192	180-200
Iodine number (g I <sub>2</sub> /100g)	max.1	max.1	max.1	max.3
Melting area (°C)	43-47	55-58	70-73	67-72

#### 1.2.1.2. PHOSPHOLIPIDS

Distearoyl-phosphatidyl-choline (DSPC, Lipoid PC 18:0/18:0) was kindly provided by Lipoid, Ludwigshafen, Germany. Lipoid PC 18:0/18:0 reveals a high chemical purity; the content of non-esterified fatty acids and the content of lysophosphatidylcholine was less than 0.5 %, respectively (certificate of analysis).

#### 1.2.1.3. MIXED-ACID TRIGLYCERIDES

Solid triglycerides of various saturated fatty acids were provided by Sasol GmbH (Witten, Germany). The features of the mixed-acid triglycerides are given in Table 4. In addition, Softisan<sup>®</sup>378 and Miglyol<sup>®</sup>812 were used in the present work. Softisan<sup>®</sup>378 is a special blend of triglycerides based on saturated even-numbered, unbranched fatty acids with a chain length of C<sub>8</sub>-C<sub>18</sub>. Miglyol<sup>®</sup>812 is a mixture of triglycerides of caprylic (C<sub>8</sub>) and capric (C<sub>10</sub>) fatty acids obtained from coconut and palmkernel oil. The used Softisan<sup>®</sup> 378 and Miglyol<sup>®</sup> 812 met the requirements of the European Pharmacopoeia for Hard Fat and for Medium Chain Triglycerides, respectively.

**Table 4: Characterisation of used mixed-acid triglycerides.**

	Triglyceride type H12	Triglyceride type E 85
C12 fatty acid,%	71.0	27.0
C14 fatty acid, %	26.8	70.1
C16 fatty acid;%	2.0	2.0
Hydroxyl number (mg KOH/g)	1.4	3.1
Saponification no. (mg KOH/g)	269.38	240.5
unsaturated fatty acids	no	no
Melting point (°C)	35.5	41.3

### 1.2.2. CHEMICALS AND REAGENTS

**Acetic acid (100 %)**, p.a., VWR International GmbH, Darmstadt, Germany

**Acetonitril**, gradient grade, VWR International GmbH, Darmstadt, Germany

**Ammonium thiocyanate**, ACS reagent, Sigma-Aldrich, Steinheim, Germany

**Chloroform**, CHCl<sub>3</sub>, VWR International GmbH, Darmstadt, Germany

**Dipotassium hydrogen phosphate**, K<sub>2</sub>HPO<sub>4</sub>, p.A., VWR International GmbH, Darmstadt, Germany

**Disodium hydrogen phosphate dihydrate**, Na<sub>2</sub>HPO<sub>4</sub> x 2 H<sub>2</sub>O, VWR Int. GmbH, Germany

**Ferric chloride**, FeCl<sub>3</sub>, VWR International GmbH, Darmstadt, Germany

**Hydroxypropyl-β-cyclodextrin (HP-β-CD)**, Cavasol W7 HP Pharma, Wacker specialities, Burghausen, Germany

**Methylene blue**, VWR International GmbH, Darmstadt, Germany

**Phenolphthalein**, C<sub>20</sub>H<sub>14</sub>O<sub>4</sub>, VWR International GmbH, Darmstadt, Germany

**Poly(ethylene glycol) 6000 (PEG)**, Clariant, Gendorf, Germany

**Potassium chloride**, KCl, p.A., VWR International GmbH, Darmstadt, Germany

**Sodium azide**, NaN<sub>3</sub>, p.A., VWR International GmbH, Darmstadt, Germany

**Sodium chloride**, NaCl, p.A., VWR International GmbH, Darmstadt, Germany

**Sodium dihydrogen phosphate monohydrate**, NaH<sub>2</sub>PO<sub>4</sub> x H<sub>2</sub>O, p.A., VWR Int. GmbH, Germany

**Sodium dodecyl sulphate**, C<sub>12</sub>H<sub>25</sub>NaO<sub>4</sub>S, VWR International GmbH, Darmstadt, Germany

**Sodium hydroxide**, NaOH, p.A., VWR International GmbH, Darmstadt, Germany

**Trifluoroacetic acid**, p.A., Merck KGaA, Darmstadt, Germany

**α,α-Trehalose-dihydrate**, British Sugar, Peterborough, UK

**Tween<sup>®</sup>20, Polysorbate 20**, Serva, Heidelberg, Germany

**Ultra pure water**, taken from Purelab Plus<sup>®</sup>, USF GmbH, Ransbach-Baumbach, Germany

## **2. METHODS**

### **2.1. PREPARATION OF LIPIDIC CONTROLLED RELEASE DEVICES**

#### **2.1.1. LYOPHILISATION OF IFN- $\alpha$**

Lyophilisation was performed in accordance with Mohl [151]. IFN- $\alpha$  was lyophilised either with trehalose or with HP- $\beta$ -CD in a protein/excipient ratio of 1 to 3. Before lyophilisation the pH of the stock solution was adjusted to 4.2 with acetic acid (30 % vol/vol). A freeze-dryer  $\varepsilon$ 12G (Christ, Osterode, Germany) was used for lyophilisation. 1 mL protein/lyoprotectant stock solution filled into 2R glass vials was frozen to  $-45\text{ }^{\circ}\text{C}$  at a rate of  $1.6\text{ }^{\circ}\text{C}/\text{min}$ . This temperature was maintained for 90 minutes. Afterwards, the temperature was increased to  $-20\text{ }^{\circ}\text{C}$  in steps of  $0.1\text{ }^{\circ}\text{C}/\text{min}$ . Simultaneously, the chamber pressure was reduced to  $10^{-2}$  mbar. This primary drying program was maintained for 30 hours. Then, the temperature was increased by  $0.1\text{ }^{\circ}\text{C}/\text{min}$  up to  $20\text{ }^{\circ}\text{C}$  and concomitantly the pressure was reduced to  $10^{-3}$  mbar. Secondary drying was performed for 15 hours. Finally, the chamber was vented with nitrogen to a pressure of 800 mbar and the vials were closed with rubber stoppers.

The average weight per lyophilisate was 64 mg, comprising 25 % IFN- $\alpha$  and 75 % excipient.

#### **2.1.2. MANUFACTURING OF IMPLANTS BY COMPRESSION**

IFN- $\alpha$  loaded, tristearin-based implants were prepared by compression as described previously [151]. Briefly, lyophilised IFN- $\alpha$  (Lot PZ 0210P017, c (IFN- $\alpha$ ) =  $1.7\text{ mg/mL}$ ) was blended with different amounts of PEG and tristearin and filled into a compaction tool (diameter: 5 mm). The powder blends were compressed with a force of 19.6 kN for 30 s using a hydraulic press (Maassen, Eningen, Germany). In order to evaluate the impact of compression force and compression time on the in-vitro release behaviour, the compression was also performed at 9.8 kN or for 2 min, respectively. The average mass and height of the implants were 50 mg and 2.3 mm, respectively. The drug loading was calculated on the total implant weight (wt/wt).

Lysozyme-loaded implants were prepared in same way, but as lysozyme was already purchased as solid powder, lyophilisation could be omitted. For matters of comparison, 7.5 % of placebo HP- $\beta$ -CD lyophilisate, 2.5 % lysozyme and optionally PEG were admixed to the tristearin material.

### **2.1.3. MANUFACTURING OF IMPLANTS BY RAM EXTRUSION**

In accordance to Chapter III.2.1.2, the lipid powder was blended with lyophilised IFN- $\alpha$  and optionally PEG in an agate mortar. This mixture was filled into the barrel of a purpose made extruder device shown in Figure 57 Chapter V. After inserting the extruder piston a force of 3.92 kN was applied for 30 s with a hydraulic press (Maassen, Eningen, Germany). Then, the extruder was lifted on a rack and the lipidic formulation was extruded with the hydraulic press.

As the extruder die was 1.2 mm, extrudates revealed a diameter of 1.2 mm. The average length of the extrudates was 15 mm.

### **2.1.4. MANUFACTURING OF IMPLANTS BY TWIN SCREW EXTRUSION**

The lipid powder comprising the low and the high melting point lipid was prepared by grinding in a mortar. Subsequently, the obtained blend was admixed with 10 % IFN- $\alpha$ /HP- $\beta$ -CD lyophilisate (IFN- $\alpha$  bulk material Lot PZ0005P025, c (IFN- $\alpha$ ) = 4.8 mg/mL) and PEG, optionally 10 % or 20 %. In the case of lysozyme 2.5 % lysozyme powder, 7.5 % HP- $\beta$ -CD and 20 % PEG were compounded with the lipids. Extrusion was performed using a twin screw extruder (MiniLab<sup>®</sup> Micro Rheology Compounder, Thermo Haake GmbH Karlsruhe, Germany, see Figure 77, Chapter V). The extruder was heated to 40 °C (D118/H12 lipid blend) or to 47 °C (D112/D118 lipid blend) prior to filling. The rotation speed of the screws was fixed at 40 rpm. Then the extruder was manually filled with the lipid blend. Extrusion was performed with closed bypass channel to allow a direct extrusion without circulation. In order to prepare extrudates of different sizes, dies with a diameter of 0.5 mm, 1.0 mm or 1.4 mm were fixed in front of the standard extruder outlet (diameter 2.0 mm). The extruded strands were cut into pieces with a length of approximately 2.3 cm.

## **2.2. MECHANICAL STABILITY OF THE LIPIDIC IMPLANTS**

The mechanical properties of extrudates prepared either by ram extrusion or by twin screw extrusion were estimated with the Texture Analyser TA XT2i (Stable Micro systems, UK). A 25 mm cylinder probe was used, and the extrudates were placed centrally under the probe. The standardised test program “Failure behaviour of tablets due to diametrical compression using a cylinder probe” (settings: pre-test speed 2mm/s, test speed 0.03 mm/s and post-test speed 10 mm/s) was applied. From the obtained force versus time plot the maximum force value was used as the longitudinal tensile strength.

### **2.3. EXTRACTION OF PROTEIN FROM THE LIPID MATRIX**

The protein was extracted with the aqueous extraction method developed by Mohl [151]. Briefly, the protein-loaded matrix was ground in an agate mortar. Subsequently, 50 mg of the sample were suspended in 1 mL pH 7.4 isotonic 0.01 M sodium phosphate buffer containing 0.05 % (wt/vol) sodium azide and 1 % (wt/vol) polysorbate 20 (PBST). After gentle agitation for 2 hours the samples were centrifuged at 5000 rpm for 5 minutes (4K15 laboratory centrifuge; Sigma, Osterode, Germany).

### **2.4. IN-VITRO RELEASE STUDIES OF IFN- $\alpha$**

The protein-loaded implants were placed into TopPac<sup>®</sup> vials (cycloolefin copolymer vials; Schott GmbH, Mainz, Germany). Depending on the mass of the studied implants the vials were filled with isotonic 0.01 M phosphate buffer pH 7.4 containing 0.05 % (wt/vol) sodium azide (PBS). In the case of ram extrudates and extrudates prepared with the twin-screw extruder revealing a diameter of 0.5 or 1 mm 1.0 mL of buffer was added. For compressed implants and rods prepared by twin screw extrusion with a diameter of 1.4 or 2.0 mm the volume of buffer was increased to 2.0 mL.

The vials were placed in a horizontal shaker (40 rpm, 37 °C, Certomat<sup>®</sup>IS; B. Braun Biotech International, Göttingen, Germany). At predetermined time points, the release medium was completely exchanged and the amounts of IFN- $\alpha$ , PEG, and HP- $\beta$ -CD in the phosphate buffer were determined as described below.

In order to investigate the pH effect on in-vitro release, the pH of PBS buffer was adjusted to pH 4.0. In vitro release was carried out as described above. The frequent buffer exchange as well as the absence of acidic/basic degradation or release products ensured a virtually constant pH in the release media throughout the experiments.

#### **2.4.1. SIZE EXCLUSION CHROMATOGRAPHY OF IFN- $\alpha$**

Protein concentration was measured by size-exclusion chromatography (SE-HPLC) using a TSKgel (G3000SWXL, 7.8 mm x 30.0 mm column; Tosoh Biosep, Stuttgart, Germany). The mobile phase consisted of 120 mM disodium hydrogen phosphate dihydrate, 20 mM sodium dihydrogen phosphate and 4 g/L sodium chloride (adjusted to pH 5.0 with hydrochloric acid), the flow rate was 0.5 mL/min, and IFN- $\alpha$  was

detected spectrophotometrically ( $\lambda = 215 \text{ nm}$ , UV 1000; Thermo Electron Cooperation, Dreieich, Germany).

#### **2.4.2. CONCENTRATION OF HP- $\beta$ -CD**

The HP- $\beta$ -CD content was determined using a modification of the method proposed by Basappa et al. [11]. The assay is based on the formation of a colourless, stable inclusion complex of HP- $\beta$ -CD and phenolphthalein (molar ratio 1:1): The fading of an alkaline phenolphthalein solution is followed spectrophotometrically. Briefly, 500  $\mu\text{L}$  freshly prepared 0.03 mM phenolphthalein solution (in 0.6 M sodium carbonate, pH 11) were added to 500  $\mu\text{L}$  sample solution. Immediately after mixing, the absorbance at 551 nm was measured (UV 1, Thermo Electron Cooperation, Dreieich, Germany). It was confirmed that the calibration curve ( $R^2 > 0.99$ ) obtained with protein- and PEG-free HP- $\beta$ -CD solutions (concentration range: 50-1000  $\mu\text{g/mL}$ ) overlaps with that obtained in the presence of IFN- $\alpha$  and PEG (0.164 mg/mL and 2.5 mg/mL, respectively).

#### **2.4.3. CONCENTRATION OF PEG**

500  $\mu\text{L}$  ammonium ferrothiocyanate reagent (16.2 g/l anhydrous ferric chloride, 30.4 g/L ammonium thiocyanate), 500  $\mu\text{L}$  chloroform and 150  $\mu\text{L}$  sample solution were vigorously mixed (21°C, 1400 rpm, 30 min, Eppendorf Thermomixer; Eppendorf, Hamburg, Germany). Subsequently, the aqueous phase was removed and the absorbance of the chloroform phase was measured at 510 nm (UV 1; Thermo Spectronic, Dreieich, Germany). A linear correlation ( $R^2 > 0.99$ ) between absorbance and PEG content was found in the range of 0.025 mg/mL - 2 mg/mL. Any interference by the presence of IFN- $\alpha$  and HP- $\beta$ -CD could be excluded (samples spiked with 0.164 mg/mL IFN- $\alpha$  and 1.875 mg/mL HP- $\beta$ -CD resulted in unchanged absorbance values).

#### **2.5. DETERMINATION OF POROSITY**

Compressed implants were prepared and incubated as described above. At predetermined points of time the implants were removed and vacuum dried (VO 200 vacuum chamber, Memmert, Schwabach, Germany) to constant weight. Then, the true volume of the implants was determined with a helium pycnometer using the 1 mL volume cell (accuPyc 1330, Micromeritics, Mönchengladbach, Germany). The geometric volume of the implants was determined by measuring implant height and

diameter with a digital calliper rule (Digimatic CD-15CD, Mitutoyo, Oberndorf, Germany).

The porosity ( $\varepsilon$ ) in % was calculated with:

$$\varepsilon = \left( 1 - \frac{V_{true}}{V_{geom}} \right) \cdot 100 \quad \{10\}$$

where  $V_{true}$  is the implant volume determined with the helium pycnometer and  $V_{geom}$  is the calculated theoretical volume.

## 2.6. WATER UPTAKE AND EROSION

Protein-loaded implants were removed from incubation buffer, wipe dried to remove adhesive water, and weighed (UMX 2, max. 2.1 g, d=0.1  $\mu$ g, Mettler Toledo, Giessen, Germany). After drying to constant weight (VO 200 vacuum chamber, Memmert, Schwabach, Germany) the implants were weighed again. The matrix erosion and the water uptake were determined with equation {11} and {12}:

$$\text{Matrix erosion} = \left( \frac{M_0 - M_d - M_c}{M_0} \right) \cdot 100 \quad \{11\}$$

$$\text{Water uptake} = \left( \frac{M_r - M_d}{M_d} \right) \cdot 100 \quad \{12\}$$

where  $M_0$  is the initial implant mass,  $M_r$  and  $M_d$  are the wet and the dry implant mass after exposure to incubation media, and  $M_c$  is the total mass of incorporated hydrophilic compounds (assuming complete release).

## 2.7. IN-VITRO RELEASE STUDIES OF LYSOZYME

Lysozyme release from implants prepared either by compression or by twin screw extrusion was studied in accordance to Chapter III.2.4. In order to determine lysozyme stability and concentration SE-HPLC analysis was carried out. A TSKgel G3000SWXL, 7.8 mm x 30.0 mm column (Tosoh Biosep, Stuttgart, Germany) was used with a mobile phase consisting of 200 mM disodium hydrogen phosphate dihydrate (adjusted to pH 6.8 with hydrochloric acid), the flow rate was 0.4 mL/min, and lysozyme was detected spectrophotometrically ( $\lambda = 215$  nm, UV 1000; Thermo Electron Cooperation, Dreieich, Germany). Calibration curves were generated with lysozyme solutions in a concentration range of 20.3 to 324.8 mg/mL.

## 2.8. SOLUBILITY STUDIES

Solutions of poly(ethylene glycol) 6000 (PEG unless otherwise indicated) with a concentration of 2-40 % (wt/vol) in PBS pH 4.0 or 7.4 were prepared. These solutions were mixed in a ratio of 1:1 with IFN- $\alpha$  bulk solutions (initial concentration of 4.9 mg/mL pH 4.0 or 7.4). Afterwards, the samples were equilibrated for 2 h at 37°C, 40 rpm (Certomat IS). Subsequently, precipitated protein was separated by centrifugation at 5000 rpm (5 °C, 5 min, 4K15 laboratory centrifuge; Sigma, Osterode, Germany) and the residual IFN- $\alpha$  concentration in the supernatant was determined. Thus, solubility is referred to the solute concentration of the supernatant in equilibrium with the precipitated phase. Protein concentration was determined by reversed phase chromatography (see below). The effect of pH on the precipitation of IFN- $\alpha$  was investigated at a final PEG concentration of 5 % (wt/vol) PEG. The pH of the PEG and protein solution was adjusted with 0.1 N NaOH or 0.1 N HCl prior mixing, respectively.

Solubility studies of lysozyme were performed by mixing different concentrated PEG solutions with lysozyme solutions (c=4.8 mg/mL, PBS). As no protein precipitation occurred and the protein concentration remained constant, lysozyme solubility was assessed by stepwise adding of lysozyme powder to buffer media (PBS, pH 7.4) until a sediment occurred. After equilibration for 2 h at 37°C, 40 rpm (Certomat IS), the samples were centrifuged (5 °C, 5 min, 4K15 laboratory centrifuge; Sigma, Osterode, Germany) and the concentration of dissolved lysozyme was determined by SE-HPLC. The same procedure was carried out with 5, 10, 15 and 20 % (wt/vol) PEG solutions (in PBS pH 7.4). (Remark: In contrast to IFN- $\alpha$ , the high solubility of lysozyme in the presence of PEG allowed a dilution of 1 to 2000 before SE-HPLC analysis. Consequently, no interference of PEG with the separation of lysozyme was observed.)

## 2.9. REVERSE PHASE CHROMATOGRAPHY OF IFN- $\alpha$

Reverse phase chromatography (RP-HPLC) of IFN- $\alpha$  was performed using a Jupiter 5u C18 300 Å 250 x 4.60 mm column (Phenomenex, Aschaffenburg, Germany). The mobile phase consisted of a 49:51 (vol/vol) acetonitrile/ultra pure water mixture which was acidified with 0.1 % (vol/vol) trifluoroacetic acid. The flow rate was adjusted to 1 mL/min; UV detection (UV 1000; Thermo Electron Cooperation, Dreieich, Germany) was performed at 215 nm wavelength.

## **2.10. SODIUM DODECYL SULPHATE POLYACRYLAMIDE GEL ELECTROPHORESIS (SDS-PAGE)**

SDS-PAGE was conducted under non-reducing conditions using an XCell II Mini cell system (Novex, San Diego, CA). The protein solutions were diluted in a pH 6.8 tris-buffer, containing 2 % SDS and 2 % glycerine. Samples were denatured at 90°C for 30 min and subsequently 20  $\mu$ L were loaded into the gel wells (NUPAGE Novex 10 % Bis Pre-Cast Gel 1.0 mm; Invitrogen, Groningen, The Netherlands). Electrophoresis was performed in a constant current mode of 30 mA in a tris-glycine/SDS running buffer (MES running buffer; Invitrogen, Groningen, The Netherlands). Gel staining and drying was accomplished with a silver staining kit (SilverXpress) and a drying system (DryEase), both provided from Invitrogen, Groningen, Netherlands.

## **2.11. FLUORESCENCE SPECTROSCOPY**

Fluorescence studies were carried out on a Varian fluorescence spectrometer Cary eclipse at 20 °C. IFN- $\alpha$  stability after precipitation with PEG and re-dissolution, was assessed by precipitating IFN- $\alpha$  with 5 to 20 % PEG and re-dissolving in excess of buffer to a final protein concentration of 0.05 mg/mL. The obtained spectra were compared to that of native IFN- $\alpha$  (also 0.05 mg/mL in PBS buffer). To study IFN- $\alpha$  HP- $\beta$ -CD interactions the cyclodextrin was added to IFN- $\alpha$  bulk solution in a mass ratio of 1 to 3. These solutions were diluted with PBS buffer to a protein concentration of 0.05 mg/mL.

In both experiments the excitation wavelength was fixed at 295 nm, and fluorescence emission scans were collected from 300 to 450 nm using a scan speed of 30 nm/min at an excitation and emission slit width of 5 nm.

## **2.12. FOURIER TRANSFORM INFRARED SPECTROSCOPY (FTIR)**

### **2.12.1. TRANSMISSION FTIR-SPECTRA OF DISSOLVED IFN- $\alpha$**

In order to evaluate the effect of precipitation and re-dissolution on the secondary protein structure, IFN- $\alpha$  was precipitated in the presence of 5 to 20 % PEG as described above. After centrifugation the supernatant was removed and the obtained protein pellet was re-dissolved in PBS buffer. The obtained solutions, as well as IFN- $\alpha$  bulk solutions were filled in a calcium fluoride flow through cell (Aquaspec AS 1110 M, Bruker Optik, Ettlingen, Germany) with 6.5  $\mu$ m path length. FTIR spectra were recorded with the Confocheck system on a Tensor 27 (Bruker Optik, Ettlingen, Germany) equipped with a nitrogen-cooled photovoltaic MCT detector at a resolution

of  $4\text{ cm}^{-1}$ . At least two measurements of 120 scans were performed. The temperature of the cell was maintained at  $25\text{ }^{\circ}\text{C}$  via a cryostat (DC 30-K20; Thermo Haake, Dreieich, Germany). The obtained spectra were background subtracted and vector normalised from for relative comparison. Finally, the second derivative spectra were generated via the spectrometer software (OPUS, Bruker Optik, Ettlingen, Germany). The FTIR spectra of IFN- $\alpha$  in the presence of HP- $\beta$ -CD (mass ratio 1 to 3) were collected in the same way.

### **2.12.2. TRANSMISSION FTIR-SPECTRA OF SOLID IFN- $\alpha$**

For transmission measurements 2 mg of lyophilised IFN- $\alpha$ , lipid/protein/PEG blend before or after extrusion were mixed with 150 mg KBr, respectively. After compression (78.4 kN for 2 minutes) the KBr pellet was fixed in the sample holder (Tensor 27, Bruker Optik, Ettlingen, Germany) and spectra were collected with a total of 256 scans at a resolution of  $2\text{ cm}^{-1}$ . The obtained absorbance spectra were automatically baseline corrected (OPUS, Bruker Optik, Ettlingen, Germany). Background correction was performed manually (described in detail in Chapter V.2.3). The obtained spectra were vector-normalised and analysed by the second derivatisation in the amid I band region (OPUS, Bruker Optik, Ettlingen, Germany).

### **2.12.3. THERMAL DENATURATION OF IFN- $\alpha$**

Investigations on the thermal protein stability were performed with the Bio-ATR unit. The spectra were collected in the wavenumber range from of  $4000\text{ to }850\text{ cm}^{-1}$ . The temperature was ramped from  $25\text{ to }70\text{ }^{\circ}\text{C}$  in 5 degree increments. Before recording the spectrum the cell was equilibrated for 120 seconds. Each spectrum was obtained with 240 scans at a resolution of  $4\text{ cm}^{-1}$ . Separately, the thermal dependence of the buffer was collected under the same conditions. The protein spectra were automatically background corrected by the buffer spectra at the respective temperature. The adsorption spectra were further processed by vector-normalisation. Afterwards, the second derivatives were calculated and again vector-normalised (OPUS, Bruker Optik, Ettlingen, Germany).

## **2.13. INVESTIGATIONS ON THE LIPID MODIFICATION**

### **2.13.1. WIDE-ANGLE X-RAY SCATTERING (WAXS)**

Lipidic controlled release systems, the pure lipids as well as lipidic blend before manufacturing were ground. Wide-angle X-ray scattering (WAXS) was performed by an X-ray Diffractometer XRD 3000 TT (Seifert, Ahrensberg, Germany), equipped with a copper anode (40 kV, 30 mA wavelength 0,154178 nm). Experiments were conducted at  $0.05^\circ$  (2 theta) within a  $5^\circ - 40^\circ$  range.

### **2.13.2. DIFFERENTIAL SCANNING CALORIMETRY (DSC)**

Samples were ground and approximately 10 mg were analysed in a sealed Al-crucible. Measurements were performed with DSC 204 Phoenix (Netzsch, Selb, Germany). Heating and cooling were conducted at a scan rate of 5 K/min within a 20-100°C (tristearin) or a -20 to 100°C (H12) temperature range.

## **2.14. MICROCALORIMETRY**

Microcalorimetry was carried out with a VP-DSC (MicroCal<sup>®</sup>, Milton Keynes, UK). Before measurement, all solutions were degassed (ThermoVac, MicroCal<sup>®</sup>, Milton Keynes, UK). IFN- $\alpha$  bulk solution with a protein concentration of either 4.8 mg/mL or 0.48 mg/mL was loaded into the sample cell using a tight Hamilton 2.5 mL glass syringe. The reference cell was loaded with bulk buffer (25 mM acetate buffer, 120 mM sodium chloride, pH 5.0). The same procedure was performed with solutions containing additional 14.4 or 1.4 mg/mL HP- $\beta$ -CD. Scans were performed from 20-80 °C at a scanning rate of 90 °C/hour.

By loading both cells with the reference a base line was recorded. This base line was subtracted from the protein thermal data and the excess heat capacity was normalised for protein concentration. Data analysis was performed with Origin<sup>Microcal</sup> software.

## **2.15. SCANNING ELECTRON MICROSCOPY**

Incubated implants (prepared by compression or by ram extrusion) were dried in a VO 200 vacuum chamber (Mettert, Schwabach, Germany) for 48 h at 37°C and subsequently, coated with a fine gold layer (MED 020, Bal-tec GmbH, Witten, Germany). Scanning electron microscopy was carried out with a 6500F, Jeol GmbH (Eching, Germany).

## 2.16. DETERMINATION OF THE DIFFUSION COEFFICIENTS OF IFN- $\alpha$

The apparent diffusion coefficient of IFN- $\alpha$  in the release medium was measured using a modification of the open-end capillary technique proposed by Anderson and Saddington [5]. IFN- $\alpha$  lyophilised either with HP- $\beta$ -CD or with trehalose was blended with PEG in a ratio of 1 to 1 or 1 to 2. The protein/PEG blend or the lyophilised protein was dissolved in PBS buffer to a final protein concentration of 2.4 mg/mL. These solutions were filled into glass capillaries (diameter: 0.8 mm, length: 2 cm, one end open), respectively. The capillaries were placed into glass vials filled with 10 mL PBS buffer. Sink conditions were provided throughout the experiments. The vials were shaken horizontally with 40 rpm, if not otherwise indicated, at 37°C (Certomat<sup>®</sup>IS). At predetermined time points the acceptor medium was removed and the IFN- $\alpha$  content within the capillary was determined by SE-HPLC as described above. For each time point three separate samples were prepared. The apparent diffusion coefficient  $D$  of IFN- $\alpha$  in the release medium was determined by fitting the following analytical solution of Fick's second law of diffusion (considering the respective initial and boundary conditions) to the experimentally measured protein release kinetics:

$$\frac{M_t}{M_\infty} = 1 - \sum_{n=0}^{\infty} \frac{8}{(2 \cdot n + 1)^2 \cdot \pi^2} \cdot \exp\left(-\frac{(2 \cdot n + 1)^2 \cdot \pi^2}{4 \cdot L^2} \cdot D \cdot t\right) \quad \{13\}$$

where  $M_t$  and  $M_\infty$  represent the absolute cumulative amounts of IFN- $\alpha$  released at time  $t$ , and infinite time, respectively;  $L$  denotes the length of the capillary. [Remark: To be sure that convective mass transfer was negligible for IFN- $\alpha$  release out of the thin capillaries, the agitation rate was increased from 40 to 80 rpm. Importantly, the determined protein release kinetics was not affected.]

## 2.17. "MACROPORE MODEL"

The developed "macropore release model" device is schematically illustrated in Figure 37, Chapter IV. The device was filled with protein, HP- $\beta$ -CD and PEG pellets prepared by compression. The pellets comprised IFN- $\alpha$  lyophilisate, IFN- $\alpha$  lyophilisate:PEG blends, as well as IFN- $\alpha$  lyophilisate:HP- $\beta$ -CD blends, respectively. The lyophilisate:PEG ratios were the same as for the implant formulations, e.g. 1:1 for devices containing 10 % PEG, 10 % lyophilised protein; and 1:2 for implants

containing 10 % lyophilised protein and 20 % PEG. The pellets were placed in a small volume container, connected with an open capillary of around 10 mm length and 2 mm diameter. Subsequently, the devices were filled with isotonic phosphate buffer (pH 7.4, 0.05 % (w/v) sodium azide) and fixed at the bottom of a sterile polypropylene tube (Greiner bio-one, Frickenhausen, Germany). Afterwards, the polypropylene tube was filled with 3 mL acceptor medium (isotonic phosphate buffer, pH 7.4, 0.05 % (w/v) sodium azide) and incubated at 37°C and 40 rpm (Certomat IS). At predetermined time points, the acceptor medium was completely replaced and the protein concentrations in the samples were determined by RP-HPLC as described above.

### 2.18. MATHEMATICAL MODELLING

IFN- $\alpha$ , PEG and HP- $\beta$ -CD release from the investigated lipidic implants into the release media was quantitatively described using an analytical solution of Fick's second law of diffusion introduced into Chapter I.5.3. The model considers protein/PEG diffusion in axial as well as in radial direction in cylindrical matrices:

$$\frac{\partial c}{\partial t} = \frac{1}{r} \cdot \left\{ \frac{\partial}{\partial r} \left( r \cdot D \cdot \frac{\partial c}{\partial r} \right) + \frac{\partial}{\partial \theta} \left( \frac{D}{r} \cdot \frac{\partial c}{\partial \theta} \right) + \frac{\partial}{\partial z} \left( r \cdot D \cdot \frac{\partial c}{\partial z} \right) \right\} \quad \{14\}$$

where  $c$  is the concentration,  $t$  represents time;  $r$ ,  $z$  denote the radial and axial coordinates and  $\theta$  the angle perpendicular to the  $r$ - $z$ -plane;  $D$  is the apparent diffusion coefficient within the lipidic implant.

The theory takes into account that perfect sink conditions are maintained throughout the experiments and considers the rotational symmetry around the  $z$ -axis (no concentration gradients in  $\theta$  direction) as well as homogeneous distributions within the implants at  $t = 0$  (before exposure to the release media). Based on these initial and boundary conditions, Equation 14 can be solved using infinite series of exponential functions, leading to [107]:

$$\frac{M_t}{M_\infty} = 1 - \frac{32}{\pi^2} \cdot \sum_{n=1}^{\infty} \frac{1}{q_n^2} \cdot \exp\left(-\frac{q_n^2}{R^2} \cdot D \cdot t\right) \cdot \sum_{p=0}^{\infty} \frac{1}{(2 \cdot p + 1)^2} \cdot \exp\left(-\frac{(2 \cdot p + 1)^2 \cdot \pi^2}{H^2} \cdot D \cdot t\right)$$

{Repetition of Equation 9, Chapter I.5.3}

where  $M_t$  and  $M_\infty$  represent the absolute cumulative amounts of protein, PEG or HP- $\beta$ -CD released at time  $t$  and infinite time, respectively;  $q_n$  are the roots of the Bessel function of the first kind of zero order [ $J_0(q_n)=0$ ];  $R$  and  $H$  denote the radius and height of the cylinder.

If release levelled off below 100 %, the experimentally determined plateau values were considered as 100 % reference values for protein/PEG diffusion. For the implementation of the mathematical model the programming language C++ was used.

## CHAPTER IV: MECHANISMS CONTROLLING THE RELEASE FROM LIPID-BASED DELIVERY SYSTEMS

Despite the steadily increasing importance of lipid-based delivery systems for controlled protein release [127, 144] the knowledge of the underlying drug release mechanisms is very limited so far. However, as illustrated in the introduction, this knowledge would help to optimise existing controlled release systems and to develop new ones.

Therefore, it was the aim of the following work to understand the mechanisms controlling the release from tristearin implants. Such systems containing IFN- $\alpha$  co-lyophilised with hydroxypropyl- $\beta$ -cyclodextrin (HP- $\beta$ -CD) were recently shown to deliver the incorporated protein in a sustained manner over a period of one month. Importantly, an excellent protein stability was proven during implant preparation, release, and storage [151-153]. Furthermore, the addition of various amounts of poly(ethylene glycol) 6000 (PEG) to the implant formulation were shown to enable a modification of the protein release. Interestingly, the presence of PEG resulted in a more sustained protein liberation, which was so far not understood. Therefore, firstly the release of IFN- $\alpha$  from tristearin implants containing different initial PEG loadings was investigated.

### **1. EFFECT OF PEG ADDITION ON RELEASE KINETICS FROM TRISTEARIN IMPLANTS**

#### **1.1. RELEASE MECHANISMS OF IFN- $\alpha$ FROM TRISTEARIN IMPLANTS**

The effects of varying the relative PEG contents of the lipidic implants on the resulting protein release kinetics in phosphate buffer pH 7.4 are illustrated in Figure 12. The initial PEG content of the formulations was varied from 0 to 20 %, in 5 % increments. As it can be seen, the resulting IFN- $\alpha$  release rate and the amount of totally released protein significantly increased with increasing PEG contents. For instance, protein release from PEG-free implants levelled off at 31 % after 7 d, whereas complete IFN- $\alpha$  release was observed from devices containing 10-20 % PEG after approximately 16 d. With 5 % PEG an intermediate release profile was obtained (i.e. 54 % after 13 d).

Thus, the addition of small amounts of PEG to the lipidic implants was a very efficient tool to provide a complete protein recovery. The enhanced recovery yields found here agreed well with the effects of PEG described in literature. Usually the impact of

PEG on the release kinetics is ascribed to its role as a pore former [40, 108, 138, 174]. Due to the elevated levels of the water-soluble fraction of the matrix the formation of an interconnected pore-network is enhanced. Hence, PEG facilitates the diffusion of the drug out of the matrix (see Chapter I.5.1).

Interestingly, not only the slope of the release curves, but also their shape was altered. The release rates from PEG-free matrices monotonically decreased with time, whereas IFN- $\alpha$  was delivered in a constant manner over at least 7 days from all PEG-containing matrices. This alteration of the release kinetics indicates differences in the underlying mass transport mechanisms.

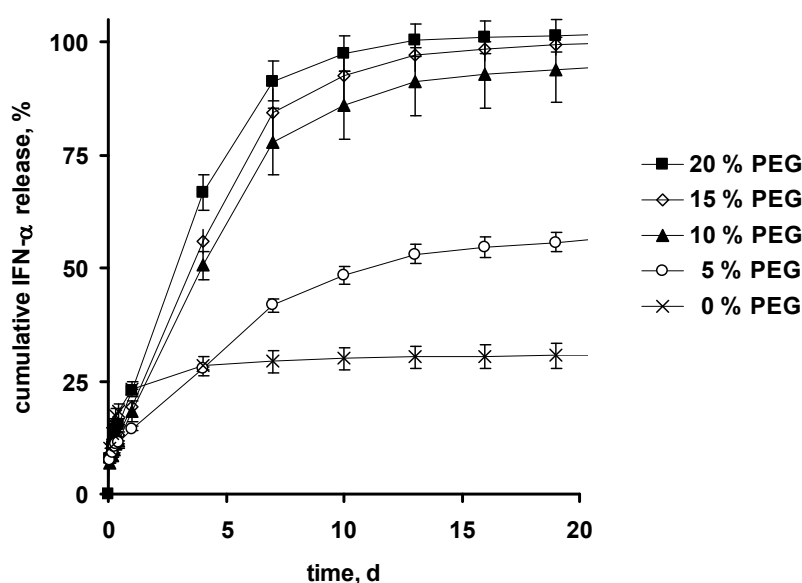


**Figure 12: Effects of the addition of various amounts of PEG on the release of IFN- $\alpha$  from tristearin-based cylindrical implants.**

The implants were prepared by compression as described in Chapter III. All devices were loaded with 10 % IFN- $\alpha$  co-lyophilised with HP- $\beta$ -CD and the indicated PEG amount (average  $\pm$  SD; n = 3).

In addition, another effect of PEG was obvious: PEG-containing implants exhibited a lower burst release than PEG-free systems (Figure 13). For example, matrices containing 0 % PEG released 18.3 % ( $\pm$  1.7 %) of the incorporated IFN- $\alpha$  within the first 10 h, whereas implants comprising 10 % PEG liberated only 11.9 % ( $\pm$  2.2 %) within the same time period.

The reduced burst release was very astonishing considering the well known role of PEG as a pore former in controlled release systems [40, 108, 138, 174]. PEG can be expected to leach rapidly from the matrix. As a result the creation of pores and channels through which the release medium can enter the device occurs in an accelerated manner. Furthermore, the enlargement of the created pore-network

mostly accounts for a reduction of the geometric restrictions of the pore-network. Thus, the addition of PEG to degradable as well as to non-degradable depot formulations was predominantly reported to be associated with an increase of the initial burst effect [40, 108, 138, 174].

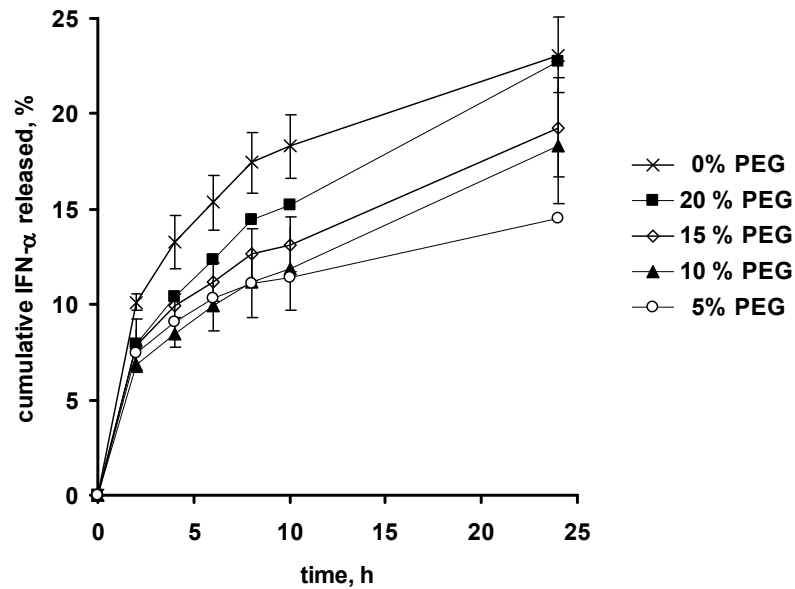


**Figure 13: Effects of the addition of various amounts of PEG on the burst release of IFN- $\alpha$ .**

The implants were prepared by compression. All devices were loaded with 10 % IFN- $\alpha$  co-lyophilised with HP- $\beta$ -CD and the indicated PEG amount (average  $\pm$  SD; n = 3).

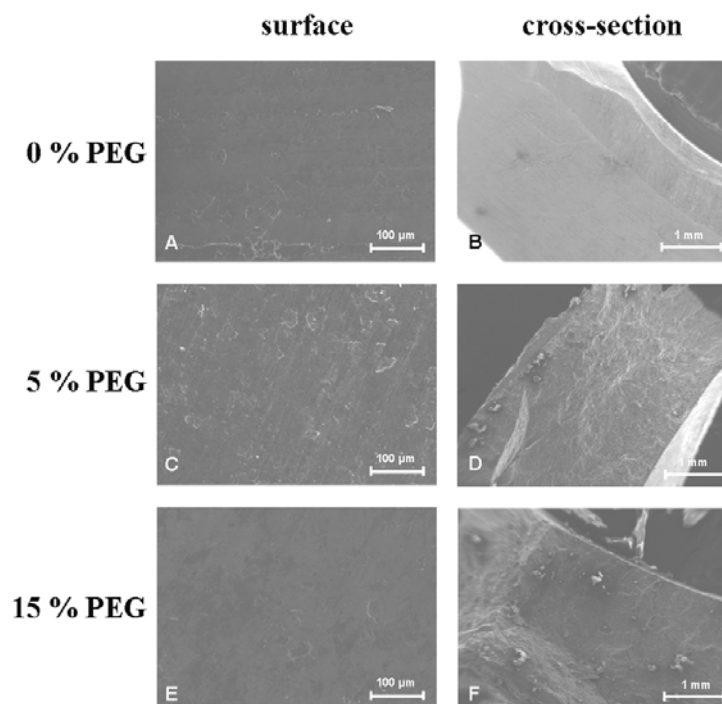


**Figure 14: External (left) and internal (right) morphology of the tristearin-based implants before exposure to the release medium.**

Scanning electron microscopy of tristearin implants before in-vitro incubation. The implants were loaded with 10 % IFN- $\alpha$ /HP- $\beta$ -CD co-lyophilisate and the indicated PEG amount.

To better understand the impact of PEG the internal and external morphology of the lipidic implants was studied before and after exposure to the release medium. Figure 14 shows examples of surfaces and cross-sections of tristearin-based implants loaded with 10 % IFN- $\alpha$ /HP- $\beta$ -CD and 0, 5, or 15 % PEG before exposure to phosphate buffer pH 7.4. Clearly, the implants were very dense, showing low initial porosity. No significant differences in the morphology were visible between the devices containing different amounts of PEG.

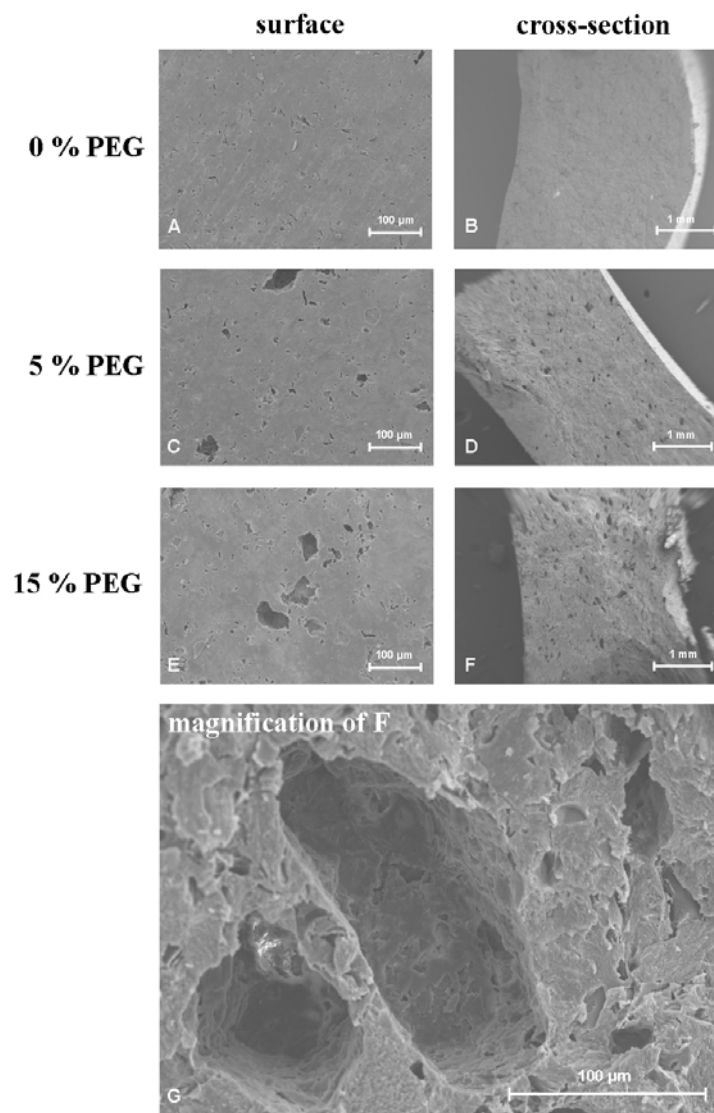


**Figure 15: External (left) and internal (right) morphology of the tristearin-based implants after in-vitro release studies.**

Scanning electron microscopy of tristearin implants after in-vitro incubation. The implants were loaded with 10 % IFN- $\alpha$ /HP- $\beta$ -CD co-lyophilisate and the indicated PEG amount.

In contrast, clear differences were visible after 28 d of incubation in phosphate buffer pH 7.4 (Figure 15). With an increasing PEG content, the inner and outer porosity of the devices significantly increased. This can be attributed to the leaching out of the

water-soluble PEG (together with IFN- $\alpha$  and HP- $\beta$ -CD) into the bulk fluid upon exposure to the release medium. The observed changes in the implants' morphology agreed very well with the protein release patterns (Figure 12): With higher PEG loadings, the porosity of the lipidic matrices increased upon exposure to the release medium, resulting in enhanced IFN- $\alpha$  mobility and, thus, in increased protein release rates. Importantly, the created pore network was highly interconnected at more elevated initial PEG contents (Figure 15G). Furthermore, it became evident that at 0 and 5 % initial PEG loadings, not all of the protein had direct access to water-filled pores. As the permeability through crystalline lipidic plates can be expected negligible, IFN- $\alpha$  surrounded completely by tristearin cannot be released. This may explain the levelling off of protein release below 100 % from PEG-free and 5 % PEG containing matrices (Figure 12).

The external and internal morphology clearly indicates that PEG acts as a pore forming agent which explains well the increased amount of delivered protein. However, the observed changes in the shape of the release curves and especially the decreasing burst effects are still unclear and cannot be ascribed to the effect of PEG as a pore former.

In order to get a deeper insight into these phenomena a mathematical model was fitted to the release data. The used tristearin implant systems revealed no swelling or erosion during in-vitro and during in-vivo release [151]. In Chapter I.5 it was explained that the release from such inert matrices can be expected to be governed by pure diffusion through a water-filled pore-network penetrating the matrix. Thus, an adequate solution of Fick's second law of diffusion was fitted to the experimental release data (see Equation 9, Chapter I.5.3 as well as Chapter III.2.18).

In Figure 16 the theoretical release curves and the experimental data are illustrated. Good agreement between theory and experiment was obtained in the case of IFN- $\alpha$ -loaded implants which did not contain any PEG ( $R^2 = 0.99$ ). This indicated that diffusion through the interconnected pore network dominated the overall control of IFN- $\alpha$  liberation. Based on this fitting, the apparent diffusion coefficient of the protein in the lipidic matrix was determined to be  $5.8 (+/- 1.2) \times 10^{-8} \text{ cm}^2/\text{s}$ .

In contrast, systematic deviations between the applied theory and the experimentally determined IFN- $\alpha$  release kinetics were observed with all PEG containing implants. In Figure 16 B the theoretical and experimental data for implants containing 10 % PEG are shown exemplarily. At early time points, protein release was overestimated,

whereas at late time points IFN- $\alpha$  release was underestimated. The observed differences between the theoretical and the experimental release profiles suggest that in PEG-containing implants, not only pure protein diffusion (with constant diffusivities) through the water-filled pores is of importance.

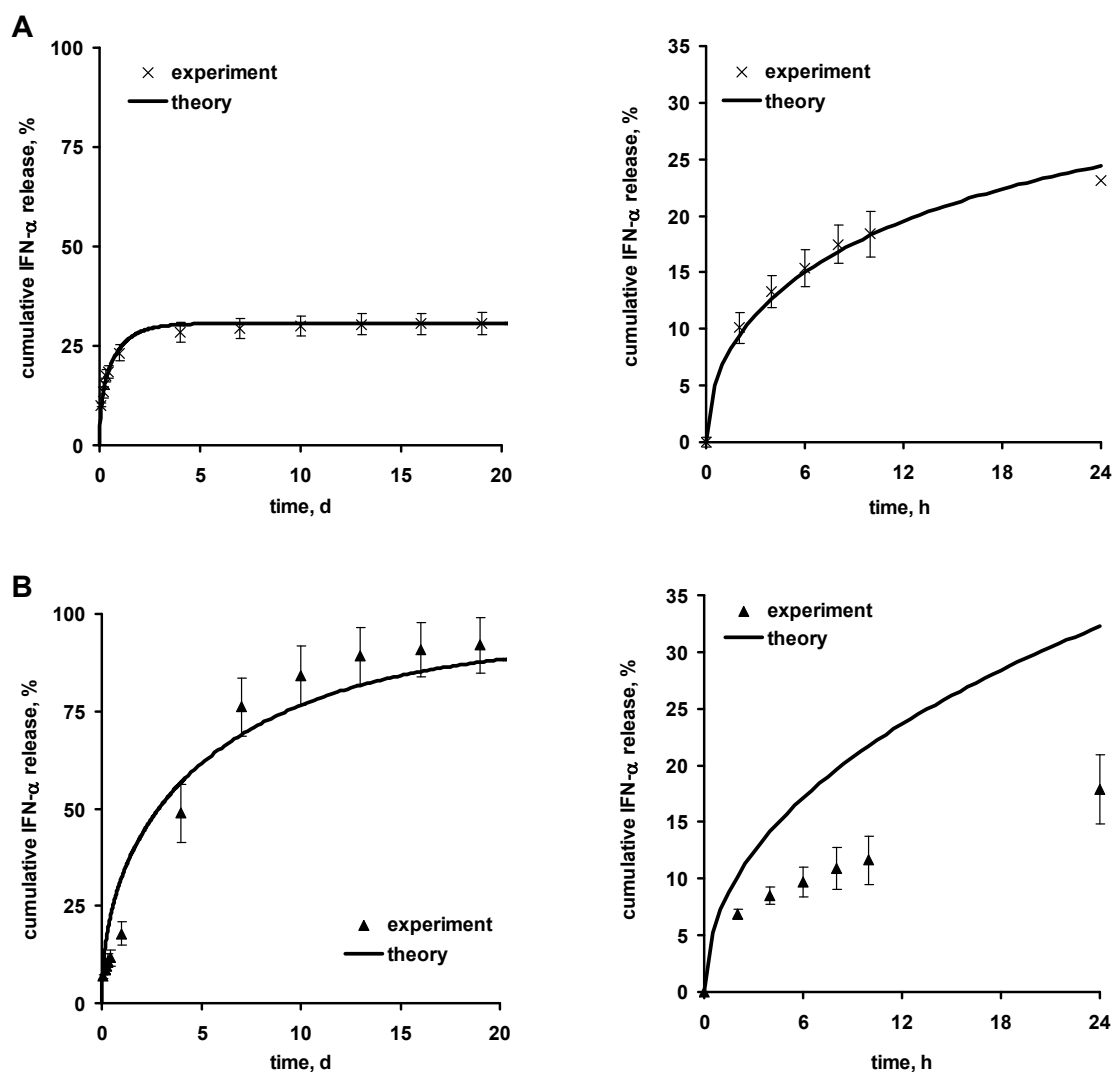


**Figure 16: Effect of the addition of PEG on the underlying drug release mechanisms of IFN- $\alpha$  from tristearin implants.**

Experiments (symbols) and theory (curves): fittings of Equation 9 Chapter I.5.3 to the experimentally determined IFN- $\alpha$  release kinetics from tristearin-based implants containing: (A) 0 % PEG, and (B) 10 % PEG in phosphate buffer pH 7.4. On the right hand-side the protein release within the first 24 h is shown, respectively (for experimental results: average  $\pm$  SD;  $n = 3$ ).

Recently, Guse et al. also used Equation {9} Chapter I.5.3 to quantify drug release from compressed lipidic implants. It was found that the release of lysozyme from implants prepared with the emulsion-compression method (see Chapter I.3.2.3) was purely diffusion-controlled, irrespective of the type of triglyceride used. In contrast, the dominating release mechanism was depended on the type of lipid in the case of

pyranine-loaded implants prepared by compression of a lyophilised lipid-drug solution: trilaurin- and tristearin-based systems were found to be purely diffusion controlled, whereas also other mass transport phenomena were of importance in trimyristin- and tripalmitin-based devices. However, when reducing the applied compression force also diffusion controlled release was reported for the latter systems, indicating that the underlying drug release mechanism was affected by the preparation method [107].

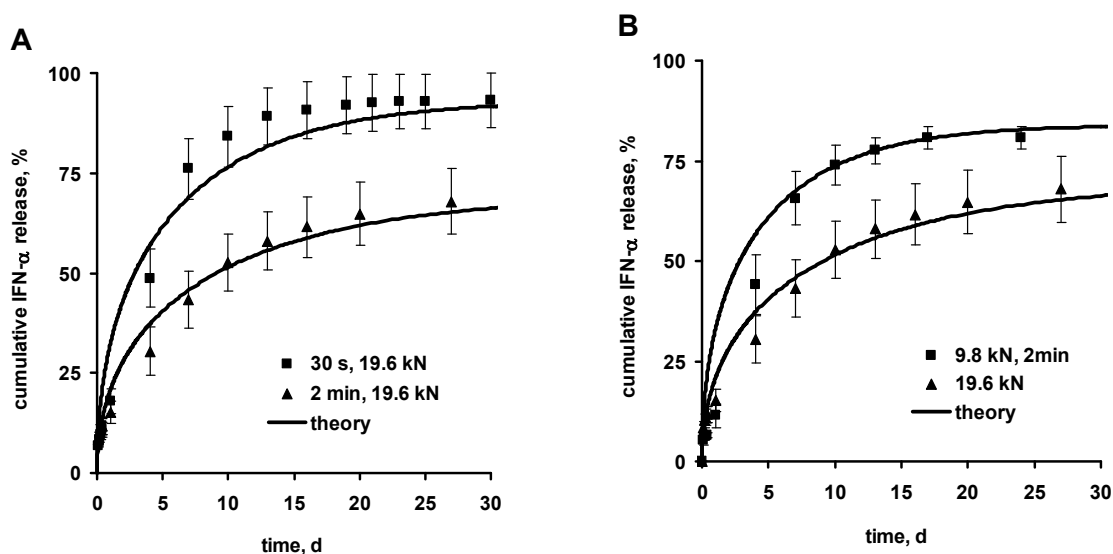


**Figure 17: Effects of compression time (A) and compression force (B) on IFN- $\alpha$  release.**

All tristearin implants were loaded with 10 % IFN- $\alpha$  co-lyophilised with HP- $\beta$ -CD and 10 % PEG (average  $\pm$  SD;  $n = 3$ ).

In order to investigate potential effects of the manufacturing procedure on the protein release mechanisms IFN- $\alpha$  loaded tristearin implants containing 10 % PEG were prepared with different compression forces and compression times, respectively. In Figure 17 A the impact of the compression time can be seen. The compression time was prolonged from 30 seconds to 2 minutes while maintaining a constant compression force of 19.6 kN. Obviously, extended compression times resulted in lower and more sustained protein liberation. Implants compressed for 30 seconds delivered 89.2 % of the incorporated IFN- $\alpha$  within 13 days, whereas exerting a compression over 2 minutes resulted in an ongoing release of 68 % of the initially incorporated protein over 27 days.

By increasing the compression forces (Figure 17 B) also decreasing liberation rates were found. Matrices yielded after applying a force of 9.8 kN revealed significantly faster protein release than matrices prepared with the doubled force.

The impact of compression force and time on the protein release kinetics can presumably be ascribed to alterations in the packing arrangement of drug, excipient, and matrix particles, which in turn influences the pore characteristics and consequently the drug release [112]. Tristearin, protein/HP- $\beta$ -CD, and PEG particles can be expected to be packed more closely with increasing compression time and force. Thus, the implant porosity decreases, resulting in decreased drug release rates.

However, the fitting of Equation {9} based on Fick's second law of diffusion to the experimental release data clearly showed that the underlying drug release mechanisms were not affected by the alteration in the manufacturing procedure (Figure 17). Irrespective of the applied compression force or time, systematic deviations between the theoretical data considering pure diffusion and the experimentally determined release values were observed. This means, that independent of the applied implant compression method the release of IFN- $\alpha$  from PEG-containing tristearin matrices was not purely governed by diffusion.

## **1.2. DETERMINATION OF THE DIFFUSION COEFFICIENT OF IFN- $\alpha$**

The simultaneous dissolution and leaching out of HP- $\beta$ -CD, PEG, and IFN- $\alpha$  continuously alters the composition of the medium generated within the implant pores during the release period. According to the Stoke-Einstein equation the diffusion coefficient is a function of the viscosity. Due to the dissolution of PEG a concentrated PEG solution of a high viscosity within the implant pores can be initially expected. As PEG leaches out the viscosity of the pore liquid decreases, which may impair the mobility of the protein diffusing within the liquid-filled pores. Consequently, it may be possible that the change of the liquid conditions within the implant pores affects the protein diffusivity. This assumption is backed by the reports on bovine serum albumin and lysozyme for which the diffusion coefficients in aqueous media decrease with an increasing concentration of poly(ethylene glycol) [170, 238].

Thus, the presence or absence of PEG within the water-filled pores of the implants may affect the mobility of IFN- $\alpha$ . This situation would provide an explanation of the aforementioned deviations between the theoretical release kinetics considering pure diffusion with constant diffusion coefficients and the experimental release data observed with PEG-containing lipidic implants.

Therefore, it was necessary to evaluate the diffusion coefficients of IFN- $\alpha$  in the release medium in the presence and absence of PEG. For the study of the protein

diffusion in gels or liquids several methods have been described in literature [252]. Dynamic Light Scattering was applied to investigate the diffusional behaviour of lysozyme [238] and bovine serum albumin [170] in the presence of various poly(ethylene glycols). Furthermore, Fluorescence Recovery after Photobleaching (FRAP) or the more elaborated Holographic Relaxation Spectroscopy (HRS) were used to evaluate the diffusion coefficient of macromolecules [173, 183].

Apart from the obvious need for advanced equipment and skills these methods impose some further restrictions. In HRS and FRAP the diffusant is tagged to a photochromic or photobleachable label, which in turn might affect the mobility [252].

Alternatively, the open-end capillary technique proposed by Anderson and Saddington provides a less laborious approach to determine the diffusion coefficient. Here, the rate at which the solute diffuses out of the open end of a capillary into the acceptor medium is monitored under perfect sink conditions [5]. In addition to its simplicity the open-end capillary technique would provide the benefit that the conditions within the pores of the controlled release system can be simulated. As the liquid generated within the implant pores would presumably compromise IFN- $\alpha$ , HP- $\beta$ -CD, and optionally PEG the capillaries were filled with these compounds dissolved in buffer medium. In contrast to the original experimental protocol, the acceptor medium did only contain phosphate buffer. This means that IFN- $\alpha$ , HP- $\beta$ -CD, and PEG would diffuse out of the capillary simultaneously, which should provide additional information on the interdependency of excipient and protein liberation.

The experimental setup applied is illustrated in Figure 18. The capillaries with a diameter of 0.9 mm and a length of 3 cm were filled with IFN- $\alpha$ /HP- $\beta$ -CD:PEG blends dissolved in isotonic phosphate buffer pH 7.4 to a final protein concentration of 2.5 mg/mL. The ratios of IFN- $\alpha$ / HP- $\beta$ -CD to PEG were chosen in analogy to the implant formulations. An IFN- $\alpha$ /HP- $\beta$ -CD:PEG ratio of 1 to 1 dissolved within the capillary corresponds to an implant formulation with a preload of 10 % IFN- $\alpha$ /HP- $\beta$ -CD co-lyophilisate and 10 % PEG. After filling, the capillaries were uprightly fixed in a beaker filled with the acceptor medium and tempered at 37 °C. The acceptor was stirred at 300 rpm.

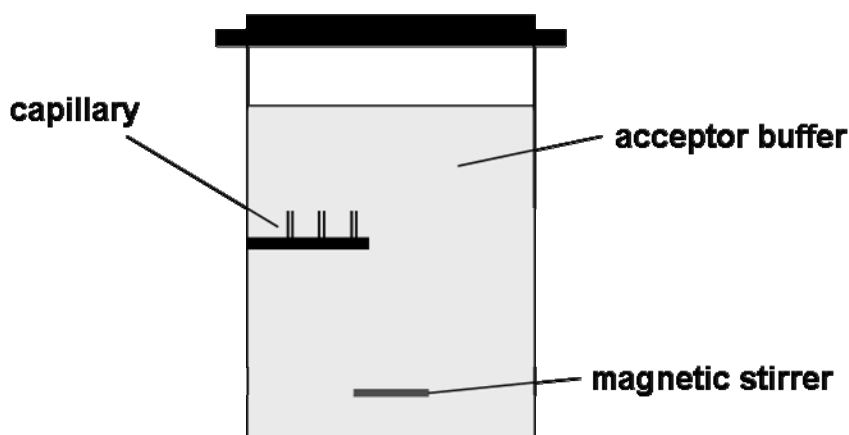


**Figure 18: Schematic presentation of the experimental setup used to determine the diffusion coefficient of IFN- $\alpha$ .**

After predetermined points of time a capillary was removed and the remaining protein content within the capillary was determined. Figure 19 represents the declining protein concentrations within the capillary over time.

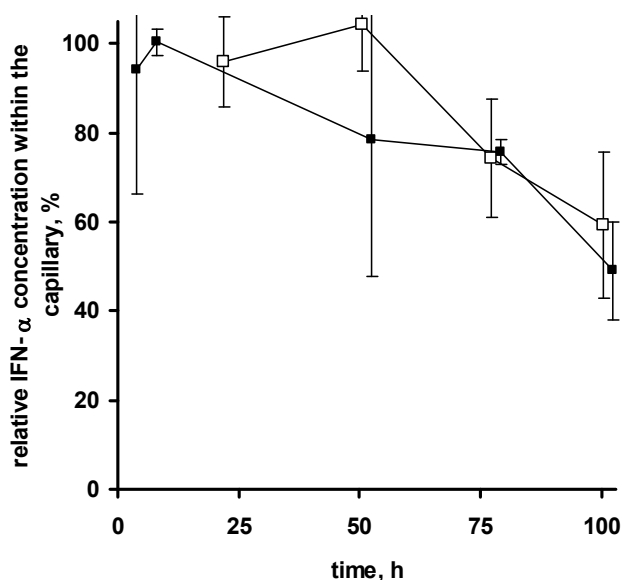


**Figure 19: Decrease of IFN- $\alpha$  concentration within the capillary.**

The diffusion out of a capillary was measured according to the experimental setup shown in Figure 18. Open symbols represent decay of IFN- $\alpha$  concentration in the absence and closed symbols in the presence of PEG (IFN- $\alpha$ /HP- $\beta$ -CD:PEG blends 1:1) (average  $\pm$  SD; n = 3).

Clearly, no important differences between PEG-containing and PEG-free samples were found. However, the standard deviations were high and thus, the calculation of accurate diffusion coefficients was not possible. Presumably, the large deviations between the samples are due to the manual withdrawal of the capillaries, which might cause an uncontrollable convective mass transfer out of the remaining capillaries.

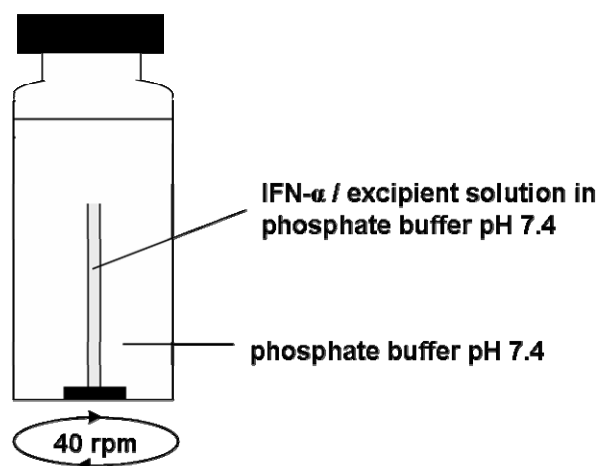


**Figure 20: Schematic presentation of the modified experimental setup used to determine the diffusion coefficient of IFN- $\alpha$ .**

In order to improve accuracy an alternative experimental setup was established (Figure 20). Each capillary was now fixed at the bottom of a separate vial. After filling the capillary the vial was carefully charged with the acceptor medium. The prepared vials were incubated at 37 °C and 40 rpm. At predetermined time points the acceptor medium was removed with a pipette. Then the content of the thin glass capillary was transferred to determine the remaining protein concentration.

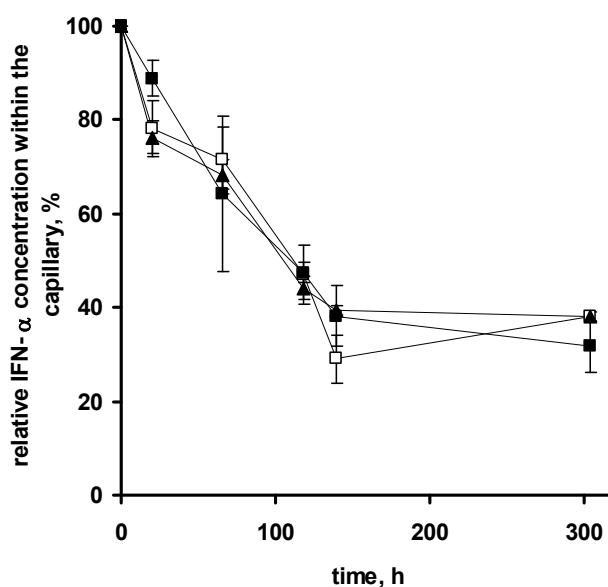


**Figure 21: Decrease of IFN- $\alpha$  concentration within the capillary.**

The diffusion out of a capillary was measured according to the experimental setup shown in Figure 20. Open symbols represent decay of IFN- $\alpha$  concentration in the absence and closed symbols in the presence of PEG (IFN- $\alpha$ /HP- $\beta$ -CD:PEG blends 1:1 ■, IFN- $\alpha$ /HP- $\beta$ -CD:PEG blends 1:2 ▲) (average  $\pm$  SD; n = 3).

In Figure 21 the obtained concentration profiles are presented. In accordance with the first experimental setup no significant differences between PEG-containing and

PEG-free samples were observed. Furthermore, the deviations between three independent vials were lower than those found with the first approach (compare Figure 19 and 21).

Based on the experimental determined protein liberation data the diffusion coefficients of IFN- $\alpha$  in the presence and in the absence of PEG were evaluated by fitting an analytical solution of Fick's second law (see Chapter III.2.16).

As the protein release could only occur via the capillaries' openings, the mathematical analysis could be restricted to one dimension with the following equation [5]:

$$\frac{M_t}{M_\infty} = 1 - \sum_{n=0}^{\infty} \frac{8}{(2 \cdot n + 1)^2 \cdot \pi^2} \cdot \exp\left(-\frac{(2 \cdot n + 1)^2 \cdot \pi^2}{4 \cdot L^2} \cdot D \cdot t\right)$$

{Repetition of equation 13}

where  $M_t$  and  $M_\infty$  represent the absolute cumulative amounts of IFN- $\alpha$  released at time  $t$ , and infinite time, respectively;  $L$  denotes the length of the capillary.

Table 5 summarises the calculated protein diffusivities of IFN- $\alpha$ . It should be mentioned that the modification of the original capillary technique might account for an apparent increase in the diffusion coefficients. As only the liquid within the capillaries contains HP- $\beta$ -CD and optionally PEG there might be an osmotic driven water influx. This effect would contribute the diffusion release of IFN- $\alpha$  resulting in diffusion coefficients higher than those which would be obtained with the original method proposed by Anderson and Saddington [5]. However, the obtained values are in good agreement with literature data reported for proteins with a comparable molecular weight. For instance, for lysozyme, a 14.4 kDa protein, diffusion coefficients between  $0.8\text{-}1.3 \times 10^{-6} \text{ cm}^2/\text{s}$  were reported [83]. Furthermore, comparing the diffusion coefficients obtained in PEG-free and in PEG-containing medium it can be concluded that the presence of different amounts of PEG did not substantially alter the mobility of IFN- $\alpha$  in the release medium.

Therefore, it can be summarised that the presence of PEG within the water-filled pores of the implants did not affect the mobility of dissolved IFN- $\alpha$  during the release from tristearin implants. As explained above, a time-dependent alteration of protein diffusivity in such a context would mainly arise from the effects of PEG on the viscosity of the buffer media.

**Table 5: Diffusion coefficients of IFN- $\alpha$  within phosphate-buffer filled capillaries comprising various amounts of PEG.**

The diffusion coefficients were determined by fitting Equation {13} to the release data shown in Figure 21.

IFN- $\alpha$ /HP- $\beta$ -CD:PEG ratio	D, x 10 <sup>-6</sup> cm <sup>2</sup> /s
1:0	1.8
1:1	1.8
1:2	1.7

However, the drug diffusivity within a controlled release device is not only a function of the composition of the liquid within the pores. In addition, the characteristics of the generated pores might be even more important for the diffusivity of the drug (see Chapter I.5).

It has to be taken into account that the continuously leaching out of the protein itself and of the incorporated hydrophilic excipients (HP- $\beta$ -CD and PEG) progressively increases the porosity of the implants. Such a time-dependent increase in porosity might enhance the diffusivities during release. However, the mathematical solution of Fick's second law of diffusion used to analyse the release data assumed constant diffusion coefficients over the entire release period. This means, a possible explanation for the observed deviations between the calculated release curves and the experimental obtained protein liberation might be a time-dependent increase in the protein mobility due to an increase in matrix porosity.

In order to evaluate if such a scenario is of relevance, the release of PEG and HP- $\beta$ -CD was monitored simultaneously to the protein delivery. If a time-dependent increase in diffusivity by changes of the pore structure is of importance, systematic deviations between the mathematical predicted release data and the experimentally obtained data should be observed also for HP- $\beta$ -CD and PEG.

### 1.3. RELEASE MECHANISMS OF THE INCORPORATED EXCIPIENTS – HP- $\beta$ -CD AND PEG

The PEG concentration was determined using a modification of the ammonium ferrothiocyanate assay described by Nag et al. [159]. The method is based on the partitioning of the ammonium ferrothiocyanate chromophore from the aqueous phase to the chloroform phase in the presence of PEG. The original assay was modified to

allow also the quantification of PEG in the concentration range from 0.025 mg/mL to 2 mg/mL (see Chapter III).

Concentrations of HP- $\beta$ -CD were determined by following the fading of an alkaline phenolphthalein solution spectrophotometrically [11]. The original assay needed to be adapted to allow the determination of small quantities of released cyclodextrin (see Chapter III).

Since the hydrophobic side chains of proteins [105] as well as of PEG [87] are able to interact with the cyclodextrin cavity the released protein or the liberated PEG might interfere with the developed assay. However, it could be shown that the calibration curve obtained with protein- and PEG-free HP- $\beta$ -CD solutions overlapped with that obtained in the presence of IFN- $\alpha$  and PEG (data not shown). Thus, any interference of released IFN- $\alpha$  or PEG with the formation of the phenolphthalein/HP- $\beta$ -CD inclusion complex was negligible in the present study.

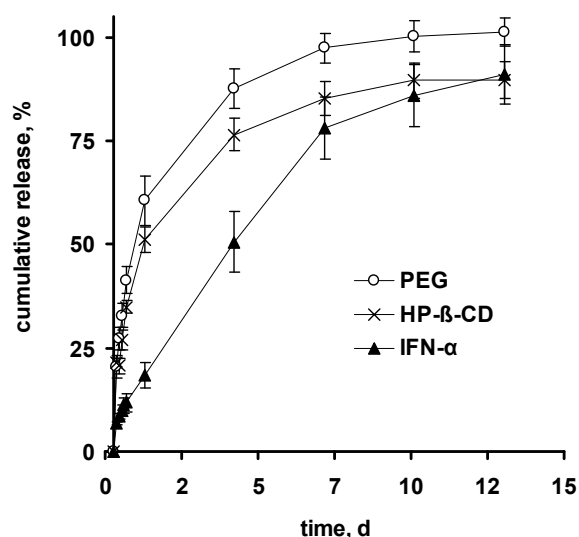


**Figure 22: Release of HP- $\beta$ -CD, PEG, and IFN- $\alpha$  from the tristearin-based implants.**

The implants were loaded with 10 % IFN- $\alpha$  / HP- $\beta$ -CD co-lyophilisate and 10 % (average  $\pm$  SD; n = 3).

Figure 22 compares the in-vitro release kinetics of IFN- $\alpha$ , PEG, and HP- $\beta$ -CD from tristearin implants containing 10 % PEG. Clearly, PEG leaching was fastest, followed by HP- $\beta$ -CD and IFN- $\alpha$  liberation. Importantly, the shape of the release curves of PEG and HP- $\beta$ -CD was different from that of IFN- $\alpha$ : the slope monotonically decreased with time for the two excipients, whereas it remained almost constant during at least 7 d for the protein. This already indicated differences in the underlying mass transport mechanisms. In order to judge the importance of diffusional mass

transport of the release of the excipients, the above described mathematical model (Equation 9, Chapter I.5.3) was fitted to the experimentally determined release rates considering PEG and HP- $\beta$ -CD as the diffusing species.

In Figure 23 the obtained releases profiles of PEG from implants with initial PEG contents of 5 - 20 % as well as the respective fittings are illustrated. Clearly, good agreement between the applied theory and experiments was obtained in all cases ( $R^2 > 0.99$ ), indicating that pure diffusion (in axial and radial direction) with constant diffusion coefficients governed the transport of this excipient. As it can be seen, the release rate significantly increased with higher initial PEG loading.

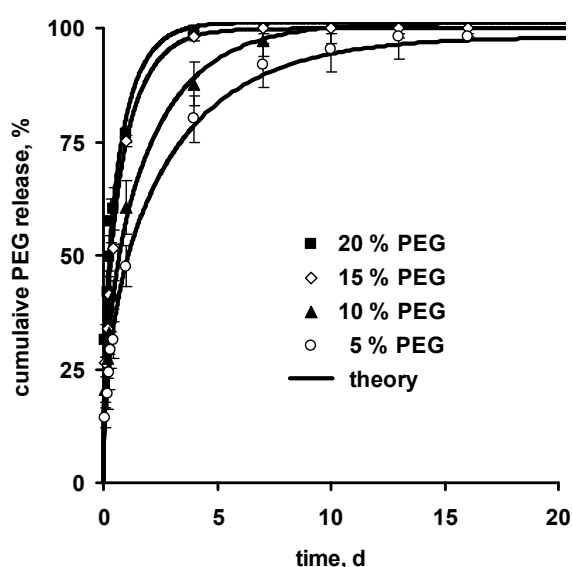


**Figure 23: Effects of the initial PEG loading on the release of PEG.**

Experimental data are shown as symbols and theoretical data based on Equation 9, Chapter I.5.3 as solid lines. All tristearin-based implants were loaded with 10 % IFN- $\alpha$ /HP- $\beta$ -CD co-lyophilisate and the indicated amount of PEG (for experimental results: average  $\pm$  SD;  $n = 3$ ).

Since the used mathematical model described well the experimental release kinetics it was possible to determine the apparent diffusion coefficients of PEG within the lipidic matrices based on theoretical fittings shown in Figure 23. This approach allowed to quantify the impact of the initial PEG loading on the diffusivity of PEG. The dependence of the calculated apparent diffusion coefficients on the PEG content of the matrix is shown in Figure 24. Obviously, the diffusivity significantly increased with higher initial PEG loading and an exponential relationship between the diffusion coefficient  $D$ , and the initial PEG content could be established ( $R^2 = 0.99$ , equation indicated in Figure 24).

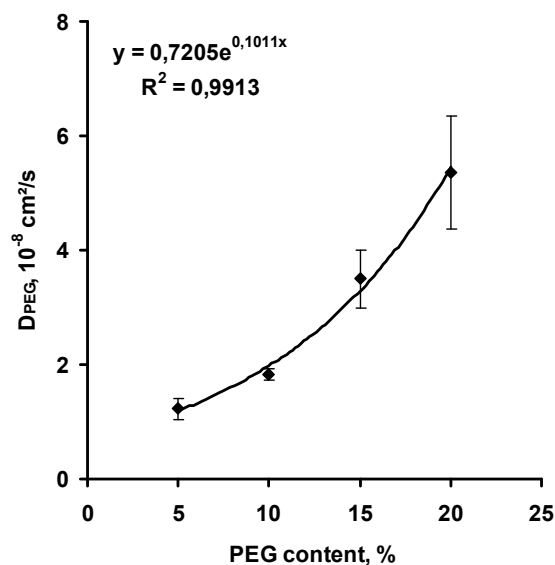


**Figure 24: Effects of the initial PEG loading on the apparent diffusion coefficient of PEG within the tristearin matrix.**

The release patterns of HP- $\beta$ -CD as well as the respective fittings based on Equation {9} (Chapter I.5.3) are illustrated in Figure 25 for various initial PEG contents. Like PEG release (and in contrast to IFN- $\alpha$  release), pure diffusion with constant diffusivities was the dominating mass transport mechanism of HP-  $\beta$ -CD. This was indicated by the good agreement between theory and experiments ( $R^2 > 0.98$ ). In accordance with the liberation of PEG from matrices with various PEG loadings, the release rates increased with rising PEG contents.

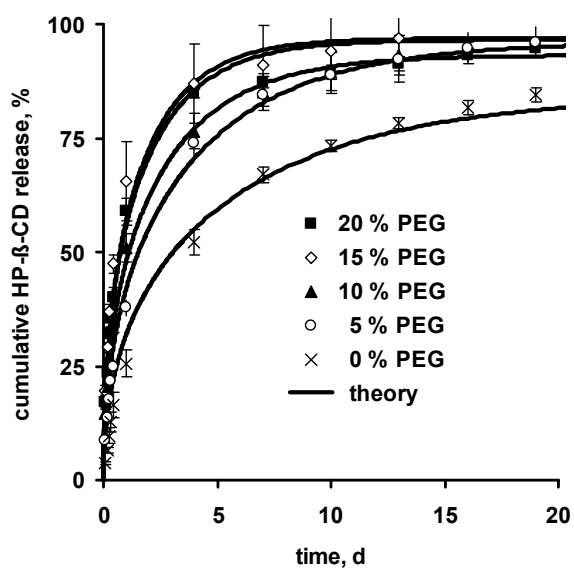


**Figure 25: Effects of the initial PEG loading on the release of HP- $\beta$ -CD.**

Experimental data are shown as symbols and theoretical data based on Equation 9, Chapter I.5.3 as solid lines. All tristearin-based implants were loaded with 10 % IFN- $\alpha$ /HP- $\beta$ -CD lyophilisate and the indicated amount of PEG (for experimental results: average  $\pm$  SD;  $n = 3$ ).

Based on the theoretical fittings shown in Figure 25, the apparent diffusion coefficient of HP- $\beta$ -CD in the lipidic matrices was calculated. The obtained D values are plotted versus the initial PEG loading of the matrix in Figure 26. Clearly, a higher PEG content of the matrix accounted for an increase in the diffusivity of HP- $\beta$ -CD, which is in well accordance with the results obtained for PEG itself (Figure 24). Furthermore, similar to the diffusion coefficient of PEG an exponential relationship between the diffusivity of HP- $\beta$ -CD and the initial PEG content could be established ( $R^2 = 0.98$ ).

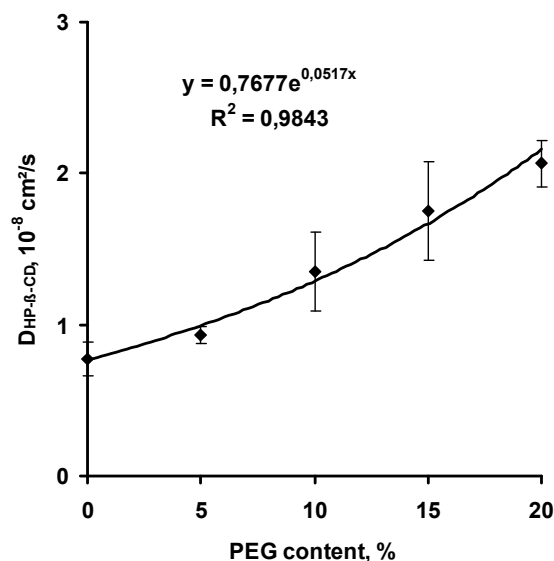


**Figure 26: Effects of the initial PEG loading on the apparent diffusion coefficient of HP- $\beta$ -CD within the tristearin matrix.**

The observation that the diffusivities of both excipients increased with rising initial PEG loading is consistent with the SEM pictures of tristearin implants after in-vitro incubation (Figure 15). Enhanced levels of initial PEG amounts clearly resulted in a more pronounced pore formation. So, less restricted pore dimensions accounted for increased mobility of the excipients within the lipidic matrix. As a result the delivery rates of both excipients from matrices comprising higher initial PEG loadings were significantly accelerated.

Since release kinetics of PEG as well as of HP- $\beta$ -CD were described well by a solution of Fick's second law of diffusion assuming constant diffusivities during release, time-dependent variations of the diffusivity during the release period were not of importance for the tristearin implants studied here. This result clearly contradicts the assumption that the observed deviations of IFN- $\alpha$  release from purely diffusion-controlled mass transport from matrices containing PEG can be attributed to the time-dependent increase in the porosity of the matrices.

#### 1.4. SUMMARY AND CONCLUSION

The admixing of PEG to tristearin implants was shown as an efficient tool to modify the protein release kinetics. In addition to an increase of the totally released protein the shape of the release curves was altered. The release rates monotonically decreased with time for PEG-free implants, whereas PEG-comprising implants revealed nearly constant liberation rates over prolonged periods of time. Interestingly, compared to PEG-free matrices the admixing of PEG to the matrix formulation resulted in reduced initial burst effects.

In order to understand the underlying drug release mechanisms an adequate mathematical solution of Fick's second law of diffusion was fitted to the release data. The protein release from PEG-free matrices was found to be purely diffusion controlled. In contrast, the addition of 5 to 20 % PEG to the formulations significantly altered the underlying mass transport mechanisms. Already the addition of only 5 % PEG resulted in systematic deviations between the experimental results and the purely diffusion-based mathematical model.

Both effects of PEG - the reduced burst release as well as the significant deviations from purely diffusion controlled protein release – are very astonishing considering the well – known role of PEG as pore forming agent. The addition of porogens generally facilitates the creation of interconnected pore networks and, thus, leads to increased total amounts of drug released (see Chapter 1.5). However, the amplified pore creation reduces the geometrical hindrance of the pore networks, what accounts for high burst effects and elevated release rates [40, 108, 113, 138, 174].

One possible reason for the observed systematic deviations between the applied mathematical model and the experimentally measured IFN- $\alpha$  release kinetics may be that the simultaneous dissolution and diffusion of PEG within the water-filled pores of the implants affects the mobility of the protein. In order to evaluate the relevance of this hypothesis, the diffusion coefficients of IFN- $\alpha$  in the release medium in the presence and the absence of PEG were determined using a modification of the open capillary method described by Anderson and Saddington [5]. However, the presence of different amounts of PEG did not substantially alter the diffusivity of IFN- $\alpha$  in the release medium.

Furthermore, the liberation rates of PEG and the co-lyophilisation agent HP- $\beta$ -CD were determined. Unlike protein release, the release of PEG and HP- $\beta$ -CD from the implants remained purely diffusion controlled, irrespective of the amount of added

PEG. Thus, different mass transport mechanisms govern the release of the drug and the excipients out of the lipidic implants.

The fact that the release of both PEG and HP- $\beta$ -CD was purely diffusion-controlled (with constant diffusivities), irrespective of the initial PEG content of the implants, is an important information: it renders the hypothesis very unlikely that the deviations of IFN- $\alpha$  release from purely diffusion-controlled mass transport can be attributed to the time-dependent increase in the porosity of the matrices. Such a time-dependent increase in matrix porosity could result in a significant time-dependent increase in protein mobility. However, in this case a similar effect should have been observed also with PEG and HP- $\beta$ -CD.

Screening the literature aside from the studies describing the impact of PEG as porogen, a few alternative features of PEG used within controlled release systems are outlined. For PLGA-based matrices, for instance, the accelerated pore formation enhanced the diffusion of acid species generated during polymer degradation. Consequently, the acidification within the devices became less pronounced and the tendency of protein aggregation is minimised [108]. Further positive effects of PEG 400 addition have been shown, when preparing PLGA microparticles by solvent extraction/evaporation methods. The major cause of protein denaturation occurring during this type of preparation techniques was the exposure of the macromolecules to the aqueous-organic interfaces. As PEG 400 adsorbed to these interfaces too, it competed with the proteins and, thus, protects them from degradation [34, 167].

It was also suggested that the amphiphilic character of PEG 6000 reduced the solubility of PLGA in methylene chloride. During the preparation of microspheres, therefore, an accelerated solidification of PLGA was observed, which in turn decreased the porosity and the initial burst release from the obtained microspheres [260].

The group of Morita employed phase separation during the lyophilisation of an aqueous protein-PEG mixture to generate spherical fine protein microparticles [155]. The obtained BSA particles were incorporated in PLGA microspheres using the “polymer-allow” technique. This methodology was based on the selective localization of solid BSA particles in a phase separated-structure between PLGA and PLA in methylene chloride. Due to the resulting reservoir type system with a outer drug-free PLA-shell the produced microspheres revealed a low burst effect (<10 %) despite the presence of PEG [154].

Although the latter two studies disclosed a low burst effect for PEG-comprising controlled release systems the provided explanations can obviously not be adapted to the lipidic implant systems studied here.

## 2. SOLUBILITY STUDIES AND INVESTIGATIONS ON THE PROTEIN STABILITY

In biotechnology the ability of PEG to reversibly precipitate/crystallise proteins has been widely used for protein separation and purification [149, 165]. However, these effects have so far not been considered in the context of controlled release.

Therefore, the solubility of IFN- $\alpha$  was experimentally determined in differently concentrated aqueous PEG solutions. Solutions of IFN- $\alpha$  with an initial protein concentration of 4.8 mg/mL were diluted in a one to one ratio with highly concentrated PEG solutions (2-40 % (wt/vol)). Immediately after mixing both solutions, a macroscopic visible precipitation of IFN- $\alpha$  occurred when the final PEG concentration exceeded 3 %. After equilibrating the samples for 2 hours at 37 °C and 40 rpm the protein concentration in the supernatant was determined. As illustrated in Figure 27, the soluble fraction of IFN- $\alpha$  decreases non-linearly with increasing PEG concentration. Interestingly, already 10 % PEG resulted in an almost negligible protein solubility (0.02 mg/mL).

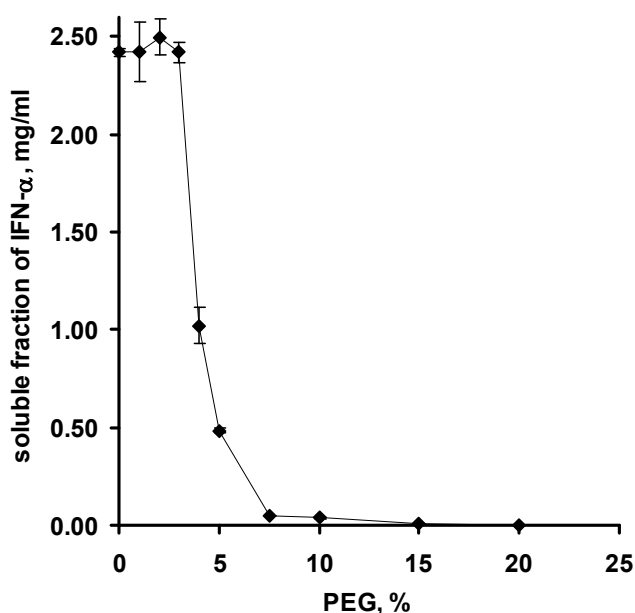
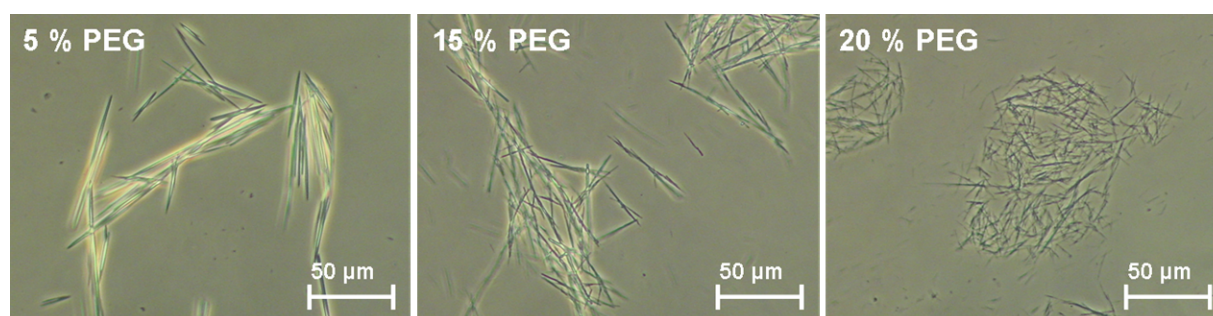


Figure 27: Effects of the PEG concentration on the apparent solubility of IFN- $\alpha$  at 37 °C in phosphate buffer pH 7.4 (average  $\pm$  SD; n = 3).

The tremendous impact of PEG on protein solubility might offer an explanation for the effects of PEG on the protein release from lipidic matrix systems. Due to the small pore volume within the lipid matrices the dissolution of the incorporated PEG should first result in a highly concentrated PEG solution. Therefore, protein solubility within the device might be reduced, resulting in a more sustained protein delivery from PEG containing implants compared to PEG-free systems.



**Figure 28: Morphology of the precipitated protein observed by light microscopy.**

The final PEG concentration of the solution is indicated in the figure.

Figure 28 visualises the appearance of the obtained solid material upon precipitation of IFN- $\alpha$  by the addition of PEG. The ordered, needle-like structures indicated a crystallisation of IFN- $\alpha$  in the presence of PEG. This was an important information considering protein stability, since the crystalline form may be more stable than the corresponding soluble or amorphous material [203]. It was further apparent from Figure 28 that increasing PEG concentrations led to smaller needles. This was in good agreement with theory: with increasing the nucleation rate due to enhanced precipitant concentrations the amount of protein available per crystal nucleus is reduced, leading to smaller crystals [67].

## 2.1. PROTEIN STABILITY AFTER PRECIPITATION AND REDISSOLUTION

Generally, the precipitation of proteins by PEG has been explained on the basis of volume exclusion effects. Mainly due to sterical hindrance, proteins are excluded from the solvent space that is occupied by the linear PEG chains. Hence, the protein is locally concentrated until the solubility is exceeded and precipitation and/or crystallization occurs [149].

From a thermodynamic point of view the preferential exclusion of PEG from the protein surface (preferential hydration) leads to an increase in the chemical potential of the protein. This thermodynamically unfavourable situation can be relieved by protein precipitation (salting-out), which reduces the total protein-solvent interface [7, 9, 204].

The potential effects of PEG on protein stability are more complicated. Therefore, in brief the general mechanism of protein stabilisation by preferential exclusion will be outlined. According to Timasheff co-solvents that are preferentially excluded from the protein surface can be classified into two distinct categories: (1) those that are totally independent of the chemical nature of the protein surface and (2) those for which the

particular chemical features of the protein surface play a role. Co-solvents of the first category are either excluded due to sterical hindrance or, due to an increase in surface tension of water by the co-solvent. The predominant driving forces of the second class are the solvophobic effect (e.g. polyols, glycerol) and electrostatic repulsions between the charged protein surface and the co-solvent (2-methyl-2,4-pentanediol, MPD) [226, 227].

Irrespective of its category a preferentially excluded co-solvent will reduce protein solubility due to an increase in the chemical potential of a protein. However, the effects on protein stability of preferentially excluded co-solvents can be very different. Whereas co-solvents of the first class are always stabilising, compounds of the second category may also be destabilising. Importantly, such destabilising effects have been reported for PEG too [14, 226, 227].

PEGs are hydrophobic in nature and have an affinity for non-polar residues on proteins. In the native state most of these non-polar residues are hidden inside the folded protein structure inaccessible to PEG. As a result the interactions of PEG with native proteins are determined predominately by the sterical exclusion. However, as the protein unfolds, hydrophobic regions of the protein become exposed. Consequently, PEG will favourably interact with these newly exposed non-polar residues, thereby stabilising the unfolded structures. This explains why PEG has been found to promote protein unfolding, especially at high temperatures [68, 136].

The extent of thermal destabilisation strongly depends on the molecular weight. For PEG 10000 sterical exclusion being the major factor, determining the interaction to human serum albumin (HSA) even during thermal denaturation. Thus, thermal stability increases. In contrast, the low molecular weight PEGs 1000 and 4000 were found to interact favourably with hydrophobic side chains exposed during thermal unfolding. This was manifested in lowering the thermal transition temperature ( $T_m$ ) [68].

The opposite was reported by Remmele.  $T_m$  of interleukin-1 receptor (IL-1R) was shifted to lower values when increasing the molecular weight of PEG ( $T_{mPEG\ 300} > T_{mPEG\ 1000} > T_{mPEG\ 3350}$ ) [181]. Presumably, in the latter case the increased hydrophobicity of the higher molecular weight PEGs overcompensates the impact of sterical exclusion.

On the other hand, Cleland et al. revealed that the presence of PEGs significantly enhanced the recovery of active protein during refolding after chemical denaturation.

It was suggested that PEG acted like chaperons - i.e. the binding to specific segments of the protein during refolding prevented intermolecular interactions (i.e. aggregation) [42, 44].

Generally, the precipitation of proteins by PEG is considered to inhere only little tendency for denaturation [104]. Thus, crystals grown from PEG-solutions are widely used to solve protein structures [149]. However, recently Sharma and Kalonia revealed irreversible alterations of the protein structure for IFN- $\alpha$  upon precipitation by high molecular weight PEGs. Attenuated total reflectance Fourier transform infrared spectroscopy (ATR-FTIR) of precipitated IFN- $\alpha$  featured slight changes in the secondary structure of the protein. After re-dissolution these changes were observed to be reversible, when IFN- $\alpha$  was precipitated by PEG 1450. However, when PEG 8000 was used, also after re-dissolution far and near UV circular dichroism (CD) indicated alterations in the secondary and tertiary structure [201].

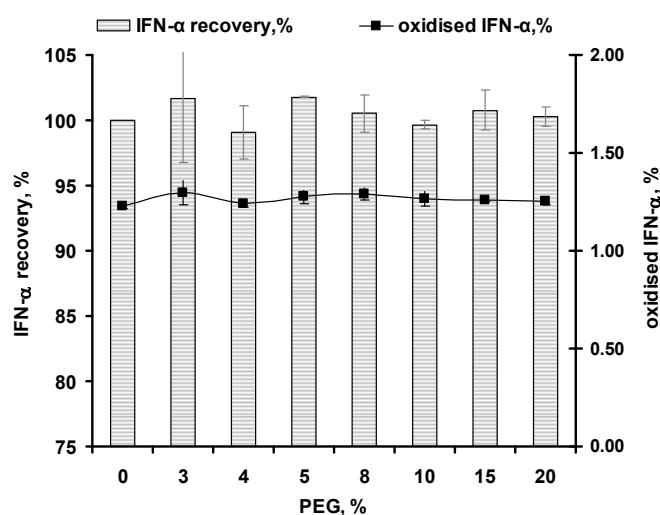


**Figure 29: Recovery and chemical protein integrity after precipitation and re-dissolution.**

After precipitation of IFN- $\alpha$  with the indicated PEG concentration the samples were diluted and analysed by RP-HPLC (average  $\pm$  SD; n = 3).

In order to investigate the stability of IFN- $\alpha$  after precipitation with PEG 6000, dispersions of protein precipitates (in the presence of 3 to 20 % (wt/vol) PEG) were diluted with buffer to PEG concentrations below 0.2 %. The protein precipitates instantaneously dissolved in an excess of buffer and the re-dissolved protein concentration was determined by RP-HPLC. As illustrated in Figure 29, a virtually complete protein recovery could be proven, irrespective of the PEG concentration used for precipitation (4-20 %). The fraction of oxidised IFN- $\alpha$  was comparable to that present in protein bulk solution and thus could not be ascribed to the precipitation

and re-dissolution process. Importantly, apart from this marginal amount of oxidised IFN- $\alpha$  no further degradation products were detected.

In addition, the reconstituted precipitates were analysed by SDS-PAGE to exclude the formation of protein aggregates and fragments associated to a precipitation. Obviously, irrespective of the applied PEG amount, only monomeric protein was determined after silver staining (Figure 30).

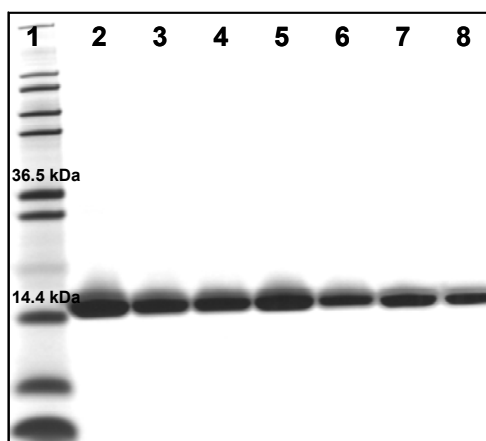


**Figure 30: SDS-PAGE of precipitated and re-constituted IFN- $\alpha$ .**

Lane 1: Molecular weight standard, lane 2: IFN- $\alpha$  standard, lanes 3-8: re-constituted IFN- $\alpha$  precipitates (precipitated in phosphate buffer pH 7.4 containing 4, 5, 7.5, 10, 15 and 20 % PEG).

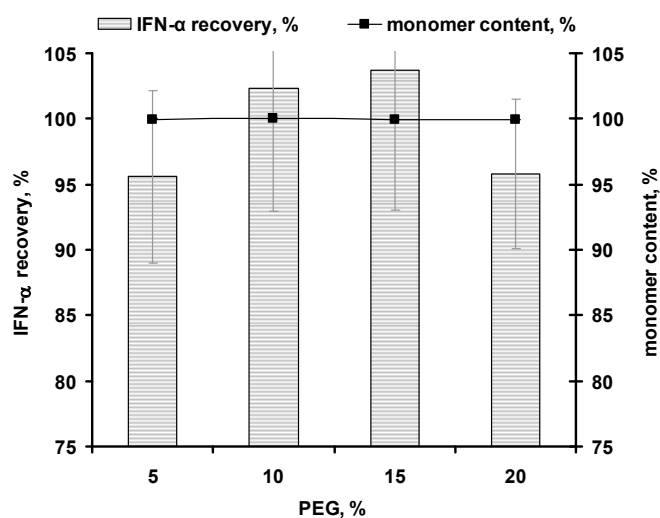


**Figure 31: Recovery and protein integrity after precipitation and re-dissolution investigated by SE-HPLC.**

After precipitation of IFN- $\alpha$  with the indicated PEG concentration, the supernatant was removed and the obtained precipitates were dissolved in phosphate buffer pH 7.4 (average  $\pm$  SD;  $n = 3$ ).

However, the presence of SDS may dissolve non-covalent aggregates during sample preparation [251]. To overcome this limitation size-exclusion chromatography was carried out. Unfortunately, even low amounts of PEG interfere with the separation of dimeric IFN- $\alpha$  (data not shown). In order to remove PEG as far as possible, the

dispersion of protein precipitates was centrifuged. After removing the supernatant, the obtained protein precipitates were diluted with buffer. Since the removal of the supernatant inheres the risk of losing a certain amount of protein this procedure cannot provide precise protein recoveries as the simple dilution of the precipitated samples used for RP-HPLC. Nevertheless, the results mirrored that at least 95 % of the protein were recovered (Figure 31). Importantly, the recovered protein comprised only monomeric IFN- $\alpha$ . Irrespective of the PEG concentration used for precipitation no formation of soluble aggregates was detectable by SE-HPLC analysis. The marginal amount of approximately 0.1 % dimer fraction was already present in the protein bulk material prior to precipitation.

For the investigation of the effects of precipitation and re-dissolution on the secondary structure of IFN- $\alpha$ , the FTIR spectra in the amid I region of reconstituted precipitates were compared to that of native IFN- $\alpha$ . As it can be seen in Figure 32, the spectra of native IFN- $\alpha$  revealed an intense peak at  $1654\text{ cm}^{-1}$ , the typical feature of an alpha helical protein [60]. Importantly, the vector-normalised FTIR spectra as well as the corresponding second derivatives of reconstituted protein precipitates were almost congruent with that of native IFN- $\alpha$ , irrespective of the PEG concentration used for precipitation. Therefore, the secondary structure of IFN- $\alpha$  remained unaffected upon precipitation and re-dissolution.

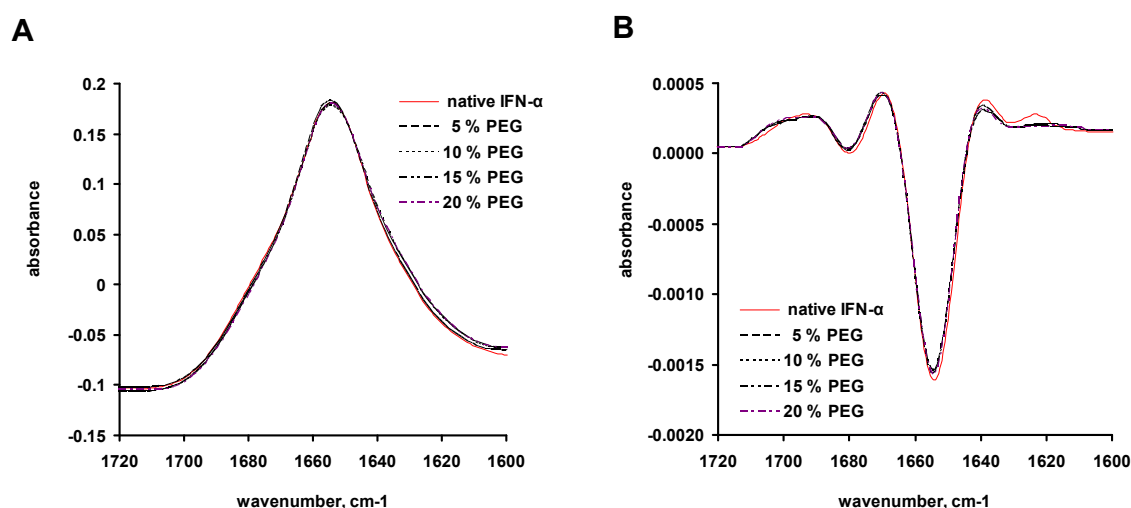


**Figure 32: Effects of precipitation and re-dissolution of IFN- $\alpha$  in phosphate buffer pH 7.4 on the secondary protein structure.**

(A) Background corrected and vector-normalised amid I FTIR-spectra; (B) Second-derivative amid I FTIR-spectra. The PEG concentrations at which IFN- $\alpha$  precipitation was performed are indicated.

Finally, the potential impact of precipitation and re-dissolution on the tertiary structure was probed with the intrinsic protein fluorescence spectroscopy. IFN- $\alpha$  contains two tryptophan (Trp) residues [202]. Trp residues of a protein can be selectively excited

at 295 nm. Depending on the microenvironment of Trp the emission spectra revealed a maximum between 302 nm and 350 nm. Emission at lower wavelengths is characteristic for Trp buried entirely in the hydrophobic environment, whereas an emission maximum at longer wavelengths indicates Trp residues on the protein surface. Due to protein unfolding hydrophobic amino residues would become more solvent exposed and, therefore, unfolding often results in a decrease of the fluorescence quantum yield and in a red shift [182, 250].

Figure 33 shows the Trp fluorescence emission scans of IFN- $\alpha$  in PBS buffer at a pH of 7.4. The observed  $\lambda_{\text{max}}$  of Trp emission at 336 nm indicated that the two Trps of IFN- $\alpha$  were partially buried in the hydrophobic core of the protein [202]. Importantly,  $\lambda_{\text{max}}$  of IFN- $\alpha$  after precipitation and re-dissolution was determined at 336 nm and the obtained fluorescence scans were almost identical with those of native IFN- $\alpha$ .

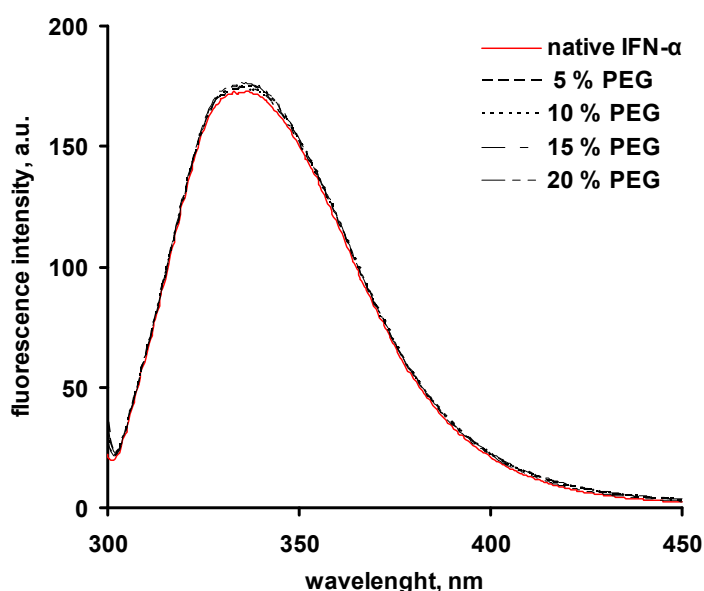


Figure 33: Trp fluorescence emission spectra of native IFN- $\alpha$  and after precipitation and re-dissolution with various amounts of PEG (as indicated in the figure).

## 2.2. SUMMARY AND CONCLUSION

The presence of PEG was shown to have a tremendous effect on IFN- $\alpha$  solubility: a concentration of 3 % PEG was already sufficient to cause protein precipitation. Importantly, precipitation was completely reversible. After re-dissolution of IFN- $\alpha$  the protein was completely recovered in its monomeric form without structural alterations detectable by SE- and RP-HPLC. Furthermore, FTIR- and fluorescence spectroscopy indicated a preservation of the native secondary and tertiary structure after precipitation and re-dissolution.

As the release of PEG occurred delayed from tristearin implants, it was hypothesised that within the water-filled pores of the tristearin implant a highly concentrated PEG solution might be generated in the first period of the release process. Taking into account the dramatic effect of PEG on the solubility of IFN- $\alpha$ , reduced protein solubility or even a reversible precipitation of IFN- $\alpha$  within PEG-containing matrices is highly likely. Not until PEG is completely leached out of the matrix, only a minor, non-precipitated fraction of the incorporated protein is available for diffusion. Thus, at an early stage of release the protein liberation from PEG-comprising implants is hindered. Furthermore, the creation of water-filled pores might be reduced due to the un-dissolved protein. Both effects could explain the reduced burst of protein release from PEG-containing implants in comparison to PEG-free implants.

In the case of purely diffusion controlled drug release, the time-dependent prolongation of the diffusion ways results in monotonically decreasing release rates. This was shown to be true for PEG-free implants. In contrast, in PEG-containing devices the solubility of IFN- $\alpha$  within the water-filled pores increases continuously due to the leaching out of PEG of the system. Thus, the amount of protein available for diffusion increases with time. Consequently, the increasing length of the diffusion pathways is partly compensated, resulting in about constant IFN- $\alpha$  release rates over prolonged periods of time. Such considerations would explain the systematic deviations between the presented mathematical model (assuming unlimited protein solubility and constant diffusion coefficients) and the experimentally determined IFN- $\alpha$  release kinetics from PEG-containing implants.

Although in-situ precipitation would explain well the effects of PEG on the release behaviour of IFN- $\alpha$ , such release controlling mechanisms by PEG are not described in literature. Protein precipitation/crystallisation in general has so far only been used to provide beneficial protein stabilisation during the fabrication process of controlled release devices. For example, the formation of an insoluble complex of rhGH and zinc enables the encapsulation and slow release of unaltered rhGH from PLGA microspheres [10, 109]. Furthermore, van de Wetering used the precipitation of rhGH by zinc or by PEG to protect the protein from reaction with gel precursors during the preparation of chemically cross-linked hydrogels [232]. In addition, the reversible precipitation of  $\alpha$ -chymotrypsin and lactate dehydrogenase in the presence of poloxamer 407 has been used to increase the protein loading of in-situ forming poloxamer gels [217].

However, in the present project IFN- $\alpha$ , PEG, and the lipid were simply mixed as solid powders and subsequently compressed to implants. Thus, in contrast to the studies mentioned above, precipitation will only occur in-situ during release.

In order to evaluate if in-situ reduced protein solubility or a protein precipitation within PEG-containing matrices is relevant, the following chapter reports on various model experiments carried out to prove the presented hypothesis.

### 3. POLY(ETHYLENE GLYCOL) ACTING AS IN-SITU PRECIPITATION AGENT – PROOF OF CONCEPT

Together with the release data of PEG the time-dependent increase in matrix porosity should provide information on the PEG concentrations generated within the implant pores. In order to determine the kinetics of pore formation three independent implants loaded with 20 % PEG and 10 % IFN- $\alpha$ /HP- $\beta$ -CD co-lyophilisate were removed from the incubation buffer at predetermined points of time. The implants were wipe-dried with an adsorbent paper to remove adhesive water and were then weighed. Subsequently, the implants were vacuum dried to constant weight. Finally, the density of the devices was determined by means of helium pycnometry. Based on these values the porosity and the absolute pore volume were calculated. Together with the release rates of PEG, presented in Chapter IV.1, the theoretical PEG concentrations within the implant pores could be determined.

After manufacturing the lipidic implants revealed a low porosity of approximately 2 %. As illustrated in Figure 34, immediately after immersion into the release media the porosity increased until the fourth day of incubation, which was followed by a plateau of approximately 25 %.

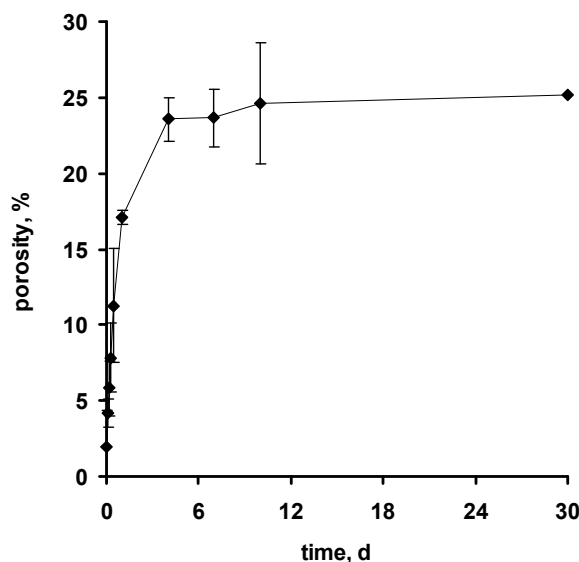


**Figure 34: Time-dependent increase in matrix porosity.**

After incubation in the release medium the implants were dried and the porosity was determined by means of a helium pycnometer. The implants were loaded with 20 % PEG and 10 % IFN- $\alpha$ /HP- $\beta$ -CD co-lyophilisate (average  $\pm$  SD;  $n = 3$ ).

Assuming that the pores were completely filled with release medium, the actual PEG concentrations within the implant pores can be calculated at each time point using the determined pore volume and the amount of PEG remaining in the implant

(Table 6). The small pore volume combined with the sustained release of PEG resulted in quite high PEG concentrations within the implant pores.

**Table 6: Calculated PEG concentrations within the implant pores.**

time, d	porosity, %	conc. dissolved PEG, % (wt/vol)
0	1.91	0.00
0.08	4.21	377.61
0.17	5.81	230.69
0.25	7.83	148.07
0.5	11.27	86.89
1	17.09	53.67
4	23.55	22.94
7	23.65	0.53
10	24.61	0.00
30	25.20	0.00

However, the presented calculation of the PEG concentrations is somewhat speculative, as it is based on the assumption that the total amount of incorporated PEG immediately dissolves after incubation in the release buffer. The real conditions may differ as it is likely that not the entire hydrophobic matrix is wetted immediately after the incubation start. In fact water will first dissolve PEG located in the outermost implant region. Then, at a later stage of release the entire matrix is percolated by the release medium and the overall amount of PEG is dissolved (Figure 35). This scenario was confirmed by the experimentally determined water uptake during in-vitro incubation (Figure 36).

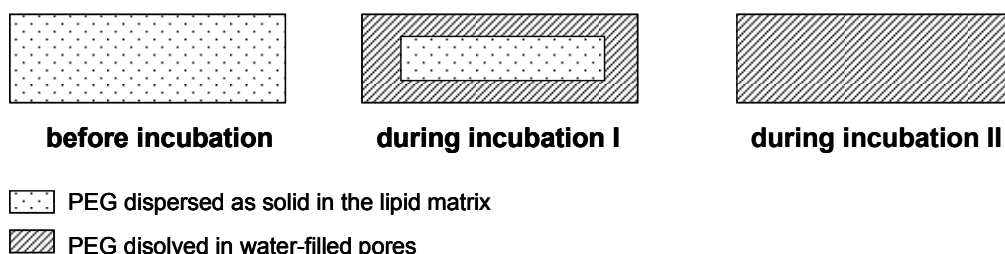


**Figure 35: Migration of the dissolution front during release.**

Before incubation PEG is dispersed as solid in the lipidic matrix (left). At an early stage (middle) of release water penetrates in the outermost areas of the implant and dissolves PEG. Finally, the lipidic matrix is completely wetted and the entire PEG is dissolved within the water-filled pores (right).

As the matrix took up water until the fourth day of incubation (Figure 36), the concentrations of PEG calculated before are overestimating the real PEG

concentrations within the water-filled pores. However, it is highly conceivable that at the fourth day of incubation the matrix is completely wetted. Therefore, it becomes realistic that a PEG solution with concentrations of approximately 20 % PEG is generated within the implant pores (Table 6). Taking into account the effect of PEG on the solubility of IFN- $\alpha$  (Figure 27), reduced protein solubility or even a reversible precipitation of IFN- $\alpha$  within these PEG-containing matrices can be assumed until day four of incubation.

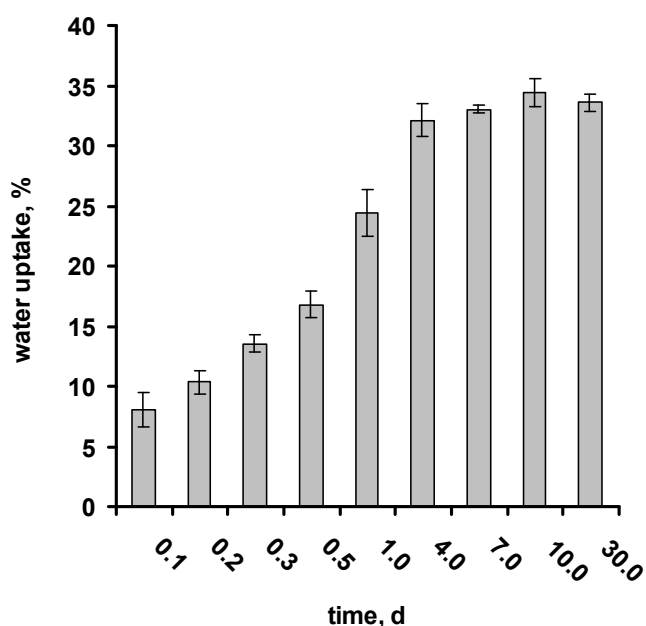


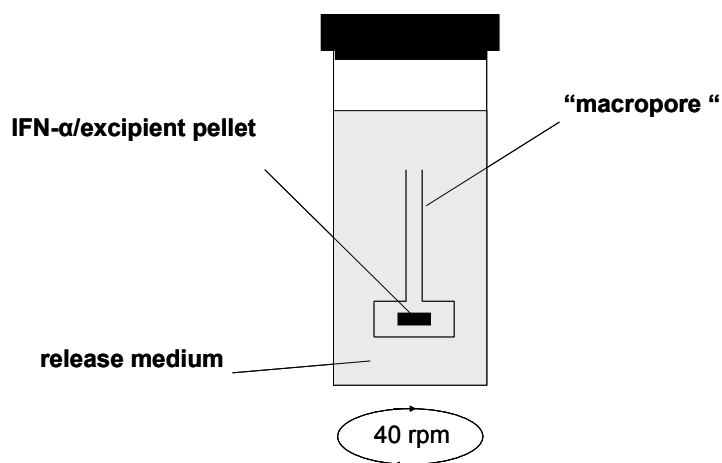
**Figure 36: Time-dependent water-uptake of tristearin implants prepared by compression.** The implants were loaded with 20 % PEG and 10 % IFN- $\alpha$ /HP- $\beta$ -CD co-lyophilisate. The water uptake was determined by weighing wet and dry implants (see Chapter III) (average  $\pm$  SD; n = 3).

In order to cope with the remaining uncertainties of the aforementioned method, and to prove the postulated hypothesis of a reversible precipitation and reduced solubility of IFN- $\alpha$  within PEG-containing matrices, further model experiments were carried out.

### 3.1. "MACROPORE MODEL"

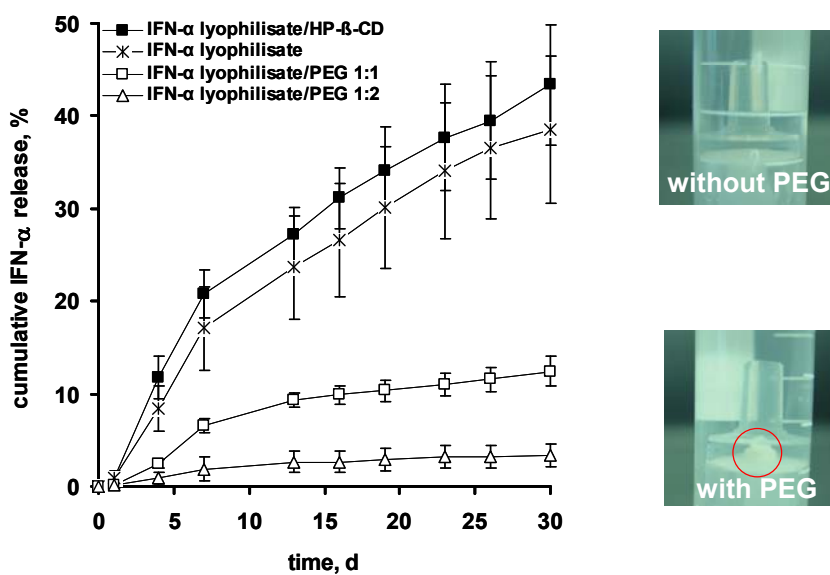
In order to determine whether the reduced protein solubility or even a reversible precipitation within the lipidic matrix could play a role for the IFN- $\alpha$  release, a model device simulating the conditions in the water-filled pores within the implant was developed. The idea was to elucidate the relevance of protein dissolution versus protein diffusion in the presence of PEG by mimicking the inner content of a pore filled with IFN- $\alpha$  and the water-soluble excipients. For that purpose a small volume container connected with a capillary was intended to imitate a drug reservoir with an

associated pore within the controlled release system. The device (schematically illustrated in Figure 37) was named “macropore model”. The container was filled with compressed lyophilised protein pellets or with compressed lyophilised protein/PEG pellets. In the latter case, lyophilisate/PEG ratios of 1:1 or 1:2 (corresponding to implants containing 10 % PEG or 20 % PEG, respectively) were studied. In addition, pellets containing HP- $\beta$ -CD instead of PEG were placed in the cylindrical chamber of the “macropore model” (in contrast to PEG, HP- $\beta$ -CD does not cause protein precipitation).



**Figure 37: Schematical presentation of the experimental setup of the “macropore model”.**

Protein, protein/PEG, or protein/HP- $\beta$ -CD pellets were placed into a cylindrical chamber with only one opening into a cylindrical capillary. This device was placed into a plastic flask filled with phosphate buffer pH 7.4. The flask was agitated at 40 rpm and kept at 37 °C.



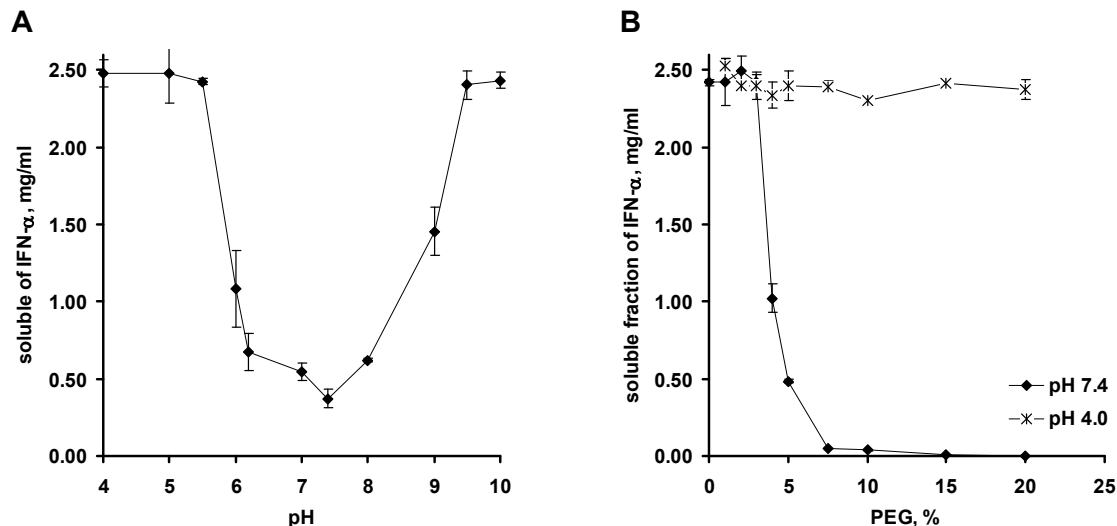
**Figure 38: IFN- $\alpha$  release from pellets consisting of IFN- $\alpha$  lyophilisates, IFN- $\alpha$  lyophilisates:PEG blends, and IFN- $\alpha$  lyophilisates:HP- $\beta$ -CD blends into phosphate buffer pH 7.4 measured using the “macropore model” (schematically illustrated in Figure 37) (average  $\pm$  SD; n = 3).**

Figure 38 demonstrates that the release of IFN- $\alpha$  from PEG-free devices was almost ten times faster than protein delivery from systems containing pellets with a lyophilisate/PEG ratio of 1:2. Interestingly, when PEG was present the pellets did not disintegrate and remained visible during the entire release period. This indicated that within the “macropores” highly concentrated PEG solutions were created and, hence, the dissolution of the protein/excipient pellets was hindered. Therefore, the dissolution step can be considered as one of the major rate limiting factors for protein release in the presence of PEG.

### 3.2. PH-DEPENDENCE OF SOLUBILITY AND RELEASE

Further insight into the significance of reduced protein solubility and reversible precipitation within PEG-containing tristearin implants was obtained by studying the pH-dependence of protein solubility and release.

As it can be seen in Figure 39 A, the solubility of IFN- $\alpha$  in phosphate buffer containing 5 % PEG was strongly affected by the pH: a minimum was observed in the pH range 6-9. At lower or higher pH values, no protein precipitation was notified under the given experimental conditions.



**Figure 39: Effects of the pH of the phosphate buffer solution on the apparent solubility of IFN- $\alpha$  at 37 °C**

(A) Solubility in the presence of 5 % PEG (B) Solubility at pH 7.4 and at pH 4.0 in the presence of different concentrated PEG solutions (average  $\pm$  SD; n = 3).

Therefore, a pH change of the release buffer offers the possibility to “switch off” the in-situ precipitation. Since several authors reported good IFN- $\alpha$  stability at low pH values [62, 142], pH 4.0 was chosen to investigate the effects of higher PEG

concentrations on protein solubility. Importantly, even PEG concentration up to 20 % did not induce protein precipitation under this experimental setup (Figure 39 B).

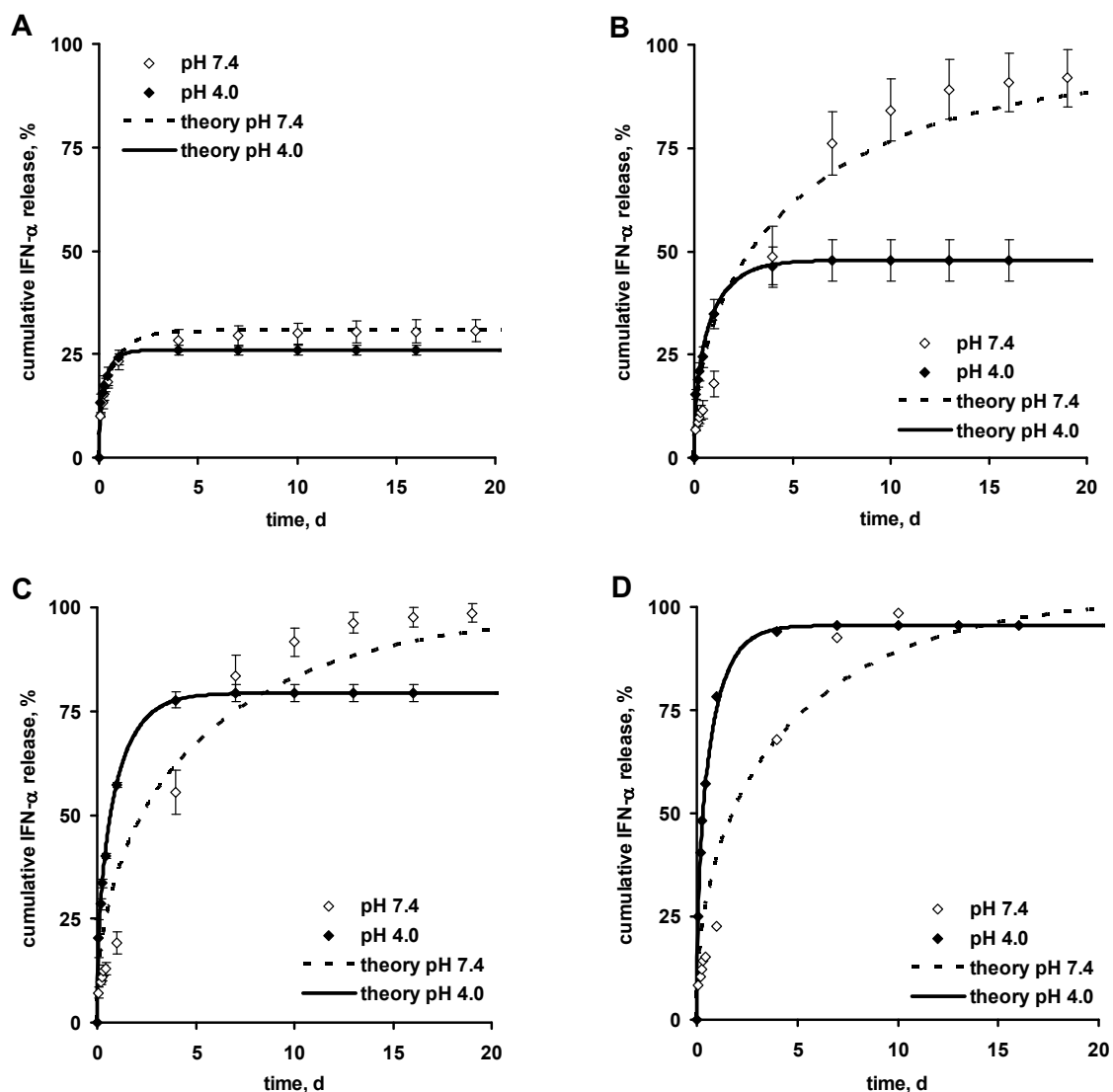


**Figure 40: Effects of the pH of the phosphate buffer solution on IFN- $\alpha$  release from tristearin-based implants.**

Matrices were loaded with 10 % IFN- $\alpha$ /HP- $\beta$ -CD lyophilisate and 0 % PEG (A), 10 % PEG (B), 15 % PEG (C) and 20 % PEG (D). The release was studied either in phosphate buffer pH 7.4 [open symbols: experimental values (average  $\pm$  SD;  $n = 3$ ), dashed curves: theory (Equation 9)] or in phosphate buffer pH 4.0 [closed symbols: experimental values (average  $\pm$  SD;  $n = 3$ ), solid curves: theory (Equation 9)].

Figure 40 compares the release kinetics of IFN- $\alpha$  from tristearin-based implants in phosphate buffer pH 7.4 and pH 4.0. In the case of PEG-free implants, the pH had no effect on the resulting in-vitro release kinetics (Figure 40 A). Protein release levelled off at approximately 30 % after 4 d, irrespective of the pH of the medium. In contrast, the pH was found to affect fundamentally IFN- $\alpha$  release patterns from lipidic implants containing PEG.

As shown in Figure 40 B-D, the lack of protein precipitation at pH 4.0 resulted in significantly accelerated protein release rates with a high burst effect. For example at pH 4.0, implants loaded with 20 % PEG exhibited a high initial release of 78.3 % ( $\pm$  0.43) after 24 h and the release was already complete after only 4 d. In contrast, sustained IFN- $\alpha$  release was observed from the same type of implant in phosphate buffer pH 7.4. Not only the slope of the release curves, but also their shapes were affected by the pH of the release medium. All release rates monotonically decreased at pH 4.0, whereas at pH 7.4 they remained about constant for 7 d.

This observation indicated differences in the underlying protein release mechanisms. To get deeper insight into the involved mass transport phenomena, an analytical solution of Fick's second law of diffusion considering radial as well as axial mass transfer in cylinders with constant diffusion coefficients (Equation 9, Chapter I.5.3) was fitted to the experimentally determined release rates. As it can be seen in Figure 40, good agreement between theory and experiment was obtained in all cases at pH 4.0, irrespective of the initial PEG loadings of the implants ( $R^2 > 0.99$ ). Thus, protein release at pH 4.0 was predominantly controlled by pure diffusion with constant diffusivities. In contrast, at pH 7.4 the presence of PEG within the lipidic systems resulted in systematic deviations between the applied mathematical theory and the measured protein release kinetics.

Furthermore, the total amounts of IFN- $\alpha$  released from PEG-containing implant systems strongly depended on the pH of the release medium. This effect will be investigated in Chapter IV.3.4.

### 3.3. ALTERNATIVE POROGEN AND ALTERNATIVE PROTEIN

Finally, either the pore forming agent or the protein of the implant formulation was substituted to prove the postulated hypothesis of an in-situ precipitation prior protein release.

#### 3.3.1. RELEASE OF IFN- $\alpha$ FROM TRISTEARIN IMPLANTS LOADED WITH AN ALTERNATIVE POROGEN

Following the postulated release mechanism an alternative porogen, that does not cause protein precipitation, should lead to an accelerated release of IFN- $\alpha$  from tristearin matrices.

HP- $\beta$ -CD was chosen as alternative porogen for three main reasons:

(1) HP- $\beta$ -CD is already present in the original implant formulation. Thus, potential unforeseeable effects (on the protein stability, matrix compressibility etc.) of the “new” porogen are improbable.

(2) Cyclodextrins are reported to form inclusion complexes with peptides and proteins [105]. Such interactions may affect protein solubility as well as diffusivity which in turn would account for various effects on the protein release kinetics. However, in Chapter IV.4 it will be shown that the formation of inclusion complexes between IFN- $\alpha$  and HP- $\beta$ -CD is unlikely.

(3) The release of HP- $\beta$ -CD from tristearin implants is slower than the release of PEG (Figure 22). Consequently, an accelerated liberation of IFN- $\alpha$  due to a faster leaching out of HP- $\beta$ -CD can be excluded.

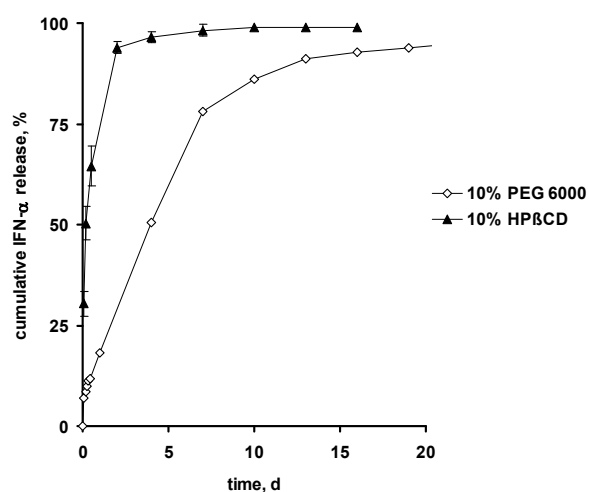


**Figure 41: Effect of porogen character on the in-vitro release of IFN- $\alpha$ .**

Matrices were loaded with 10 % IFN- $\alpha$ /HP- $\beta$ -CD lyophilisate and with 10 % lyophilised HP- $\beta$ -CD or with 10 % PEG (average  $\pm$  SD; n = 3).

The replacement of PEG by HP- $\beta$ -CD tremendously altered the release behaviour of IFN- $\alpha$  from tristearin implants (Figure 41). As expected, accelerated protein delivery from implants comprising 10 % HP- $\beta$ -CD as porogen was observed. IFN- $\alpha$  was completely liberated within the first 24 hours. This result demonstrated the importance of the protein precipitation for a sustained protein release.

### 3.3.2. RELEASE OF LYSOZYME FROM TRISTEARIN IMPLANTS

In a second attempt the effect of PEG on the in-vitro release behaviour of an alternative protein was investigated. Due to volume exclusion effects it is highly expectable that the addition of polyethyleneglycols reduces protein solubility in general [204, 226]. However, the extent of “salting out” depends on the protein.

Thus, in the following experiment the impact of different PEG loadings on the release kinetics of a protein with a less strong precipitation in the presence of PEG was studied. Based on the postulated release mechanism PEG should mainly act as a porogen resulting in accelerated protein release with enhances burst effects [40, 108, 138, 174].

Atha et al. (1981) investigated the effect of PEG 4000 on the solubility of various proteins. It was shown that proteins with a molecular weight between 150 to 670 kDa tend to precipitate at lower PEG concentrations than proteins with a molecular weight between 14 and 66 kDa [9]. Since a massive variation of the protein's molecular weight would affect diffusivity and in consequence the release behaviour, an alternative protein with a molecular weight comparable to IFN- $\alpha$ , but with a less distinct precipitation in the presence of PEG 6000 was chosen.

In the study of Atha [9], lysozyme revealed the highest solubility in the presence of PEG 4000. Since the molecular weight of lysozyme (14.4 kDa) is comparable to that of IFN- $\alpha$  (19.2 kDa) lysozyme was used in these studies.

First, the solubility of lysozyme in the presence of PEG 6000 was investigated. As shown in Figure 42, the influence of PEG on protein solubility was significantly lower than that observed for IFN- $\alpha$ . Even at a PEG concentration of 20 % (wt/vol) a high lysozyme solubility of 63.9 mg/mL (SD 4.0 mg/mL, n=3) was determined. In comparison, PEG concentrations of 10 % resulted in an almost negligible IFN- $\alpha$  solubility (soluble fraction of IFN- $\alpha$  0.02 mg/mL).

Thus, it could be expected that in-situ precipitation is of minor importance for the release of lysozyme from PEG containing matrices compared to IFN- $\alpha$ .

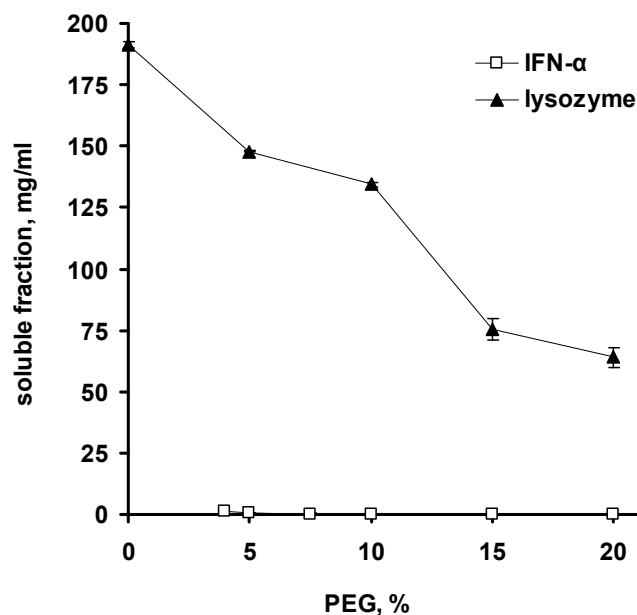


**Figure 42:** Effects of the PEG concentration on the apparent solubility of IFN- $\alpha$  and lysozyme at 37 °C in phosphate buffer pH 7.4 (average  $\pm$  SD; n = 3).

The release patterns of lysozyme from tristearin implants containing various amounts of PEG are illustrated in Figure 43. In analogy to the release of IFN- $\alpha$ , the addition of PEG enhanced the total amount of liberated lysozyme. However, an important distinction between IFN- $\alpha$  and lysozyme liberation is evident from Figure 43 B: the burst release of lysozyme increased with increasing the PEG loading. For instance, implants loaded with 20 % PEG delivered approximately 61 % of the incorporated lysozyme within the first 24 h. In contrast, the burst release of IFN- $\alpha$  from tristearin implants was substantially lowered by the addition of PEG (compare to Figure 13). Even with an initial PEG loading of 20 % no more than 23 % of IFN- $\alpha$  was released within 24 hours. The accelerated release of lysozyme from PEG-containing tristearin implants was also reflected in the overall release kinetics. As it can be seen in Figure 44 lysozyme liberation was less sustained. Moreover, the liberation curve of lysozyme revealed a parabolic shape, whereas a linear phase up to 7 days was observed in the case of IFN- $\alpha$ . Actually, the mathematical analysis of the release profiles of lysozyme with the aforementioned solution of Fick's second law of diffusion (Equation 9, Chapter 1.5.3) revealed good agreement between the theoretical and the experimental data (data not shown, [206]). Consequently, the release of lysozyme was predominantly governed by pure diffusion irrespective of the PEG content of the matrix. In contrast, in the case of IFN- $\alpha$  delivery from PEG-containing matrices pure diffusion controlled release could be excluded since

systematic deviations between the applied mathematical model and the experimental release data were found.

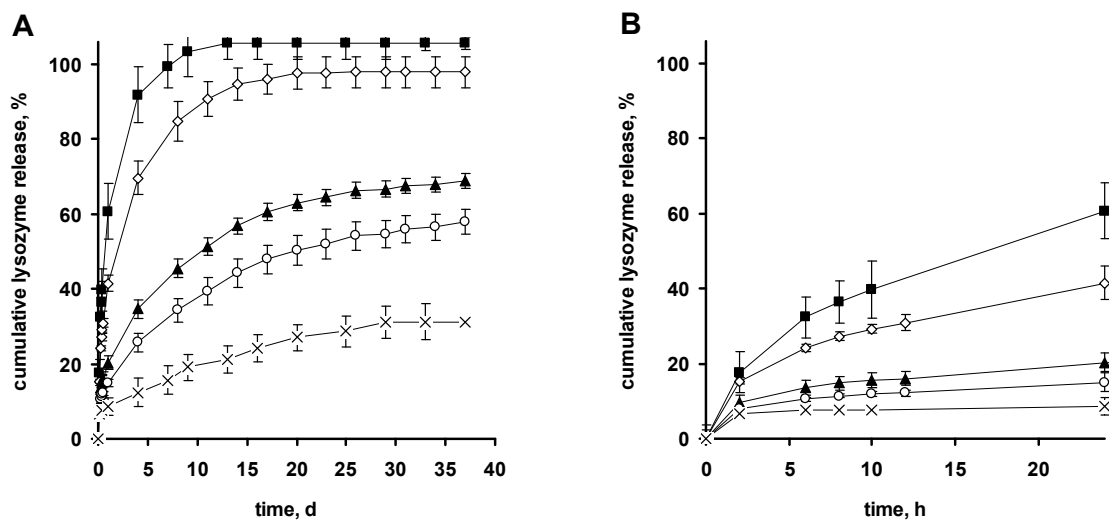


**Figure 43: Effects of various PEG loadings on release of lysozyme from tristearin-based cylindrical implants.**

In (A) the release over 40 days is illustrated. (B) Represents a zoom of the lysozyme release within 24 hours. All devices were loaded with 2.5 % lysozyme and 7.5 % HP- $\beta$ -CD. The admixed PEG amount was: (\*) 0 %, (○) 5 %, (▲) 10 %, (◇) 15 % and (■) 20 %, respectively (average  $\pm$  SD;  $n = 3$ ).

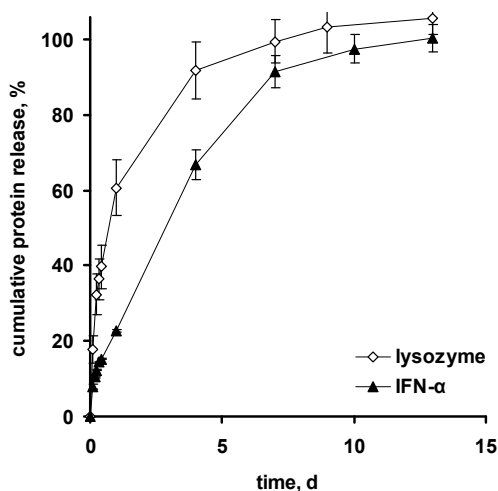


**Figure 44: Comparison of IFN- $\alpha$  and lysozyme release from tristearin-based implants.**

Matrices were loaded with 20 % PEG. The release was studied in phosphate buffer pH 7.4 (average  $\pm$  SD;  $n = 3$ ).

The release kinetics of lysozyme from PEG-containing matrices led to the conclusion that the impact of PEG can be fully explained in this case by its role as a pore forming agent. Due to the leaching out of PEG the creation of water-filled pores is facilitated. As a result the amount of totally delivered protein increases compared to PEG-free matrices. On the other hand, the accelerated creation of pores and the

concomitant reduction of geometrical hindrances by the pore network account for less sustained protein liberation and enhanced burst effects.

### 3.4. IMPORTANCE OF THE PRECIPITATION MECHANISM FOR PROTEIN STABILITY

In the case of release studies at pH 7.4 the addition of 10 % PEG (or more) to a lipidic matrix allowed a complete recovery of IFN- $\alpha$  (totally 93.6 % SD=6.8 % of the incorporated protein were delivered). In contrast IFN- $\alpha$  release levelled off at 47.8 % (SD=4.91) after 4 days when incubation of the same implants took place at pH 4.0 (Figure 45). Possible reasons for the different IFN- $\alpha$  recovery rates will be discussed in the following section.

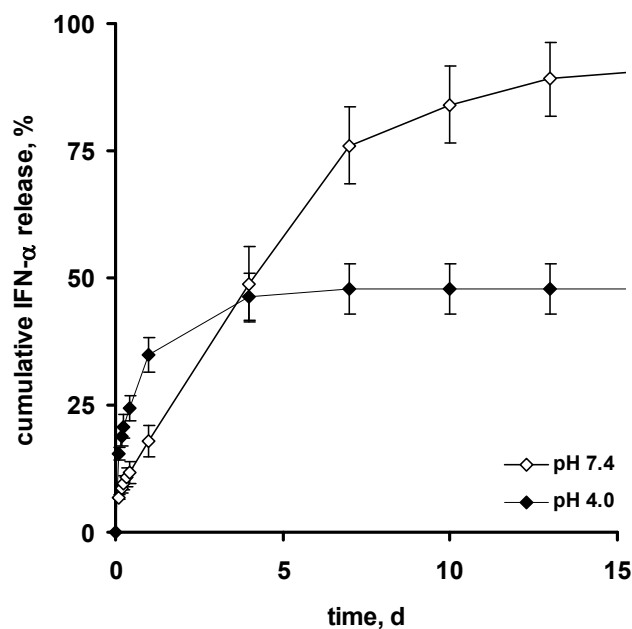


**Figure 45: Effects of the pH of the phosphate buffer solution on IFN- $\alpha$  release from tristearin-based implants.**

Matrices were loaded with 10 % IFN- $\alpha$ /HP- $\beta$ -CD lyophilisate and 10 % PEG. The release was studied either in phosphate buffer pH 7.4 or in phosphate buffer pH 4.0 (average  $\pm$  SD; n = 3).

As described in Chapter I.5.1 the creation of an interconnected pore-network is essential for the diffusion of proteins from inert matrices. Thus, one explanation for different protein recoveries might be a pH-dependence of the kinetics of pore creation. Since the formation of water-filled pores occurs upon the dissolution and leaching out of the incorporated hydrophilic excipients PEG and HP- $\beta$ -CD, the release rates of both were determined simultaneously with protein release at pH 4.0 and at pH 7.4.

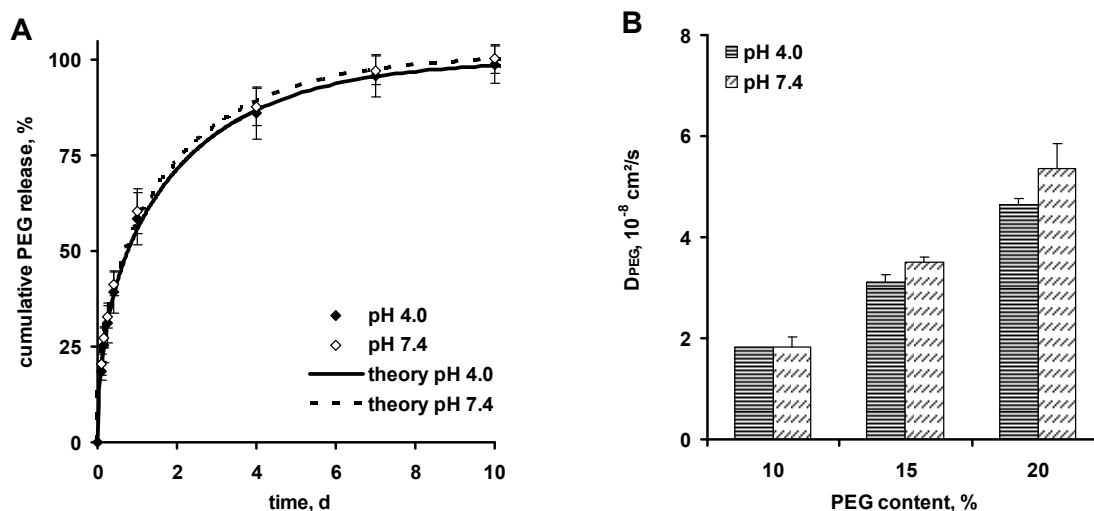


**Figure 46: (A) PEG release from tristearin-implants at pH 4.0 and at pH 7.5 (B) The apparent diffusion coefficients of PEG in lipidic implants at different PEG loadings and different pH values.**

(A) The release of PEG from implants loaded with 10 % IFN- $\alpha$ /HP- $\beta$ -CD lyophilisate and 10 % PEG was studied at pH 7.4 or 4.0 [symbols: experimental results (average  $\pm$  SD; n = 3), curves: theory (Equation 9, Chapter I.5.3)].

(B) Based on the fittings the apparent diffusion coefficients of PEG were determined. The indicated PEG content represents the initial PEG loading of the investigated implant formulation, respectively (average  $\pm$  SD; n = 3).

However, as shown in Figure 46 A the pH of the release medium did not affect the release of PEG from tristearin-based implants. Exemplarily, the results obtained with devices (initially) containing 10 % PEG are shown. The tendencies with 15 and 20 % PEG-loaded implants were similar. Fitting an adequate solution of Fick's law of diffusion (Equation 9, Chapter I.5.3) to the experimentally determined PEG release kinetics, good agreement between theory and experiment was obtained in all cases (two examples are illustrated in Figure 46 A). This clearly indicated that PEG release was primarily controlled by pure diffusion with constant diffusivities, irrespective of the pH of the release medium.

Based on the obtained fittings, the apparent diffusion coefficients of PEG within the lipidic implants were determined. For all investigated PEG loadings the pH of the phosphate buffer (pH 7.4 or 4.0) was only of minor importance for the mobility of PEG within the tristearin-based implants (Figure 46 B).

The results obtained when studying the pH-dependence of the release of the co-lyophilisation agent HP- $\beta$ -CD are given in Figure 47. The diffusivity of HP- $\beta$ -CD increased at pH 4.0 for higher PEG-loadings, but obviously this effect was not helpful to explain the levelling off of the protein release at pH 4.0 due to reduced pore formation as it leads into the opposite direction.

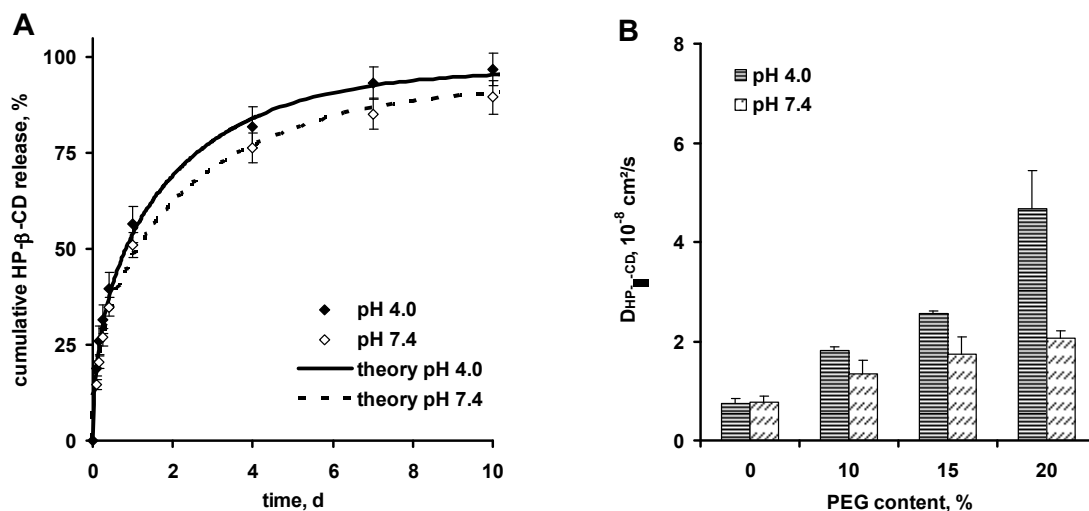


**Figure 47: (A) HP-β-CD release from tristearin-implants at pH 4.0 and pH 7.4 (B) The apparent diffusion coefficient of HP-β-CD in the lipidic implants.**

(A) The release of HP-β-CD from implants loaded with 10 % IFN-α/HP-β-CD lyophilisate and 10 % PEG was studied at pH 7.4 or 4.0 [symbols: experimental results (average +/- SD; n = 3), curves: theory (Equation 9, Chapter I.5.3)].

(B) Based on the fittings the apparent diffusion coefficients of HP-β-CD were determined. The indicated PEG content represents the initial PEG loading of the investigated implant formulation, respectively (average +/- SD; n = 3).

The release kinetics of PEG and HP-β-CD suggest that potential differences in the creation of water-filled pores at different pH values of the bulk fluid can be excluded as reason for the observed significant effects of the pH on protein release.

At pH 7.4 the solubility of IFN-α is reduced in the presence of PEG. As a consequence only low protein concentrations within the implant pores are generated. In contrast, at pH 4.0 the water-uptake and the subsequent dissolution of IFN-α will result in highly concentrated protein solutions, which may favour intermolecular interactions and, thus, leading to increased aggregation [250].

In order to investigate the possibility of IFN-α aggregation during release at pH 4.0 within the matrix, the protein drug remaining within the lipidic implants after in-vitro incubation was extracted and analysed by SDS-PAGE. As visualised in Figure 48, irrespective of the initial PEG loading the formation of dimers as well as the presence of higher-order aggregates within the implants was evident at pH 4.0. In contrast, it has been shown early that the stability of IFN-α within the same implants was not compromised at pH 7.4 [151, 153]. Mohl and Winter extracted IFN-α from tristearin implants after in-vitro incubation at pH 7.4. SDS-PAGE of the samples revealed only marginal dimer formation [151, 153].

It was shown for PLGA matrices that the creation of higher-order aggregates within the controlled release devices is one of the major causes for incomplete release. Due

to their large sizes such specimens are not able to diffuse through the restrictive pore-network [52, 119].

Thus, it can be concluded that the precipitation of IFN- $\alpha$  by PEG at pH 7.4 ensures low protein concentration within the water-filled pores, which in turn contributes to the stabilisation of the protein during release. In contrast, the lack of protein precipitation at pH 4.0 resulted in high protein concentrations within the implant pores favouring protein aggregation.

In addition, a further contribution to lower protein stability at pH 4.0 might be provided by the fact that the diffusivity of HP- $\beta$ -CD is increased at pH 4.0. Consequently, low concentrations of HP- $\beta$ -CD might be available within the implant pores. Considering that HP- $\beta$ -CD presumably stabilises IFN- $\alpha$  during the release period (see Chapter IV.4), this stabilisation of IFN- $\alpha$  by HP- $\beta$ -CD might be less effective at pH 4.0.

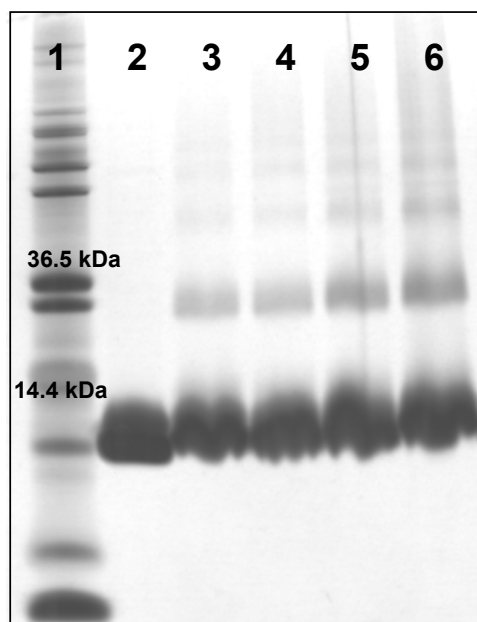


**Figure 48: SDS-PAGE of IFN- $\alpha$  extracted from tristearin implants at pH 4.0.**

Lane 1: Molecular weight standard, lane 2: IFN- $\alpha$  standard, lane 3-6: IFN- $\alpha$  extracted from tristearin implants after in-vitro incubation at pH 4.0. The implants were loaded with 0 %, 10 %, 15 % and 20 % PEG, respectively.

### 3.5. SUMMARY AND CONCLUSION

This chapter clearly pointed out that the role of PEG as protein precipitant is crucial for the full understanding of IFN- $\alpha$  release from PEG-containing lipidic matrices. The hypothesis of reduced protein solubility within the PEG-loaded lipidic implants presented in Chapter IV.2 was confirmed by several additional and independent experiments.

The developed “macropore model”, which enabled to evaluate simultaneously the relative importance of dissolution and diffusion of IFN- $\alpha$ , HP- $\beta$ -CD, and PEG revealed that within the “macropores” a highly concentrated PEG solution was created. Thus, the dissolution of the protein was restricted and, compared to PEG-free “macropores”, only a minor fraction of IFN- $\alpha$  was available for diffusion. As a result, the release of IFN- $\alpha$  from PEG-containing “macropores” was drastically reduced, suggesting that the dissolution step is one of the major rate limiting factors for protein release in the presence of PEG.

Further insight into the significance of reduced protein solubility and reversible precipitation within PEG-containing tristearin implants was obtained by studying the pH-dependence of protein solubility and release. At pH 7.4 already low PEG concentrations of about 3 % resulted in the precipitation of IFN- $\alpha$ . In contrast, at pH 4.0 PEG concentrations of up to 20 % did not cause protein precipitation under the investigated conditions. This means that the selection of different pH values for in-vitro release studies offers the possibility to “switch on/off” the “limited protein solubility” release mechanism. Lacking protein precipitation at pH 4.0 the release patterns of IFN- $\alpha$  from PEG-containing implants showed a significantly accelerated protein release with a high burst effect. In this case, protein release was purely diffusion controlled with constant diffusion coefficients and monotonically decreasing release rates, irrespective of the initial PEG loading.

Whereas the addition of 10 % PEG (or more) to a lipidic matrix allowed complete protein recovery at pH 7.4, at pH 4.0 IFN- $\alpha$  release levelled off at 48 % after 4 d. In contrast to protein liberation, the release of both hydrophilic excipients – PEG and HP- $\beta$ -CD – revealed only marginal pH-dependence. Therefore, pH dependent differences in the creation of water-filled pores can be neglected and very similar pore volumes at pH 7.4 and pH 4.0 can be assumed.

As mentioned before (Chapter I) incomplete protein release is often ascribed to protein aggregation/denaturation within the matrix [156, 199, 233]. Since the solubility of IFN- $\alpha$  is reduced in the presence of PEG, only low protein concentrations within the implant pores were generated at pH 7.4. In contrast at pH 4.0, the water imbedding and the subsequent dissolution of IFN- $\alpha$  resulted in highly concentrated protein solutions. Therefore, intermolecular interactions are favoured and thus increased aggregation within the matrix can be expected [250].

Consequently, the presented sustained release mechanism offers two major benefits for its practical application. Firstly, the reversible precipitation of IFN- $\alpha$  facilitates the sustained protein delivery with nearly constant release rates and a low burst effect. Secondly, the precipitation also ensures low protein concentrations within the implant pores, which in turn reduces the tendency towards protein aggregation.

Furthermore, the hypothesis of a reversible precipitation was confirmed by the replacement of PEG by an alternative porogen. Compared to the implant formulation containing PEG, the use of HP- $\beta$ -CD as porogen resulted in a markedly accelerated IFN- $\alpha$  liberation from tristearin matrices.

In an alternative experimental setup, IFN- $\alpha$  was replaced by lysozyme, which inherited a minor tendency to precipitate. Comparing the release kinetics of lysozyme from PEG-free and PEG-loaded tristearin implants the typical features described in literature for the addition of PEG to controlled release devices were evident: the total amount of delivered protein increased due to the formation of an interconnected pore-network. Concomitantly, the burst release significantly increased with rising up the PEG content.

The latter experiment can be regarded as further proof for the postulated in-situ precipitation of IFN- $\alpha$  within PEG-containing tristearin implants. On the other hand, the results obtained with lysozyme pointed out the fragile balance between PEG acting as porogen and PEG acting as protein precipitant. Aiming at a prolongation of the delivery period powerful precipitation is crucial. In the case of lysozyme high protein solubility persisted in the presence of high PEG concentrations. Hence, the PEG content within the implant pores was not sufficient to limit the release of lysozyme from such implants. The liberation of lysozyme was therefore less sustained compared to the delivery of IFN- $\alpha$ .

It is highly conceivable that the described in-situ precipitation mechanism might be transferable to other protein precipitants than PEG. In order to achieve benefits similar to the case of the IFN- $\alpha$ -PEG system the precipitant should fulfil the following features: (1) high efficiency to precipitate even in low concentrations, (2) reversible precipitation without affecting protein stability, and (3) water-solubility. The first point is evident with respect to the comparison of the release data for lysozyme and IFN- $\alpha$ . The second request arises from the scientific knowledge that protein denaturation and aggregation can be claimed as one of the major causes for incomplete recovery [169, 199, 233]. Furthermore, the release of proteins which are not properly folded

and in particular the delivery of aggregates from controlled release devices inheres the risk of inducing an immune response [93, 194]. Thus, reversibility of precipitation needs to be carefully evaluated. Third, the water-solubility of the precipitation agent will allow a concomitant leaching out of precipitant and drug. As the diffusion pathways increase with advanced release times the release rates monotonically decrease. Such effects can be compensated by increasing the drug solubility within the matrix, which can be accomplished by decreasing the concentration of the available precipitant due to permanent leaching out of the same.

Analysing the literature plenty of solvent conditions are available for reducing protein solubility. According to McPherson precipitants of macromolecules can be categorised into four classes: (1) organic solvents, (2) salts, (3) long-chain polymers, and (4) low molecular weight polymers [149].

#### **4. POTENTIAL EFFECT OF HP- $\beta$ -CD ON IFN- $\alpha$ RELEASE AND STABILITY**

Before implant manufacturing IFN- $\alpha$  has to be lyophilised in order to obtain a solid protein powder. As freezing and dehydration can induce protein denaturation, the presence of lyoprotectants during lyophilisation is crucial for maintaining protein stability [249]. It has been shown that trehalose and HP- $\beta$ -CD are suitable for conserving the stability of IFN- $\alpha$  during lyophilisation [151].

By comparing tristearin implants loaded either with IFN- $\alpha$ /trehalose or with IFN- $\alpha$ /HP- $\beta$ -CD lyophilisates, the use of HP- $\beta$ -CD co-lyophilisates resulted in a faster and more complete protein liberation [153]. Furthermore, co-lyophilisation with HP- $\beta$ -CD increased protein stability during the release period in comparison to co-lyophilisates containing trehalose [153]. This superiority of HP- $\beta$ -CD was also reflected during long-term storage: lyophilisation with HP- $\beta$ -CD ensured an excellent protein integrity and highly reproducible release kinetics. In contrast, the delivered amount of dimer and trimer species, as well as of oxidised protein increased during storage when trehalose was used as lyoprotectant. Moreover, the release profiles changed and IFN- $\alpha$  delivery became incomplete after six-months storage [152].

From these studies it can be concluded that HP- $\beta$ -CD compared to trehalose has two main effects: (1) accelerating the protein release and (2) increasing protein stability during release and storage. Therefore, it was aimed in the following section to provide additional experiments that should help to understand the effects of HP- $\beta$ -CD on IFN- $\alpha$  release and stability.

##### **4.1. POTENTIAL EFFECTS OF HP- $\beta$ -CD ON THE RELEASE OF IFN- $\alpha$ FROM TRISTEARIN IMPLANTS**

Cyclodextrins are a group of cyclic oligosaccharides that have a hydrophilic exterior and a hydrophobic internal cavity. This hydrophobic interior enables cyclodextrins to form inclusion complexes with the hydrophobic side chains accessible at the protein surface. In particular, aromatic amino acids are considered to be inserted into the hydrophobic cavity and these interactions are reported to stabilise and to solubilise various peptides and proteins [105]. For instance, the aqueous solubility of ovine growth hormone (O-GH) at pH 7.4 was increased by the use of HP- $\beta$ -CD [26].

For low molecular weight drugs it was shown that such effects on the solubility increased the drug release rates from various polymeric controlled release systems [15]. Furthermore, cyclodextrins are able to complex PEG [87].

Therefore, the interactions of HP- $\beta$ -CD with IFN- $\alpha$  and/or with PEG 6000 may affect the ability of PEG to precipitate IFN- $\alpha$ . In order to determine such effects the protein solubility in the presence of both excipients was investigated. However, the presence/absence of this co-lyophilisation agent did not alter the impact of PEG on the protein solubility (Figure 49).

This suggested that in-situ precipitation of IFN- $\alpha$  within PEG-containing tristearin implants occurs to the same extent regardless whether HP- $\beta$ -CD is present or not.

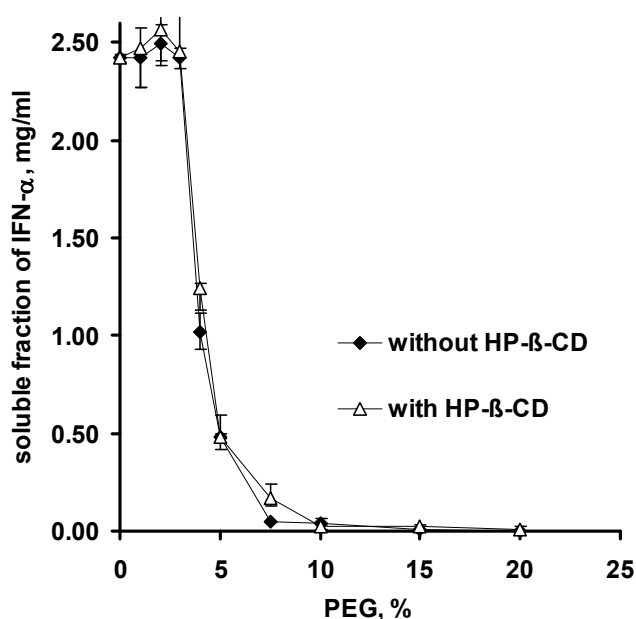


**Figure 49:** Effects of HP- $\beta$ -CD on the precipitation of IFN- $\alpha$  in the presence of PEG (average  $\pm$  SD; n = 3).

Apart from the effect of cyclodextrins on solubility, the formation of inclusion complexes may modify the drug diffusivity and consequently the drug release from delivery systems [15]. De Rosa et al. applied Attenuated Total Reflection (ATR)-FTIR spectroscopy to investigate the influence of HP- $\beta$ -CD incorporation on the properties of insulin-loaded PLGA microspheres prepared by spray drying. Upon addition of HP- $\beta$ -CD, insulin embedded within microspheres revealed an extended content of  $\beta$ -sheet structures, which was ascribed to the formation of an insulin/CD complex within the microspheres. Since the mobility of this complex within the polymeric matrix was considered to be lower than the mobility of free protein, the overall release rate was slowed down by the addition of HP- $\beta$ -CD [54].

In the case of tristearin implants the solubility of IFN- $\alpha$  was primarily affected by PEG (Figure 49). However, interactions between IFN- $\alpha$  and HP- $\beta$ -CD might affect the diffusivity of IFN- $\alpha$  as well. Various techniques such as competitive spectroscopy

[101], isothermal titration calorimetry, and nuclear magnetic resonance [56] are proposed to gain insight into the interactions of cyclodextrins with peptides and proteins after dissolution. Furthermore, spectroscopic techniques like FTIR, circular dichroism, and fluorescence spectroscopy were shown to be suitable for characterising protein cyclodextrin interactions.

For instance, Chen et al. revealed that the interactions of HP- $\beta$ -CD with the 40 kDa protein horseradish peroxidase were sufficient to increase the amount of  $\alpha$ -helical structure detectable by FTIR spectroscopy [37].

The potential of steady state fluorescence for monitoring cyclodextrin-peptide interactions was outlined by Khajehpour et al. for melittin interacting with HP- $\beta$ -CD. In the presence of HP- $\beta$ -CD a blue shift of the fluorescence maxima and a slight increase in the intrinsic fluorescence emission maxima of melittin were observed. The blue shift was ascribed to the reduction of the polarity around Trp. This might be a result of interactions with the cyclodextrin cavity or of an overall change of the peptide structure upon cyclodextrin addition [116].

In the course of this thesis fluorescence and FTIR spectroscopy were used to evaluate potential cyclodextrin-protein interactions. The protein to cyclodextrin mass ratio applied for lyophilisation and subsequent implant loading was 1 part protein to 3 parts cyclodextrin. This can be regarded as the highest protein to cyclodextrin ratio achievable within the implants, as HP- $\beta$ -CD was found to leach out faster from the lipidic implant than IFN- $\alpha$  (see Figure 22). The following experiments were, therefore, consistently carried out with a protein to cyclodextrin mass ratio of 1 to 3.

Figure 50 A illustrates the vector-normalised spectra as well as the vector-normalised second derivative spectra of IFN- $\alpha$  in the presence and in the absence of HP- $\beta$ -CD. As it can be seen, no differences were detectable in the amid I region between both samples. Furthermore, the addition of HP- $\beta$ -CD had no effect on the Trp fluorescence emission spectrum of IFN- $\alpha$  (Figure 50 B). In both spectra the emission maxima were detected at 336 nm with an identical intensity.

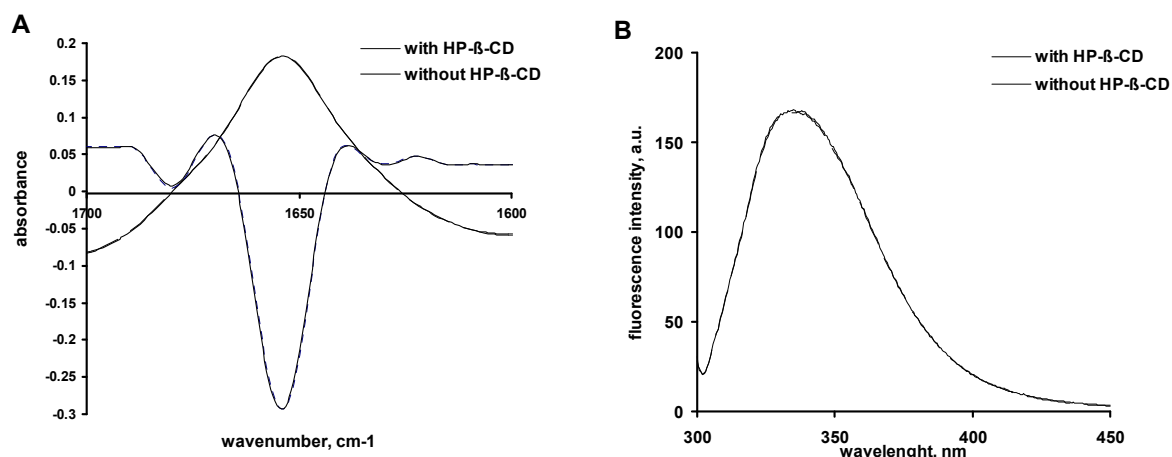


**Figure 50: (A) Vector-normalised and second derivative transmission FTIR-spectra; (B) Trp fluorescence emission scans of IFN- $\alpha$  in the presence and in the absence of HP- $\beta$ -CD (n=2).**

FTIR and Fluorescence spectroscopy provided information on the secondary and on the tertiary protein structure, respectively. Since both, FTIR and fluorescence spectra of IFN- $\alpha$  were not affected by the presence of HP- $\beta$ -CD it could be assumed that potential interactions with the cyclodextrin had no influence on the overall protein structure. Since such an alteration of the three-dimensional protein structure as well as the formation of stable complexes would affect the protein diffusivity, it can be supposed that the mobility of IFN- $\alpha$  within the water-filled pores of tristearin implants was not affected by the presence of HP- $\beta$ -CD.

In order to prove this experimentally the diffusion coefficients of IFN- $\alpha$  in the presence and in the absence of HP- $\beta$ -CD were determined by the open-end capillary technique introduced in Chapter IV.1.2. The improved experimental setup illustrated in Figure 20 was applied. For matters of comparison HP- $\beta$ -CD was replaced by trehalose as alternative stabilising agent.

This experiment was supposed to provide information on the diffusivity of IFN- $\alpha$  within the water-filled implant pores. In addition to IFN- $\alpha$  and HP- $\beta$ -CD some implants were loaded with PEG as porogen and precipitant. Thus, after water penetration, IFN- $\alpha$ , HP- $\beta$ -CD, and PEG will be dissolved within the implants pores. Hence, the effects of HP- $\beta$ -CD on the diffusion coefficient of IFN- $\alpha$  were determined additionally with and without PEG. In agreement to implant formulation comprising 10 % IFN- $\alpha$ /HP- $\beta$ -CD co-lyophilisate and 10 % or 20 % PEG, the IFN- $\alpha$ /HP- $\beta$ -CD co-lyophilisate to PEG ratio was 1 to 1 or 1 to 2, respectively.

In Figure 51 the protein concentrations determined within the capillary over time are depicted. Obviously, the release of IFN- $\alpha$  out of capillaries containing HP- $\beta$ -CD or

trehalose was comparable (Figure 51 A). The same tendency was observed when PEG was present (Figure 51 B and C).

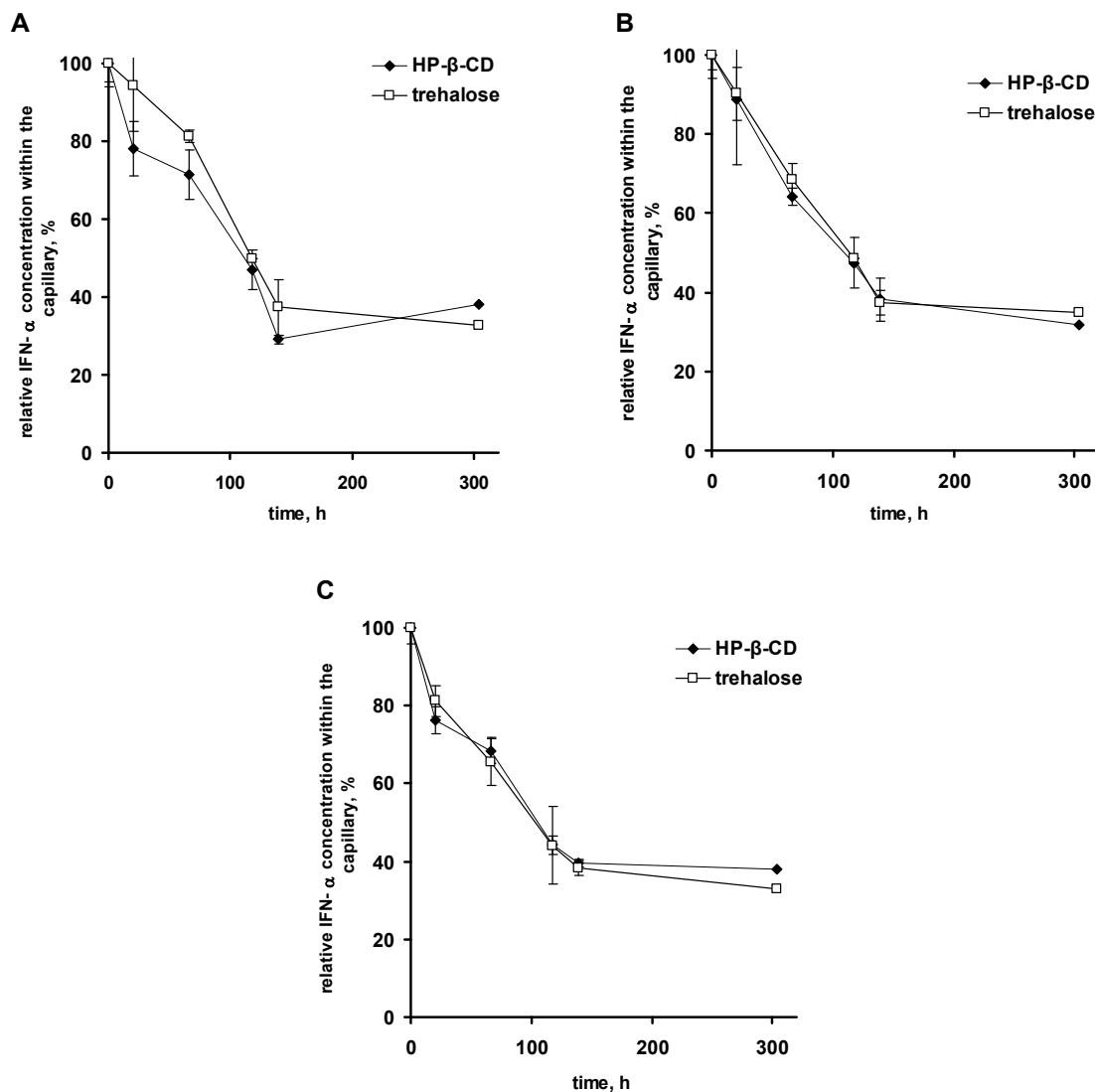


**Figure 51: Determination of the diffusion coefficient of IFN- $\alpha$ : decrease of IFN- $\alpha$  concentration within the capillary.**

Open symbols represent the IFN- $\alpha$  concentration in the presence of trehalose and closed symbols represent the IFN- $\alpha$  concentration in the presence of HP- $\beta$ -CD. Protein concentration within capillaries containing no PEG (A), lyophilisate:PEG blend in the ratio 1:1 (B), and lyophilisate:PEG ratio of 1:2 (C) (average  $\pm$  SD;  $n = 3$ , experimental setup according to Figure 20).

The diffusion coefficients of IFN- $\alpha$  were calculated based on the liberation rates (as described in Chapter IV.1.2). The determined diffusivities of IFN- $\alpha$  are listed in Table 7. As the diffusivities of IFN- $\alpha$  in samples containing HP- $\beta$ -CD and in samples containing trehalose were in the same order of magnitude, it could be concluded that HP- $\beta$ -CD neither affected the release of IFN- $\alpha$  from tristearin implants by a modulation of the protein solubility nor by an alteration of the protein diffusivity.

However, as a water-soluble excipient HP- $\beta$ -CD will promote the creation of water-filled pores and in this regard HP- $\beta$ -CD will surely contribute to the formation of water-filled pores allowing protein release from lipidic implants.

Moreover, unlike natural cyclodextrins, HP- $\beta$ -CD is surface active [106]. Recently, Koennings et al. revealed that the incorporation of surface active compounds accounted for increased water imbedding and consequently for increased release rates from lipidic implants [124].

**Table 7: Diffusion coefficients of IFN- $\alpha$  within phosphate-buffer filled capillaries comprising various amounts of PEG. IFN- $\alpha$  was lyophilised either with HP- $\beta$ -CD or with trehalose.**

The diffusion coefficients were determined by fitting Equation {13} to the release data shown in Figure 51.

	lyophilisate:PEG ratio	D, x 10 <sup>-6</sup> cm <sup>2</sup> /s
	1:0	1.80
HP- $\beta$ -CD	1:1	1.77
	1:2	1.71
	1:0	1.48
trehalose	1:1	1.29
	1:2	1.72

#### 4.2. POTENTIAL EFFECTS OF HP- $\beta$ -CD ON THE STABILITY OF IFN- $\alpha$

The effects of cyclodextrins on protein stability are often investigated under stress conditions such as during thermally or chemically induced unfolding. Since in vitro release studies are carried out at 37 °C, a thermal stabilisation of IFN- $\alpha$  by HP- $\beta$ -CD may be important to inhibit unfolding and aggregation during the release period.

Differential scanning calorimetry (DSC) is commonly used to characterise the thermal stability of a protein and to obtain information on the thermodynamics of protein unfolding. In Figure 52 the heat capacity curves of IFN- $\alpha$  in the presence and in the absence of HP- $\beta$ -CD are shown. Protein unfolding due to the increasing temperature was reflected by a single endothermic transition. The midpoint of this denaturation peak is generally referred to the melting temperature  $T_m$ , and the integrated area under the peak corresponds to the overall enthalpy change  $\Delta H$ , associated with the unfolding of IFN- $\alpha$ . It is obvious from Figure 52 that the addition of HP- $\beta$ -CD had no effect on both  $T_m$  and  $\Delta H$ . Furthermore, a steep decrease in the DSC signal was

observed after reaching  $T_m$  irrespective of the cyclodextrin. This is typically ascribed to protein aggregation suggesting irreversibility of IFN- $\alpha$  unfolding during heating.

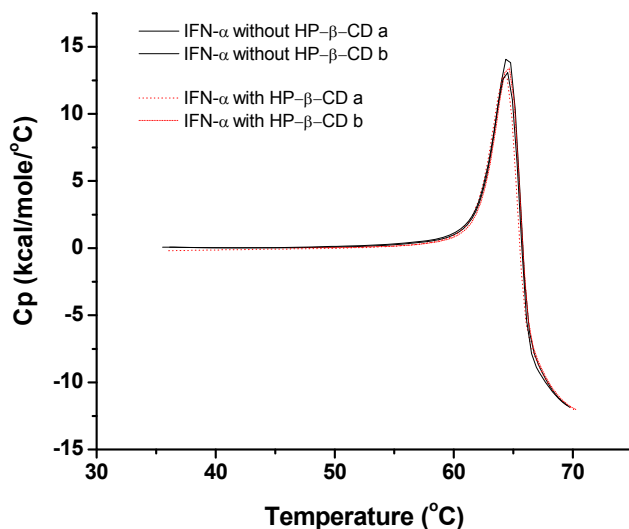


**Figure 52: DSC scans of IFN- $\alpha$  in the presence and in the absence of HP- $\beta$ -CD.**

The protein concentration was 4.8 mg/mL corresponding to a cyclodextrin concentration of 14.4 mg/mL.

Apart from DSC measurements the thermal stability of proteins can be evaluated spectroscopically. The temperature-induced changes in the secondary structure of IFN- $\alpha$  were monitored by attenuated total reflection (ATR)-FTIR.

In Figure 53 the original background corrected spectra of IFN- $\alpha$  as well as the corresponding second derivatives recorded during heating are shown. The overall intensity of the adsorption spectra rose when the temperature was ramped up (Figure 53 A). Generally, such an intensity increase during heating can be ascribed to protein precipitation [27]. The normalised second derivative spectra (Figure 53 B) revealed drastic perturbations of the structural components underlying the amid I and the amid II bands. At 25 °C IFN- $\alpha$  exhibited an amid I band maximum at 1653  $\text{cm}^{-1}$  which is characteristic for proteins containing predominantly  $\alpha$ -helical structures [60]. Elevating the temperature to 50 °C resulted in a decrease of the amid I band at 1653  $\text{cm}^{-1}$  which was accompanied by an intensity increase at 1622  $\text{cm}^{-1}$ . Bands in the range of 1620  $\text{cm}^{-1}$  were interpreted as intermolecular  $\beta$ -sheets [35, 147, 230], indicating protein denaturation and the beginning of aggregation. Furthermore, at higher temperatures a smaller peak around 1692  $\text{cm}^{-1}$  became evident. This peak

has also been associated with the formation of intermolecular  $\beta$ -sheets during protein denaturation [35, 147, 230].

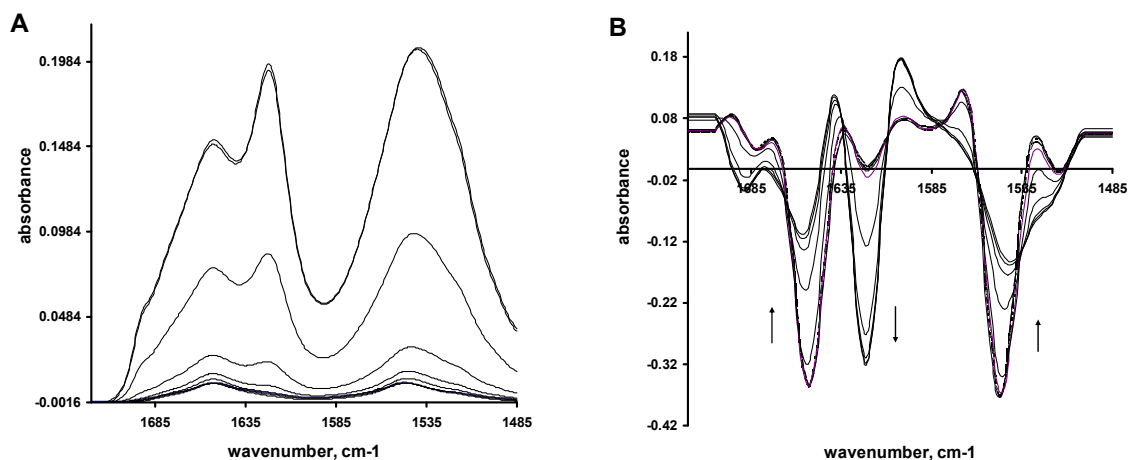


**Figure 53: Background corrected ATR-FTIR absorbance spectra (A) and vector-normalised second derivatives (B) during heating of IFN- $\alpha$  from 25 to 70 °C.**

Interestingly, the presence of HP- $\beta$ -CD seemed to increase the thermal stability of IFN- $\alpha$ . Exemplarily, in Figure 54 the spectra at 25 °C, 50 °C, 60 °C, and 70 °C are illustrated. At the starting temperature the spectra of IFN- $\alpha$  in the presence and in the absence of HP- $\beta$ -CD were nearly identical. In contrast, at elevated temperatures during heating clear differences were visible: samples without HP- $\beta$ -CD revealed significant unfolding and aggregation, whereas in the presence of HP- $\beta$ -CD only slight spectral changes occurred (Figure 54 B). Until a temperature of 70 °C was reached the addition of HP- $\beta$ -CD resulted in a lower decrease of helical elements and in a reduced formation of intermolecular  $\beta$ -sheets compared to IFN- $\alpha$  without HP- $\beta$ -CD. Finally, when the temperature ramp reached 70 °C no differences between HP- $\beta$ -CD-free and HP- $\beta$ -CD-containing samples were detectable and both spectra showed the same extent of protein denaturation.

This suggested that the presence of HP- $\beta$ -CD protects the native protein up to a critical value. Nevertheless, exceeding this temperature will also result in irreversible protein aggregation and precipitation as shown for samples without HP- $\beta$ -CD.

Protein stability is generally depending on protein concentration [250]. In order to evaluate whether the observed effects can also be expected for other protein concentrations the concentration of IFN- $\alpha$  was reduced from 4.8 to 1.6 mg/mL. This corresponds to a reduction of the cyclodextrin concentration from 14.4 mg/mL to 4.8 mg/mL. Here, a similar stabilisation of IFN- $\alpha$  against thermal induced denaturation was observed (data shown in Figure 55).

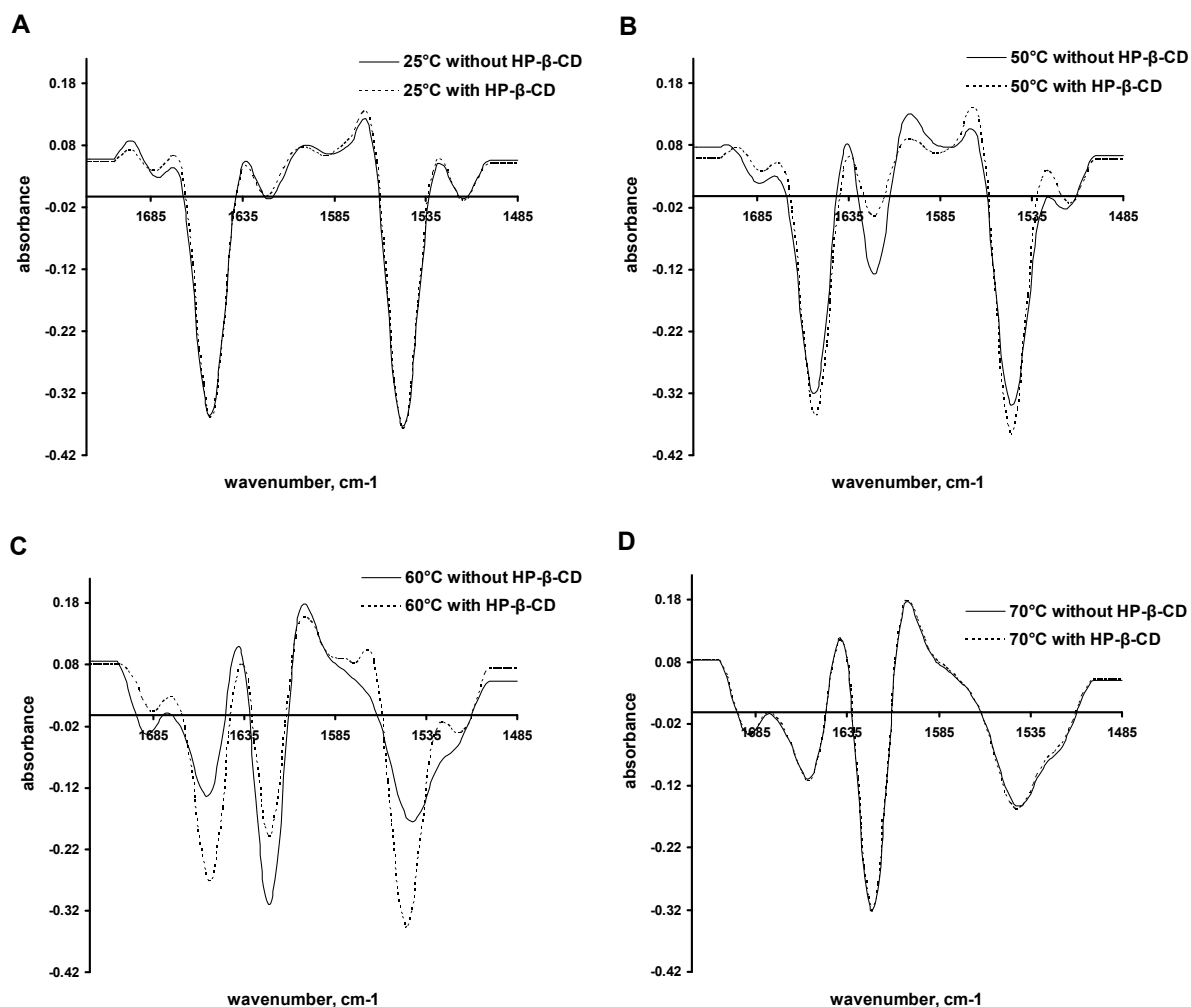


**Figure 54: Vector-normalised second derivative ATR-FTIR spectra at 25 °C (A), 50 °C (B), 60 °C (C), and 70 °C (D).**

The spectra of IFN- $\alpha$  ( $c=4.8$  mg/mL) were recorded in the absence (solid lines) and in the presence (broken line) of HP- $\beta$ -CD ( $c=14.4$ mg/mL).

The effects of cyclodextrin addition on the thermal stability of IFN- $\alpha$  can be quantified by calculating the melting temperature based on the ATR-FTIR spectra. Different interpretation methods are available in the literature to extract  $T_m$  from the spectral changes [147]. One possibility is plotting the intensities of the decreasing or increasing bands over the changing temperature. The decreasing  $\alpha$ -helical bands at  $1653\text{ cm}^{-1}$  and the increasing intermolecular  $\beta$ -sheet bands at  $1622\text{ cm}^{-1}$  and their temperature dependency is shown in Figure 55.

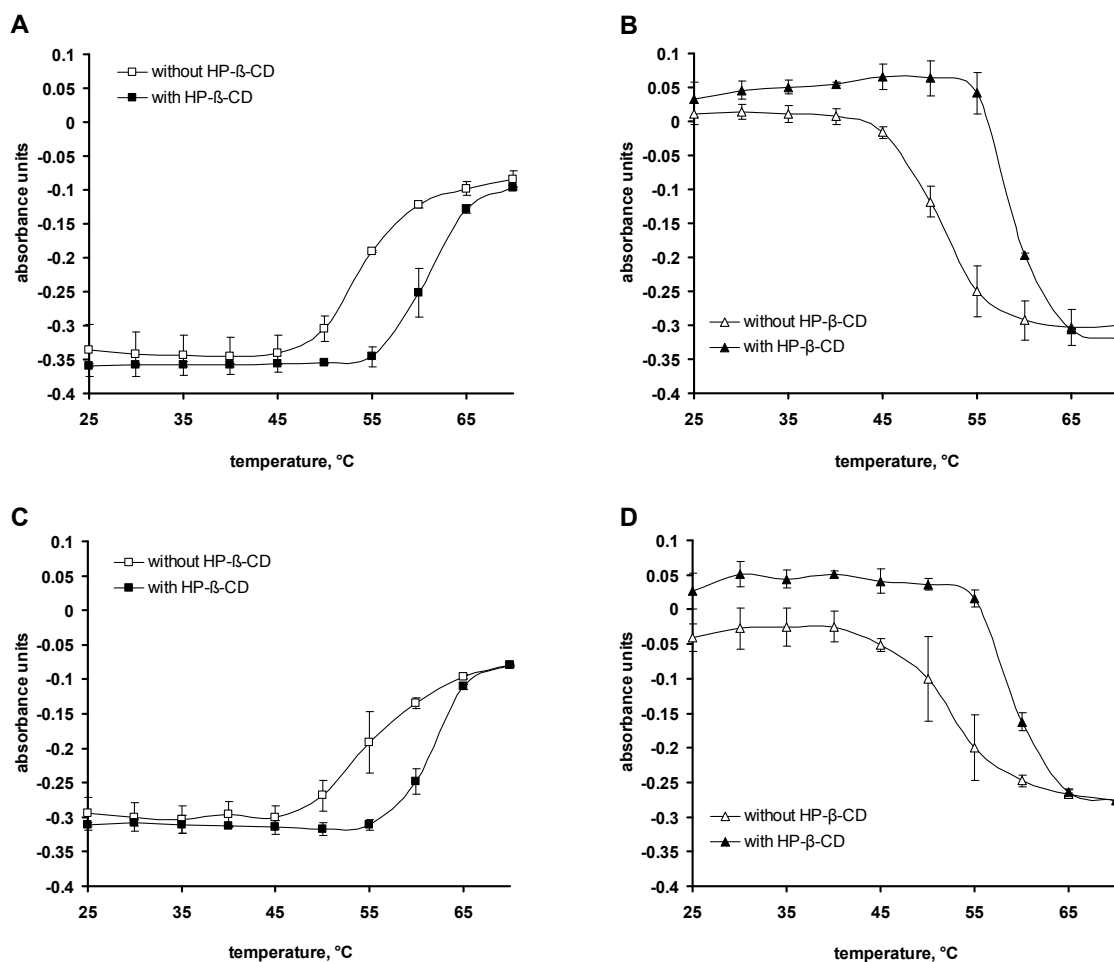


**Figure 55: Intensity change of the  $\alpha$ -helical band at  $1653\text{ cm}^{-1}$  (left) and intensity change of the  $\beta$ -sheet band at  $1622\text{ cm}^{-1}$  (right) during heating.**

Figure A and B represent the thermal transition curves obtained with a protein concentration of  $4.8\text{ mg/mL}$ . Figure C and D the thermal transition curves received with a protein concentration of  $1.6\text{ mg/mL}$  (average  $\pm$  SD;  $n = 3$ ).

Obviously, the presence of HP- $\beta$ -CD during thermal denaturation shifted the loss of the  $\alpha$ -helical structure and the increase of the  $\beta$ -sheet to higher temperatures, respectively. This observation was consistent at a protein concentration of  $4.8\text{ mg/mL}$  as well as at a protein concentration of  $1.6\text{ mg/mL}$ . Based on the plots shown in Figure 55 the midpoint of thermal denaturation was obtained by performing a sigmoid fit.

Alternatively, it has been suggested to use the cross section point between the increasing and the decreasing denaturation curve as  $T_m$  [147]. In accordance with the aforementioned methods this data evaluation also indicated a shift of  $T_m$  to higher values (Figure 56).

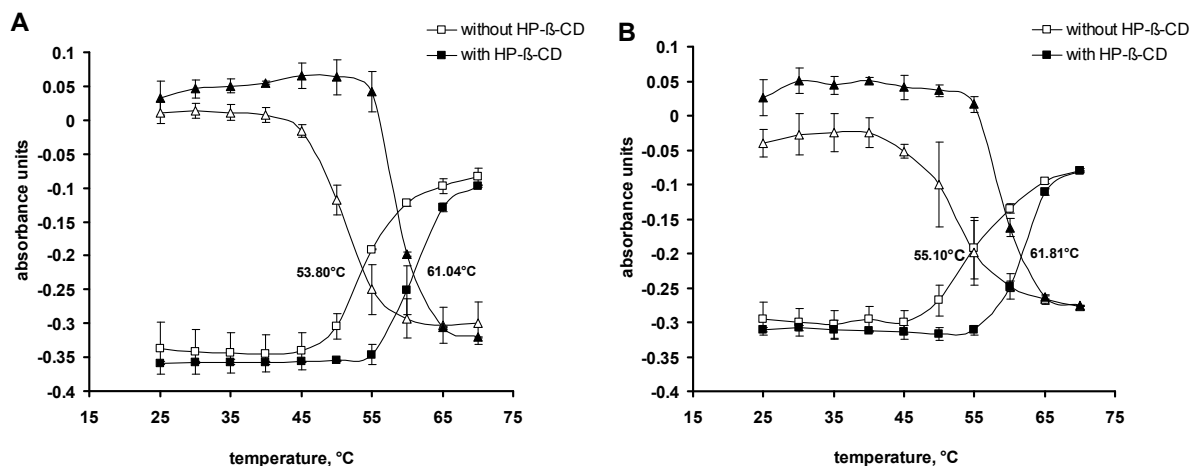


**Figure 56:** Intensity of band at  $1653\text{ cm}^{-1}$  (■/□) and at  $1622\text{ cm}^{-1}$  (▲/△) in the temperature range from 25 to 70 °C.

The protein concentration was either 4.8 mg/mL (A) or 1.6 mg/mL (B) (average  $\pm$  SD;  $n = 3$ ).

**Table 8: Melting temperature  $T_m$  of IFN- $\alpha$  in the presence and in the absence of HP- $\beta$ -CD.**

The melting temperatures based on ATR-FTIR experiments were obtained from the inflection point of thermal denaturation curves of the band at  $1653\text{ cm}^{-1}$  (method I) or the band at  $1622\text{ cm}^{-1}$  (method II). Alternatively, the cross section point of both intensity-temperature curves was referred as denaturation temperature (method III) (average  $\pm$  SD;  $n = 3$  for FTIR measurements, average  $\pm$  SD;  $n = 2$  for  $\mu$ DSC measurements).

conc. IFN- $\alpha$	formulation	FTIR			$\mu$ DSC
		method I	method II	method III* <sup>1</sup>	
0.48 mg/mL	without HP- $\beta$ -CD	n.d.	n.d.	n.d.	67.67°C* <sup>2</sup>
	with HP- $\beta$ -CD	n.d.	n.d.	n.d.	67.99°C* <sup>2</sup>
1.6 mg/mL	without HP- $\beta$ -CD	57.99 $\pm$ 2.02°C	48.60°C	55.16°C	65.34°C* <sup>2</sup>
	with HP- $\beta$ -CD	61.67 $\pm$ 0.46°C	57.99 $\pm$ 2.02°C	61.81°C	65.46°C* <sup>2</sup>
4.8 mg/mL	without HP- $\beta$ -CD	54.1 $\pm$ 0.96°C	50.98 $\pm$ 0.62°C	53.80°C	64.30 $\pm$ 0.30°C
	with HP- $\beta$ -CD	60.74 $\pm$ 1.18°C	59.21 $\pm$ 0.63°C	61.04°C	64.52 $\pm$ 0.23°C

\*<sup>1</sup> data represent the cross section of the average curves shown in Figure 56

\*<sup>2</sup> only one experiment performed

The different melting temperatures of IFN- $\alpha$  determined with ATR-FTIR and with  $\mu$ DSC measurements are given in Table 8. From the comparison of the results obtained with FTIR and  $\mu$ DSC two observations are evident: first, the  $T_m$  determined by means of ATR-FTIR strongly differed from that obtained with the  $\mu$ DSC technique.  $T_m$  values detected by the FTIR spectra were up to 10 degrees lower than that measured with  $\mu$ DSC. Second, the addition of HP- $\beta$ -CD had a drastic impact on the melting temperature of IFN- $\alpha$  determined with FTIR measurements, whereas no differences between HP- $\beta$ -CD-containing and HP- $\beta$ -CD-free samples were

detectable by  $\mu$ DSC experiments. Irrespective of the method applied for interpreting the FTIR spectra a significant increase in the melting temperature was observed.

Variations of  $T_m$  dependent on the applied method to evaluate the thermal stability were also reported by other authors. For instance, Matheus et al. recently demonstrated differences between the  $T_m$  values of lysozyme determined by ATR-FTIR spectroscopy and by  $\mu$ DSC experiments [147]. One explanation for the observed deviations might be the differences in the applied heating rates. FTIR spectroscopy requires an interruption of the heating at each temperature point to collect the spectral information and to average the signal. In contrast, normally a completely linear temperature profile is applied with  $\mu$ DSC measurements [147].

On the other hand, the presented data suggested that subtle changes in the protein structure occurring at moderate temperatures were detectable by FTIR but not by the DSC technique. Without the addition of HP- $\beta$ -CD IFN- $\alpha$  revealed the first perturbation of the secondary structure at 50 °C. In contrast, no change in the heat capacity was detectable by  $\mu$ DSC up to a temperature of 57 °C. Likewise results have been mentioned by Sharma and Kolonia for IFN- $\alpha$  [202]. It was shown that near- and far-UV CD were capable to identify slight changes in secondary and in tertiary protein structure at moderate temperatures. However, at these temperatures no changes in the baseline of DSC thermograms were detectable indicating that subtle conformational changes may not induce changes in the heat capacity sensitive enough to be picked up by  $\mu$ DSC [201].

These inherent differences between FTIR spectroscopy and  $\mu$ DSC may also explain the observed differences between FTIR and  $\mu$ DSC experiments regarding the thermal stability of IFN- $\alpha$  in the presence of HP- $\beta$ -CD.

The interactions between cyclodextrins and proteins depend on the type of cyclodextrin used as well as on the characteristics of the protein; therefore, the impact of cyclodextrins on the thermally or chemically induced unfolding is described heterogeneously in literature.

For instance, humane growth hormone revealed a reduced tendency to undergo thermally induced aggregation in the presence of hydrophilic cyclodextrins, which was manifested by an increase in the melting temperature ( $T_m$ ) of rhGH measured by means of differential scanning calorimetry [223]. In accordance with this observation Charman et al. [36] reported that HP- $\beta$ -CD was very effective in preventing precipitation of porcine growth hormone during heating. On the other hand, most

other studies described another scenario: due to interactions between cyclodextrins and hydrophobic side chains exposed during heating, cyclodextrins stabilised the unfolded state. Consequently, the equilibrium between folded and unfolded state was shifted to the unfolded state, which was associated with a lowering of  $T_m$  values [47]. After chemically induced denaturation cyclodextrins often act as artificial chaperons. For instance, Tavornvipas et al. investigated the influence of various cyclodextrins on the refolding of lysozyme, of basic fibroblast growth factor (bFGF) [222], and of human growth hormone [223]. First, the proteins were denaturated with guanidinium hydrochloride. Afterwards the denaturated protein solution was diluted and it was shown that the addition of branched  $\beta$ -cyclodextrins significantly reduced the tendency towards aggregation for all proteins, whereas HP- $\beta$ -CD,  $\alpha$ -CD-derivatives, and  $\gamma$ -CD-derivatives were less or not effective in preventing aggregation. As protein unfolding induced by GdnHCl is associated with solvent exposure of hydrophobic side chains, it has been suggested by the authors that the interactions of cyclodextrins to these exposed hydrophobic residues result in an inhibition of aggregation.

#### **4.3. SUMMARY AND CONCLUSION**

Due to the lack of any detectable interactions between IFN- $\alpha$  and HP- $\beta$ -CD in the mass ratio used for implant formulation, it is highly conceivable that the release of IFN- $\alpha$  is not affected by the formation of inclusion complexes. Such complexation would affect the protein solubility as well as the diffusivity of IFN- $\alpha$ . However, it was shown experimentally that the protein solubility is mainly affected by PEG rather than by the presence of the cyclodextrin. Furthermore, the diffusion coefficient determined by using the open-end capillary technique remained unaffected upon HP- $\beta$ -CD addition. Thus, these results suggested that HP- $\beta$ -CD will predominantly influence the protein release by increasing the matrix porosity and/or promoting the hydration of the controlled release system.

On the other hand, thermal protein denaturation monitored with ATR-FTIR spectroscopy indicated a stabilisation of IFN- $\alpha$  at elevated temperature. In comparison to HP- $\beta$ -CD-free samples thermally induced unfolding occurred at higher temperatures in the presence of HP- $\beta$ -CD. This stabilisation of IFN- $\alpha$  due to the addition of HP- $\beta$ -CD is in good agreement to the observation that HP- $\beta$ -CD ensured the preservation of the protein stability during release as well as during long-term storage [152, 153].

## CHAPTER V: DEVELOPMENT OF IMPROVED LIPID BASED DELIVERY SYSTEMS FOR PHARMACEUTICAL PROTEINS

### 1. MANUFACTURING OF EXTRUDATES BY RAM EXTRUSION

Tristearin implants were deemed as promising platform for the continuous delivery of IFN- $\alpha$  over a period of 1 month [153]. However, the geometry of these implants (average diameter and height of 5 mm and 2.4 mm, respectively) necessitates a surgical intervention for application. To overcome this limitation the manufacturing of small cylindrical rods that can be deposited subcutaneously via a trochar is highly desirable. As explained in the introduction section extrusion is applied most commonly to produce injectable implant systems. Since ram extrusion can be conducted in lab-scale with comparable low material costs (see Chapter I.4.3) the potential of implant preparation by means of a ram extruder was evaluated first.

#### 1.1. EXPERIMENTAL SETUP

Based on the general assembly of ram extruders (see Chapter I, Figure 2) a purpose-built extruder device was designed (Figure 57). To allow the softening of the lipid mixture prior to or during extrusion the extruder could optionally be equipped with a heatable coat. In a pilot study different heating temperatures were applied. It was found that a temperature of around 60 °C allowed the manual extrusion of tristearin material. However, temperature exposure may induce a polymorphic transition of the lipidic matrix material or a destabilisation of the protein drug (see Chapter I.3.3 and I.4.4, respectively). Therefore, an extrusion at room temperature was favoured and an alternative procedure was developed.

Since tristearin is very brittle, high pressures were needed to allow the flow through the extruder die. In consequence, extrusion was only possible by the employment of a hydraulic press to force tristearin through the extruder die. The obtained extrudates revealed high surface roughness and a low mechanical stability. In order to improve the extrudate quality a separate compression step before extrusion was introduced. After filling the extruder barrel with the lipophilic material a force of 3.92 kN was applied for 30 seconds. Afterwards, the extruder device was lifted on a rack and the extrusion was performed with a hydraulic press.

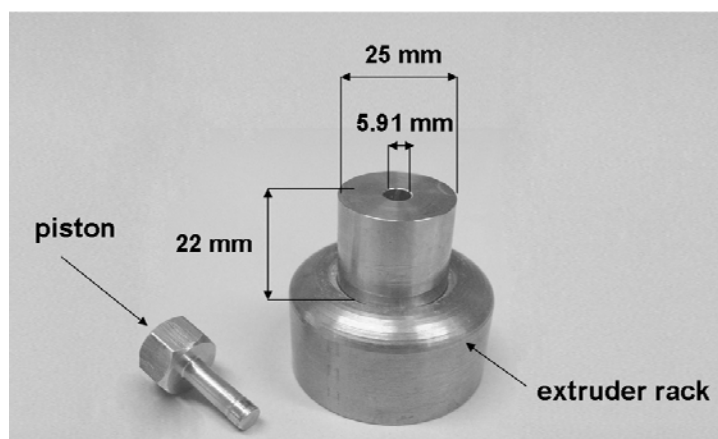


**Figure 57: Ram extruder device.**

After this manufacturing procedure the surface appeared smooth, with only low ruggedness (Figure 58). Furthermore, the mechanical stability of the extrudates was increased; to quantify this effect the forces needed for breaking the extrudates perpendicularly to the longitudinal axis were measured. Without a compression step the extrudates revealed a breaking strength of 26.5 N ( $n=3$ ,  $SD=5.9$  N), whereas after compression the extrudates resisted a force of 42.9 N ( $n=3$ ,  $SD=1.0$  N).

With the developed extrusion method not only tristearin could be processed, but also the manufacturing of extrudates based on various lipidic matrix materials (triglycerides of C12-C20, phospholipids etc.) with different amounts of hydrophilic excipients (0-30 %) was realised. Thus, the possibility to extrude various matrix compositions in a standardised way was given.

The prepared extrudates had an average length of 1.5 cm and a diameter of 1.2 mm according to the used extruder die. Importantly, the achieved geometry enables to fill the obtained extrudates in an injection device approved as suitable method for application of peptide containing extrudates, like Zoladex<sup>®</sup>.

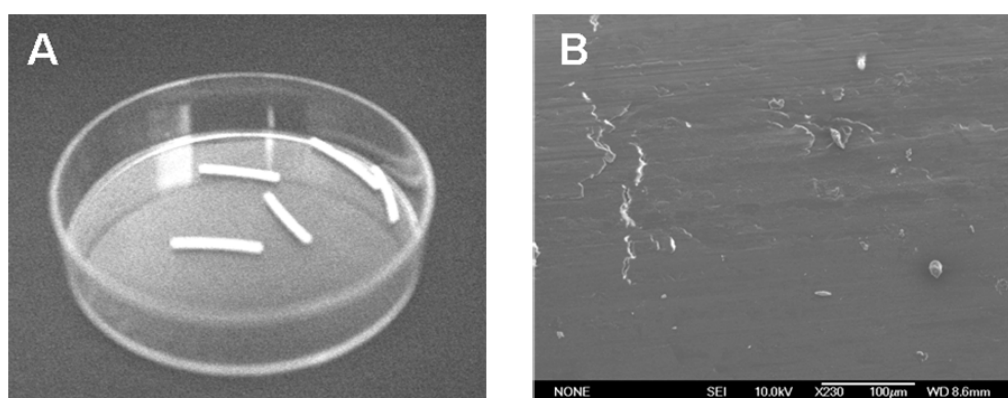


**Figure 58: Improved extrudates (A) macroscopic appearance (B) SEM zoom of the extrudate surface.**

## 1.2. INFLUENCE OF THE MANUFACTURING PROCESS ON THE LIPID MODIFICATION

When lipids are used as matrix material the preparation of sustained release devices may induce a polymorphic transformation from the stable  $\beta$ - to the  $\alpha$ -modification, which in turn may influence the quality of the end product during storage or may affect the release behaviour (see Chapter 1.3.3).

In order to determine the effect of the extrusion process on the lipid modification, the thermal behaviour of lipidic extrudates was investigated by differential scanning calorimetry. The heating and cooling curves of tristearin bulk material are shown in Figure 59. During the first heating step an endothermic peak at 70.8 °C ( $n=3$ ,  $SD=1.15$  °C) was observed that corresponds to the melting of the stable  $\beta$ -modification [77]. On cooling, crystallisation of the  $\alpha$ -polymorph occurred at 43.0 °C ( $n=3$ ,  $SD=0.9$  °C). Reheating of the solidified melt revealed an endotherm at 52.5 °C ( $n=3$ ,  $SD=0.75$  °C), indicating the melting of the unstable  $\alpha$ -modification. This peak was followed by an exotherm, attributed to the rearrangement of the  $\alpha$ -form to the crystalline  $\beta$ -form. By further heating a second endothermic peak was obtained, which displays the melting of the  $\beta$ -polymorph [77].

Importantly, the thermograms recorded from freshly prepared extrudates revealed only one melting peak at 70.8 °C ( $n=3$ ,  $SD=0.21$  °C). Hence, freshly prepared extrudates comprised the lipid in the stable  $\beta$ -modification.

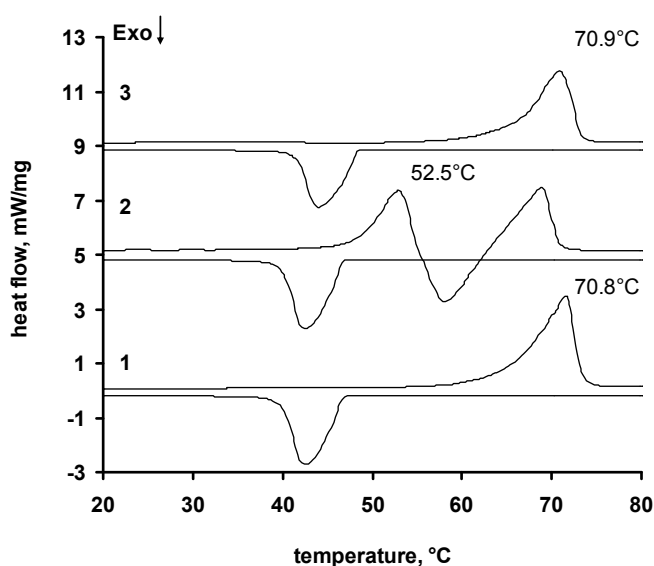


**Figure 59: Influence of the extrusion procedure on the lipid modification.**

DSC analyses of tristearin bulk material (1), melted and solidified tristearin (2), and tristearin extrudates directly after preparation at room temperature (3).

To confirm these results the crystalline states of tristearin bulk material, melted tristearin and extrudates were investigated by wide angle X-ray diffraction. As illustrated in Figure 60 tristearin bulk material showed three diffraction peaks at  $2\theta=19.5^\circ$ ,  $23.3^\circ$ ,  $24.3^\circ$ , respectively. The corresponding short spacings at 0.46 nm, 0.38 nm and 0.37 nm are typical for the  $\beta$ -modification [77]. In contrast, the solidified melt featured one single short spacing at about 0.415 nm that can be ascribed to the chain packing of the  $\alpha$ -modification [77].

Obviously, the extrudates possessed the specific short spacings of the stable  $\beta$ -polymorph. Therefore, both - WAXS and DSC experiments - confirmed that the extrusion process did not induce a polymorphic transformation of the lipidic matrix material.

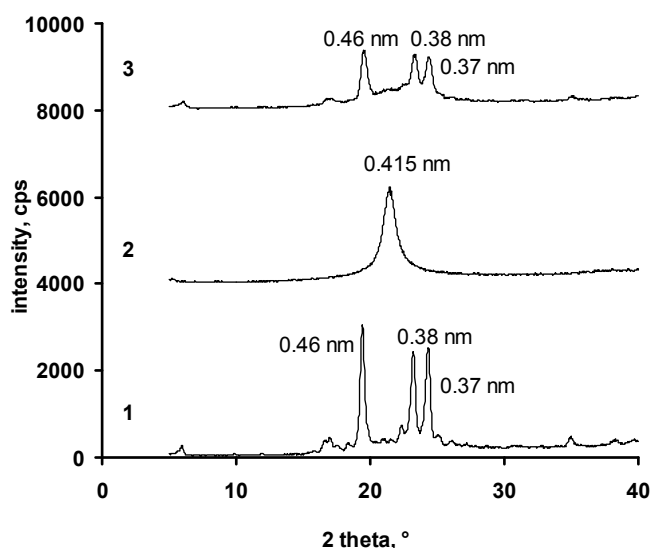


**Figure 60: Influence of the extrusion procedure on the lipid modification.** WAXS analyses of tristearin bulk material (1), melted and solidified tristearin (2), and tristearin extrudates directly after preparation (3).

### 1.3. INFLUENCE OF THE MANUFACTURING PROCESS ON PROTEIN STABILITY

The preservation of the native protein structure is one of the major challenging tasks during the manufacturing of controlled release devices. As pointed out in Chapter I.2.1 the harsh environmental conditions proteins are often exposed to during the preparation of controlled release devices trigger chemical and/or physical degradation pathways. However, since proteins that are not properly folded show less or no bioactivity, this will imperil the therapeutical efficiency of the product. Furthermore, the delivery of non-native protein specimen inheres the risk of inducing an immune response [71, 250].

Recombinant proteins that are structural identical or nearly identical to endogenous proteins might induce an immune reaction based on a break down of the immune tolerance to self-antigens. Thereby, impurities and protein aggregates are considered as main elucidators [194]. The participation of aggregates in the immunogenicity of recombinant proteins was shown, for example, for IFN  $\alpha$ -2a [24]. Therefore, specific attention should be paid to the stability of the formulation in regard to the prevention of protein aggregation.

In order to survey that the extrusion procedure did not induce a protein destabilisation IFN- $\alpha$  was extracted from the extrudates. The obtained samples were analysed by gel electrophoreses with subsequent silver staining (Figure 61). As shown in lane 3 and lane 6 only the band of monomeric IFN- $\alpha$  was detectable irrespective of the extrudate formulation.

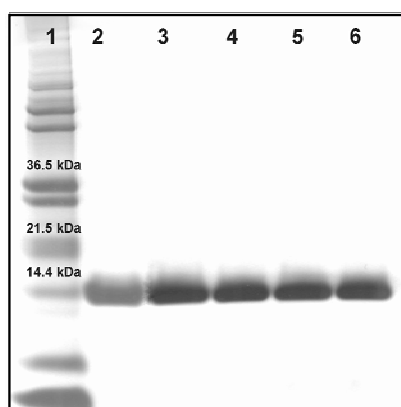


**Figure 61: Proof of protein integrity after extrusion.**

Lane 1: molecular weight marker, lane 2: IFN- $\alpha$  standard material, lane 3 to lane 6: IFN- $\alpha$  extracted from extrudates containing 0 %, 5 %, 10 % or 20 % PEG.

Consequently, it can be stated that the manufacturing process neither induced protein aggregation or fragmentation nor a polymorphic transformation of the lipid matrix. These encouraging results suggested further investigation of the in-vitro release kinetics.

#### 1.4. IN-VITRO RELEASE STUDIES

The addition of PEG to the lipidic matrix was an efficient tool to adjust the desired release kinetics of disc shaped lipid implants prepared by compression (see Chapter IV.1). Therefore, the in-vitro release behaviour of tristearin extrudates comprising various amounts of PEG was initially investigated.

It is obvious from Figure 62 that the addition of PEG to the lipidic formulation significantly affects the in-vitro release kinetics of IFN- $\alpha$ . Extrudates containing no

PEG liberated just 32.71 % (n=3, SD= 1.17 %) of the incorporated protein within 16 days. The protein was delivered mainly in the first seven days.

Admixing of 5 % PEG prolonged the liberation period to 16 days. Furthermore, the amount of totally delivered protein was raised to 66.43 % (n=3, SD=1.54 %). Complete protein recovery was achieved after 16 days when using a formulation with 10 % PEG or more.

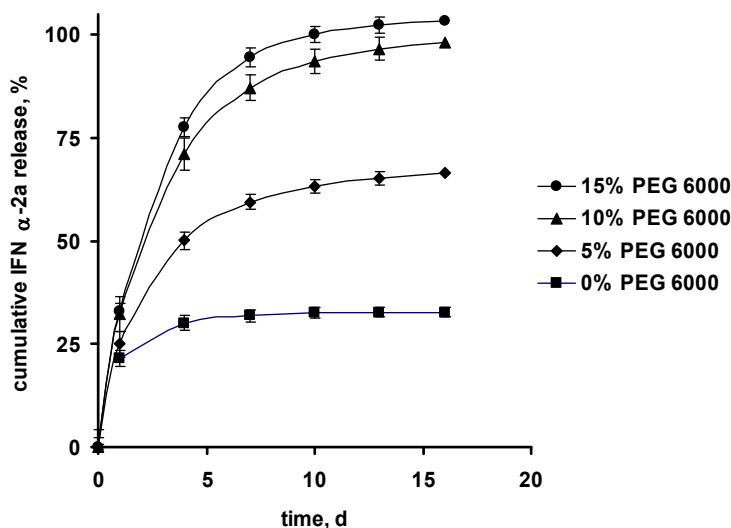


**Figure 62: Effects of the addition of various amounts of PEG on the release of IFN- $\alpha$  from extrudates (average,  $\pm$  SD; n = 3).**

The extrudates were prepared by ram extrusion. All devices were loaded with 10 % IFN- $\alpha$  co-lyophilised with HP- $\beta$ -CD and the indicated PEG amount (average  $\pm$  SD; n = 3).

In contrast to the results obtained with lipid implants prepared by compression, the addition of PEG enhanced the burst effects. For instance, PEG-free extrudates liberate 21.62 % (n=3, SD=1.97 %) within the first 24 hours, whereas admixing of 10 % PEG enhanced the burst effect to 32.36 % (n=3, SD=0.77 %).

It has to be noted that the released protein almost exclusively existed in its monomeric form. The amount of dimer fraction detected with size exclusion chromatography was less than 1.5 % during the entire in-vitro release study and irrespective of the PEG amount. To confirm this excellent protein integrity, liberated IFN- $\alpha$  was analysed by means of gel electrophoreses followed by silver staining. As visualised in Figure 63, gel electrophoresis featured that the protein was delivered in its monomeric form.

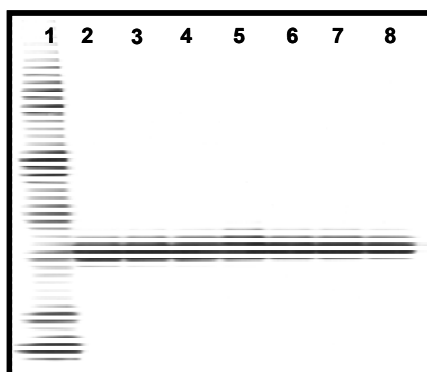


**Figure 63: Protein stability during in-vitro release.**

SDS-PAGE of IFN- $\alpha$  liberated from tristearin implants comprising 10 % PEG. Lane 1: molecular weight marker, lane 2: IFN- $\alpha$  standard material, lane 3: IFN- $\alpha$  released after 24 hours, lane 4: IFN- $\alpha$  released after 4 days, lane 5: IFN- $\alpha$  released after 7 days, lane 6: IFN- $\alpha$  released after 10 days, lane 7: IFN- $\alpha$  released after 13 days, lane 8: IFN- $\alpha$  released after 16 days.

The elevated amounts of liberated drug as well as the accelerated burst release observed with increasing PEG loadings are often ascribed to the ability of PEG to act as a porogen. When water soluble hydrophilic excipients, such as PEG, are added to an inert sustained release matrix these substances facilitate the creation of an interconnected pore network (see Chapter 1.5). As a result, a larger portion of the incorporated protein has access to water-filled pores and can diffuse out of the matrix, which accounts for increased recovery rates. On the other hand, the amplified pore formation reduces the geometric hindrance of the pore network, consequently the release is accelerated and the burst effect is often elevated [40, 40, 138, 174].

To investigate whether such effects occur due to the addition of PEG, the external morphology of the lipidic extrudates was studied by scanning electron microscopy before and after exposure to the release medium.

Before in-vitro release studies no significant differences in the morphology were visible between extrudates containing different amounts of PEG (data not shown). During incubation water-soluble substances (IFN- $\alpha$ , together with HP- $\beta$ -CD and PEG) were leaching out of the matrix into the bulk fluid. Accordingly, the SEM pictures of incubated extrudates revealed the formation of pores. A few small pores with a size between 2 to 5  $\mu\text{m}$  were formed at the surface of extrudates comprising no PEG (Figure 64 A). By increasing the PEG content the pore number per area and the pore size increased (Figure 64 B, C, D).

Interestingly, the shape of the pores changed: on the surface of PEG-free matrices circular pores were found, whereas the surface of PEG-comprising extrudates revealed more slit-like pores. This geometry might be generated in the course of

extrusion. The mechanical properties of PEG range from soft and plastic material for low molecular weights to hard and brittle for high molecular weights. For PEGs with an intermediate molecular weight, such as the here used PEG 6000, it was shown that the particles were easy to deform at low compaction speed and pressures [135]. Thus, it can be assumed that the stretched pores were formed due to the deformation of PEG particles during extrusion. By forcing the lipid/PEG blend through the small extruder die the PEG particles are racked along the extrudate axis. This hypothesis is further backed by the comparison to the pore structure of PEG-loaded compressed implants. In contrast to the morphology observed for extrudates, compressed samples revealed large, irregular formed pores at the implant surface (see Chapter IV, Figure 15).

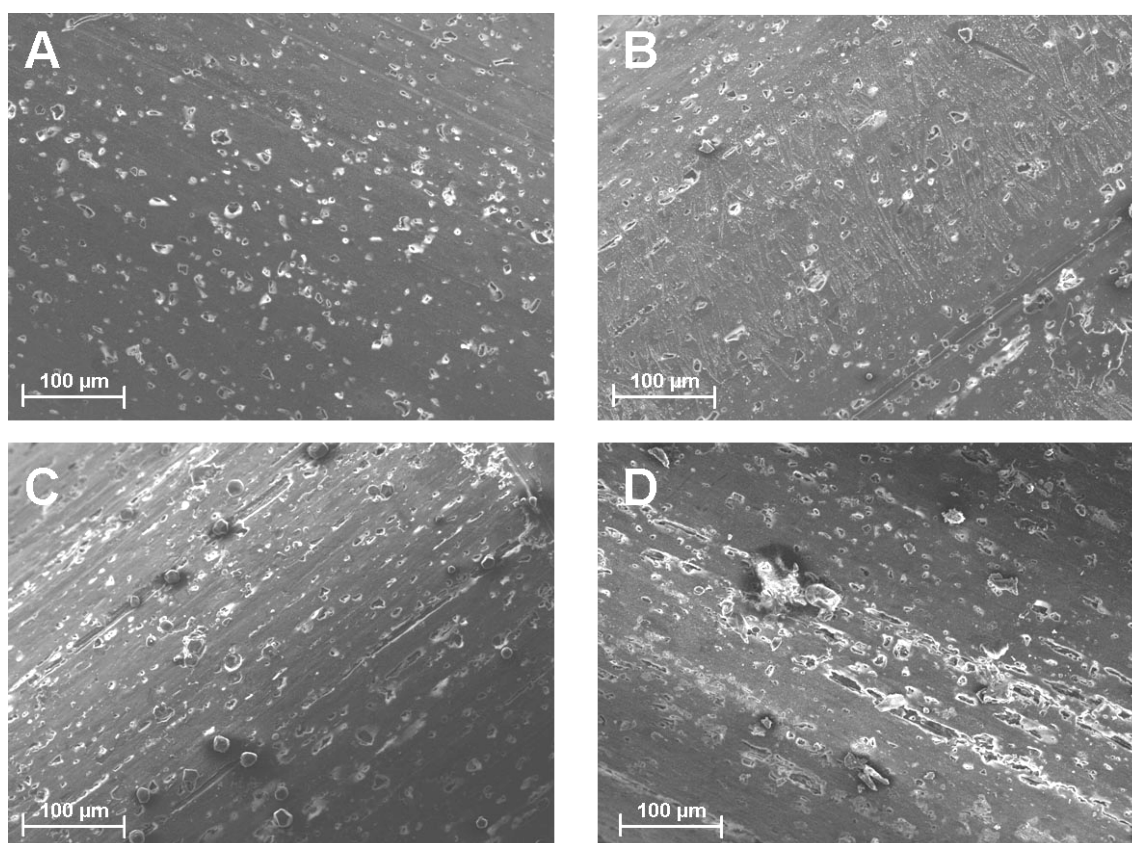


**Figure 64: External morphology of extrudates containing no PEG (A), 5%PEG (B), 15 % PEG (C) and 20 % PEG (D) after in-vitro release studies.**

As the extrudates featured a low coherence after in-vitro incubation, it was not possible to obtain cross-sections of incubated extrudates to study the internal implant morphology. On the other hand, the samples were too small to determine reliable implant porosities with a helium pycnometer or with mercury porosimetry (data not shown). Nevertheless, to get an idea about the relative ability of the pores to percolate the inert lipid matrix the water uptake of PEG-free and PEG-loaded

extrudates was investigated (Figure 65). This attempt was based on the report of Rabelo and Coutinho, that showed that the water uptake was in good agreement with the pore volume determined by means of mercury porosimetry measurements [177]. The water uptake was obtained from the weight difference between dry and wetted samples [177]. Recently, Pongjanyakul et al. used this simple technique to estimate the water uptake of lysozyme loaded glyceryl palmitostearate implants after in-vitro release studies [174]. Accordingly, at predetermined point of time the implants were removed from the incubation buffer, blotted dry, and weighed. Afterwards the extrudates were dried to constant mass and weighed again (see Chapter III.2.6).

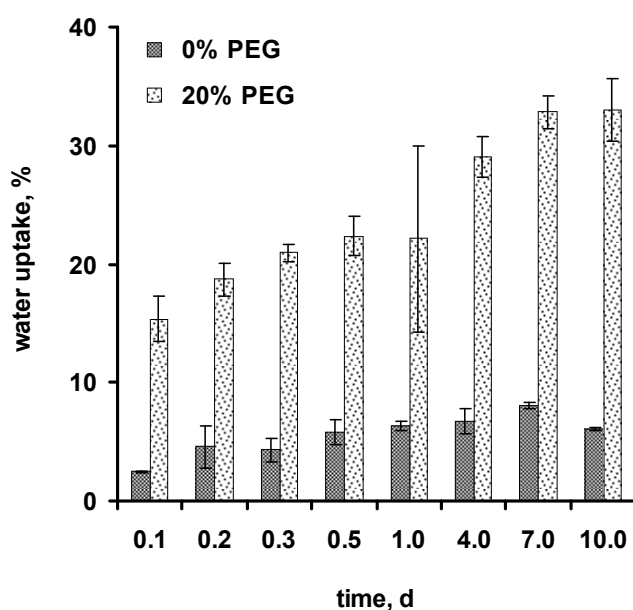


**Figure 65: Effect of PEG loading on the water uptake of tristearin extrudates.**

The extrudates were loaded with 10 % IFN- $\alpha$ /HP- $\beta$ -CD lyophilisate and the indicated amount of PEG. (average  $\pm$  SD; n = 3),

PEG-free extrudates incorporated not more than 7 % water (relative to the implant weight). In generally, it was suggested that at least 30-35 % water-soluble drug (and excipient) are necessary to create percolating diffusion pathways within inert matrices (see Chapter I.5). As the extrudates were only loaded with 10 % IFN- $\alpha$ /HP- $\beta$ -CD co-lyophilisate, an incomplete pore network through the matrix seemed probable. This assumption was backed by the restricted entry of water which indicated that the observed pores of PEG-free extrudates (Figure 64 A) were only located at the implant surface and were not penetrating the matrix. As a result, not all of the incorporated IFN- $\alpha$  had access to water-filled pores connected to the implant surface. Since tristearin matrices themselves did not erode [85, 240] and the

permeability of IFN- $\alpha$  through crystalline lipid can be considered as negligible, IFN- $\alpha$  was trapped within in the matrix. As a result, only 32.71 % (n=3, SD= 1.17 %) of the totally incorporated IFN- $\alpha$  were delivered from PEG-free extrudates (Figure 62).

In contrast, extrudates loaded with 20 % PEG revealed a water uptake of up to 36 % (Figure 65). Therefore, inside the implant an increased space for the imbedding of water was provided which indicated the formation of pores penetrating the matrix.

It can be concluded that the observed implant morphology as well as the water uptake agreed well with the protein release patterns shown in Figure 62. With a higher PEG content, the porosity of the lipidic matrices increased upon exposure to the release medium, resulting in enhanced IFN- $\alpha$  mobility and, hence, in increased protein release rates.

### **1.5. MECHANISMS OF PROTEIN RELEASE FROM EXTRUDED IMPLANTS**

In Figure 66 the in-vitro release kinetics of IFN- $\alpha$  from extruded and compressed implants are compared. Irrespective of the manufacturing method, implants comprising no PEG revealed nearly the same protein liberation characteristics. Bearing in mind that the initial protein/excipients load of these formulations was not sufficient to create an interconnected pore network through the device, only the fraction of protein located on the surface and/or in cavities adjacent to the surface was released upon immersion in aqueous buffer. As the relative amount of surface touched protein is a function of the matrix composition the protein liberation from extrudates and implants should be comparable.

A completely different scenario was found with PEG-loaded devices. Here, the protein release was significantly more extended when using compression as manufacturing method. Especially the burst release, which is shown exemplarily for a PEG loading of 20 % in Figure 66 F, was more accelerated from extruded implants. Furthermore, it was obvious that the total amount of recovered IFN- $\alpha$  at intermediate PEG loadings (5 and 10 %) was higher for extrudates.

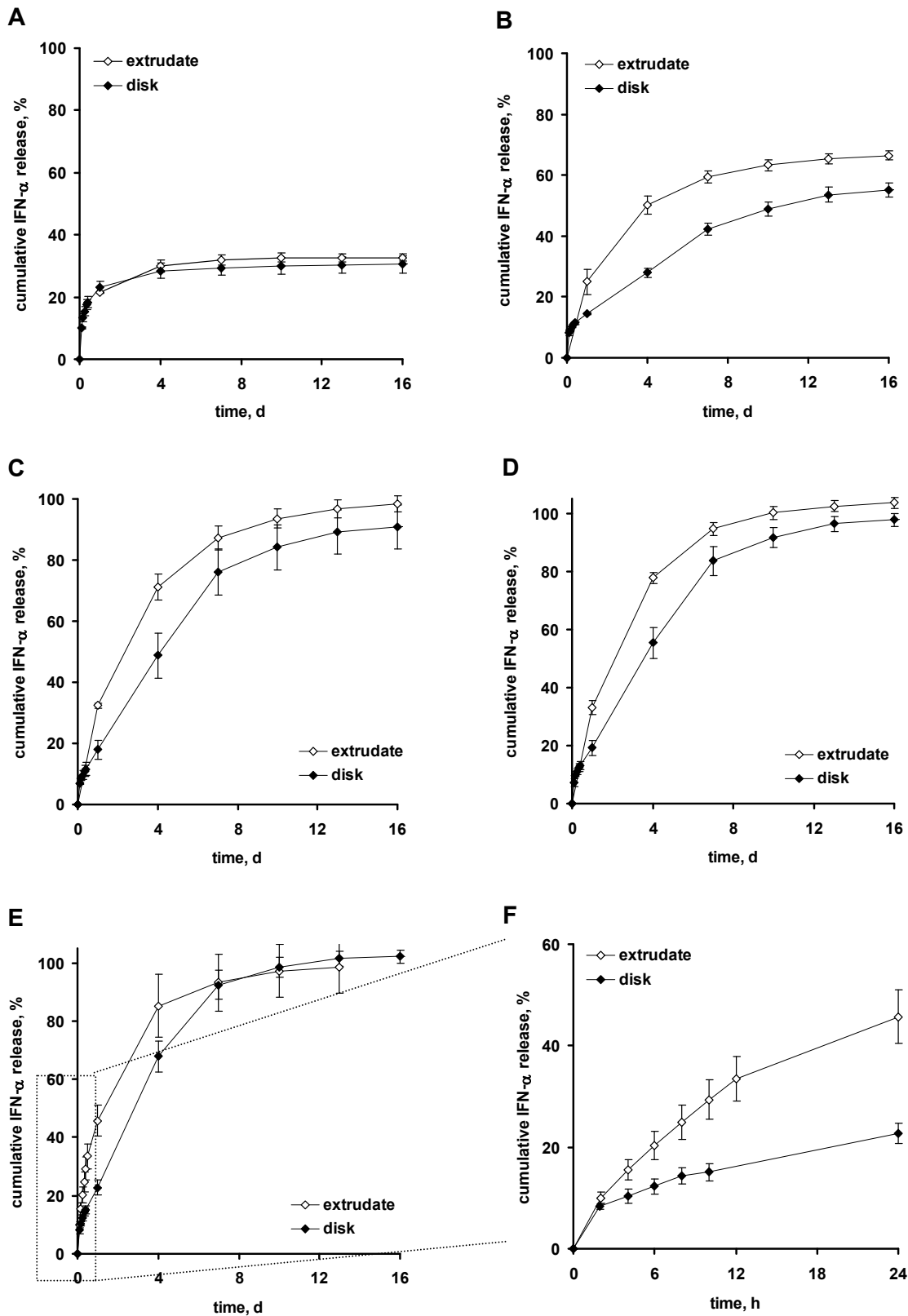


**Figure 66: Effect of the manufacturing procedure on the protein release.**

Cumulative in-vitro release rates from extruded (open symbols) and compressed (closed symbols) implants comprising 0 % (A), 5 % (B), 10 % (C), 15 % (D) or 20 % PEG (E, F). Each matrix was loaded with 10 % IFN  $\alpha$ -2a/HP- $\beta$ -CD lyophilisate (average,  $\pm$  SD;  $n = 3$ ).

The general acceleration of the protein release kinetics from extrudates can be ascribed to the modification of the cylinder geometry. The transfer of the manufacturing process to extrusion involved an extension of the implant height and a reduction of the implant diameter. The device shape changed from flat disks to slim rods (Figure 67).

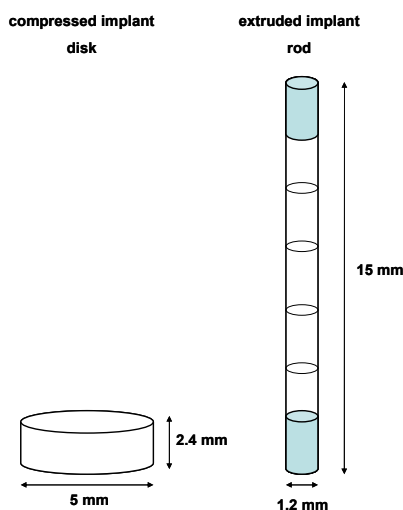


**Figure 67: Geometry of compressed and extruded implants.**

When decreasing the radius while keeping constant the height accelerated drug liberation can be expected. The same is observed when decreasing the height and maintaining the implant radius. When modifying the implant shape from disks to rods in order to enable adequate application, both parameters radius and length were varied simultaneously. Thus, the prediction of the impact on the release kinetics is difficult.

The available surface area is one of the crucial factors for the drug release. Thus, reduced or increased surface to volume ratios are often used to explain differences in the drug liberation rates. The accomplished change of the manufacturing procedure from compression to extrusion implied an increase in the surface to volume of the implants from 1.2 to 1.8. However, compared to literature such a slight increase in the surface to volume ratio cannot completely explain the tremendous alteration of the release profiles. For instance, a quite similar alteration of the surface to volume ratio - achieved by decreasing the height - did not affect the release kinetics of pyranine from lipidic implants based on tripalmitin [86].

This distinction can presumably be ascribed to the fact that the surface to volume ratios does not depict the actual geometric situation and the resulting diffusion pathways. To illustrate these effects the extrudate was schematically divided into

implants with the height of the disked shaped devices (Figure 67). Obviously, the axial diffusion ways were increased for five systems, whereas the radial diffusion pathways decreased for all seven subunits. Furthermore, due to the symmetry conditions the latter aspect is important for the diffusion along two dimensions, the x- and the z-plane. It can, therefore, be considered as being the more influential parameter.

Apart from the distinctions in the device geometry, the preparation procedures for rod and disk-shaped implants were quite different. Prior extrusion a force of 3.92 kN was applied for 30 s to compress the lipidic formulation within the extruder barrel. In comparison the standard method for the preparation of disked shaped implants included a compression at 19.6 kN for 30 s. In Chapter IV.1.1 the impact of various compression forces on the protein delivery rates was outlined. Although disk-shaped implants were investigated, it is highly conceivable that the reduced compression forces applied during extrusion will result in a less dense particle packaging. In fact, the calculated apparent densities of extrudates declined by 13 % compared to disk-shaped implants.

In summary, the presented considerations suggested that the accelerated protein release from extruded implants compared to compressed implants can be explained by both the alteration of the implant geometry and the reduction of the matrix compactness.

It is furthermore evident from Figure 66 that not only the release rates were affected by the manufacturing method, but also the shape of the release curves. PEG-containing disks revealed a nearly constant IFN- $\alpha$  release rate over at least seven days. In contrast, this linear phase was completely missed in the case of extrudates. Irrespective of the added PEG amount the release rates monotonically decreased with time, which led to a parabolic release profile.

In addition, the impact of PEG on the early protein liberation was found to be different for extruded and compressed implants. As described in Chapter IV.1.1, for the compressed implants the admixing of PEG resulted in a decrease of the burst effect. However, the opposite was observed with extruded implants.

To get a deeper insight into the involved mass transport phenomena, an analytical solution of Fick's second law of diffusion considering radial as well as axial mass transfer in cylinders with constant diffusion coefficients (see Equation 9,

Chapter I.5.3) was fitted to the experimentally determined release rates. This model takes into account the homogeneous distribution of the protein within the implants before exposure to the release media (at  $t = 0$ ), as well as sink conditions maintained throughout the experiments.

For the extruded implants good agreement between the theoretical and the experimental data was obtained in all cases, irrespective of the initial PEG loading of the implant ( $R^2 > 0.98$ ) (Figure 68 A). The release kinetics of IFN- $\alpha$  from compressed implants, however, showed systematic deviations between the applied mathematical theory and the experimentally measured protein release kinetics when PEG was added (Figure 68 B). This means, that the preparation method affected the drug release mechanism of PEG-loaded lipidic matrices. The protein release from a PEG-containing matrix was predominantly controlled by pure diffusion with constant diffusivities when the matrix was prepared by extrusion. Contrarily, for compressed matrices it was found that also other mass transport mechanisms were of importance for the protein liberation.

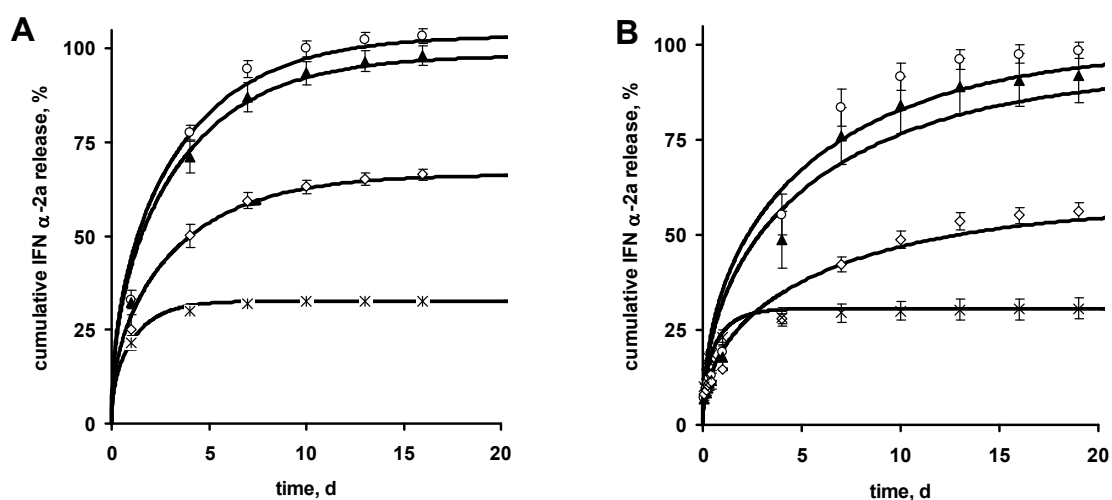


**Figure 68: Experiments (symbols) and theory (solid lines).**

Fittings of Equation 9, Chapter I.5.3 to the experimentally determined IFN- $\alpha$  release kinetics from implants prepared by ram extrusion (A) or by compression (B) containing various amounts of PEG: (\* ) 0 %, (◇) 5 %, (▲) 10 %, (○) 15 % (average  $\pm$  SD;  $n = 3$ ).

In Chapter IV the lower burst effect, the initial constant release rates, as well as the resulting deviations from pure diffusion controlled protein release from PEG-comprising disk-shaped implants were explained. It was shown that these phenomena can be ascribed to a reversible in-situ precipitation of IFN- $\alpha$  within the lipidic matrix. Therefore, the protein release from compressed devices was governed by both, the limited solubility of the protein and the diffusion through tortuous liquid-

filled pores. However, the reduced protein solubility in the presence of PEG seemed to be unimportant when using extruded matrices, since the release from these systems was primarily dominated by diffusion.

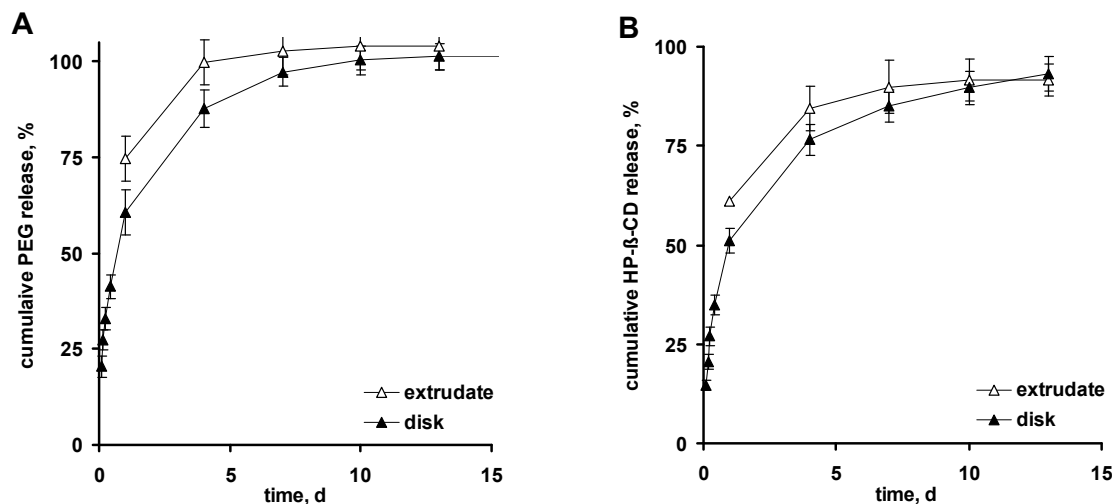


**Figure 69: Effect of the manufacturing procedure on the in-vitro release of PEG (A) and HP-β-CD (B).**

The release of PEG and of HP-β-CD was studied from implants prepared by compression (closed symbols) or by ram extrusion (open symbols) loaded with 10 % IFN-α/HP-β-CD lyophilisate and 10 % PEG (average  $\pm$  SD;  $n = 3$ ).

In order to understand these distinctions the in-vitro release kinetics of the incorporated excipients (PEG and HP-β-CD) were studied. In accordance with the protein release, the delivery of PEG and HP-β-CD from compressed implants was more sustained than the liberation from extrudates (in Figure 69 the release kinetics of matrices comprising 10 % PEG are shown, similar results were obtained with other PEG loadings).

Therefore, the accelerated leaching out of IFN-α, PEG, and HP-β-CD from extruded rods would lead to a faster creation of water-filled pores compared to compressed implants. Simultaneously, the amounts of PEG and IFN-α available within the implant pores were reduced. For instance, after 4 days PEG was already completely washed out from extrudates, whereas compressed disks still contained PEG. Summing up both effects – the accelerated increase of the available pore volume and the reduced amounts of PEG and IFN-α within the pores – it is highly conceivable that the actual concentrations of PEG generated within the extruded matrices were not high enough to cause precipitation of IFN-α. As a result, the protein liberation was purely governed by diffusion through water-filled pores. Therefore, in contrast to the “precipitation controlled release” from compressed implants, monotonically decreasing release

rates as well as increased burst effects were observed in the case of extruded implants.

## **1.6. FORMULATION FACTORS INFLUENCING PROTEIN RELEASE**

### **1.6.1. INFLUENCE OF THE USED TRIGLYCERIDE**

The matrix material itself is one of the crucial parameters for the design of controlled release devices. However, the impact of different triglycerides on the in-vitro release behaviour was sparsely investigated and from the few reports available no consistent conclusion can be drawn.

Guse et al. reported that the release of lysozyme from lipidic implants was accelerated when reducing the chain length of the esterified fatty acid. An exception from this rule was the protein liberation from tristearin matrices, which was found to be faster than the release from tripalmitin matrices (C12>C14>C18>C16) [84]. Recently, it was suggested that the decreasing velocities of lysozyme release with extension of the esterified fatty acid chain length can be explained with reduced wettability of the lipid [124]. However, the opposite was found for the release of the low molecular weight model compound pyranine. The triglyceride with the shortest fatty acids revealed the slowest release (C14>C18>C16>C12) [84].

Considering the work of Vogelhuber et al. [240], who also investigated the release of pyranine from different triglyceride matrices, the impact of the manufacturing process on the ranking order becomes apparent. In contrast to Guse, the drug loading was not performed by dissolving but by emulsifying the drug within the lipid solution. After vacuum drying the obtained drug-loaded lipid powder was compressed. Interestingly, the ranking order observed by Vogelhuber [240] was completely different from that reported by Guse [84]: the shorter the carbohydrate chain the faster the release.

More recently, Koennings et al. showed that lysozyme was liberated with decreasing velocity from mini-cylinders composed of trilaurin, trimyristin, tripalmitin or tristearin [124].

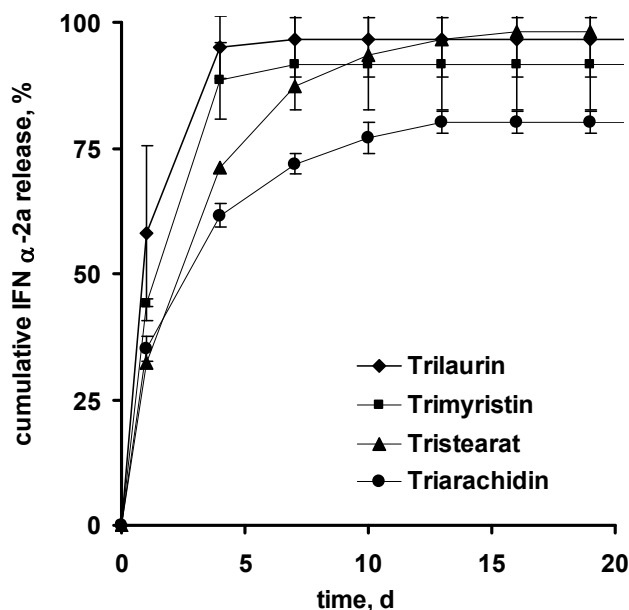


**Figure 70: Effect of different triglyceride matrices on the in-vitro release of IFN- $\alpha$ .**

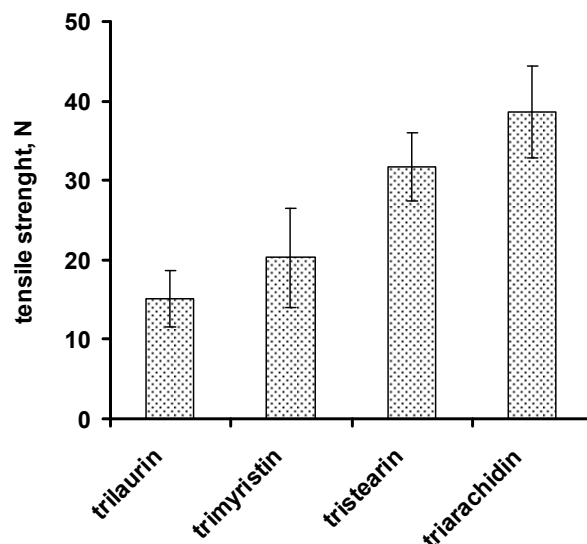
All extrudates were loaded with 10 % IFN/HP- $\beta$ -CD lyophilisate and 10 % PEG (average  $\pm$  SD; n=3).

Figure 70 illustrates the release profiles of IFN- $\alpha$  from ram extruded tristearin matrices in comparison to matrices based on other triglycerides. A total of approx. 32-35 % of IFN- $\alpha$  was released within the first 24 hours from matrices comprising tristearin and triarachidin, respectively. The initial burst was amplified to 44-58 % when the carbohydrate chain was shortened. After the burst, matrices of trimyristin and trilaurin delivered the remaining protein within 4 days. Contrarily, the usage of the longer chained triglycerides facilitates a more delayed protein liberation, enduring over 13 days.

Apart from the release rate the amount of totally delivered protein was also affected by the utilised triglyceride. Protein release was found to be complete in the case of tristearin, trilaurin and trimyristin extrudates. Matrices comprising triarachidin liberated around 80 % of the incorporated drug within 20 days.

It was observed that extrudates based on triglycerides of the short-chained fatty acids revealed a reduced mechanical stability. To investigate this effect the crushing strength of freshly prepared extrudates was determined (Chapter III.2.2). As it can be seen in Figure 71, the mechanical strength of triglyceride extrudates increased in the same order as the fatty chain length of the used triglyceride increased. Since the crushing strength is determined by the interparticular bonding forces and the density of the matrix, it can be assumed that the more sustained release from extrudates

based on triglycerides with longer carbohydrate chains might be a result of the more consolidated particle arrangement.



**Figure 71: Effect of triglyceride type on the crushing strength of freshly prepared extrudates (average  $\pm$  SD; n=3).**

### 1.6.2. INFLUENCE OF PARTICLE SIZE

Particle size and shape are important parameters for the arrangement of drug and matrix particles during compression [112]. Since the particle arrangement determines the pore characteristics, the in-vitro release kinetics may depend on the particle size. Generally, an increase in particle size of the drug material causes increased release rates because the direct contact to the matrix surface is more likely [112, 205]. In addition, the particle size of the matrix substance is crucial, when the release occurs from an interconnected pore network. The use of larger particles usually extends the interparticular voids within compressed matrices. Accordingly, accelerated release rates were found [84, 112].

To investigate whether such relations between particle size and release kinetics are also relevant for extruded matrices the particle size of the lipid material was varied. Particle size measurement of tristearin bulk material by laser light scattering revealed that 90 % of the particles of tristearin bulk material already have a size smaller than  $96.74 \mu\text{m}$  ( $d(0.9)$ ). Aiming for a prolongation of the IFN- $\alpha$  release, the large particles were eliminated by sieving the lipid bulk material.

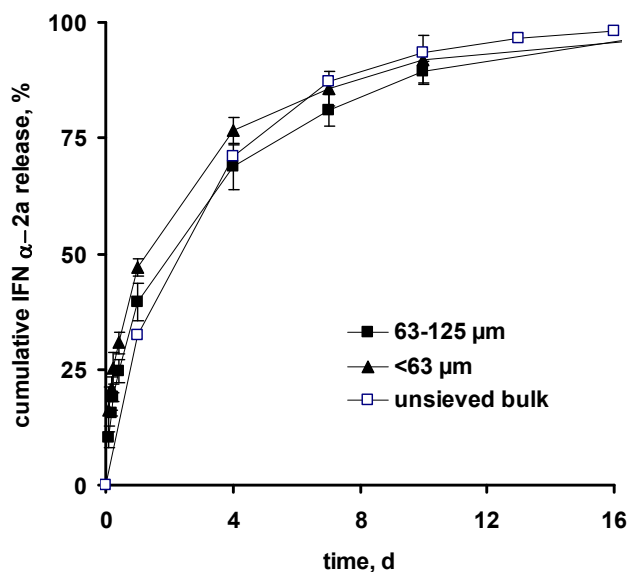


**Figure 72: Effects of different particle size of the lipid powder on the in-vitro release kinetics of IFN- $\alpha$ .**

All extrudates were loaded with 10 % PEG and 10 % IFN- $\alpha$  co-lyophilised with HP- $\beta$ -CD (average  $\pm$  SD; n = 3).

Applying the additional sieving step the width of the particle size distribution (span) was reduced from 3.0 to 2.2 and the  $d(0.9)$  value was shifted to 48.69  $\mu\text{m}$ . However, as shown in Figure 72, the reduction of the particle size did not lead to a more extended in-vitro release. The release kinetics of IFN- $\alpha$  from extrudates containing the sieved tristearin material are almost superimposed with that obtained from extrudates containing unsieved bulk material.

Therefore, it can be concluded that the pore characteristics of extruded implants were not importantly affected by the modification of the particle size distribution of the matrix material. To back up this observation the mesh-plus was also utilised for extrudate preparation. Obviously, extrudates prepared from this sieve fraction liberated IFN- $\alpha$  in the same manner as extrudates prepared with smaller lipid particles.

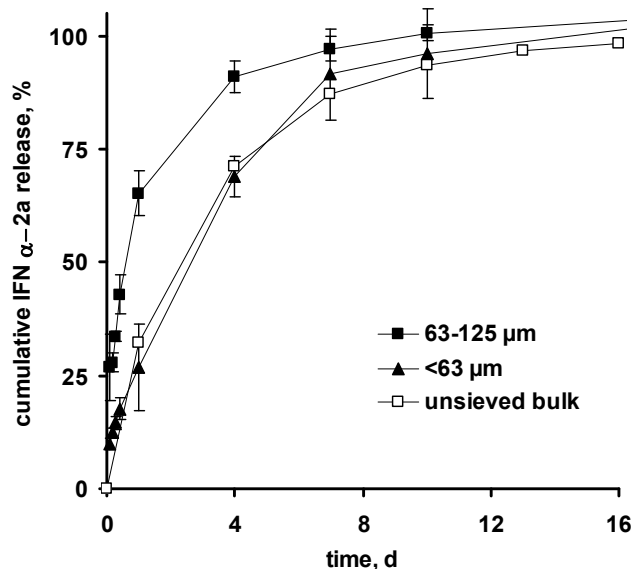


**Figure 73: Effects of different particle size of the porogen on the in-vitro release kinetics of IFN- $\alpha$ .**

All extrudates were loaded with 10 % PEG and 10% IFN- $\alpha$  co-lyophilised with HP- $\beta$ -CD (average  $\pm$ SD; n = 3)

In a second experiment the particle size distribution of the pore-forming agent PEG was modified. In analogy to the lipid powder, PEG was sieved and the fraction below 63  $\mu\text{m}$  and between 63 and 125  $\mu\text{m}$  were collected for implant preparation. In Figure 73 the impact of the particle size of PEG on the in-vitro release behaviour of IFN- $\alpha$  is illustrated. Faster protein release was observed with larger particles.

The impact of the size of porogen particles on the drug release kinetics from inert matrices is non-consistently discussed in literature. Accelerated as well as more delayed drug delivery profiles are reported. For instance, when sucrose acts as porogen in tripalmitin implants, the use of smaller particles resulted in a faster release of the model drug pyranine [86]. On the other hand, it is conceivable that the porogen particle sizes act on the release kinetics in a similar way like different particle sizes of the drug. In that case the loading of larger particle would provide the formation of larger channels and pores within inert matrices. Thus, the diffusion of water into and of drug out of the device is facilitated which in turn accounts for accelerated drug release rates. Such effects were reported for the liberation of the low molecular weight drugs cefadroxil as well as for the release of the polypeptide hirudin from polyurethane matrices with PEG 1450, mannitol, or BSA as porogen [118, 120].

### 1.6.3. EXCIPIENTS TO MODIFY THE EROSION BEHAVIOUR

During in-vitro release compressed matrices based on tristearin showed no erosion [151, 153]. These findings were recently verified in-vivo. After a 2 months subcutaneous implantation into rabbits, the tristearin matrices maintained their geometry and showed no signs of matrix erosion [141].

In accordance to these results, extruded tristearin matrices featured no signs of erosion during in-vitro release studies. However, with regard to patient compliance erodible systems are preferred, since non-erodible controlled release devices need to be removed surgically after drug depletion.

Recently, it was shown for cylindrical implants based on tripalmitin that the admixing of phospholipids to a triglyceride matrix enabled in-vivo and in-vitro erosion [85, 86].

Therefore, it was decided to investigate the potential of phospholipid incorporation to facilitate erosion of the tristearin-based extrudates. Phospholipids are amphiphile compounds that belong to the class of water insoluble lipids, which swell in water and form a liquid crystalline hydrated phase [200]. Hence, the addition of distearoyl-phosphatidyl-choline (DSPC) to the triglyceride formulation resulted in an increased water uptake of the matrix (Figure 74). Compared to pure tristearin extrudates, matrices containing 5 % DSPC already revealed a 5-fold increased water uptake. It can be assumed that this amplified water infiltration in combination with the swelling behaviour of phospholipids diminished the coherence of the tristearin particles during release. Consequently, the mechanical stability of the device was reduced and erosion of the lipidic device took place. As it can be seen in Figure 74, the water-uptake correlated well with the erosion behaviour of the implants.

However, if erosion and release occurred simultaneously, this would be accompanied with accelerated drug liberation. For lipid based drug delivery systems Khan et al. showed good correlation between the release rates of BSA and the erosion rates of matrices comprising cholesterol and lecithin [117].

In accordance with this study, an increase in the DSPC amount resulted in less sustained protein liberation (Figure 75). The protein delivery from extrudates comprising 20 % DSPC was already completed within one day. Contrarily, the liberation of IFN- $\alpha$  occurred in a sustained manner over 16 days when no more than 5 % DSPC were added. The overall protein release from these matrices was comparable to that without DSPC. With 10 % DSPC an intermediate release profile was obtained.

Obviously, the effects of DSPC on the protein release behaviour agreed well with the increased water-uptake and erosion rates of DSPC-loaded matrices. For instance, the enormous burst release from extrudates containing 20 % DSPC was accompanied by a macroscopic visible erosion of the extrudate surface. Within 16 days of incubation these extrudates strongly disintegrated. However, the protein delivery was not sustained and thus, the addition of such high amounts of DSPC should be avoided.

Matrix erosion still occurred when 10 % or 5 % DSPC are incorporated. Since matrices still revealed a delayed protein delivery such formulations propose an appropriate balance between sustained release and degradation.

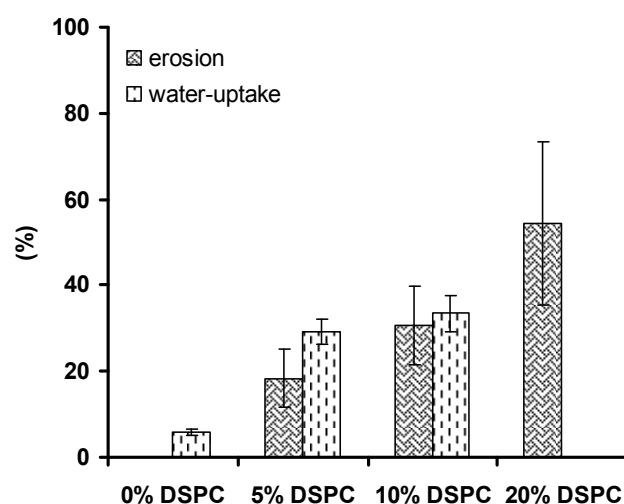


**Figure 74: Effect of DSPC on the water uptake and the in-vitro erosion behaviour of tristearin extrudates.**

Besides the indicated DSPC amount, all implants were loaded with 10 % PEG and 10 % IFN- $\alpha$ /HP- $\beta$ -CD lyophilisate. Since samples containing 20 % DSPC disintegrated to a large extent, the determination of the water uptake was not possible.

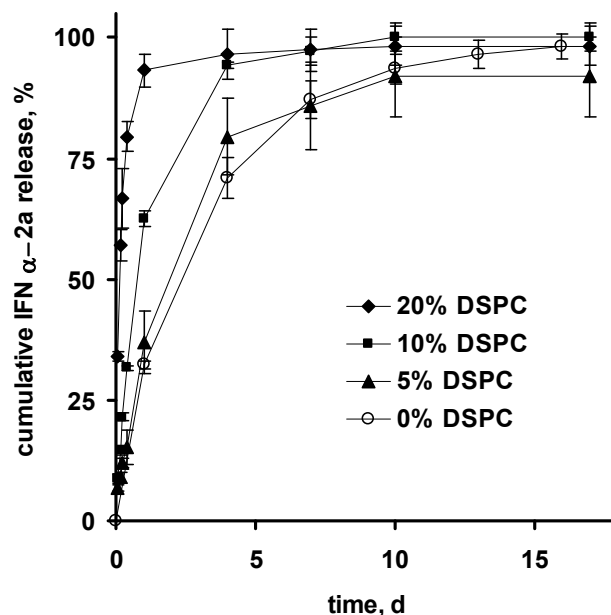


**Figure 75: Effect of distearyl-phosphatidyl-choline (DSPC) on the in-vitro release kinetics of IFN- $\alpha$  from tristearin based extrudates.**

All extrudates were loaded with 10 % PEG and 10 % IFN- $\alpha$  co-lyophilised with HP- $\beta$ -CD (average  $\pm$  SD; n = 3).

For PLGA matrices it was proven that degradation products and/or increased hydration of the matrix affect protein stability during release (see Chapter I.2.2). However, SEC-HPLC analysis of released IFN- $\alpha$  revealed only a minor fraction of dimer specimen (less than 1.5 %). This excellent protein integrity was further backed by gel electrophoresis. As illustrated in Figure 76 only monomeric IFN- $\alpha$  was detectable over the entire incubation period.

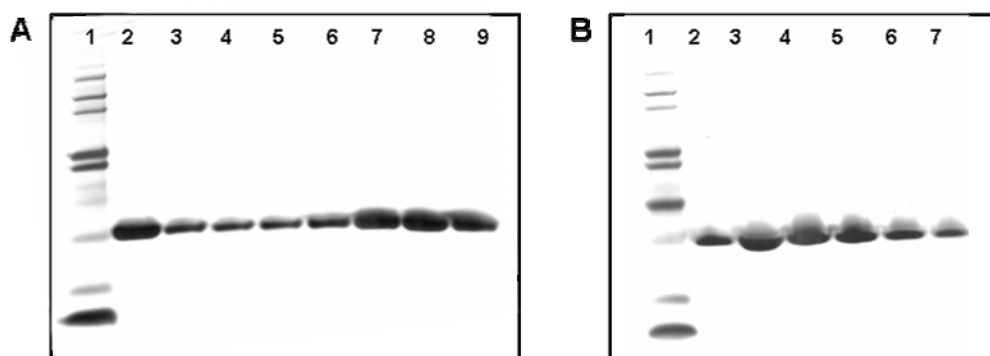


**Figure 76: Effect of DSPC on the protein stability.**

SDS-PAGE of IFN- $\alpha$  liberated from tristearin implants comprising 5 % DSPC (A) and 20 % DSPC (B), respectively. Lane 1: molecular weight marker, lane 2 IFN- $\alpha$  standard material, lane 3 IFN- $\alpha$  released after 2 hours, lane 4 IFN- $\alpha$  released after 4 hours, lane 5 IFN- $\alpha$  released after 6 hours, lane 6 IFN- $\alpha$  released after 10 hours, lane 7 IFN- $\alpha$  released after 24 hours, lane 8: IFN- $\alpha$  released after 4 days, lane 9: IFN- $\alpha$  released after 7 days.

## 1.7. SUMMARY AND CONCLUSION

This chapter shows that lipidic extrudates loaded with IFN- $\alpha$  can be prepared as controlled release systems. The developed extrusion procedure did not induce any polymorphic transformations. Hence, the obtained implants comprised the lipid material in the stable  $\beta$ -modification. With respect to increased storage stability and more sustained protein liberation the stable modification is preferable (see Chapter I.3.3). Furthermore, an important attainment of this study was that the protein integrity was not affected by the extrusion process. Moreover, no detrimental effects occurred during release. Thus, protein stability was maintained within the lipidic matrix, and IFN- $\alpha$  was delivered from tristearin extrudates almost exclusively in its monomeric form.

The addition of PEG was shown to be an efficient tool to adjust the in-vitro release kinetics. Below a PEG loading of 10 % the protein recovery was incomplete but with increasing the PEG loading the amount of liberated IFN- $\alpha$  increased. The observed implant morphology agreed well with the protein release patterns – due to the addition of PEG the creation of an interconnected pore network was facilitated.

Interestingly, the comparison to compressed tristearin implants introduced in Chapter IV revealed that not only the protein release kinetics, but also the underlying drug release mechanism was affected by the change of the manufacturing method. The implant shape was changed from disk-like implants to slim rods. Furthermore, the density of the implants decreased, as significantly lower compression forces were applied to prepare extrudates. Both effects accounted for less sustained protein delivery from extruded implants. The fitting of an adequate solution of Fick's second law of diffusion to the experimental release data revealed a purely diffusion controlled protein release, irrespective of the initial PEG load of the matrix. In contrast, in PEG-loaded disk-shaped implants IFN- $\alpha$  was precipitated within the pores and thus systematic deviations to a pure diffusion controlled release were found (see Chapter IV). This distinction between compressed and extruded implants could be correlated well with the release of PEG, which was much faster from extrudates. As a result, the actual PEG concentrations within the implant pores can be assumed to be insufficient to cause protein precipitation.

Since the release of IFN- $\alpha$  from extrudates was only sustained over 16 days, several attempts to extend the release time were investigated. Within this framework the effect of various particle sizes of the porogen and the matrix material were

investigated. An increase in the particle size of PEG resulted in accelerated protein delivery, whereas little deviations of the particles size of tristearin had no impact on the release properties.

Another important parameter was the triglyceride used. It was found that the liberation of IFN- $\alpha$  proceeded faster from matrices comprising triglycerides of shorter chain length fatty acids. This acceleration of the release can presumably be explained by a reduced consolidation of the device, as the compactness of the implant decreased with decreasing the chain length of the esterified fatty acids.

However, none of the approaches led to an appropriate prolongation of the IFN- $\alpha$  release. Therefore, it was decided to investigate the potential of twin screw extrusion for the preparation of protein-loaded lipidic implants.

## 2. MANUFACTURING OF EXTRUDATES BY TWIN SCREW EXTRUSION

The manufacturing of commercially available, subcutaneous implants is mostly accomplished by means of screw extrusion [121]. Compared to ram extrusion screw extrusion offers the advantage of a continuous operation mode facilitating the processing of large amounts of material (see Chapter I.4.3). In the previous section it was shown that ram extrusion is generally capable to produce small-sized implants for subcutaneous injection via a trochar. However, the liberation period of IFN- $\alpha$  was terminated after 16 days. The need for a prolonged release period in combination with the ease of up-scaling in later stages gave reason to investigate the potential of twin-screw extrusion for the production of lipid-based implants.

### 2.1. EXPERIMENTAL SETUP

The possibility to produce lipidic implants by twin screw extrusion was evaluated in lab-scale with the micro twin-screw MiniLab<sup>®</sup> Micro Rheology Compounder (Thermo Haake GmbH) illustrated in Figure 77. Compared to common twin screw extruders which usually require large amounts (>100 g) for extrusion, this extruder was especially designed for the handling of small amounts (starting at 5 g). Via an integrated back flow channel the filled-in sample can be circulated, allowing the blending of the material during extrusion. In addition, this back flow channel was constructed as rheological slit capillary with two pressure sensors. This enabled to obtain rheological information on the flow behaviour of the sample.

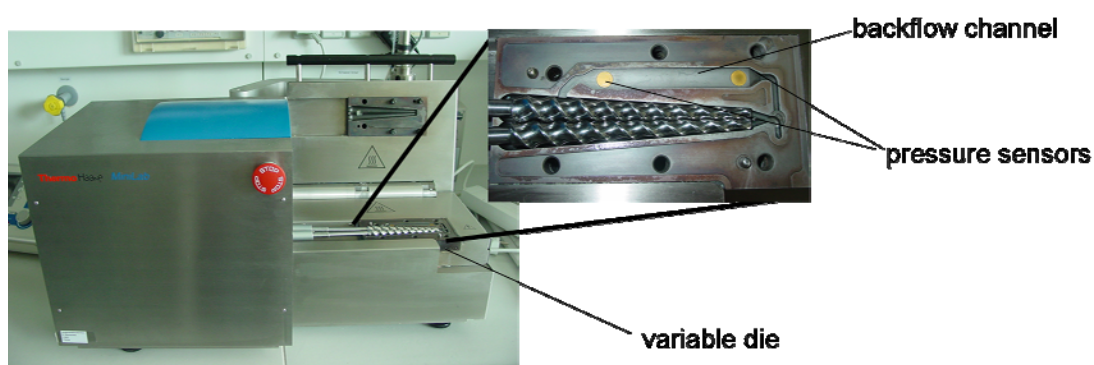


Figure 77: Twin screw extruder MiniLab<sup>®</sup> Micro Rheology Compounder

As explained above (Chapter I.4) the preparation of polymeric implants is mostly realised by hot-melt extrusion. Therefore, it was tried to prepared placebo implants based on the standard formulation (80 % tristearin, 10 % HP- $\beta$ -CD lyophilisate and 10 % PEG) by heating the extruder barrel.

The melting point of tristearin is at 71 °C. Thus, the applied temperature was varied from 65 to 72 °C in steps of one degree. Before loading the barrel, the extruder was heated for 30 minutes to ensure a uniform tempering.

However, clogging of the extruder occurred after loading, when the applied temperatures were lower than 70 °C. Variations in the rotation speed of the screws also failed to avoid this clogging and a complete filling of the extruder was not achieved.

On the other hand, tristearin was completely molten within the extruder at higher temperatures. Due to the associated decrease in viscosity, this attempt failed to create sufficient pressures for forcing the material through the extruder die.

Tristearin exhibits a very sharp melting point, which presumably explains the failure of hot-melt extrusion of pure tristearin material: below the melting point filling of the extruder was not possible, whereas temperatures above the melting resulted in low viscosity melts inapplicable for extrusion.

In order to obtain an extrudable lipidic mass the following approaches were evaluated:

- (1) admixing of oils or semi-softened lipids,
- (2) suspending the lipid in highly concentrated PEG solutions,
- (3) dissolving the lipid in an organic solvents,
- (4) admixing of low-melting point lipids.

All manufacturing strategies were conducted with a formulation comprising 10 % PEG and 10 % HP- $\beta$ -CD placebo-lyophilisate. The approaches were ranked according to the quality of the obtained extrudates and to the extrudability of the obtained lipidic mass.

### **2.1.1. ADMIXING OF OILS OR SEMI-SOFTENED LIPIDS**

In the first attempt various amounts of tristearin were replaced by Miglyol 812<sup>®</sup>. Miglyol 812<sup>®</sup> is a neutral oil based on triglycerides of caprylic and capric acid. An addition of 27 % Miglyol<sup>®</sup> to the standard formulation resulted in the formation of a rubbery mass that was convertible to extrudates without heating.

As the rods revealed a quite low breaking strength of around 8 N the amount of Miglyol<sup>®</sup> was reduced. For instance, for extrudates with a Miglyol<sup>®</sup> content of 16 % a tensile strength of approximately 15 N was measured. However, a further decrease of the Miglyol<sup>®</sup> fraction did not further enhanced the mechanical stability of the

extrudates and on the other hand, a minimum amount of 13 % Miglyol<sup>®</sup> was necessary to provide extrusion.

Alternatively to Miglyol<sup>®</sup>, the semi-soften lipid Softisan 378<sup>®</sup> was admixed to the blend of tristearin, PEG, and cyclodextrin. In analogy to the results obtained with Miglyol<sup>®</sup>, extrusion could be handled after admixing of 16 % Softisan 378<sup>®</sup>. However, these extrudates were less compact compared to those obtained by the addition of Miglyol<sup>®</sup>.

In Figure 78 Miglyol<sup>®</sup>-containing extrudates are displayed. In order to estimate the homogeneity of the produced extrudates 1 % of methylene blue was added to the lipidic formulation. The extrudates revealed a uniform blue staining, independent whether the rods were received at the start or at the end of the extrusion procedure. As a consequence, it can be concluded that a homogeneous drug distribution can be achieved.

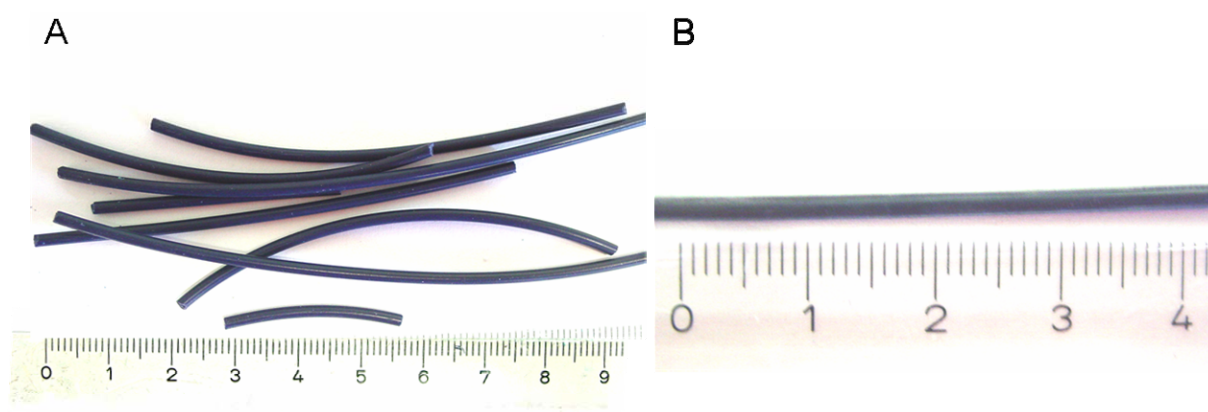


**Figure 78: Appearance of extrudates based on 10 % PEG, 10 % HP- $\beta$ -CD, 16 % Miglyol<sup>®</sup>, 64 % tristearin and 1 % methylene blue.**

### **2.1.2. SUSPENDING THE LIPIDIC MATERIAL IN A HIGHLY CONCENTRATED PEG SOLUTION**

Here an adjustment of the viscosity of the lipidic mass for extrusion was aimed by wetting the lipidic blend with a highly concentrated PEG solution. The idea behind this experiment was to avoid the lyophilisation step of IFN- $\alpha$  before implant manufacturing. IFN- $\alpha$  can be quantitatively precipitated/crystallised by a highly concentrated PEG solution (Chapter IV.2). These protein crystals may provide a higher protein stability, allowing the handling at elevated pressures and shear stresses.

Tristearin powder was wetted with a solution comprising either 40 % (wt/wt) PEG or 50 % (wt/wt) PEG (5 g of lipidic mass were wetted with 2.5 mL or 2.0 mL PEG solution, respectively). Extrusion was possible with the obtained lipid slurry. However,

extrusion ground to a halt after the delivery of a strand with a length of approximately 10 cm. Due to this low yield extrusion by wetting of the lipidic mass with an aqueous PEG solution was not further investigated.

### 2.1.3. DISSOLVING THE LIPIDIC MATERIAL IN AN ORGANIC SOLVENT

As illustrated in Chapter 1.4.3, Zhu and Schwendeman prepared PLGA minicylinders by suspending the protein in a solution of PLGA. The obtained PLGA-slurry was then extruded through a needle [262]. In order to transfer such a manufacturing procedure to twin screw extrusion of lipids various quantities of hexane were added to dissolve a certain amount of the lipid. The dissolution of the lipid was supposed to provide a softening of the lipidic mass. On the other hand, a certain minimal viscosity of the material was needed for increasing the pressure within the extruder and thereby forcing the material through the extruders die. Hexane was chosen as solvent providing an acceptable stability of lyophilised IFN- $\alpha$  suspended within this solvent [94].

The addition of 25 %, 30 %, and 40 % hexane to the blend of tristearin, PEG, and HP- $\beta$ -CD, respectively, facilitated extrusion at room temperature. After evaporating the organic solvent the extrudates exhibited an improved mechanical stability. In comparison to the extrudates containing Miglyol<sup>®</sup> the tensile strength increased up to 37.3 N (SD=8.7, n=5).

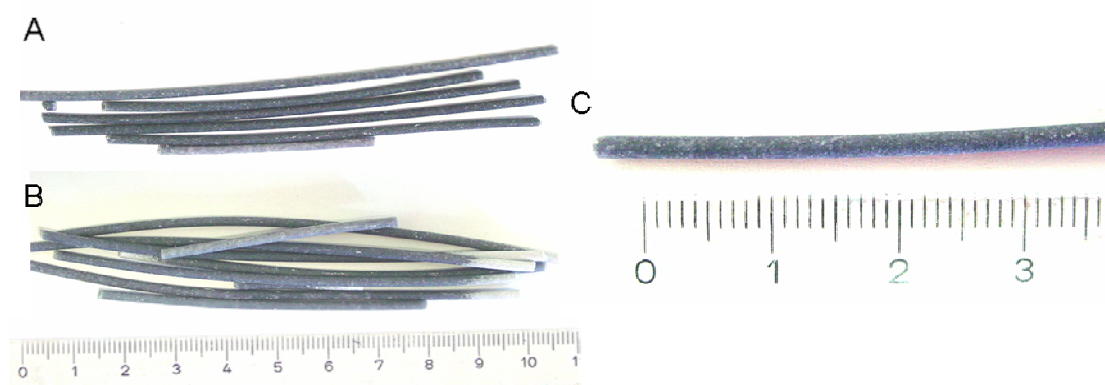


**Figure 79: Extrudates based on tristearin, PEG, and HP- $\beta$ -CD wetted with various amounts of hexane.**

1.5 g hexane (A) and 2 g hexane (B) were added to 5 g of lipidic formulation comprising 10 % PEG, 10 % HP- $\beta$ -CD, 79 % tristearin, and 1 % methylene blue. Figure C is a magnification of A.

However, as illustrated in Figure 79 the extrudates revealed a non-uniform methylene blue staining – darker and brighter areas were visible within one rod (Figure 79 C) – indicating different methylene blue contents in these regions. In addition, some extrudates revealed a complete depletion of methylene blue at their edges.

This heterogeneous methylene blue distribution as well as the general concerns associated with the use of organic solvents (see Chapter I) led to the decision that manufacturing of extrudates by suspending the material within organic solvents is unsuitable for the preparation of lipidic extrudates.

#### 2.1.4. ADMIXING OF LOW MELTING POINT LIPIDS

Finally various amounts of tristearin were replaced by alternative lipids with a melting point lower than that of tristearin. Thereby, selective melting of the low-melting point lipid should provide a softening of the lipidic mass during the manufacturing procedure. On the other hand, the re-solidification of the lipid mass after extrusion should offer the benefit of an increased mechanical stability.

First, tristearin was replaced by the mixed-acid triglyceride H12. H12 is a triglyceride based on saturated, even-numbered, unbranched, natural fatty acids. In particular the fatty acid composition is: 71 % lauric acid, 27 % myristic acid and 2 % palmitic acid. As H12 melts at 36 °C, the extruder was heated to 40 °C in order to ensure a complete melting of H12 during manufacture.

In a preliminary study the amount of H12 needed for acceptable extrusion was explored. Initially, 40 % H12 were applied, allowing the filling of the extruder. However, as visualised in Figure 80 A, the obtained rods were not solidified after leaving the extruder outlet. By stepwise reduction of the amount of the low melting point fat stable extrudates could be produced. The optimum amount of H12 was found to be 16 % (Figure 80 C).

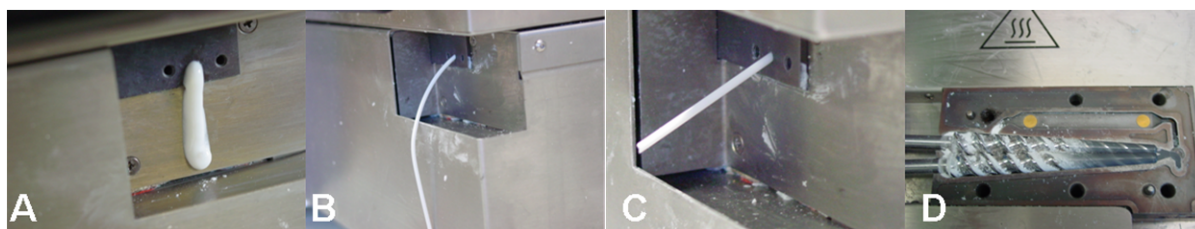


**Figure 80: Effect of H12 addition on extrusion.**

The formulations based on 10 % HP- $\beta$ -CD, 10 % PEG and 40 % H 12 and 40 % tristearin (A), 24 % H12 and 56 % tristearin (B), 16 % H12 and 64 % tristearin (C), and 8 % H12 and 72 % tristearin (D) were extruded, respectively.

Reducing the admixed content of H12 from 40 % to 16 % led to an increase in the torque from ~7 Ncm to ~14 Ncm. At a constant screw rotation speed of 40 rpm this increase suggested an increasing viscosity of the semi-soft mass generated during extrusion. A further reduction of the H12 content to 8 % resulted in a torque of 100-150 Ncm which was accompanied with a grey staining of the extrudates (Figure 80 D), which implied material abrasion from the barrel.

Based on these results it was concluded that an extrudable formulation should contain 16 % to 24 % of a compound which melts during extrusion. In order to evaluate if this formulation strategy was transferable to other lipid combinations the low-melting point lipid or high-melting point lipid were substituted.

Instead of H12 the triglyceride E85 was used. E85 is also a mixed-acid triglyceride but in comparison to H12 the amount of myristic acid is increased accounting for a melting point of 41 °C. Thus, extrusion was performed at a temperature of 45 °C. In accordance with formulations containing H12 an addition of 16 % E85 facilitated a continuous extrusion. In order to evaluate if the developed manufacturing procedure is also applicable for lipidic blends based solely on mono-acid triglycerides H12 was replaced by trilaurin. As the melting point of trilaurin is 43 °C the extruder barrel was heated to 47 °C which allowed extrusion with a trilaurin content of 16 %.

In a second attempt tristearin was substituted by tripalmitin or triarachidin. As H12 was used as low-melting point lipid, the extruder was heated to 40 °C to allow softening. However, only with triarachidin a convenient extrusion procedure could be established. Substituting tristearin by tripalmitin rendered filling of the extruder possible, but no extrusion occurred. To increase the pressure within the barrel the extruder was cooled down to 35 °C. Afterwards extrusion could also be performed with the triplamitin material.

Irrespective of the formulation the extrudates revealed a uniform methylene blue distribution. In Figure 81 extrudates comprising a H12/tristearin blend and extrudates based on trilaurin/tristearin are exemplarily illustrated.

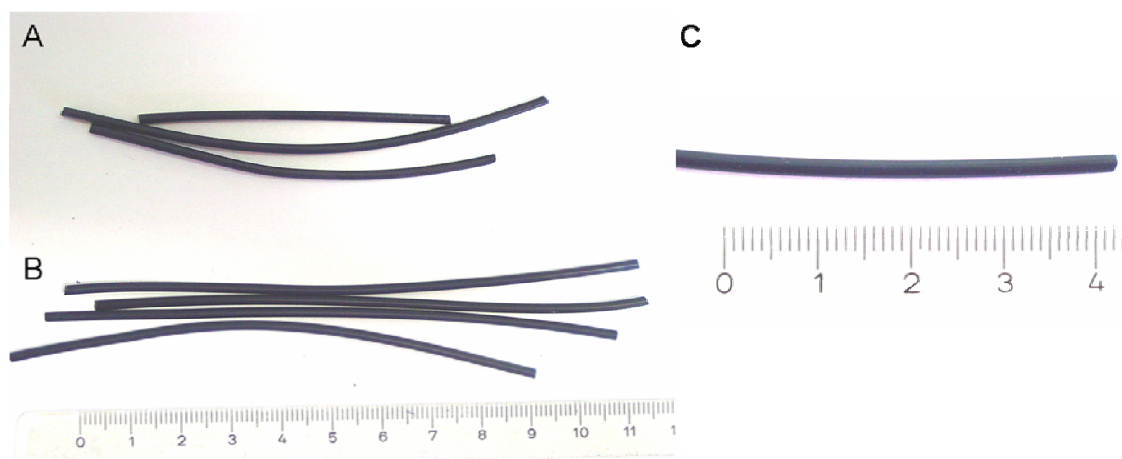


**Figure 81: Appearance of extrudates based on 10 % PEG, 10 % HP- $\beta$ -CD placebo lyophilisate, 64 % tristearin and 16 % H12 (A) or 16 % trilaurin (B), respectively. Figure C represents a magnification of A.**

From these formulation studies it was concluded that (1) the combination of solid triglycerides and semi-softened fat or oils, or (2) the combination of low- and high-melting point lipids can be considered as most promising manufacturing strategies regarding both, feasibility of the extrusion process and product homogeneity.

Comparing the mechanical properties of the obtained rods a clear superiority of extrudates comprising low-melting point lipids became evident. The forces needed to induce longitudinal breakage increased from  $\sim 15$  to  $\sim 37$  N, when replacing Miglyol<sup>®</sup> by a low-melting lipid.

## 2.2. INFLUENCE OF THE MANUFACTURING PROCESS ON THE LIPID MODIFICATION

During extrusion the applied temperatures must lead to a melting of the low-melting point lipid enabling the mass flow within the barrel. Therefore, manufacturing may induce a polymorphic transformation from the stable  $\beta$ - to the  $\alpha$ -polymorph.

As such a transformation can be associated with various problems during storage and during release (see Chapter 1.3.3) the thermal behaviour of freshly prepared extrudates was investigated by DSC experiments.

These studies were carried out with extrudates consisting solely of the lipid materials because the melting points of other excipients as for example PEG ( $T_m=58.7^\circ\text{C}$ ,  $SD=0.87$ ,  $n=3$ ) may overlap with the transitions temperatures relevant for studying the polymorphism of the lipids. In accordance with the formulations described above the ratio of low melting point to high melting point lipid was 1 to 4.

### 2.2.1. EXTRUDATES BASED ON A MIXTURE OF MONO-ACID TRIGLYCERIDES

The polymorphic properties of mixed-acid triglycerides (H12 and E85) are more complex than those described for monoacid-triglycerides [193]. Therefore, the effect of extrusion was first evaluated for extrudates based on a trilaurin/tristearin blend.

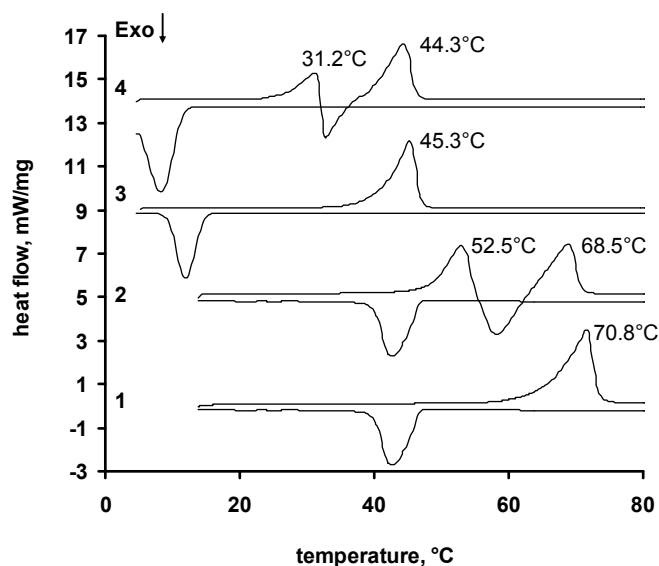


**Figure 82: Thermal behaviour of mono-acid triglycerides.**

The first heating scan of the used lipid bulk materials tristearin (1) and trilaurin (3) as well as the respective second heating scans in 2 and 4.

In order to determine the melting points and the polymorphic behaviour of the pure triglycerides, DSC analysis of trilaurin and tristearin was initially carried out. The thermograms of trilaurin and of tristearin revealed one single endothermic transition at 45.3 °C ( $n=2$ ,  $SD=0.07$  °C) and at 70.8 °C ( $n=3$ ,  $SD=1.15$  °C), respectively (Figure 82). Both melting endotherms are characteristics of the stable  $\beta$ -modification of trilaurin and tristearin [77]. As the triglycerides re-crystallised from melt firstly in the metastable  $\alpha$ -form, the second heating scan demonstrated an endothermic peak at 31.2 °C ( $n=2$ ,  $SD=0.21$  °C) for trilaurin and an endothermic peak at 52.5 °C ( $n=3$ ,  $SD=0.75$  °C) for tristearin. These endotherms were followed by an exothermic transition representing the re-crystallisation to the  $\beta$ -modification. Upon further heating the melting of the  $\beta$ -modification was observed at 44.3 ( $n=2$ ,  $SD=0.21$  °C) and at 68.5 °C ( $n=3$ ,  $SD=0.75$  °C), respectively.

In Figure 83 the thermograms of the lipid blend comprising trilaurin and tristearin are shown before extrusion (scan 1) and after extrusion (scan 3). In order to illustrate the

polymorphic behaviour of the lipid blend the respective second heating scans are included.

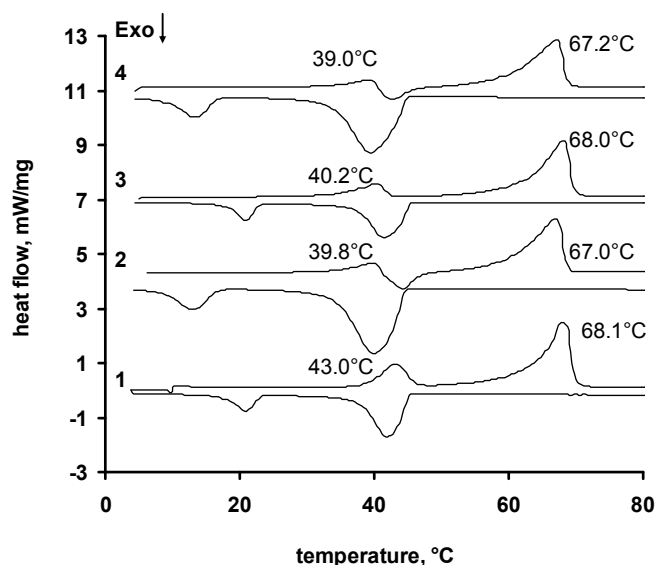


**Figure 83 : Influence of the extrusion procedure on the lipid modification.**

In (1) the first heating scan and in (2) the second heating scan of tristearin blended with trilaurin are illustrated. The first and the second heating scans of the extrudates based on the trilaurin/tristearin blend are shown in (3) and (4), respectively.

Two endothermic transitions were observed for the blend of trilaurin and tristearin (ratio 1 to 4, Figure 83 (1)). The similarities of these peaks to the melting temperatures of trilaurin and tristearin alone allowed the assignment of the low-melting to trilaurin and of the high-melting peak to tristearin. In accordance, the extrudates (Figure 83 (3)) also revealed two endothermic transitions presumably corresponding to the transitions of trilaurin and tristearin.

However, the melting points of blended triglycerides were lower compared to the melting endotherms of pure trilaurin and tristearin, respectively. In particular after extrusion, the first melting event occurred already at 40.2 °C ( $n=2$ ,  $SD=0.07$  °C), whereas pure trilaurin revealed an endotherm at 45.3 °C ( $n=2$ ,  $SD=0.07$  °C).

In literature it has been described that the phase behaviour and the crystallisation of binary systems comprising saturated mono-acid triglycerides both depend mainly on the chain length difference of the triglycerides. Two phase types can be distinguished: (1) triglycerides of a similar chemical structure form a miscible solid-solution phase and (2) triglycerides with different chemical structures form a eutectic phase. Polymorphism makes the phase behaviour even more complicated. For instance, when triglycerides of a binary mixtures differ in their chain length by two

carbons, solid solution phases are formed in the metastable  $\alpha$  and  $\beta'$  modification, whereas a eutectic phase with a limited region of solid solution is formed for the stable  $\beta$  form [192, 193].

Takeuchi et al. [221] investigated the phase behaviour and the polymorphism of binary mixtures based on various mono-acid triglycerides by synchrotron radiation x-ray diffraction. When the mass content of trilaurin was below 50 % no crystallisation of the trilaurin fraction occurred during the heating and cooling process [221]. Considering this information the transitions observed in the second heating scan of the trilaurin/tristearin blend (Figure 83 (2)) might reflect the transformation of tristearin from the  $\alpha$  to the  $\beta$  modification.

However, as illustrated in Figure 83 the cooling curves after heating revealed two exothermic transitions, indicating the crystallisation in two distinct phases.

Bunjes et al. [29] investigated the thermal behaviour of solid lipid nanoparticles containing various amounts of trilaurin and tristearin. During heating two melting maxima were observed, which were ascribed to the trilaurin and the tristearin fraction, respectively. In accordance to the present work, the melting peaks were shifted to lower temperatures compared to the pure triglycerides. The authors suggested, that this depression of the melting temperatures can be explained by eutectic phase behaviour [29].

Summing up, the main characteristics of the DSC-scans shown in Figure 83 – the two crystallisation peaks upon cooling in combination with the depression of the melting points – implied the formation of a eutectic phase for the physically mixed blends as well as for the extrudates. Due to the fact that trilaurin was completely molten during extrusion the depression of the melting point was more pronounced after extrusion than after physical mixing.

Moreover, the first melting endotherms in the second heating scans were followed by an exothermic crystallisation peaks (Figure 83 (2) and (4)). This suggests that the melting endotherm can be ascribed to the instable  $\alpha$ -modification. As the melting point of the  $\alpha$ -tristearin modification might be depressed due to the formation of a solid solution of trilaurin in tristearin [29], a clear distinction whether this transition can be ascribed to trilaurin or tristearin fraction is not possible based on the presented DSC data.

However, more important for the present work was the observation that no re-crystallisation was detectable in the thermograms of the freshly prepared extrudates.

This clearly indicated that the extrudates comprise both the low- and high-melting point lipid in the stable  $\beta$ -modification.

The absence of the  $\alpha$ -modification after extrusion was confirmed by WAXS experiments. As shown in Figure 84 the freshly prepared extrudates revealed the short-spacings typical for the stable  $\beta$ -modification at 0.46, 0.38 and 0.37 nm [77].

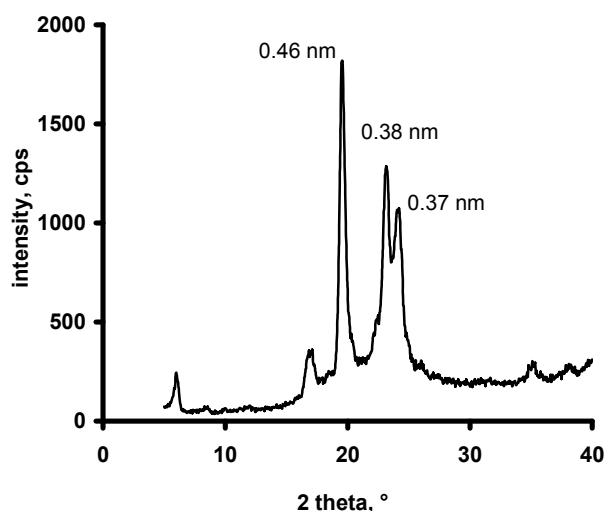


**Figure 84: Influence of the extrusion procedure on the lipid modification.**  
WAXS analyses of tristearin/trilaurin extrudates directly after twin screw extrusion.

The presence of both lipids in a stable modification even after melting one of them during extrusion might be explained by: (1) crystal seeding effects or (2) by the effect of shear stress on the fat solidification. It is known that the presence of seeding crystals can control polymorphic transitions [192]. As the high melting lipid is present in the stable  $\beta$ -modification during extrusion this might trigger a crystallisation of trilaurin into the  $\beta$ -form. On the other hand, it has been reported that shearing of hydrogenated cottonseed oil facilitates the crystallisation into stable polymorphs [69]. In the cited study mechanical “tempering” was performed by repeated extrusion through a sodium press [69].

### 2.2.2. EXTRUDATES BASED ON A MIXTURE OF MONO-ACID AND MIXED-ACID TRIGLYCERIDES

In order to confirm the promising results obtained with extrudates containing a mixture of trilaurin and tristearin a similar study was performed with extrudates based on a mixture of mono-acid and mixed-acid triglycerides.

As the polymorphic properties of mixed-acid triglycerides are quite complex, they need to be evaluated for each individual species. For example, Sato et al. [193]

reported for some mixed triglycerides the absence of the  $\beta'$ -form. In this case the  $\beta'$ -form became the most stable modification. However, other mixed-acid triglycerides were characterised by the existence of several  $\beta$  forms [193].

In Figure 85 the thermal behaviour of the triglyceride H12 is illustrated. The bulk material revealed one single endothermic peak at 35.6 °C. When cooling down (5 K/min) and performing a second heating scan the endotherm shifted to 32.9 °C. Moreover, a small exotherm was observed in front of the endothermic peak, suggesting that the re-crystallisation during cooling was not complete [157]. Contrarily, when H12 was slowly re-crystallised from melt at room temperature the exothermic transition was missing and a melting endotherm was detected at 35.6 °C.

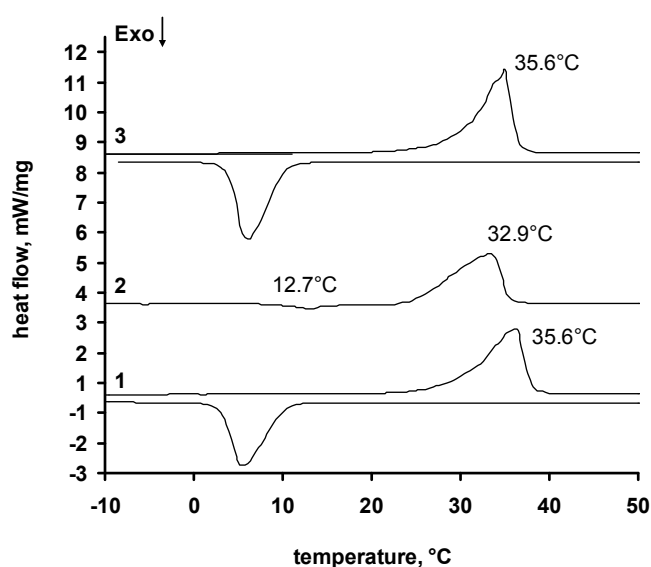


**Figure 85: DSC experiments of H12 bulk material.**

The following thermograms are illustrated: (1) first heating scan of H12 bulk, (2) second heating scan (after melting and cooling down during the DSC measurement), and (3) first heating scan of H12 bulk material melted and solidified at room temperature.

In order to supplement the obtained results WAXS experiments were carried out. In Figure 86 the corresponding X-ray diffraction patterns for H12 bulk material, for molten H12 bulk material cooled down with liquid nitrogen as well as for molten H12 re-solidified at room temperature are shown.

For H12 bulk material two short spacings at 0.42 nm and at 0.38 nm ( $2\theta = 21.1^\circ$  and  $23.4^\circ$ ) were determined, which are characteristic for the orthorhombic chain packing of the  $\beta'$  polymorph [77]. After melting and cooling down with liquid nitrogen the typical short spacings of the  $\beta'$  modification were also measured. However, a decrease in the intensity of the reflection was obvious, which can be attributed to a

lower crystallinity. In contrast, when molten H12 was slowly solidified at room temperature the obtained diffraction patterns were comparable to those of the bulk material (Figure 86B).

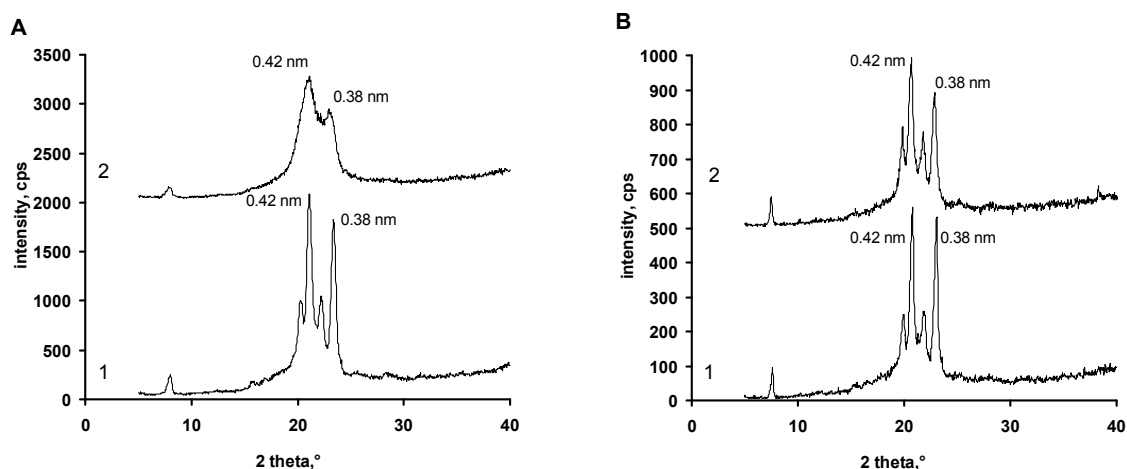


**Figure 86: WAXS experiments of H12 bulk material.**

In Figure A the diffraction patterns of H12 bulk material (1) as well as the diffraction patterns of molten H12 solidified with liquid nitrogen (2) are illustrated. Figure B demonstrates the diffraction patterns of H12 bulk material (1) and of molten H12 solidified at room temperature (2).

The results of the WAXS analysis suggest that H12 bulk material consists of the  $\beta'$  modification. Furthermore, H12 re-crystallised in this modification when the molten lipid was slowly solidified. Thus, a polymorphic transformation during extrusion became unlikely.

In order to confirm this assumption the thermal behaviour of a H12/tristearin blend before and after extrusion was investigated (Figure 87). In accordance to the results observed with the trilaurin/tristearin blend, the compounding resulted in a depression of the melting points. Whereas H12 bulk material revealed a melting endotherm at 35.6 °C, tristearin blended H12 featured an endothermic transitions at 32.3 °C prior to extrusion and at 30.0 °C after extrusion. It can be assumed that the reasons for these shifts of the melting points are similar to that discussed for the trilaurin/tristearin formulation.

Importantly, no re-crystallisation of unstable modifications was detectable for freshly prepared extrudates.

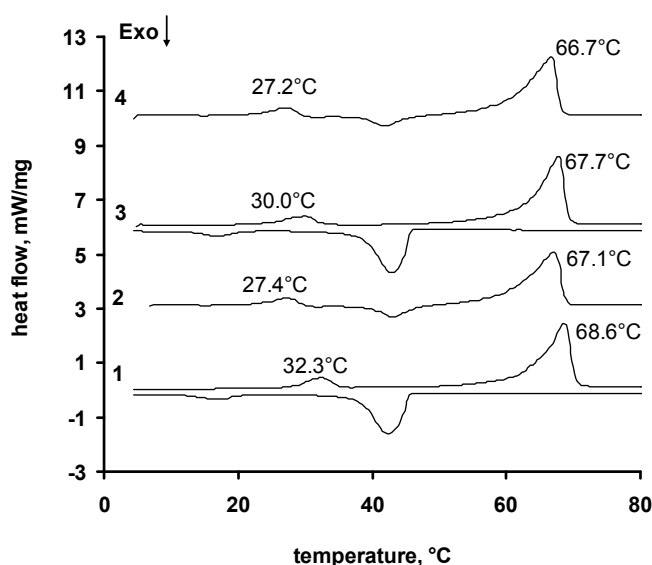


**Figure 87: Influence of the extrusion procedure on the lipid modification.**

In (1) the first heating scan and in (2) the second heating scan of tristearin blended with H12 are illustrated. The first and the second heating scans of the extrudates based on the H12/tristearin blend are shown in (3) and (4), respectively.

In addition, the absence of a polymorphic transformation during extrusion was confirmed by WAXS analysis. As illustrated in Figure 88 the admixture of H12 and tristearin produced reflections, which were intermediate between those of the pure substances. The strong diffraction lines at  $2\theta=19.6^\circ$ ,  $23.4^\circ$ , and  $24.4^\circ$  correspond to the crystal spacings of the  $\beta$  modification of tristearin at 0.46, 0.38, and 0.37 nm. Considering the diffraction pattern of pure H12 at  $2\theta=23.4^\circ$ ,  $d=0.38$  nm an overlapping with the  $\beta'$  modification of H12 occurred at this  $2\theta$  angle. In addition, the  $\beta'$  modification of H12 was detected at 0.42 nm (respective at  $2\theta=21.1^\circ$ ). Importantly, the same short spacings were featured after extrusion, leading to the conclusion that tristearin was present in the  $\beta$ -modification and H12 in the  $\beta'$ -modification.

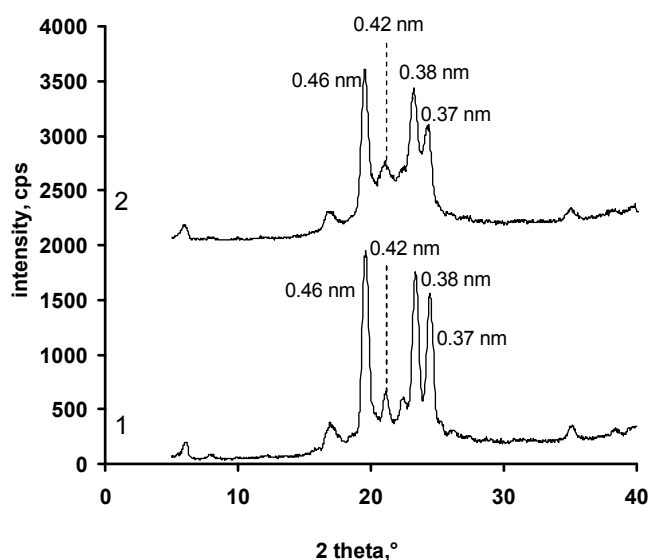


**Figure 88: Influence of the extrusion procedure on the lipid modification.** WAXS analyses of the tristerain/H12 before (1) and after extrusion (2).

Since both WAXS and DSC analysis of the lipids after extrusion featured the characteristics of the modification of the bulk materials, unforeseeable and hardly controllable polymorphic transformations upon storage or during release are improbable. The next experiments will, therefore, deal with the second potentially critical point of the manufacturing procedure: the effects of extrusion on protein stability.

### 2.3. INFLUENCE OF THE MANUFACTURING PROCESS ON THE PROTEIN STABILITY

Potential effects of elevated temperatures on the protein stability were discussed in Chapter I.4.4. Based on the literature data presented, it might be possible that proteins suspended in molten lipids can resist thermally induced denaturation and aggregation at moderate temperatures.

IFN- $\alpha$  loaded extrudates were prepared based on the formulations presented before. In particular, a combination of H12 with tristearin as well as a Miglyol<sup>®</sup>/tristearin blend was used as lipidic matrix material. With the latter formulation extrusion can be performed at room temperature and heat will only be generated by friction. Thus, potential thermally induced aggregation should be lower than in the case of a combination between low and high melting point lipids.

After extrusion IFN- $\alpha$  was extracted (as described previously [151], see Chapter III.2.3) and the samples were analysed by SDS-PAGE with subsequent silver staining (Figure 89).

The presence of dimer specimen was evident in all IFN- $\alpha$  samples. Furthermore, samples extruded in the presence of Miglyol<sup>®</sup> featured the creation of higher-order aggregates (Figure 89, lane 8).

The dimer fraction detected in all extruded samples was already present in the IFN- $\alpha$  bulk material and in the lyophilisates used for extrusion. (In contrast to the experiments described before (Chapter IV and V.1, here a different lot of protein standard was used.) Thus, the formation of dimers cannot be ascribed to the extrusion procedure of the H12/tristearin formulation. Only the extrusion in the presence of Miglyol<sup>®</sup> (Figure 89, lane 8) seemed to compromise protein stability.

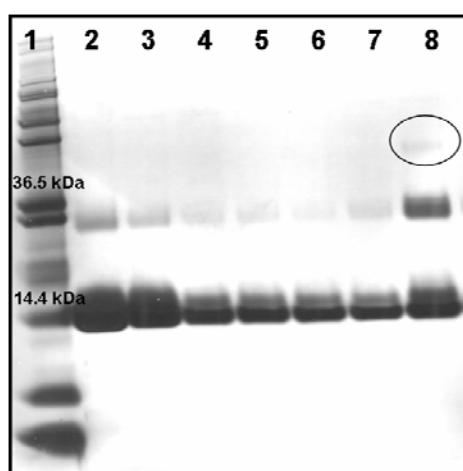


**Figure 89: SDS-PAGE of IFN- $\alpha$  extracted from lipidic extrudates.**

Lane 1: Molecular weight standard, lane 2: IFN- $\alpha$  standard, lane 3: IFN- $\alpha$  after lyophilisation, lane 4-8: IFN- $\alpha$  extracted from lipidic implants. The extrudates formulations were 80 % H12/tristearin  $\frac{1}{4}$ , 10 % lyophilised IFN- $\alpha$  and 10 % PEG (lane 4 and lane 5 extrudates received at the beginning and at the end of the extrusion procedure, respectively) and 70 % H12/tristearin  $\frac{1}{4}$ , 10 % lyophilised IFN- $\alpha$  and 20 % PEG (lane 6 and lane 7 extrudates received at the beginning and at the end of the extrusion procedure, respectively). In lane 8 IFN- $\alpha$  extracted from extrudates comprising 80 % of a Miglyol<sup>®</sup>/tristearin  $\frac{1}{4}$  blend, 10 % lyophilised IFN- $\alpha$  and 10 % PEG is shown.

### 2.3.1. CHARACTERISATION OF THE SECONDARY PROTEIN STRUCTURE WITHIN THE LIPIDIC EXTRUDATE

FTIR-spectroscopy has been suggested to analyse the secondary structure of proteins embedded within controlled release devices [75, 228, 256]. This method inheres the benefit that extraction of the protein is not necessary as the protein structure is directly studied within the delivery system.

FTIR-spectra of solid protein can be obtained for instance with the ATR-technique or with the transmission-technique using infrared-transparent salts. The main advantage of the ATR-technique is that it obviates time consuming sample preparation. In brief, the basis of ATR-spectroscopy is a beam of infrared radiation entering an optically transparent crystal of a higher refraction index than the sample. At the crystal-sample

interface the beam is totally reflected and consequently an evanescent wave penetrates the sample located at the crystal surface at the reflections point. In comparison, the IR-beam passes directly through the sample when the KBr transmission method is applied to collect the spectra [230].

In a pilot survey the potential of ATR- and transmission-technique to characterise the secondary structure of IFN- $\alpha$  embedded in a lipidic powder formulation was investigated. In accordance to the extrudate formulations presented in Chapter V.2.1 a lipid mixture based on H12 and tristearin in a ratio of 1 to 4 was blended with 10 % IFN- $\alpha$  and with 10 % PEG. As illustrated in Figure 90 the spectra recorded by the ATR-technique revealed a protein signal in the amid I/amid II region. However, better signal to noise ratio was obtained in the transmission mode. Thus, it was decided to use this technique for further investigations.

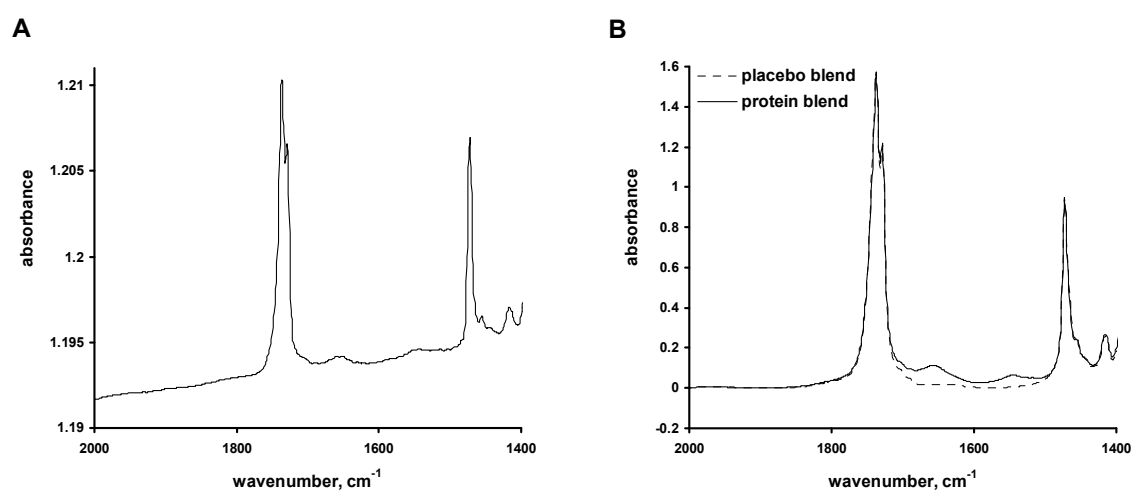


**Figure 90: ATR-spectrum (A) and KBr pellet transmission spectrum (B) of the physically mixed lipid, PEG and protein formulation**

As many proteins revealed spectral changes upon lyophilisation [33, 230] first the KBr transmission spectra of lyophilised IFN- $\alpha$  were recorded. The second derivative transmission spectra of IFN- $\alpha$  lyophilised with HP- $\beta$ -CD and that of the protein in solution are shown in Figure 91.

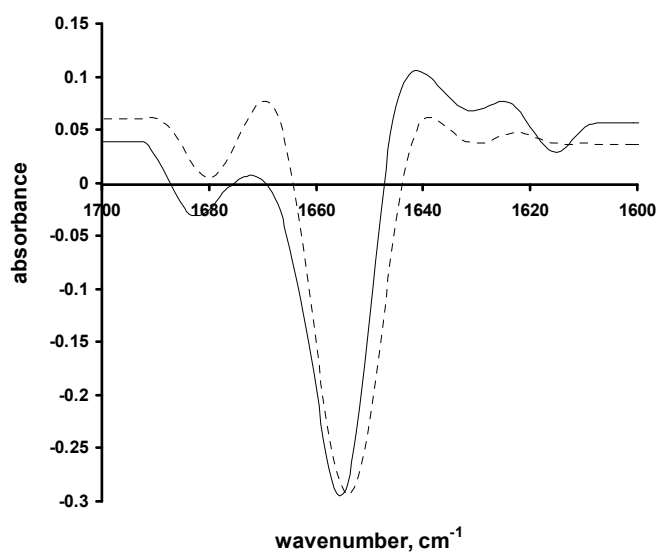


**Figure 91: Vector-normalised second-derivative spectra of IFN- $\alpha$ .**

The solid line represents the second-derivative spectra of lyophilised IFN- $\alpha$  obtained with the KBr pellet method. The dashed line shows the second-derivative spectra native IFN- $\alpha$  in solution.

Upon lyophilisation the dominant band ascribed to the helical structure was shifted from  $1654\text{ cm}^{-1}$  to  $1656\text{ cm}^{-1}$ . A shift of the band positions upon lyophilisation may indicate variations in the order of the  $\alpha$ -helical structure [175]. Furthermore, a broader amid I band in the KBr spectra was observed and a new band at  $1615\text{ cm}^{-1}$  arose. The occurrence of new bands at  $1619\text{ cm}^{-1}$  upon lyophilisation was related to intermolecular  $\beta$ -sheet formation [229].

Though Carpenter and co-workers showed that the extent of spectral changes occurring upon lyophilisation correlated with the storage stability [33], there is still a debate about the reasons for these structural changes. For instance, Van de Weert et al. [229] figured out that both structural changes as well as the removal of water might induce differences in the absorption characteristics of the amid bond.

Within the scope of the present work the origin of the spectra differences was not further investigated. The spectra of lyophilised IFN- $\alpha$  should only serve as standard to evaluate the effects of the extrusion procedure on the secondary protein structure.

As shown before, the C=O stretch vibrations of the triglyceride matrix material occurred at  $1737$ , at  $1729$ , and at  $1690\text{ cm}^{-1}$  (see Figure 90). In particular the latter band overlapped with the amid I band of the protein. Hence, it was necessary to evaluate the possibility of background correction. These investigations were performed with IFN- $\alpha$  blended in a mortar with the lipidic matrix material to exclude potential changes of the protein structure. The obtained spectra of the lipid/protein powder blend (10 % IFN- $\alpha$ /HP- $\beta$ -CD co-lyophilisate, 10 % PEG, 64 % tristearin, and

16 % H12) were corrected by the spectra of the respective placebo blend. Yang et al. [256] suggested as criterion for successful background subtraction a flat baseline in the region at  $1730 - 1710 \text{ cm}^{-1}$  (final protein spectra obtained after correction with PLGA background). However, it was not possible to fulfil this request with the lipidic/protein blend studied here (Figure 92).

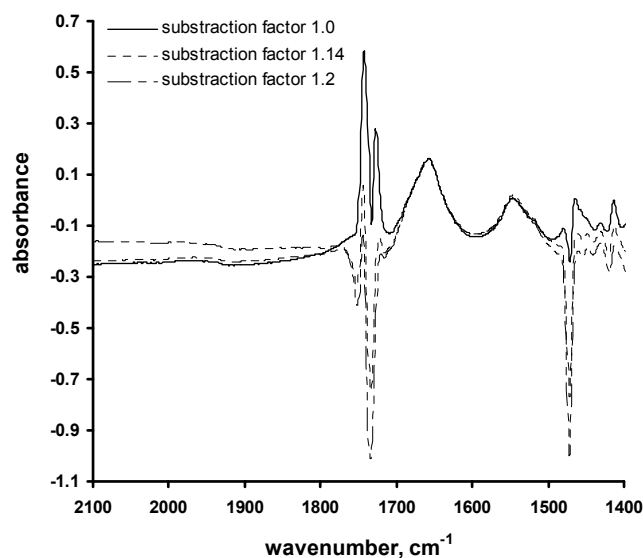


**Figure 92: Effect of background subtraction on the KBr pellet transmission spectra of IFN- $\alpha$  embedded in a lipid/PEG blend**

Variations of the subtraction factor either involved an oversubtraction or an undersubtraction of the lipid contributions, leading to negative or positive features in the spectrum between  $1700$  to  $1800 \text{ cm}^{-1}$ . The same problem was noted by van de Weert et al. [228]. In the cited work it was tried to correct the spectra of lysozyme embedded within PLGA microspheres by the spectra of the blank PLGA microspheres. The fact that the background could not completely cancelled out was explained by baseline slopes and distorted peak shapes especially in the carbonyl stretch vibration of PLGA due to the compression in KBr pellets. In addition, it was suggested that different absorption characteristics of protein-loaded microspheres restricted the subtraction of the spectrum of blank PLGA microspheres [228].

However, in accordance to the work of van de Weert et al. [228], the peak positions below  $\sim 1670 \text{ cm}^{-1}$  in the absorbance spectra as well as in the second derivative spectra were not markedly affected by the used subtraction factor (Figure 93). Importantly, the obtained spectra were quite similar to that of lyophilised protein before blending with the lipid matrix material. Taking all together led to the conclusion

that the subtraction of the lipid background did not cause spectral artefacts in the amid I region below  $1670\text{ cm}^{-1}$  (Figure 93).

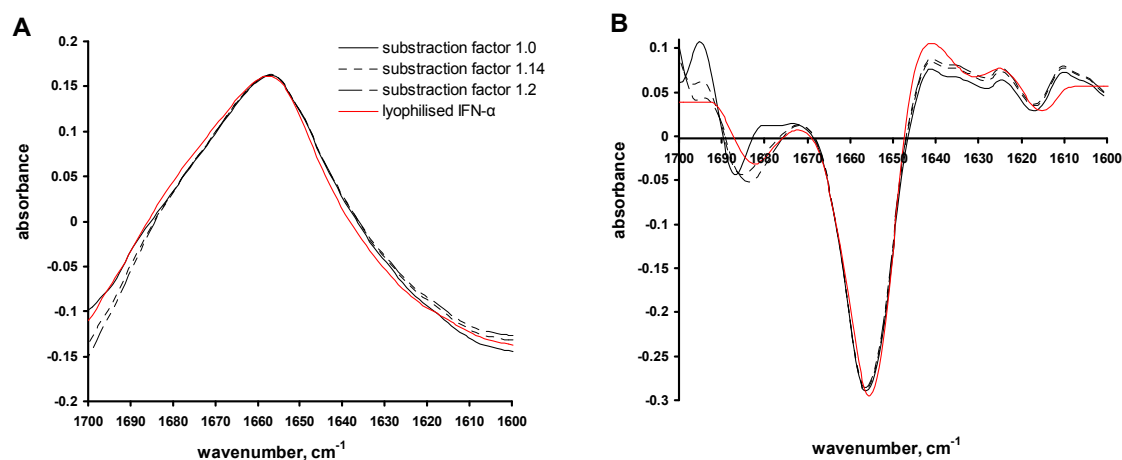


**Figure 93: Vector-normalised KBr-pellet-transmission spectra (A) and respective second derivatives (B) of IFN- $\alpha$  embedded in a lipid/PEG blend after background correction.**

In Figure 94 the obtained second derivatives of IFN- $\alpha$  after extrusion with a H12/tristearin blend are illustrated. Compared to the physical blended protein no significant differences in the amid I region below  $\sim 1670\text{ cm}^{-1}$  were detected.

The formation of intermolecular  $\beta$ -sheets would be detectable by the appearance of new bands at  $1623-1641\text{ cm}^{-1}$  and at  $1674-1695\text{ cm}^{-1}$  [230], but there were uncertainties in the latter band region with the described KBr transmission technique. However, a structural rearrangement should be associated with a decrease in the  $\alpha$ -helical content (compare Figure 54 (FTIR-spectra during thermal induced denaturation)). As shown in Figure 94 the band at  $1653\text{ cm}^{-1}$  was largely unaffected by the extrusion procedure. Thus, it is highly likely that extrusion of IFN- $\alpha$  embedded in a H12/tristearin blend comprising either 10 % or 20 % PEG did not induce important changes in secondary protein structure.

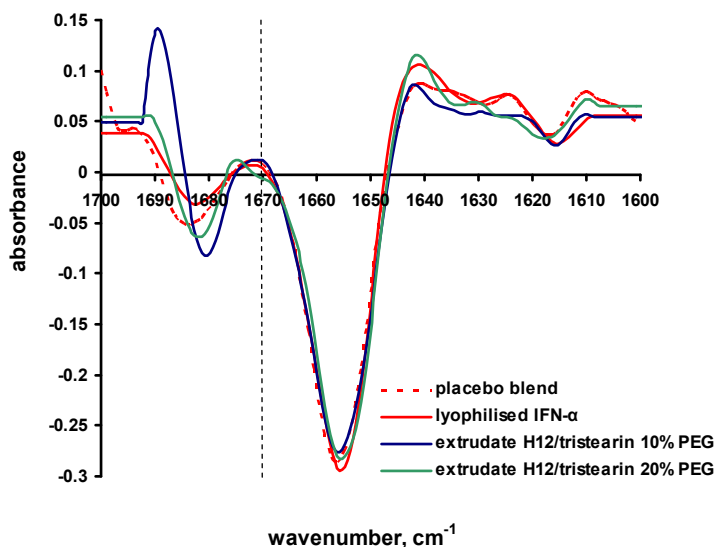


**Figure 94: Second derivative KBr-pellet-transmission spectra before extrusion and after extrusion with a lipidic blend based on H12 and tristearin.**

In contrast, the second derivatives of IFN- $\alpha$  after extrusion with a Miglyol<sup>®</sup>/tristearin blend revealed a number of differences compared to the spectra of the physical blend (Figure 95). The band arising from  $\alpha$ -helical structures was shifted to  $1653\text{ cm}^{-1}$  with a decrease in the relative intensity. In addition, the absorption bands at  $1635\text{ cm}^{-1}$  and at  $1619\text{ cm}^{-1}$  gained in intensity. Based on the overall spectral perturbations, a modification of the secondary structure of IFN- $\alpha$  could be supposed upon extrusion with a Miglyol<sup>®</sup>/tristearin blend.

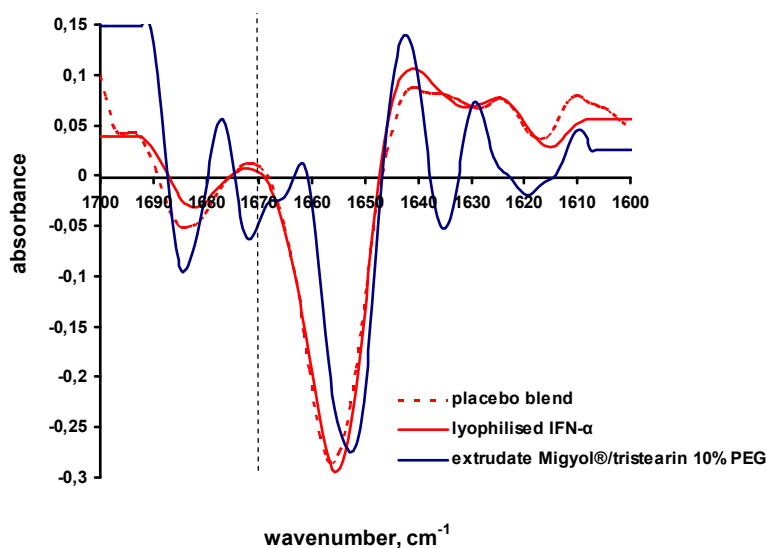


**Figure 95: Second derivative KBr-pellet-transmission spectra before extrusion and after extrusion with a lipidic blend based on Miglyol<sup>®</sup> and tristearin.**

In summary, SDS-PAGE analysis and FTIR-spectroscopy demonstrated that protein integrity was kept during extrusion at 40 °C with a lipid blend comprising H12 and tristearin. In contrast, SDS-PAGE analysis and FTIR-spectroscopy of IFN- $\alpha$  processed with the Miglyol<sup>®</sup>/tristearin blend revealed the occurrence of higher-order aggregates and significant perturbations of the secondary protein structure even though extrusion was performed at room temperature.

#### 2.4. IN-VITRO RELEASE STUDIES

In the next step the in-vitro release behaviour of IFN- $\alpha$  from lipidic extrudates was investigated. In order to facilitate the creation of an interconnected pore network enabling complete protein release the extrudates were loaded with 10 % or 20 % PEG, respectively. In addition, the influence of different extrudate diameters on the protein liberation was studied. For this, dies of 0.5 mm or 1 mm were fixed in front of the normal extruder outlet (diameter 2.0 mm)

The reduction of the extrudate diameter resulted in an accelerated protein delivery (Figure 96). For instance, extrudates comprising 10 % PEG liberated IFN- $\alpha$  in a sustained manner over 13 days, when the implant diameter was 0.5 mm. In comparison, the use of extrudates with a diameter of 1.0 or 1.9 mm extended the release period up to 30 or up to 60 days, respectively. Coexistent to this prolongation of the release period the total amount of IFN- $\alpha$  released differed in dependence on the implant diameter. Almost complete release (95.40 % (SD=5.51 %, n= 3)) was determined with the smallest extrudates, whereas increasing the implant diameter resulted in less complete protein release. Extrudates with a diameter of 1.0 mm delivered 83.53 % of the incorporated protein within 30 days and a further decrease in the overall released amount was observed with extrudates of a diameter of 1.9 mm (62.09 % (SD=0.85 %; n=3) within 60 days).

A similar influence of the extrudate diameter was observed with implants loaded with 20 % PEG. Here almost complete protein recovery was observed with extrudates of a diameter of 0.5 and 1 mm. The delivery of 91.18 % (SD=0.17, n=3) or 93.14 % (SD=0.6, n=3) IFN- $\alpha$  from these extrudates was retarded over 10 days and over 23 days, respectively. Furthermore, extrudates with a diameter of 1.9 mm revealed a sustained IFN- $\alpha$  release over 2 month. Compared to extrudates comprising only 10 % PEG the released fraction of IFN- $\alpha$  rose up to 84.12 % (SD=3.71, n=3).

The stepwise decrease of the totally liberated IFN- $\alpha$  by increasing the implant diameter, indicated that the incomplete protein recovery from larger extrudates can be ascribed to the implant geometry rather than to protein aggregation within the extrudates. With increasing the diameter of extrudates the diffusion pathways increase. Therefore, it seems that the enlargement of the lipidic matrix required higher amounts of hydrophilic drug/excipient to allow the creation of a connected pore-network.

However, further investigations should clarify whether the incomplete release from thicker extrudates can be ascribed to non-connected diffusing pathways or to protein aggregation within the matrix. For instance, the mechanisms of incomplete protein release can be investigated by the extraction of non-released protein with different types of incubation media. Solutions of sodium chloride would give information on potential electrostatic interactions, whereas the denaturants GdnHCl and SDS would dissolve non-covalent aggregates trapped within the matrix. From the comparison of the released protein amounts in the presence of GdnHCl and SDS information on protein adsorption can be obtained, as the strong surface active SDS can additionally displace protein molecules adsorbed onto surfaces [52, 119, 164].

Beside the possibility to adapt the release kinetics by using extrudates with different diameters the addition of various amounts of PEG was an effective tool to modify IFN- $\alpha$  release (Figure 96). Increasing the amount of incorporated PEG from 10 to 20 % resulted in a more accelerated IFN- $\alpha$  release. For example extrudates with a diameter of 1.0 mm comprising 10 % PEG liberated IFN- $\alpha$  in a sustained manner over 37 days, whereas the delivery was only retarded over 19 days when 20 % PEG were used as pore former.

Interestingly, the release kinetics of extrudates with a diameter of 1.9 mm (partly also extrudates with a diameter of 1.0 mm) revealed a lag-phase after the initial burst release. Extrudates loaded with 10 % PEG released 10.41 % (SD=2.02%, n=3) within the first day of incubation. After that, a lag-phase until day 16 occurred. Enhancing the amount of admixed PEG to 20 % reduced the burst release to 7.19 % (SD=0.65 %, n=3) and shortened the lag-phase to 7 days (Figure 96 C). After the lag-period IFN- $\alpha$  was delivered from extrudates with 10 % PEG in a constant manner over 30 days until day 53 of incubation. In comparison to that, extrudates with 20 % PEG revealed a linear phase over 24 days.

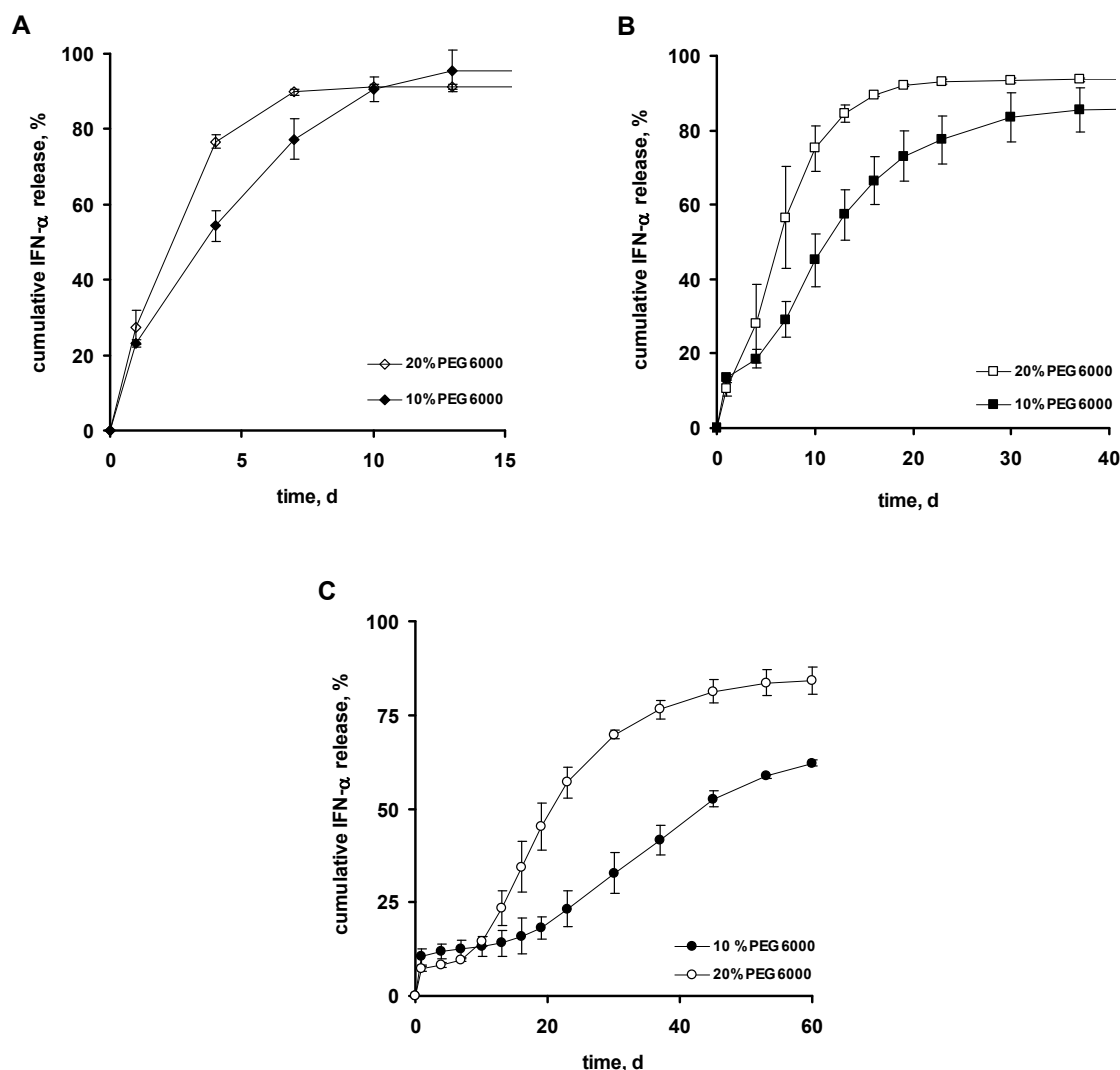


**Figure 96: Effect of PEG content and implant diameter on the in-vitro release behaviour of IFN- $\alpha$  from lipidic extrudates.**

For extrusion 10 % IFN- $\alpha$ /HP- $\beta$ -CD co-lyophilisate were blended with 10 % or 20 % PEG and 80 % or 70 % H12/tristearin  $\frac{1}{4}$ . Extrusion was performed with the described twin screw extruder at 40 °C. The diameter of the prepared rods was 0.5 mm (A), 1.0 mm (B), or 1.9 mm (C) (average  $\pm$  SD; n = 3).

Such a triphasic release profile (burst, lag-phase, linear release period) was reported for protein delivery from degradable matrix systems. As explained in Chapter I.5. the burst is ascribed to protein delivery from the surface. The lag-phase is characterised by diffusion controlled release and finally, when erosion starts, the release rates rise up. However, extrudates based on a H12/tristearin blend maintained there geometric dimensions during in-vitro incubation and no mass loss occurred during incubation. One explanation for the triphasic release profile might be the in-situ precipitation mechanism of IFN- $\alpha$  within PEG-containing delivery systems outlined in Chapter IV. Assuming high concentrations of PEG within the implant pores over prolonged periods of time this would explain the observed non-release phase.

It is evident from Figure 96 that the burst effects from extrudates prepared by twin screw extrusion were quite low. Even implants with a diameter of 0.5 mm loaded with 20 % PEG liberated not more than 27.27 % (SD=4.54, n=3) within the first 24 hours. Importantly, thicker extrudates revealed a reduction of the burst release with rising up the PEG content from 10 % to 20 %. Such an observation was already described before for the protein release from PEG-containing compressed tristearin matrices and it was shown that this contradiction to the effects of PEG as porogen could be explained well by the reduced solubility of IFN- $\alpha$  within PEG-containing matrices (see Chapter IV).

In order to evaluate whether a reduced protein solubility or even an in-situ precipitation is relevant for extrudates prepared by twin screw extrusion the release behaviour of lysozyme from these implant systems was investigated. As shown in Chapter IV.3.3 lysozyme revealed less distinct precipitation in presence of PEG. Thus, if precipitation is really important for the sustained liberation of IFN- $\alpha$  from extrudates the substitution of IFN- $\alpha$  by lysozyme should result in an acceleration of the release kinetics.

#### **2.4.1. LYSOZYME AS MODEL PROTEIN**

In order to exclude detrimental effects of the manufacturing procedure on lysozyme stability, lysozyme was extracted from the lipidic extrudates and analysed by SDS-PAGE.

As shown in Figure 97 lysozyme bulk material contains dimeric protein (quantification with SE-HPLC revealed approximately 0.3 % dimer) and an impurity with molecular weight of approximately 18 kDa. Such contaminations of commercially available hen egg-white lysozyme were already noted before [225]. In addition, SDS-PAGE revealed a weak band at a molecular weight of about 6 kDa.

Importantly, it was shown that no further protein degradation occurred upon extrusion, indicating that the developed extrusion procedure did not compromise the stability of lysozyme.

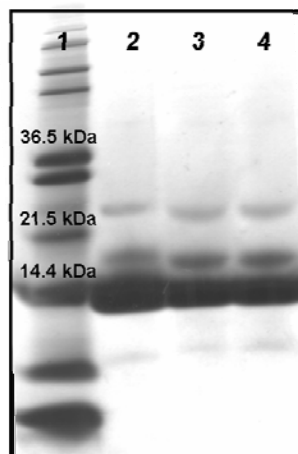


**Figure 97: Effect of the extrusion procedure on the integrity of lysozyme.**

Lane 1: Molecular weight standard, lane 2: lysozyme standard, lane 3: lysozyme extracted from extrudates received at the start of the extrusion procedure, lane 4: lysozyme extracted from extrudates received at the end of the extrusion procedure.

In Figure 98 the in-vitro release kinetics of lysozyme from extrudates based on a H12/tristearin blend and containing 20 % PEG are illustrated. In accordance to the delivery of IFN- $\alpha$ , the reduction of the implant diameter resulted in a less retarded lysozyme release. For instance, the amount of lysozyme delivered within the first 24 hours increased from 23.76 % (SD=5.33 %, n=3) to 69.51 % (SD=3.85 %, n=3) when the implant diameter was reduced from 1.9 mm to 0.5 mm.

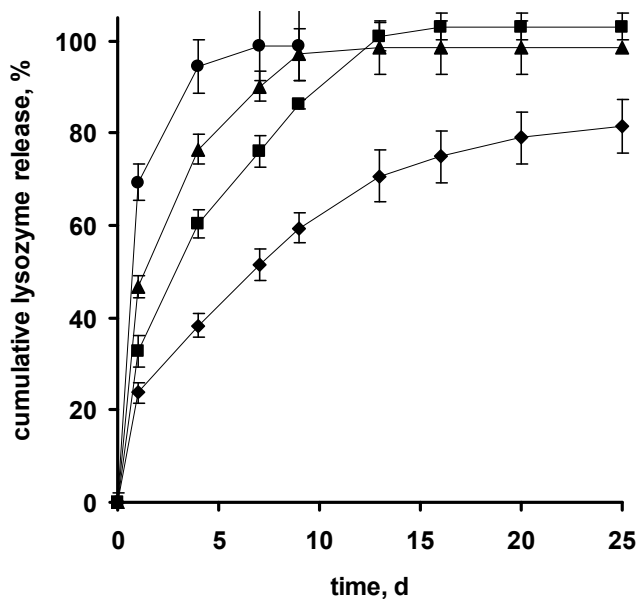


**Figure 98: Effect of implant diameter on lysozyme release.**

For extrusion 2.5 % lysozyme was blended with 20 % PEG, 70 % H12/tristearin  $\frac{1}{4}$  and 7.5 % HP- $\beta$ -CD. Extrusion was performed with the described twin screw extruder at 40 °C. The diameter of the extrudates was 0.5 mm (●), 1.0 mm (▲), 1.4 mm (■), or 1.9 mm (◆), respectively (average  $\pm$  SD; n = 3).

However, in comparison to the IFN- $\alpha$  release a significant faster lysozyme delivery was found for all rods irrespective of the implant diameter. As illustrated in Figure 99 a lag-time was missed when analysing lysozyme release from extrudates with a diameter of 1.9 mm. Furthermore, release of lysozyme levelled off at 81.51 % (SD=4.61, n=3) already after 25 days whereas 84.13 % of IFN- $\alpha$  (SD=3.71, n=3) were liberated over 60 days. Obviously, the burst effect of lysozyme was significantly higher than that of IFN- $\alpha$ .

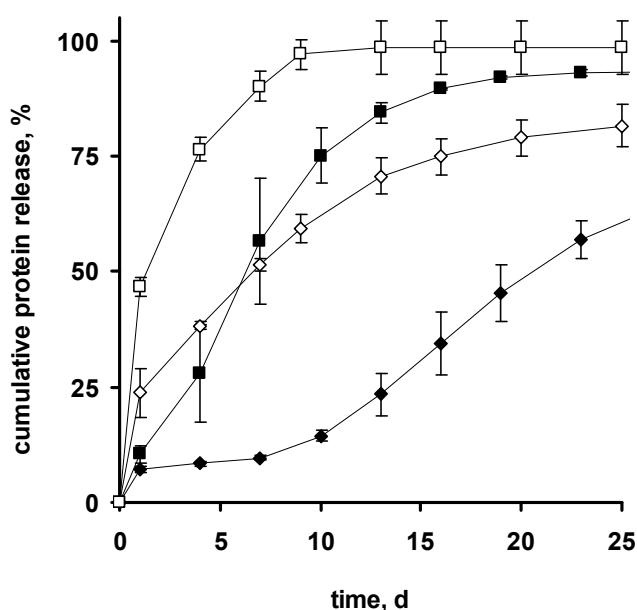


**Figure 99: Comparison between lysozyme and IFN- $\alpha$  release from extrudates prepared by twin screw extrusion.**

Open symbols indicate the liberation of lysozyme and closed symbols the delivery of IFN- $\alpha$ . The investigated extrudate diameters were 1.9 mm ( $\blacklozenge/\diamond$ ) and 1.0 mm ( $\blacksquare/\square$ ) (average  $\pm$  SD; n = 3).

In Chapter IV it was shown that reduced burst effects as well as deviations from purely diffusion controlled release of IFN- $\alpha$  from PEG-containing compressed tristearin matrices were a result of the reduced solubility of IFN- $\alpha$  in the presence of PEG. Considering this information the comparison of lysozyme and IFN- $\alpha$  indicated that the precipitation of IFN- $\alpha$  in the presence of PEG might be of important for the sustained protein liberation from extrudates as well. As lysozyme featured a rather high solubility in presence of PEG, high protein concentrations within the implant pores would allow lysozyme to diffuse out of the matrix. In contrast, the presence of PEG within the implant pores would reduce the protein solubility of IFN- $\alpha$ . As a consequence, only a minor fraction of the embedded IFN- $\alpha$  might be available for diffusion. This would result in low burst effects. Furthermore, the maintenance of

high PEG concentration within the pores might restrict the release of IFN- $\alpha$  over prolonged periods. This would explain why the burst release (of surface adjacent protein) is followed by a non-release period of IFN- $\alpha$ .

However, in contrast to the release of IFN- $\alpha$  from compressed matrices, a lag-phase was observed with extrudates prepared by twin screw extrusion (diameter 1.9 mm). Therefore, in the following section the inherent differences of the manufacturing methods, which might contribute to the observed differences in the release profiles, were discussed.

## 2.5. INFLUENCE OF THE MANUFACTURING PROCEDURE ON THE IN-VITRO RELEASE KINETICS OF IFN- $\alpha$

The influence of the three manufacturing strategies used within the scope of the present thesis - ram extrusion, twin screw extrusion and compression - on the release of IFN- $\alpha$  was investigated. The lipid/protein mixture comprising 10 % IFN- $\alpha$ /HP- $\beta$ -CD lyophilisate, 20 % PEG, and a lipidic powder blend of H12 and tristearin in a mass ratio of 1 to 4 was compressed at 19.6 kN for 30 s (see Chapter IV) or extruded by means of the ram extruder (see Chapter V.1).

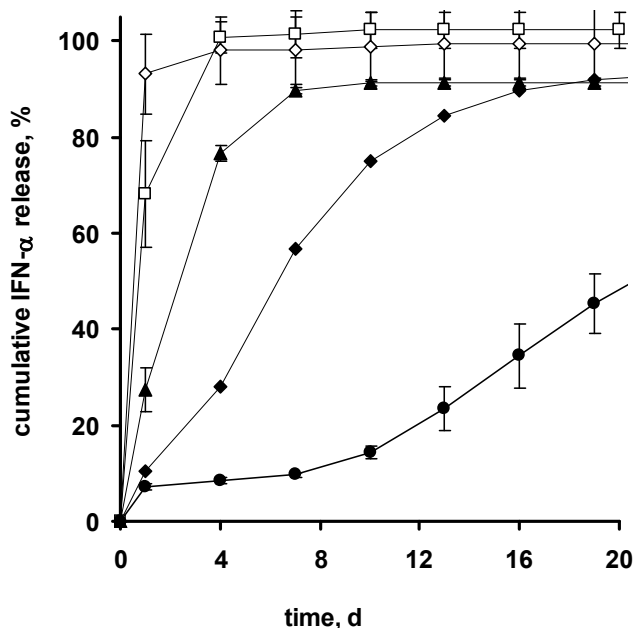


**Figure 100: Influence of the implant manufacturing method on the in-vitro release of IFN- $\alpha$ .**

In-vitro release kinetics of IFN- $\alpha$  from implants based on a H12/tristearin blend  $\frac{1}{4}$  prepared by compression ( $\square$ ), by ram extrusion ( $\diamond$ ) or by twin screw extrusion (extrudates with a diameter 1.9 mm ( $\bullet$ ), 1.0 mm ( $\blacklozenge$ ), or 0.5 mm ( $\blacktriangle$ )). All matrices were loaded with 10 % IFN- $\alpha$  co-lyophilised with HP- $\beta$ -CD and with 10 % PEG (average  $\pm$  SD;  $n = 3$ ).

As illustrated in Figure 100 the protein liberation occurred in a significantly accelerated manner when the manufacturing of implants was accomplished by

compression or by ram extrusion. Interestingly, despite of the reduction of the implant diameter associated with the change of the manufacturing procedure, twin screw extrusion resulted in a more sustained protein delivery. This suggested that twin screw extrusion per se causes more delayed protein release. However, it should be noted that concomitantly to the reduction of the implant diameter the implant height was varied. By compression implants with a height of 2.5 mm were produced, whereas extruded rods were cut into pieces of 2.3 cm.

To get a further insight into the impact of the twin-screw extrusion procedure on the release of IFN- $\alpha$ , extrudates prepared by twin screw extrusion were ground and then compressed to cylindrical implants. This manufacturing procedure should eliminate the influence of the implant geometry on the in-vitro release. If the blending and compaction during twin screw extrusion has an influence on the protein liberation the release profiles should markedly differ from those obtained from implants prepared by compression of the physical protein/lipid/PEG mixture.

Indeed, release profiles from implants prepared from the extruded lipid/protein blend revealed a triphasic release curve (Figure 101). After the burst release a lag-period over 9 days was followed. Finally, the delivery rates of IFN- $\alpha$  increased.

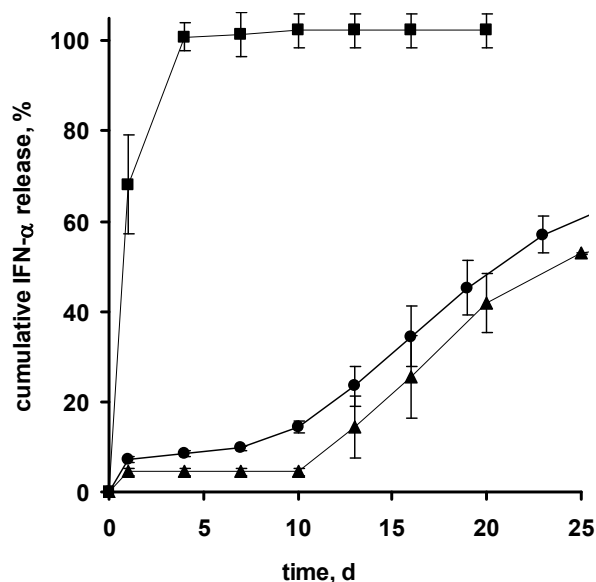


**Figure 101: Influence of the extrusion procedure on the protein release.**

For the preparation of lipidic implants a physical powder blend of 10 % IFN- $\alpha$ /HP- $\beta$ -CD co-lyophilisate, 20 % PEG, and 70 % H12/tristearin  $\frac{1}{4}$  was compressed (■). Alternatively the powder was extruded with the twin screw extruder, ground and compressed (▲). For comparison only the protein release kinetics from extrudates with a diameter of 1.9 mm (prepared by twin-screw extrusion) are included (●) (average  $\pm$  SD; n = 3).

Three possible process inherent features might explain the more sustained release from extrudates prepared by twin screw extrusion: (1) the intense compaction, (2) the fine compounding during extrusion, and (3) the melting of the low melting lipid during extrusion.

As shown in Chapter V.1.6.1 the acceleration of IFN- $\alpha$  release by using different triglyceride matrices was associated with a decrease in the compactness of the matrix. The change of the manufacturing procedure from ram to twin screw extrusion also significantly improved the mechanical stabilities of the extrudates (Table 9). Therefore, the more compact matrix structure might be one reason for the more sustained protein release from twin screw extrudates.

**Table 9: Mechanical properties of implants prepared by various manufacturing methods.**

The implants were based on a lipidic powder blend of H12 and tristearin in a ratio of  $\frac{1}{4}$  (average  $\pm$  SD; n = 5).

manufacturing method	tensile strenght, N
compression	15.2 $\pm$ 2.3
ram extrusion	10.7 $\pm$ 1.5
twin screw extrusion	37.1 $\pm$ 2.6

In addition, homogeneity studies by the admixture of methylene blue to the extrudate formulation showed a uniform staining of extruded rods prepared by twin screw extrusion. In contrast, implants of the same formulation processed by compression or ram extrusion revealed darker and brighter zones (Figure 102).



**Figure 102: Optical appearance of the different implant systems.**

A lipidic powder blend of H12 and tristearin in a ratio of  $\frac{1}{4}$  was admixed with 1 % methylene blue in mortar. The powder blend was (A) compressed at 19.8 kN for 30 seconds, (B) extruded with a ram extruder, or (C) extruded with a twin-screw extruder.

Based on these observations it can be assumed that the compounding during twin screw extrusion accounts for a more finely distribution of PEG and IFN- $\alpha$  within the lipidic matrix.

It has been suggested recently, that the homogeneity of the protein distribution within a lipidic matrix correlates with the resulting release profiles [126]. Considering this information, the high homogeneity after twin screw extrusion may contribute to the more delayed protein recovery from extrudates prepared by twin screw extrusion.

In addition, it can be assumed that the melting of the low melting lipid during extrusion resulted in a welding of the lipid matrix, which in turn would account for a very dense structure with a low amount of pores and void spaces. Such effects of a melting step during implant manufacturing were reported, for instance, by Pongjanyakul [174]. The implants were prepared by casting the molten lipid into polyethylene tubes (see Chapter 1.3.2.3), which entailed a significantly lower water uptake and a lower porosity of the implants compared to compressed implants. This was considered as reason for the reduced overall protein release from molten lipidic implants [174].

Taken together – the compaction, the blending and the melting – during twin screw extrusion can be considered as complementary reasons for the more sustained release of IFN- $\alpha$  from implants prepared by this manufacturing technique. Furthermore, assuming that these features of twin screw extrusion might also affect the release kinetics of the incorporated excipients, in comparison to ram extrudates and to compressed implants, a more sustained release of HP- $\beta$ -CD and of PEG can be expected. As explained above, the latter would contribute to the understanding of the observed lag-phase during release studies from twin screw extruded implants.

The verification of these hypothesis was beyond the scope of the present thesis. However, further studies should investigate the release of the excipients from the implants prepared by twin screw extrusion. In addition, it would be interesting to explore the matrix morphology of twin screw extruded implants before and after in-vitro release and to compare those observations with the morphology of compressed (Chapter IV) and of ram extruded (Chapter V.1) implants. Finally, in order to evaluate whether the uniform distribution of the model compound methylene blue is conferrable to the distribution of IFN- $\alpha$  within the implant, a staining of the protein embedded within the lipidic matrix should be performed. For instance, van de Weert et al. revealed that the use of the red dye Ponceau S allowed a visualisation of

lysozyme embedded within PLGA microspheres [228]. Alternatively, FTIR-microscopy or the incorporation of a model protein labelled with fluorescent dyes could provide further information on the drug distribution [126].

## 2.6. PROTEIN STABILITY DURING RELEASE

In Figure 103 the monomer content of released IFN- $\alpha$  versus incubation time is illustrated. Over the entire liberation period the IFN- $\alpha$  monomer content remained at a high level (>95 %). Beside monomeric IFN- $\alpha$  only dimer specimen were detected by SE-HPLC. Mostly, the released protein resembled between 0.5 % and 2 % dimer. Extrudates with a diameter of 1.0 mm delivered an increased amount of dimer of up to 5 % after 16 days. In comparison to that, implants prepared by ram extrusion or by compression revealed a higher integrity of released protein. The delivered dimer fraction from these kinds of implant was smaller than 1.5 %.

As protein destabilisation during the manufacturing procedure is unlikely, one reason for this more pronounced deterioration of the protein might be a destabilisation during release. Such a destabilisation during release is mostly associated with a time-dependent decrease in the monomer content. However, such a dependency of the protein stability on the incubation time was not observed. Considering that the protein raw material used for twin screw extrusion already comprised a higher content of dimer specimen this might further explain the reduced protein integrity. SE-HPLC of the reconstituted lyophilisates applied for twin-screw extrusion revealed a dimer content of 0.75 %. In comparison, reconstituted lyophilisates processed by ram extrusion or by compression revealed in average less than 0.1 % dimeric IFN- $\alpha$ . The higher amount of dimer specimen presented within the used raw material used for twin screw extrusion potentially triggered further aggregation during in-vitro release studies from these implants.

As shown in Figure 104 lysozyme was delivered almost entirely in its monomeric form (>98 %) from extrudates prepared by twin screw extrusion. Size exclusion chromatograms of lysozyme revealed a main protein peak with a retention time of 24.5 minutes. In addition, a small peak with a retention time of 21 minutes was detected, which presumably corresponded to dimeric lysozyme.

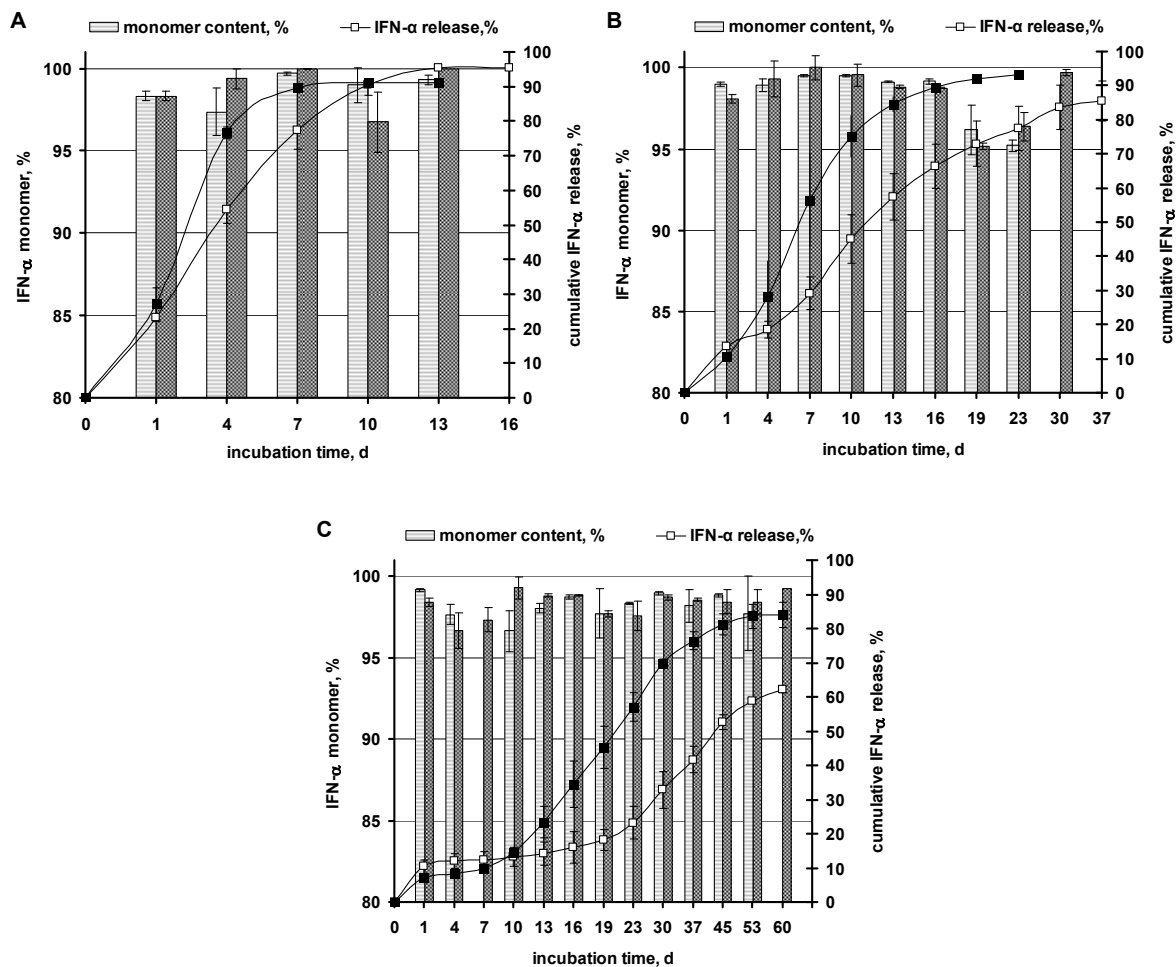


**Figure 103: IFN-α integrity during in-vitro release.**

Symbols indicate the total amount of delivered protein from extrudates comprising 10 % (open symbols) and 20 % (closed symbols) PEG. The bars illustrate the monomer content of delivered IFN-α (brighter bars: extrudates loaded with 10 % PEG, darker bars: extrudates loaded with 20 % PEG) Extrudates with a diameter of 0.5 mm (A), 1.0 mm (B) and 1.9 mm (C) were investigated (average +/- SD; n = 3).

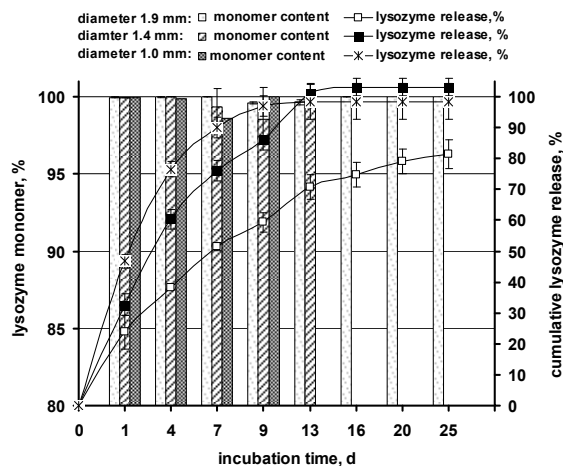


**Figure 104: Lysozyme integrity during in-vitro release.**

Symbols indicate the total amount of delivered lysozyme from extrudates with different diameters. The bars illustrate the monomer content of delivered lysozyme (average +/- SD; n = 3).

## 2.7. SUMMARY AND CONCLUSION

In the first part of this section various manufacturing strategies to produce lipidic implants by means of twin screw extrusion were investigated. Due to the sharp melting point of tristearin, implant formulations based solely on tristearin could not be processed. By tempering the extruder below the melting point of tristearin clogging of the extruder occurred, whereas employing temperatures close to the melting point of tristearin failed to increase the pressure within the barrel.

In order to circumvent these problems a semisolid lipidic mass was prepared by admixing of semisolid lipids or oils. The obtained rubbery consistence enabled filling and extrusion in a continuous way. Moreover, homogeneity studies using methylene blue as model compound featured a uniform distribution of the drug load within the lipidic matrix.

Alternatively, extrudates with an excellent homogeneity of the methylene blue distribution could be produced by the preparation of lipidic blends based on low- and high-melting point lipids. Due to the selective melting of the low-melting lipid during extrusion, clogging was avoided. On the other hand, after extrusion the lipidic matrix solidified which resulted in superior mechanical properties of the obtained extrudates compared to extrudates produced by the admixing of oils or semisolid fats.

Using the admixing of low-melting point lipids as manufacturing strategy a broad spectrum of lipid combinations can be processed by twin-screw extrusion. An optimal percentage of the low-melting fat was found between 16 and 24 %.

Although the low-melting point triglyceride was molten during extrusion, no polymorphic transformation occurred. Both, DSC and WAXS analysis revealed that extruded matrices comprised the lipids in their stable modification.

Furthermore, the extrusion of IFN- $\alpha$  at 40 °C, with a lipidic blend comprising H12 as low-melting point component and tristearin as high-melting point fraction did not compromise protein integrity. SDS-PAGE analysis of IFN- $\alpha$  extracted from the lipidic matrix revealed beside of dimeric IFN- $\alpha$  no further aggregates or fragments. As the dimeric fraction was already present within the used protein bulk material before extrusion, no detrimental effects of the extrusion procedure could be detected by SDS-PAGE. In addition, FTIR-spectroscopy of IFN- $\alpha$  embedded in an extruded H12/tristearin matrix indicated that the secondary protein structure was not affected by the extrusion procedure.

In contrast to these encouraging results, the extrusion of IFN- $\alpha$  with a Miglyol<sup>®</sup>/tristearin blend resulted in the formation of higher-order aggregates as well as in conformational changes. Thus, despite the fact that the preparation requires the employment of elevated temperatures (40 °C) with respect to protein stability a clear superior of extrudates based on H12 and tristearin can be stated.

As neither lipid modification nor protein stability were affected by the preparation methods the prerequisites for a successful sustained release system based on lipids were fulfilled and in-vitro release studies were carried out.

The manufacturing of extrudates with different diameters was shown as an effective tool to adjust protein release kinetics. By increasing the implant diameter from 0.5 mm to 1.0 mm and finally to 1.9 mm the liberation of IFN- $\alpha$  occurred in a prolonged manner over 15, 40, or 60 days.

In addition, the release kinetics could be tailored by varying the amount of incorporated PEG. Elevation of the admixed amounts of PEG from 10 % to 20 % resulted in a more accelerated protein liberation. Furthermore, extrudates with a diameter of 1.0 mm or 1.9 mm revealed a virtually complete protein recovery when increasing the PEG content. Importantly, IFN- $\alpha$  was mainly delivered in its monomeric form. Over the entire incubation period for all investigated extrudates the relative amount of released monomeric IFN- $\alpha$  did not fall below 95 %. Beside the monomer fraction only dimeric IFN- $\alpha$  was detectable in the release medium using SE-HPLC.

Interestingly, IFN- $\alpha$  release from extrudates with a diameter of 1.9 mm revealed a triphasic profile, consisting of a burst- and a lag-period and a nearly linear release phase. Since the implants were geometrically stable during the entire incubation period, matrix erosion as reason for the triphasic liberation patterns can be excluded (see Chapter I.5.2)

Bearing in mind the in-situ precipitation of IFN- $\alpha$  within PEG-containing tristearin implants prepared by compression, it might be possible that such a scenario also contributes to the occurrence of a lag-release period.

The assumption that protein precipitation might be of importance, was backed by the observation that the burst release from extrudates was rather low. For extrudates with a diameter of 1.0 mm and 1.9 mm the admixing of higher PEG quantities even resulted in a reduction of the burst effect. Such contradictions to the effects of PEG

as a porogen described in literature [40, 108, 138, 174] were shown to be a result of the postulated in-situ precipitation mechanism (Chapter IV).

In order to investigate the relevance of in-situ precipitation for the sustained release from extrudates, IFN- $\alpha$  was substituted by lysozyme. As lysozyme revealed a less distinct precipitation in the presence of PEG the liberation of lysozyme occurred markedly accelerated compared to the delivery of IFN- $\alpha$  from the same formulation. Moreover, a triphasic release profile was not longer observed and liberation patterns of lysozyme featured rather high burst effects.

Therefore, it can be concluded that the in-situ precipitation mechanism in the presence of PEG elucidated for tristearin implants prepared by compression (Chapter IV) presumably causes a sustained IFN- $\alpha$  liberation for extrudates prepared by twin screw extrusion, as well.

In the final section of this chapter the three manufacturing methods used within the scope of this thesis were compared. A lipidic blend of H12 and tristearin containing 20 % PEG and 10 % IFN- $\alpha$ /HP- $\beta$ -CD co-lyophilisate was either processed by compression, by ram extrusion, or by twin screw extrusion. Although the implant diameter of extrudates prepared by twin screw extrusion was reduced, protein delivery was more sustained from this kind of implants. One explanation for this more delayed delivery might be the increase in matrix compactness (see Chapter V.1.6.1). Furthermore, it is highly conceivable that the melting and re-solidification of the low melting lipid filled open pore space of the implant and led to a welding between the incorporated compounds and the lipid material. In addition, homogeneity studies employing methylene blue as model compound revealed a finer distribution of methylene blue within the lipidic matrix. It was shown by Koennings et al. that a more homogeneous drug distribution within lipidic implants correlated with a prolongation of the release patterns [126]. As twin screw extruded implants revealed the most uniform methylene blue distribution, this might further contribute to the more delayed release from these extrudates.

## CHAPTER VI: FINAL SUMMARY

Two main objectives were to be accomplished within the scope of the present thesis. Firstly, it was aimed at an understanding of the mechanisms controlling protein release from lipidic implants, and secondly, focus was put on the development of new, improved protein delivery systems based on lipids.

In *Chapter I* the reader is introduced to the concerns associated with protein delivery from polymeric sustained release systems which gave rise to investigate the potential of lipids as alternative matrix materials. Screening the current literature increasing interest in such lipidic controlled release devices could be stated. However, it turned out that the manufacturing strategies for lipidic implants mostly rely on the compression of a lipid/protein blend and alternative manufacturing techniques were only sparsely investigated for protein-loaded lipidic implants. An overview on the currently applied manufacturing strategies for lipidic and for polymeric implants was also given, which led to the conclusion that extrusion should be evaluated as manufacturing procedure for lipidic implants. Furthermore, the protein release mechanisms from degradable and from non-degradable systems as well as the respective mathematical models describing release are illustrated in Chapter I.

Recently, lipidic implants prepared by compression were shown as promising platform for the continuous delivery of rh-interferon  $\alpha$ -2a (IFN- $\alpha$ ). The developed implant formulation is based on tristearin as matrix material comprises 10 % IFN- $\alpha$  co-lyophilised with hydroxypropyl- $\beta$ -cyclodextrin (HP- $\beta$ -CD) and different amounts of poly(ethylene glycol) 6000 (PEG) as porogen [151].

The objectives of the thesis are summarised in *Chapter II*.

Materials and Methods that were applied in the present work are listed in *Chapter III*. In order to get insights into the release controlling mechanisms; investigations on the in-vitro release kinetics of IFN- $\alpha$ , PEG, and HP- $\beta$ -CD from the described implants system are outlined in *Chapter IV.1*. The addition of PEG to the lipidic implants resulted in a more sustained protein delivery with lower burst effects, whereas the liberation of both excipients, HP- $\beta$ -CD and PEG, was accelerated when increasing the initial PEG loading. These different effects of PEG could be ascribed to the underlying mass transport mechanisms. As tristearin implants revealed no erosion during in-vitro incubation, the experimental release data were analysed with a mathematical solution of Fick's second law of diffusion. Interestingly, the release of IFN- $\alpha$  from PEG-free implants was purely diffusion controlled, whereas also other

types of transport phenomena were of importance when the release modifier PEG was present. In contrast, the release of PEG as well as of HP- $\beta$ -CD remained purely diffusion controlled, irrespective of the presence of PEG.

In literature the role of PEG within controlled release systems has so far mostly been explained by its function as a pore forming agent [40, 108, 138, 174]. Due to an increase in the matrix porosity elevated levels of drug were recovered with an accelerated release rate.

As PEG of various molecular weights was reported to precipitate IFN- $\alpha$  [201], it was assumed that a reduced protein solubility or even an in-situ protein precipitation may explain the sustained release of IFN- $\alpha$  from PEG-containing tristearin implants and the observed deviations from pure diffusion control. The assumption was backed in *Chapter IV.2* where it was shown that IFN- $\alpha$  spontaneously precipitates in the presence of more than 3 % (wt/vol) PEG. Importantly, protein precipitation was completely reversible. IFN- $\alpha$  was recovered in its monomeric form without chemical degradation according to SE- and RP-HPLC measurements after re-dissolving the precipitates. Furthermore, FTIR- and fluorescence spectroscopy indicated a preservation of the native secondary and tertiary structure after precipitation and re-dissolution.

The in-situ precipitation of IFN- $\alpha$  during the delivery from PEG-containing matrices was proven in *Chapter IV.3*. A “macropore model” was developed, which revealed that the dissolution of IFN- $\alpha$  in the presence of PEG was the rate-limiting factor for protein release. Furthermore, the pH-dependence of IFN- $\alpha$  solubility in the presence of PEG was reflected by the protein release kinetics from lipidic implants. Finally, evidence for an in-situ precipitation of IFN- $\alpha$  was provided by both the replacement of PEG by an alternative porogen as well as by the substitution of IFN- $\alpha$  by lysozyme.

In summary, the in-situ precipitation mechanism had two main benefits. The reversible precipitation of IFN- $\alpha$  in PEG-containing lipidic implants facilitated a low burst effect and a sustained protein release with nearly constant release rates. Moreover, the precipitation also ensured low concentrations of dissolved protein within the implant pores. Therefore, the tendency towards protein aggregation was reduced.

*Chapter IV.4* deals with the effects of the second hydrophilic excipient of the matrix formulation – HP- $\beta$ -CD. In brief, the obtained findings indicated that HP- $\beta$ -CD influenced the release of IFN- $\alpha$  rather by increasing the matrix porosity than by

protein complexation. In addition, a stabilisation of IFN- $\alpha$  during release can be supposed, as thermal protein denaturation studies, monitored with attenuated total reflection Fourier transform infrared spectroscopy (ATR-FTIR), figured out that HP- $\beta$ -CD reduced the tendency of IFN- $\alpha$  to undergo protein denaturation and aggregation at elevated temperatures (50-60 °C).

In order to overcome the restrictions of administration associated with the large size of the above described implant system, various extrusion techniques were evaluated regarding their potential to produce small-sized lipidic protein delivery devices (*Chapter V*).

Initially, the possibilities of ram extrusion were evaluated and an extrusion procedure was developed which did neither induced a polymorphic transformation nor compromised protein integrity. Moreover, the achieved geometry enabled filling of the extrudates in an injection device approved for subcutaneous application of polymeric implants.

However, protein release was only sustained over 16 days and various attempts, such as variations in the particle sizes of the used raw materials or the change of the lipidic matrix material, did not substantially extend the release period. The less sustained protein liberation, compared to compressed implants, can be ascribed to the transfer of the manufacturing procedure from compression to ram extrusion, which provoked a reduction of the diffusion pathways as well as a decrease in matrix density. Since the changes of implant geometry and compactness also affect the in-vitro release kinetics of the excipients, a more accelerated release of HP- $\beta$ -CD and of PEG occurred from extruded implants. The enhanced leaching out of PEG was, furthermore, shown to be associated with distinctions in the underlying drug release mechanism between the implant systems. As the actual concentrations of PEG within the water-filled pores of extruded implants seemed to be lower compared to that generated within compressed implants, IFN- $\alpha$  release was purely governed by diffusion irrespective of the initial PEG loading.

In *Chapter V.2* twin screw extrusion was evaluated as alternative manufacturing technique. Apart from the initial problems associated with the handling of tristearin material, different formulation strategies enabling extrusion were identified. Among them the processing of proteins with a combination of low-melting point and high-melting point lipids was deemed as most promising. Implants with diameters between

0.5 mm to 1.9 mm could be prepared, allowing subcutaneous injection via a large gauge needle.

The produced implants based on a blend of the mixed-acid triglyceride H12 and of tristearin were shown to contain IFN- $\alpha$  in the quality of the raw material. In order to render investigations on the secondary structure of IFN- $\alpha$  embedded within lipidic implants, FTIR spectroscopy was utilised. As the obtained absorption spectra in the amid I region revealed no significant alterations compared to the lyophilised IFN- $\alpha$  prior extrusion, perturbations of the secondary protein conformation due to the extrusion procedure could be regarded as unlikely. Moreover, the produced extrudates comprised the lipids with their stable modification. Based on these positive outcomes regarding protein stability and lipid polymorphism, the main criteria for a new lipidic delivery device were met and release studies could be performed on a meaningful basis.

During in-vitro release the developed implant system delivered IFN- $\alpha$  mainly in its monomeric form over time periods of up to 60 days. Moreover, the employment of small implant diameters or high initial PEG loadings facilitated a complete protein recovery.

Importantly, the in-vitro release profiles could be easily controlled. One option to adapt the in-vitro release kinetics of IFN- $\alpha$  was the variation of the implant diameter. Protein liberation could be controlled in a prolonged manner over 15, 40, or 60 days by producing extrudates with a diameter of 0.5 mm, 1.0 mm or 1.9 mm, respectively. Furthermore, protein delivery could be tailored by the admixing of various amounts of PEG.

The comparison of the release of IFN- $\alpha$  and lysozyme pointed out that in-situ protein precipitation is again important for the delayed protein liberation from extrudates prepared by twin screw extrusion. Although the lysozyme liberation occurred less delayed compared to the IFN- $\alpha$  delivery, a sustained lysozyme release over 25 days could be achieved. Furthermore, release studies carried out with implants prepared either by compression, by ram, or by twin screw extrusion indicated that twin screw extrusion per se resulted in more sustained protein delivery. Presumably, the blending, melting, and compaction during extrusion may explain this observation.

Summing up the attainments, twin screw extrusion can be considered as promising manufacturing technique for lipidic implants. The developed extrudate formulation can be easily manufactured. As twin screw extrusion is commonly applied to produce

commercial polymeric implants, up-scaling of the manufacturing appears feasible. It was shown that the designed manufacturing procedure did not compromise protein integrity. Furthermore, IFN- $\alpha$  as well as lysozyme could be delivered in their monomeric form over prolonged periods of time.

In conclusion two major achievements were reached with respect to the development of lipid-based sustained release devices for pharmaceutical proteins. First, a novel release mechanism based on an in-situ precipitation within inert matrices has been identified. Second, a new extruded lipidic implant system has been developed. As former concerns regarding implant administration and manufacture were overcome, the developed lipidic implant system can be deemed as promising platform for the controlled delivery of pharmaceutical proteins. The system was shown to be particularly suitable for the delivery of IFN- $\alpha$ , however, the knowledge obtained on the mechanisms controlling IFN- $\alpha$  release, should enable to transfer the developed system to a variety of other pharmaceutical proteins.

## CHAPTER VII: REFERENCES

1. European Medicines Agency: Committee for medical products for human use, Press release 2005 <http://www.emea.europa.eu/pdfs/human/press/pr/34146305en.pdf>.
2. Abdekhodaie, M. J. and Cheng, Y. L., Diffusional release of a dispersed solute from a spherical polymer matrix, *Journal of Membrane Science*. 115: 171-178 (1996).
3. Allababidi, S. and Shah, J. C., Efficacy and pharmacokinetics of site-specific cefazolin delivery from biodegradable implants in the prevention of postoperative wound infections, *Pharmaceutical research*. 15: 325-333 (1998).
4. Almeida, A. J., Runge, S., and Mueller, R. H., Peptide-loaded solid lipid nanoparticles (SLN): influence of production parameters, *International Journal of Pharmaceutics*. 149: 255-265 (1997).
5. Anderson, J. S. and Saddington, K., The use of radioactive isotopes in the study of the diffusion of ions in solution, *Journal of the Chemical Society*. Supplement 381-386 (1949).
6. Appel, B., Maschke, A., Weiser, B., Sarhan, H., Englert, C., Angele, P., Blunk, T., and Goepferich, A., Lipidic implants for controlled release of bioactive insulin: Effects on cartilage engineered in vitro, *International Journal of Pharmaceutics*. 314: 170-178 (2006).
7. Arakawa, T. and Timasheff, S. N., Mechanism of polyethylene glycol interaction with proteins, *Biochemistry*. 24: 6756-6762 (1985).
8. Arifin, D. Y., Lee, L. Y., and Wang, C. H., Mathematical modeling and simulation of drug release from microspheres: Implications to drug delivery systems, *Advanced Drug Delivery Reviews*. 58: 1274-1325 (2006).
9. Atha, D. H. and Ingham, K. C., Mechanism of precipitation of proteins by polyethylene glycols: analysis in terms of excluded volume, *Journal of Biological Chemistry*. 256: 12108-12117 (1981).
10. Bartus, R. T., Tracy, M. A., Emerich, D. F., and Zale, St. E., Sustained delivery of proteins for novel therapeutic products, *Science*. 281: 1161-1162 (1998).
11. Basappa, C., Rao, P. R., Narasimha D., and Divakar, S.A., Modified colorimetric method for the estimation of b-cyclodextrin using phenolphthalein, *International Journal of Food Science and Technology*. 33: 517-520 (1998).
12. Batycky, R. P., Hanes, J., Langer, R., and Edwards, D. A. A., Theoretical model of erosion and macromolecular drug release from biodegrading microspheres, *Journal of Pharmaceutical Sciences* 86: 1464-1477 (1997).

13. Bawa, R., Siegel, R. A., Marasca, B., Karel, M., and Langer, R., An explanation for the controlled release of macromolecules from polymers, *Journal of Controlled Release*. 1: 259-267 (1985).
14. Bhat, R. and Timasheff, S. N., Steric exclusion is the principal source of the preferential hydration of proteins in the presence of polyethylene glycols, *Protein Science*. 1: 1133-1143 (1992).
15. Bibby, D. C., Davies, N. M., and Tucker, I. G., Mechanisms by which cyclodextrins modify drug release from polymeric drug delivery systems, *International Journal of Pharmaceutics*. 197: 1-11 (2000).
16. Bittner, B., Morlock, M., Koll, H., Winter, G., and Kissel, T., Recombinant human erythropoietin (rhEPO) loaded poly(lactide-co-glycolide) microspheres: influence of the encapsulation technique and polymer purity on microsphere characteristics, *European Journal of Pharmaceutics and Biopharmaceutics*. 45: 295-305 (1998).
17. Blake, C. C. F., Koenig, D. F., Mair, G. A., North, A. C. T., Phillips, D. C., and Sarma, V. R., Structure of hen egg-white lysozyme-a three-dimensional Fourier synthesis at 2 Å resolution, *Nature*. 206: 757-761 (1965).
18. Bodmeier, R., Wang, J., and Bhagwatwar, H., Process and formulation variables in the preparation of wax microparticles by a melt dispersion technique. I. Oil-in-water technique for water-insoluble drugs, *Journal of Microencapsulation*. 9: 89-98 (1992).
19. Bodmeier, R., Wang, J., and Bhagwatwar, H., Process and formulation variables in the preparation of wax microparticles by a melt dispersion technique. II. W/O/W multiple emulsion technique for water-soluble drugs, *Journal of Microencapsulation*. 9: 99-107 (1992).
20. Bodmer, D., Kissel, T., and Traechslin, E., Factors influencing the release of peptides and proteins from biodegradable parenteral depot systems, *Journal of Controlled Release*. 21: 129-137 (1992).
21. Boonyaratanakornkit, B. B., Park, C. B., and Clark, D. S., Pressure effects on intra- and intermolecular interactions within proteins, *Biochimica et Biophysica Acta, Protein Structure and Molecular Enzymology*. 1595: 235-249 (2002).
22. Bot, A. I., Smith, D. J., Bot, S., Dellamary, L., Tarara, T. E., Harders, S., Phillips, W., Weers, J. G., and Woods, C. M., Receptor-mediated targeting of spray-dried lipid particles coformulated with immunoglobulin and loaded with a prototype vaccine, *Pharmaceutical research*. 18: 971-979 (2001).
23. Bot, A. I., Tarara, T. E., Smith, D.J., Bot, S. R., Woods, C. M., and Weers, Jeffrey G., Novel lipid-based hollow-porous microparticles as a platform for immunoglobulin delivery to the respiratory tract, *Pharmaceutical research*. 17: 275-283 (2000).

24. Braun, A., Kwee, L., Labow, M. A., and Alsenz, J., Protein aggregates seem to play a key role among the parameters influencing the antigenicity of interferon alpha (IFN-alpha) in normal and transgenic mice, *Pharmaceutical research*. 14: 1472-1478 (1997).
25. Breitenbach, J., Melt extrusion: from process to drug delivery technology, *European Journal of Pharmaceutics and Biopharmaceutics*. 54: 107-117 (2002).
26. Brewster, M. E., Hora, M. S., Simpkins, J. W., and Bodor, N., Use of 2-hydroxypropyl b-cyclodextrin as a solubilizing and stabilizing excipient for protein drugs, *Pharmaceutical research*. 8: 792-795 (1991).
27. Bruker application note. FT-IR-Accessory for protein folding/unfolding studies. 2003.
28. Brunner, A., Mader, K., and Gopferich, A., pH and osmotic pressure inside biodegradable microspheres during erosion, *Pharmaceutical research*. 16: 847-853 (1999).
29. Bunjes, H., Westesen, K., and Koch, M. H. J., Crystallization tendency and polymorphic transitions in triglyceride nanoparticles, *International Journal of Pharmaceutics*. 129: 159-173 (1996).
30. Cady, S. M., Steber, W. D, and Fishbein, R., Development of a sustained release delivery system for bovine somatotropin. Proceed. Inter. Symp. Control. Rel. of Bioact. Mater. 1989.
31. Cady, Susan M. Sustained-release parenterals and implants containing peptide fatty acid salts. American Cyanamid Co., USA. 91-661787[5137874], 11. US. 25-2-1991.
32. Caraballo, I., Fernandez-Arevalo, M., Holgado, M. A., and Rabasco, A. M., Percolation theory: Application to the study of the release behavior from inert matrix systems, *International Journal of Pharmaceutics*. 96: 175-181 (1993).
33. Carpenter, J. F., Prestrelski, S. J., and Dong, A., Application of infrared spectroscopy to development of stable lyophilized protein formulations, *European Journal of Pharmaceutics and Biopharmaceutics*. 45: 231-238 (1998).
34. Castellanos, I. J., Crespo, R., and Griebenow, K., Poly(ethylene glycol) as stabilizer and emulsifying agent: a novel stabilization approach preventing aggregation and inactivation of proteins upon encapsulation in bioerodible polyester microspheres, *Journal of Controlled Release*. 88: 135-145 (2003).
35. Cauchy, M., D'aoust, S., Dawson, B., Rode, H., and Hefford, M. A., Thermal Stability: A Means to Assure Tertiary Structure in Therapeutic Proteins, *Biologicals*. 30: 175-185 (2002).
36. Charman, S. A., Mason, K. L., and Charman, W. N., Techniques for assessing the effects of pharmaceutical excipients on the aggregation of porcine growth hormone, *Pharmaceutical research*. 10: 954-962 (1993).

37. Chen, J. B. Xu, Y., X., Chun G., and Li, S. B., Effect of cyclodextrin on the activity and secondary structure of horseradish peroxidase, *Protein and Peptide Letters*. 11: 509-513 (2004).
38. Chi, E. Y., Krishnan, S., Randolph, T. W., and Carpenter, J. F., Physical Stability of Proteins in Aqueous Solution: Mechanism and Driving Forces in Nonnative Protein Aggregation, *Pharmaceutical research*. 20: 1325-1336 (2003).
39. Choy, Y. W., Khan, N., and Yuen, K. H., Significance of lipid matrix aging on in vitro release and in vivo bioavailability, *International Journal of Pharmaceutics*. 299: 55-64 (2005).
40. Cleek, R. L., Ting, K. C., Eskin, S. G., and Mikos, A. G., Microparticles of poly(DL-lactic-co-glycolic acid)/polyethylene glycol blends for controlled drug delivery, *Journal of Controlled Release*. 48: 259-268 (1997).
41. Cleland, J. L., Protein delivery from biodegradable microspheres, *Pharmaceutical biotechnology*. 10: 1-43 (1997).
42. Cleland, J. L., Builder, S. E., Swartz, J. R., Winkler, M., Chang, J. Y., and Wang, D., Polyethylene glycol enhanced protein refolding, *Nature Biotechnology*. 10: 1013-1019 (1992).
43. Cleland, J. L. and Jones, A. J., Stable formulations of recombinant human growth hormone and interferon-gamma for microencapsulation in biodegradable microspheres, *Pharmaceutical research*. 13: 1464-1475 (1996).
44. Cleland, J. L. and Randolph, T. W., Mechanism of polyethylene glycol interaction with the molten globule folding intermediate of bovine carbonic anhydrase B, *Journal of Biological Chemistry*. 267: 3147-3153 (1992).
45. Cleland, J. L., Daugherty, A., and Mersny, R. Emerging protein delivery methods, *Current Opinion in Biotechnology*. 12: 212-219 (2001).
46. Clogston, J. and Caffrey, M., Controlling release from the lipidic cubic phase. Amino acids, peptides, proteins and nucleic acids, *Journal of Controlled Release*. 107: 97-111 (2005).
47. Cooper, A., Effect of cyclodextrins on the thermal stability of globular proteins, *Journal of the American Chemical Society*. 114: 9208-9209 (1992).
48. Cortesi, R., Esposito, E., Luca, G., and Nastruzzi, C., Production of lipospheres as carriers for bioactive compounds, *Biomaterials*. 23: 2283-2294 (2002).
49. Costantino, H. R., Langer, R., and Klibanov, A. M., Moisture-induced aggregation of lyophilized insulin, *Pharmaceutical research*. 11: 21-29 (1994).
50. Costantino, H. R., Langer, R., and Klibanov, A. M., Aggregation of a lyophilized pharmaceutical protein, recombinant human albumin: effect of moisture and stabilization by excipients, *Biotechnology (N Y)*. 13: 493-496 (1995).

51. Crank, J., *The Mathematics of Diffusion*. 2d Ed, 414 (1975).
52. Crotts, G. and Park, T. G., Protein delivery from poly(lactic-co-glycolic acid) biodegradable microspheres: release kinetics and stability issues, *Journal of Microencapsulation* 15: 699-713 (1998).
53. Davis, B. K., Diffusion in polymer gel implants, *Proceedings of the National Academy of Sciences of the United States of America*. 71: 3120-3123 (1974).
54. De Rosa, Giuseppe, Larobina, Domenico, Immacolata La Rotonda, Maria, Musto, Pellegrino, Quaglia, Fabiana, and Ungaro, Francesca How cyclodextrin incorporation affects the properties of protein-loaded PLGA-based microspheres: the case of insulin/hydroxypropyl- $\beta$ -cyclodextrin system, *Journal of Controlled Release*. 102: 71-83 (2005).
55. Del Curto, M. D., Chicco, D., D'Antonio, M., Ciolli, V., Dannan, H., D'Urso, S., Neuteboom, B., Pompili, S., Schiesaro, S., and Esposito, P., Lipid microparticles as sustained release system for a GnRH antagonist (Antide), *Journal of Controlled Release*. 89: 297-310 (2003).
56. Denadai, A. M. L., Santoro, M. M., Lopes, M. T. P., Chenna, A., de Sousa, F. B., Avelar, G. M., Gomes, M. R. T., Guzman, F., Salas, C. E., and Sinisterra, R. D. A., Supramolecular complex between proteinases and  $\beta$ -cyclodextrin that preserves enzymatic activity: physicochemical characterization, *BioDrugs*. 20: 283-291 (2006).
57. Dingermann, T., Hansel, R., and Zundorf, I., *Pharmaceutical Biology: Molecular Basis and Clinical Application*, 497 (2002).
58. Diwan, M. and Park, T. G., Pegylation enhances protein stability during encapsulation in PLGA microspheres, *Journal of Controlled Release*. 73: 233-244 (2001).
59. Domb, Abraham J. Lipospheres for controlled delivery of pharmaceuticals, pesticides, and fertilizers. Nova Pharmaceutical Corp., USA. 90-US6519[9107171], 79. WO. 8-11-1990.
60. Dong, A., Huang, P., and Caughey, W. S., Protein secondary structures in water from second-derivative amide I infrared spectra, *Biochemistry*. 29: 3303-3308 (1990).
61. Dong, W. Y., Koerber, M., Lopez, E., V., and Bodmeier, R., Stability of poly(D,L-lactide-co-glycolide) and leuprolide acetate in in-situ forming drug delivery systems, *Journal of Controlled Release*. 115: 158-167 (2006).
62. Drustrup, J., Interferon formulations. Maxygen Aps, Den. 2002-186962[2003138403], 41. US. 28-6-2002.
63. Ehtezazi, T. and Washington, C., Controlled release of macromolecules from PLA microspheres: using porous structure topology, *Journal of Controlled Release*. 68: 361-372 (2000).

64. Eldem, T., Speiser, P., and Altorfer, H., Polymorphic behavior of sprayed lipid micropellets and its evaluation by differential scanning calorimetry and scanning electron microscopy, *Pharmaceutical research*. 8: 178-184 (1991).
65. Eldem, T., Speiser, P., and Hincal, A., Optimization of spray-dried and -congealed lipid micropellets and characterization of their surface morphology by scanning electron microscopy, *Pharmaceutical research*. 8: 47-54 (1991).
66. Fagain, C. O., Understanding and increasing protein stability, *Biochimica et Biophysica Acta, Protein Structure and Molecular Enzymology*. 1252: 1-14 (1995).
67. Falkner, J. C., Al-Somali, A. M., Jamison, J. A., Zhang, J., Adrianse, S.L., Simpson, R. L., Calabretta, M. K., Radding, W., Phillips, G. N., Jr., and Colvin, V. L., Generation of size-controlled, submicrometer protein crystals, *Chemistry of Materials*. 17: 2679-2686 (2005).
68. Farruggia, B., Garcia, G., D'Angelo, C., and Pico, G., Destabilization of human serum albumin by polyethylene glycols studied by thermodynamical equilibrium and kinetic approaches, *International Journal of Biological Macromolecules*. 20: 43-51 (1997).
69. Feuge, R. O., Landmann, W., Mitcham, D., and Lovegren, N. V., Tempering triglycerides by mechanical working, *Journal of the American Oil Chemists' Society*. 39: 310-313 (1962).
70. Fini, A., Moyano, J. R., Gines, J. M., Perez-Martinez, J. I., and Rabasco, A. M., Diclofenac salts, II. Solid dispersions in PEG 6000 and Gelucire 50/13, *European Journal of Pharmaceutics and Biopharmaceutics*. 60: 99-111 (2005).
71. Frokjaer, S. and Otzen, D. E., Protein drug stability: a formulation challenge, *Nature Reviews Drug Discovery*. 4: 298-306 (2005).
72. Fu, J. C., Hagemer, C., and Moyer, D. L., A unified mathematical model for diffusion from drug-polymer composite tablets, *Journal of Biomedical Materials Research*. 10: 743-758 (1976).
73. Fu, K., Klibanov, A. M., and Langer, R., Protein stability in controlled-release systems, *Nature Biotechnology*. 18: 24-25 (2000).
74. Fu, K., Pack, D. W., Klibanov, A. M., and Langer, R., Visual evidence of acidic environment within degrading poly(lactic-co-glycolic acid) (PLGA) microspheres, *Pharmaceutical research*. 17: 100-106 (2000).
75. Fu, K., Griebenow, K., Hsieh, L., Klibanov, A. M., and Langer, R., FTIR characterization of the secondary structure of proteins encapsulated within PLGA microspheres, *Journal of Controlled Release*. 58: 357-366 (1999).
76. Fujioka, K., Takada, Y., Sato, S., and Miyata, T., Novel delivery system for proteins using collagen as a carrier material: the minipellet, *Journal of Controlled Release*. 33: 307-315 (1995).

77. Garti, N., Sato, K., and Editors., Surfactant Science Series, Vol. 31: Crystallization and Polymorphism of Fats and Fatty Acids, 450 Marcel Dekker, New York (1988).
78. Genentech press release, Jun 1 2004. web . 4-6-0004. Ref Type: Electronic Citation
79. Goepferich, A., Polymer degradation and erosion. Mechanisms and applications, *European Journal of Pharmaceutics and Biopharmaceutics*. 42: 1-11 (1996).
80. Gombotz, W. R. and Pettit, D. K., Biodegradable polymers for protein and peptide drug delivery, *Bioconjug Chem*. 6: 332-351 (1995).
81. Gorovits, B. M. and Horowitz, P. M., High Hydrostatic Pressure Can Reverse Aggregation of Protein Folding Intermediates and Facilitate Acquisition of Native Structure, *Biochemistry*. 37: 6132-6135 (1998).
82. Grassi, M. and Grassi, G., Mathematical modelling and controlled drug delivery: matrix systems, *Current Drug Delivery*. 2: 97-116 (2005).
83. Grigsby, J. J., Blanch, H. W., and Prausnitz, J. M., Diffusivities of Lysozyme in Aqueous MgCl<sub>2</sub> Solutions from Dynamic Light-Scattering Data: Effect of Protein and Salt Concentrations, *Journal of Physical Chemistry B*. 104: 3645-3650 (2000).
84. Guse, C., Koennings, S., Kreye, F., Siepmann, F., Goepferich, A., and Siepmann, J., Drug release from lipid-based implants: Elucidation of the underlying mass transport mechanisms, *International Journal of Pharmaceutics*. 314: 137-144 (2006).
85. Guse, C., Koennings, S., Maschke, A., Hacker, M., Becker, C., Schreiner, S., Blunk, T., Spruss, T., and Goepferich, A., Biocompatibility and erosion behavior of implants made of triglycerides and blends with cholesterol and phospholipids, *International Journal of Pharmaceutics*. 314: 153-160 (2006).
86. Guse, C., Triglyceride matrices for controlled release. Characteristics for manufacturing and release - biocompatibility and erosion behavior, Ph.D. Thesis, University of Regensburg (2004).
87. Harada, A., Construction of supramolecular structures from cyclodextrins and polymers, *Carbohydrate Polymers*. 34: 183-188 (1997).
88. Hastedt, J. E. and Wright, J. L., Diffusion in porous materials above the percolation threshold, *Pharmaceutical research*. 7: 893-901 (1990).
89. Hastedt, J. E. and Wright, J. L., Percolative Transport and Cluster Diffusion Near and Below the Percolation Threshold of a Porous Polymeric Matrix, *Pharmaceutical research*. 23: 2427-2440 (2006).
90. Heller, Jorge, Barr, John, Ng, Steve, Shen, Hui Rong, Gurny, Robert, Schwach-Abdelaoui, Khadija, Rothen-Weinhold, Alexandra, and van de Weert, Marco Development of poly(ortho esters) and their application for bovine serum albumin and bupivacaine delivery, *Journal of Controlled Release*. 78: 133-141 (2002).

91. Hennink, W. E., Talsma, H., Borchert, J. C. H., De Smedt, S. C., and Demeester, J., Controlled release of proteins from dextran hydrogels, *Journal of Controlled Release*. 39: 47-55 (1996).
92. Hennink, W. E. and van Nostrum, C. F., Novel crosslinking methods to design hydrogels, *Advanced Drug Delivery Reviews*. 54: 13-36 (2002).
93. Hermeling, S., Crommelin, D. A., Schellekens, H., and Jiskoot, W., Structure-Immunogenicity Relationships of Therapeutic Proteins, *Pharmaceutical research*. 21: 897-903 (2004).
94. Herrmann, S., Mohl, S., Winter, G., Enhanced stability of Interferon  $\alpha$ -2a in non aqueous solutions by using highly hydrophobic solvents. BioPerspectives 2005, May 10-12th, Wiesbaden, Germany . 2005.
95. Herrmann, S., Mohl, S., Winter, G., Strategies to circumvent polymorphism in sustained release systems based on lipids. 5th World Meeting on Pharmaceutics, Biopharmaceutics and Pharmaceutical Technology, Geneva. 2006.
96. Higuchi, T., Mechanism of sustained-action medication. Theoretical analysis of rate of release of solid drugs dispersed in solid matrices, *Journal of Pharmaceutical Sciences*. 52: 1145-1149 (1963).
97. Higuchi, T., Rate of release of medicaments from ointment bases containing drugs in suspension, *Journal of Pharmaceutical Sciences*. 50: 874-875 (1961).
98. Hildebrand, G. E. and Harnisch, S., Advanced drug delivery systems for biopharmaceuticals, *Modern Biopharmaceuticals*. 4: 1361-1391 (2005).
99. Hombreiro-Perez, M., Siepmann, J., Zinutti, C., Lamprecht, A., Ubrich, N., Hoffman, M., Bodmeier, R., and Maincent, P., Non-degradable microparticles containing a hydrophilic and/or a lipophilic drug: preparation, characterization and drug release modeling, *Journal of Controlled Release*. 88: 413-428 (2003).
100. Hora, M. S., Rana, R. K., Nunberg, J. H., Tice, T. R., Gilley, R. M., and Hudson, M. E., Release of human serum albumin from poly(lactide-co-glycolide) microspheres, *Pharmaceutical research*. 7: 1190-1194 (1990).
101. Horsky, J. and Pitha, J., Inclusion complexes of proteins: interaction of cyclodextrins with peptides containing aromatic amino acids studied by competitive spectrophotometry, *Journal of Inclusion Phenomena and Molecular Recognition in Chemistry*. 18: 291-300 (1994).
102. Hsieh, D. S., Rhine, W. D., and Langer, R., Zero-order controlled-release polymer matrices for micro- and macromolecules, *Journal of Pharmaceutical Sciences*. 72: 17-22 (1983).

103. Huang, X. and Brazel, C. S., On the importance and mechanisms of burst release in matrix-controlled drug delivery systems, *Journal of Controlled Release*. 73: 121-136 (2001).
104. Ingham, K. C., Precipitation of proteins with polyethylene glycol, *Methods in Enzymology*. 182: 301-306 (1990).
105. Irie, T. and Uekama, K., Cyclodextrins in peptide and protein delivery, *Advanced Drug Delivery Reviews*. 36: 101-123 (1999).
106. Izutsu, K., Yoshioka, S., and Terao, T., Stability of b-galactosidase by amphiphilic additives during freeze-drying, *International Journal of Pharmaceutics*. 90: 187-194 (1993).
107. J.M.Vergnaud. Controlled Drug Release of Oral Dosage Forms, Ellis Horwood Limited, Chichester, 1993.
108. Jiang, W. and Schwendeman, S. P., Stabilization and controlled release of bovine serum albumin encapsulated in poly(D, L-lactide) and poly(ethylene glycol) microsphere blends, *Pharmaceutical research*. 18: 878-885 (2001).
109. Johnson, O. L., Jaworowicz, W., Cleland, J. L., Bailey, L., Charnis, M., Duenas, Eileen, W., Chichih, S., Douglas, M., Sheila, L., Thomas, J., Andrew J. S., and Putney, S. D., The stabilization and encapsulation of human growth hormone into biodegradable microspheres, *Pharmaceutical research*. 14: 730-735 (1997).
110. Jolles, P. and Jolles, J., What's new in lysozyme research? Always a model system, today as yesterday, *Molecular and Cellular Biochemistry*. 63: 165-189 (1984).
111. Jorgensen, L., Moeller, E. H., van de Weert, M., Nielsen, H. M., and Frokjaer, S., Preparing and evaluating delivery systems for proteins, *European Journal of Pharmaceutical Sciences*. 29: 174-182 (2006).
112. Kaewvichit, S. and Tucker, I. G., The release of macromolecules from fatty acid matrixes: complete factorial study of factors affecting release, *Journal of Pharmacy and Pharmacology*. 46: 708-713 (1994).
113. Kang, F. and Singh, J., Effect of additives on the release of a model protein from PLGA microspheres, *AAPS PharmSciTech*. 2 : 30 (2001).
114. Kanjickal, D. G. and Lopina, S. T., Modeling of drug release from polymeric delivery systems-a review, *Critical Reviews in Therapeutic Drug Carrier Systems*. 21: 345-386 (2004).
115. Kent, J. S., Cholesterol matrix delivery system for sustained release of macromolecules. Syntex (U.S.A.), Inc. USA. 82-446749[4452775], 8. US. 3-12-1982.

116. Khajehpour, M., Troxler, T., Nanda, V., and Vanderkooi, J. M., Melittin as model system for probing interactions between proteins and cyclodextrins, *Proteins: Structure, Function, and Bioinformatics*. 55: 275-287 (2004).
117. Khan, M. Z., Tucker, I. G., and Opdebeeck, J. P., Cholesterol and lecithin implants for sustained release of antigen: release and erosion in vitro, and antibody response in mice, *International Journal of Pharmaceutics*. 76: 161-170 (1991).
118. Kim, D. D., Takeno, M. M., Ratner, B. D., and Horbett, T. A., Glow discharge plasma deposition (GDPD) technique for the local controlled delivery of hirudin from biomaterials, *Pharmaceutical research*. 15: 783-786 (1998).
119. Kim, H. K. and Park, T. G., Microencapsulation of human growth hormone within biodegradable polyester microspheres: protein aggregation stability and incomplete release mechanism, *Biotechnol Bioeng*. 65: 659-667 (1999).
120. Kim, J. E., Kim, S. R., Lee, S. H., Lee, C. H., and Kim, D. D., The effect of pore formers on the controlled release of cefadroxil from a polyurethane matrix, *International Journal of Pharmaceutics*. 201: 29-36 (2000).
121. Kissel, T., Li, Y., and Unger, F., ABA-triblock copolymers from biodegradable polyester A-blocks and hydrophilic poly(ethylene oxide) B-blocks as a candidate for in situ forming hydrogel delivery systems for proteins, *Advanced Drug Delivery Reviews*. 54: 99-134 (2002).
122. Klaus, W., Gsell, B., Labhardt, A. M., Wipf, B., and Senn, H., The three-dimensional high resolution structure of human interferon alpha-2a determined by heteronuclear NMR spectroscopy in solution, *Journal of Molecular Biology*. 274: 661-675 (1997).
123. Klibanov, A. M., Improving enzymes by using them in organic solvents, *Nature*. 409: 241-246 (2001).
124. Koennings, S., Berie, A., Tessmar, J., Blunk, T., and Goepferich, A., Influence of wettability and surface activity on release behavior of hydrophilic substances from lipid matrices, *Journal of Controlled Release*. 119: 173-181 (2007).
125. Koennings, S., Garcion, E., Faisant, N., Menei, P., Benoit, J. P., and Goepferich, A., In vitro investigation of lipid implants as a controlled release system for interleukin-18, *International Journal of Pharmaceutics*. 314: 145-152 (2006).
126. Koennings, S., Sapin, A., Blunk, T., Menei, P., and Goepferich, A., Towards controlled release of BDNF - Manufacturing strategies for protein-loaded lipid implants and biocompatibility evaluation in the brain, *Journal of Controlled Release*. 119: 163-172 (2007).
127. Koennings, S. and Goepferich, A., Lipospheres as delivery systems for peptides and proteins, *Lipospheres in Drug Targets and Delivery*. Editor(s): Nastruzzi, Claudio. 67-86 CRC Press LLC, Boca Raton, (2005).

128. Krishnamurthy, R., Lumpkin, J. A., and Sridhar, R., Inactivation of lysozyme by sonication under conditions relevant to microencapsulation, *International Journal of Pharmaceutics*. 205: 23-34 (2000).
129. Krishnamurthy, R. and Manning, M. C., The stability factor: importance in formulation development, *Current Pharmaceutical Biotechnology*. 3: 361-371 (2002).
130. Kwon, Y. M., Baudys, M., Knutson, K., and Kim, S. W., In situ study of insulin aggregation induced by water-organic solvent interface, *Pharmaceutical research* 18: 1754-1759 (2001).
131. Lai, M. C., Hageman, M. J., Schowen, R. L., Borchardt, R. T., Laird, B. B., and Topp, E. M., Chemical stability of peptides in polymers. 2. Discriminating between solvent and plasticizing effects of water on peptide deamidation in poly(vinylpyrrolidone), *Journal of Pharmaceutical Sciences*. 88: 1081-1089 (1999).
132. Langer, R. and Moses, M., Biocompatible controlled release polymers for delivery of polypeptides and growth factors, *Journal of Cellular Biochemistry*. 45: 340-345 (1991).
133. Langer, R. and Folkman, J., Polymers for the sustained release of proteins and other macromolecules, *Nature*. 263: 797-800 (1976).
134. Langston, M. V., Ramprasad, M. P., Kararli, T. T., Galluppi, G. R., and Katre, N. V., Modulation of the sustained delivery of myelopoietin (Leridestim) encapsulated in multivesicular liposomes (DepoFoam), *Journal of Controlled Release*. 89: 87-99 (2003).
135. Larhrib, H., Wells, J. I., and Rubinstein, M. H., Compressing polyethylene glycols: the effect of compression pressure and speed, *International Journal of Pharmaceutics*. 147: 199-205 (1997).
136. Lee, L. L. Y. and Lee, J. C., Thermal stability of proteins in the presence of poly(ethylene glycols), *Biochemistry*. 26: 7813-7819 (1987).
137. Leuenberger, H., Bonny, J. D., and Kolb, M., Percolation effects in matrix-type controlled drug release systems, *International Journal of Pharmaceutics*. 115: 217-224 (1995).
138. Lin, W. J. and Yu, C. C., Comparison of protein loaded poly( $\epsilon$ -caprolactone) microparticles prepared by the hot-melt technique, *Journal of Microencapsulation*. 18: 585-592 (2001).
139. Liu, S. J., Chi, P. S., Lin, S. S., Ueng, S. W.N., Chan, E. C., and Chen, J. K., Novel solvent-free fabrication of biodegradable poly-lactic-glycolic acid (PLGA) capsules for antibiotics and rhBMP-2 delivery, *International Journal of Pharmaceutics*. 330: 45-53 (2007).

140. Lucke, A., Kiermaier, J., and Gopferich, A., Peptide acylation by poly( $\alpha$ -hydroxy esters), *Pharmaceutical research*. 19: 175-181 (2002).
141. Schwab, M., Kessler, B., Wolf, E., Jordan, G., Mohl, S., Winter, G., Correlation of in vivo and in vitro release data for rh-INF- $\alpha$  lipid implants. 2007. Unpublished Work
142. Maeyer, E. de and de Somer, P., Influence of pH on interferon production and activity, *Nature*. 194: 1252-1253 (1962).
143. Manning, M. C., Patel, K., and Borchardt, R. T., Stability of protein pharmaceuticals, *Pharmaceutical research*. 6: 903-918 (1989).
144. Maschke, A., Lucke, A., Vogelhuber, W., Fischbach, C., Appel, B., Blunk, T., and Goeperich, A., Lipids: An alternative material for protein and peptide release, *ACS Symposium Series*. 879: 176-196 (2004).
145. Maschke, A., Becker, C., Eyrich, D., Kiermaier, J., Blunk, T., and Goeperich, A., Development of a spray congealing process for the preparation of insulin-loaded lipid microparticles and characterization thereof, *European Journal of Pharmaceutics and Biopharmaceutics*. 65: 175-187 (2007).
146. Maschke, A., Cali, N., Appel, B., Kiermaier, J., Blunk, T., and Goeperich, A., Micronization of Insulin by High Pressure Homogenization, *Pharmaceutical research*. 23: 2220-2229 (2006).
147. Matheus, S., Friess, W., and Mahler, H. C., FTIR and nDSC as Analytical Tools for High-Concentration Protein Formulations, *Pharmaceutical research*. 23: 1350-1363 (2006).
148. Mattos, C, and Ringe, D., Proteins in organic solvents, *Current Opinion in Structural Biology*. 11: 761-764 (2001).
149. McPherson, A., Introduction to protein crystallization, *Methods (San Diego, CA, United States)*. 34: 254-265 (2004).
150. Miller, E. S., Peppas, N. A., and Winslow, D. N., Morphological changes of ethylene/vinyl acetate-based controlled delivery systems during release of water-soluble solutes, *Journal of Membrane Science*. 14: 79-92 (1983).
151. Mohl, S., The Development of a Sustained and Controlled Release Device for Pharmaceutical Proteins based on Lipid Implants, No (2003).
152. Mohl, S. and Winter, G., Continuous release of Rh-interferon ( $\alpha$ -2a) from triglyceride implants: storage stability of the dosage forms, *Pharmaceutical development and technology*. 11: 103-110 (2006).
153. Mohl, S. and Winter, G., Continuous release of rh-interferon  $\alpha$ -2a from triglyceride matrices, *Journal of controlled release*. 97: 67-78 (2004).
154. Morita, T., Horikiri, Y., Suzuki, T., and Yoshino, H., Applicability of various amphiphilic polymers to the modification of protein release kinetics from

- biodegradable reservoir-type microspheres, *European Journal of Pharmaceutics and Biopharmaceutics*. 51: 45-53 (2001).
155. Morita, T., Horikiri, Y., Yamahara, H., Suzuki, T., and Yoshino, H., Formation and isolation of spherical fine protein microparticles through lyophilization of protein-poly(ethylene glycol) aqueous mixture, *Pharmaceutical research*. 17: 1367-1373 (2000).
156. Morlock, M., Koll, H., Winter, G., and Kissel, T., Microencapsulation of r-erythropoietin, using biodegradable poly(D, L-lactide-co-glycolide). Protein stability and the effects of stabilizing excipients, *European Journal of Pharmaceutics and Biopharmaceutics*. 43: 29-36 (1997).
157. Mueller, B. W. and Editor., *Suppositories: Pharmacology, Biopharmacy, and Galenical Aspects of Drug Forms for Rectal and Vaginal Use*, Wissenschaftliche Verlagsgesellschaft mbH, Stuttgart (1986).
158. Muller, R. H., Mader, K., and Gohla, S., Solid lipid nanoparticles (SLN) for controlled drug delivery - a review of the state of the art, *European Journal of Pharmaceutics and Biopharmaceutics*. 50: 161-177 (2000).
159. Nag, A., Mitra, G., and Ghosh, Prahlad C., A colorimetric assay for estimation of polyethylene glycol [PEG] and polyethylene glycolated protein using ammonium ferrothiocyanate, *Analytical Biochemistry*. 237: 224-231 (1996).
160. Narasimhan, B. and Langer, R., Zero-order release of micro- and macromolecules from polymeric devices: the role of the burst effect, *Journal of Controlled Release*. 47: 13-20 (1997).
161. Oliveira, A., C., Gaspar, L., P., Da Poian, A, T., and Silva, J. L., Arc repressor will not denature under pressure in the absence of water, *Journal of Molecular Biology*. 240: 184-187 (1994).
162. Park, T. G., Yong, L. H., and Sung, N.Y., A new preparation method for protein loaded poly(D, L-lactic-co-glycolic acid) microspheres and protein release mechanism study, *J Control Release*. 55: 181-191 (1998).
163. Park, T, G., Degradation of poly(D,L-lactic acid) microspheres: effect of molecular weight, *Journal of Controlled Release*. 30: 161-173 (1994).
164. Patel, S., Cudney, B., and McPherson, A., Polymeric precipitants for the crystallization of macromolecules, *Biochemical and Biophysical Research Communications*. 207: 819-828 (1995).
165. Patel, S., Cudney, B., and McPherson, A., Polymeric precipitants for the crystallization of macromolecules, *Biochemical and Biophysical Research Communications*. 207: 819-828 (1995).

166. Pavlou, A. K. and Reichert, J. M., Recombinant protein therapeutics-success rates, market trends and values to 2010, *Nature Biotechnology*. 22: 1513-1519 (2004).
167. Pean, J. M., Boury, F., Venier-Julienne, M. C., Menei, P., Proust, J. E., and Benoit, J. P., Why does PEG 400 co-encapsulation improve NGF stability and release from PLGA biodegradable microspheres?, *Pharmaceutical research*. 16: 1294-1299 (1999).
168. Perez, C. and Griebenow, K., Improved activity and stability of lysozyme at the water/CH<sub>2</sub>Cl<sub>2</sub> interface: enzyme unfolding and aggregation and its prevention by polyols, *Journal of Pharmacy and Pharmacology*. 53: 1217-1226 (2001).
169. Perez, C., Castellanos, I. J., Costantino, H. R., Al-Azzam, W., and Griebenow, K., Recent trends in stabilizing protein structure upon encapsulation and release from bioerodible polymers, *Journal of Pharmacy and Pharmacology*. 54: 301-313 (2002).
170. Phillies, G. D. J., Diffusion of bovine serum albumin in a neutral polymer solution, *Biopolymers*. 24: 379-386 (1985).
171. Pinto, J. F. and Silverio, N. P., Assessment of the extrudability of three different mixtures of saturated polyglycolized glycerides by determination of the specific work of extrusion and by capillary rheometry, *Pharmaceutical development and technology*. 6: 117-128 (2001).
172. Pitt, C. G., The controlled parenteral delivery of polypeptides and proteins, *International Journal of Pharmaceutics*. 59: 173-196 (1990).
173. Pluen, A., Netti, P. A., Jain, R. K., and Berk, D. A., Diffusion of macromolecules in agarose gels: Comparison of linear and globular configurations, *Biophysical Journal*. 77: 542-552 (1999).
174. Pongjanyakul, T., Medicott, N. J., and Tucker, I. G., Melted glyceryl palmitostearate (GPS) pellets for protein delivery, *International Journal of Pharmaceutics*. 271: 53-62 (2004).
175. Prestrelski, S. J., Tedeschi, N., Arakawa, T., and Carpenter, J. F., Dehydration-induced conformational transitions in proteins and their inhibition by stabilizers, *Biophysical Journal*. 65: 661-671 (1993).
176. Quintanar-Guerrero, D., Allemann, E., Fessi, H., and Doelker, E., Applications of the ion-pair concept to hydrophilic substances with special emphasis on peptides, *Pharmaceutical research*. 14: 119-127 (1997).
177. Rabelo, D. and Coutinho, F. M. B., Porous volume determination of styrene-divinylbenzene copolymers by water uptake measurements, *Polymer Bulletin*. 30: 725-728 (1993).
178. Redfield, C. and Dobson, C. M., Sequential proton NMR assignments and secondary structure of hen egg white lysozyme in solution, *Biochemistry*. 27: 122-136 (1988).

179. Reithmeier, H., Herrmann, J., and Gopferich, A., Development and characterization of lipid microparticles as a drug carrier for somatostatin, *International Journal of Pharmaceutics*. 218: 133-143 (2001).
180. Reithmeier, H., Herrmann, J., and Gopferich, A., Lipid microparticles as parenteral controlled release device for peptides, *Journal of Controlled Release*. 73: 339-350 (2001).
181. Remmele, R. L., Nightlinger, N. S., Srinivasan, S., and Gombotz, W. R., Interleukin-1 receptor (IL-1R) liquid formulation development using differential scanning calorimetry, *Pharmaceutical research*. 15: 200-208 (1998).
182. Reubsæet, J. L., Beijnen, J. H., Bult, A., Van Maanen, R. J., Marchal, J. A. D., and Underberg, W. J. M., Analytical techniques used to study the degradation of proteins and peptides: physical instability, *Journal of Pharmaceutical and Biomedical Analysis*. 17: 979-984 (1998).
183. Rhee, K. W., Gabriel, D. A., and Johnson, C. S., Jr., Diffraction from multiple gratings in holographic relaxation spectroscopy: application to bovine serum albumin labeled with benzospiropyran, *Journal of Physical Chemistry*. 88: 4010-4015 (1984).
184. Ribeiro Dos Santos, I., Richard, J., Pech, B., Thies, C., and Benoit, J. P., Microencapsulation of protein particles within lipids using a novel supercritical fluid process, *International Journal of Pharmaceutics*. 242: 69-78 (2002).
185. Ribeiro Dos Santos, I., Richard, J., Thies, C., Pech, B., and Benoit, J. P., A supercritical fluid-based coating technology. 3: Preparation and characterization of bovine serum albumin particles coated with lipids, *Journal of Microencapsulation*. 20: 110-128 (2003).
186. Rothen-Weinhold, A., Besseghir, K., Vuaridel, E., Sublet, E., Oudry, N., and Gurny, R., Stability studies of a somatostatin analog in biodegradable implants, *International Journal of Pharmaceutics*. 178: 213-221 (1999).
187. Rothen-Weinhold, A., Schwach-Abdellaoui, K., Barr, J., Ng, S. Y., Shen, H. R., Gurny, R., and Heller, J., Release of BSA from poly(ortho ester) extruded thin strands, *Journal of Controlled Release*. 71: 31-37 (2001).
188. Sah, H., Stabilization of proteins against methylene chloride/water interface-induced denaturation and aggregation, *Journal of Controlled Release*. 58: 143-151 (1999).
189. Sah, H., Protein Behavior at the Water/Methylene Chloride Interface, *Journal of Pharmaceutical Sciences*. 88: 1320-1325 (1999).
190. Sah, H., Protein instability toward organic solvent/water emulsification: implications for protein microencapsulation into microspheres, *PDA Journal of Pharmaceutical Science and Technology*. 53: 3-10 (1999).

191. San, V. A., Hernandez, R. M., Gascon, A. R., Calvo, M. B., and Pedraz, J. L., Effect of aging on the release of salbutamol sulfate from lipid matrices, *International Journal Pharmaceutics*. 208: 13-21 (2000).
192. Sato, K., Crystallization behaviour of fats and lipids - a review, *Chemical Engineering Science*. 56: 2255-2265 (2001).
193. Sato, K., Ueno, S., and Yano, J., Molecular interactions and kinetic properties of fats, *Progress Lipid Research*. 38: 91-116 (1999).
194. Schellekens, H., Factors influencing the immunogenicity of therapeutic proteins, *Nephrology Dialysis Transplantation* 20 Suppl 6: vi3-vi9 (2005).
195. Schubert, M. A. and Muller-Goymann, C. C., Characterisation of surface-modified solid lipid nanoparticles (SLN): influence of lecithin and nonionic emulsifier, *European journal of pharmaceutics and biopharmaceutics*. 61: 77-86 (2005).
196. Schwartz, J. B., Simonelli, A. P., and Higuchi, W. I., Drug release from wax matrices. II. Application of a mixture theory to the sulfanilamide-wax system, *Journal of Pharmaceutical Sciences*. 57: 278-282 (1968).
197. Schwartz, J. B., Simonelli, A. P., and Higuchi, W. I., Drug release from wax matrices. I. Analysis of data with first-order kinetics and with the diffusion-controlled model, *Journal of Pharmaceutical Sciences*. 57: 274-277 (1968).
198. Schwendeman, S. P., Recent advances in the stabilization of proteins encapsulated in injectable PLGA delivery systems, *Critical Reviews in Therapeutic Drug Carrier Systems*. 19: 73-98 (2002).
199. Schwendeman, S. P., Cardamone, M., Klibanov, A., Langer, R., and Brandon, M. R., Stability of proteins and their delivery from biodegradable polymer microspheres, *Drugs and the Pharmaceutical Sciences*. 77: 1-49 (1996).
200. Shah, J. C., Sadhale, Y., and Chilukuri, D. M., Cubic phase gels as drug delivery systems, *Advanced Drug Delivery Reviews*. 47: 229-250 (2001).
201. Sharma, V. K. and Kalonia, D. S., Polyethylene glycol-induced precipitation of interferon alpha-2a followed by vacuum drying: Development of a novel process for obtaining a dry, stable powder, *AAPS PharmSci*. 6: (2004).
202. Sharma, V. K. and Kalonia, D. S., Temperature- and pH-Induced Multiple Partially Unfolded States of Recombinant Human Interferon-a2a: Possible Implications in Protein Stability, *Pharmaceutical research*. 20: 1721-1729 (2003).
203. Shenoy, B., Wang, Y., Shan, W., and Margolin, A. L., Stability of crystalline proteins, *Biotechnology and Bioengineering*. 73: 358-369 (2001).
204. Shulgin, I. L. and Ruckenstein, E., Preferential hydration and solubility of proteins in aqueous solutions of polyethylene glycol, *Biophysical Chemistry*. 120: 188-198 (2006).

205. Siegel, R. A. and Langer, R., Controlled release of polypeptides and other macromolecules, *Pharmaceutical research* 1: 2-10 (1984).
206. Siepmann, J. Personal Communication 2007.
207. Siepmann, J. and Gopferich, A., Mathematical modeling of bioerodible, polymeric drug delivery systems, *Advanced Drug Delivery Reviews*. 48: 229-247 (2001).
208. Siepmann, J., Lecomte, F., and Bodmeier, R., Diffusion-controlled drug delivery systems: calculation of the required composition to achieve desired release profiles, *Journal of Controlled Release*. 60: 379-389 (1999).
209. Siepmann, J. and Peppas, N. A., Modeling of drug release from delivery systems based on hydroxypropyl methylcellulose (HPMC), *Advanced Drug Delivery Reviews*. 48: 139-157 (2001).
210. Siepmann, J., Streubel, A., and Peppas, N. A., Understanding and predicting drug delivery from hydrophilic matrix tablets using the sequential layer model, *Pharmaceutical research*. 19: 306-314 (2002).
211. Siepmann, J., Faisant, N., and Benoit, J. P., A new mathematical model quantifying drug release from bioerodible microparticles using monte carlo simulations, *Pharmaceutical research*. 19: 1885-1893 (2002).
212. Sinha, V. R. and Trehan, A., Biodegradable microspheres for protein delivery, *Journal of controlled release*. 90: 261-280 (2003).
213. Steber, W., Stable microsphere compositions of biologically active proteins for parenteral administration. American Cyanamid Co., USA. 91-100650 [448930], 11. EP. 21-1-1991.
214. Steber, W., Fishbein, R., and Cady, S. M., Compositions for parenteral administration of biologically active proteins and peptides. American Cyanamid Co., USA. 87-111217 [257368], 26. EP. 4-8-1987.
215. Steber, W. D., Cady, S. M., Johnson, D. F., and Haughey, T. R., Implant compositions containing a biologically active protein, peptide or polypeptide. American Cyanamid Co., USA. 95-456167 [5801141], 14. US. 31-5-1995.
216. Storm, G., Koppenhagen, F., Heeremans, A., Vingerhoeds, M., Woodle, M. C., and Crommelin, D. J. A., Novel developments in liposomal delivery of peptides and proteins, *Journal of Controlled Release*. 36: 19-24 (1995).
217. Stratton, L. P., Dong, A., Manning, M. C., and Carpenter, J. F., Drug delivery matrix containing native protein precipitates suspended in a poloxamer gel, *Journal of Pharmaceutical Sciences*. 86: 1006-1010 (1997).
218. Sutananta, W., Craig, D. Q. M., and Newton, J. M., An investigation into the effects of preparation conditions and storage on the rate of drug release from pharmaceutical glyceride bases, *Journal of Pharmacy and Pharmacology*. 47: 355-359 (1995).

219. Swarbick, J. and Boylan J.C. Extrusion and Extruder. In *Encyclopedia of pharmaceutical technology*, Marcel Dekker, Inc., New York, 1992, pp. 395-442.
220. Swarbick, J. and Boylan J. C., Lipids in pharmaceutical dosage forms. In *Encyclopedia of pharmaceutical technology*, Marcel Dekker, Inc., New York, 1992, pp. 417-476.
221. Takeuchi, M., Ueno, S., and Sato, K., Synchrotron Radiation SAXS/WAXS Study of Polymorph-Dependent Phase Behavior of Binary Mixtures of Saturated Monoacid Triacylglycerols, *Crystal Growth & Design*. 3: 369-374 (2003).
222. Tavorovipras, S., Hirayama, F., Takeda, S., Arima, H., and Uekama, K., Effects of cyclodextrins on chemically and thermally induced unfolding and aggregation of lysozyme and basic fibroblast growth factor, *Journal of Pharmaceutical Sciences*. 95: 2722-2729 (2006).
223. Tavorovipras, S., Tajiri, S., Hirayama, F., Arima, H., and Uekama, K., Effects of hydrophilic cyclodextrins on aggregation of recombinant human growth hormone, *Pharmaceutical research*. 21: 2369-2376 (2004).
224. Thies, C., Ribeiro Dos Santos, I., Richard, J., VandeVelde, V., Rolland, H., and Benoit, J. P., A supercritical fluid-based coating technology 1: Process considerations, *Journal of Microencapsulation*. 20: 87-96 (2003).
225. Thomas, B. R., Vekilov, P. G., and Rosenberger, F., Heterogeneity determination and purification of commercial hen egg-white lysozyme, *Acta Crystallographica, Section D: Biological Crystallography*. D52: 776-784 (1996).
226. Timasheff, S. N., Solvent effects on protein stability, *Current Opinion in Structural Biology*. 2: 35-39 (1991).
227. Timasheff, S. N., The control of protein stability and association by weak interactions with water: How do solvents affect these processes?, *Annual Review of Biophysics and Biomolecular Structure*. 22: 67-97 (1993).
228. van de Weert, M., van't Hof, R., van der Weerd, J., Heeren, R. M. A., Posthuma, G., Hennink, W. E., and Crommelin, D. J. A., Lysozyme distribution and conformation in a biodegradable polymer matrix as determined by FTIR techniques, *Journal of Controlled Release*. 68: 31-40 (2000).
229. van de Weert, M., Haris, P. I., Hennink, W. E., and Crommelin, D. J. A., Fourier transform infrared spectrometric analysis of protein conformation: Effect of sampling method and stress factors, *Analytical Biochemistry*. 297: 160-169 (2001).
230. van de Weert, M., Hering, J. A., and Haris, P. I., Fourier transform infrared spectroscopy, *Biotechnology: Pharmaceutical Aspects*. 3: 131-166 (2005).

231. van de Weert, M, Jorgensen, L., Moeller, E. H., and Frokjaer, S., Factors of importance for a successful delivery system for proteins, *Expert Opinion on Drug Delivery*. 2: 1029-1037 (2005).
232. van de Wetering, P., Metters, A. T., Schoenmakers, R. G., and Hubbell, J. A., Poly(ethylene glycol) hydrogels formed by conjugate addition with controllable swelling, degradation, and release of pharmaceutically active proteins, *Journal of Controlled Release*. 102: 619-627 (2005).
233. van de, Weert M., Hennink, W. E., and Jiskoot, W., Protein instability in poly(lactico-glycolic acid) microparticles, *Pharmaceutical research*. 17: 1159-1167 (2000).
234. van de, Weert M., Hoehstetter, J., Hennink, W. E., and Crommelin, D. J., The effect of a water/organic solvent interface on the structural stability of lysozyme, *Journal of Controlled Release*. 68: 351-359 (2000).
235. van Laarhoven, J. A. H., Krufft, M. A. B., and Vromans, H., Effect of supersaturation and crystallization phenomena on the release properties of a controlled release device based on EVA copolymer, *Journal of Controlled Release*. 82: 309-317 (2002).
236. van Laarhoven, J. A. H., Krufft, M. A. B., and Vromans, H., In vitro release properties of etonogestrel and ethinyl estradiol from a contraceptive vaginal ring, *International Journal of Pharmaceutics*. 232: 163-173 (2002).
237. Van Tomme, S. R. and Hennink, W. E., Biodegradable dextran hydrogels for protein delivery applications, *Expert Review of Medical Devices*. 4: 147-164 (2007).
238. Vergara, A., Paduano, L., and Sartorio, R., Mechanism of Protein-Poly(ethylene glycol) Interaction from a Diffusive Point of View, *Macromolecules*. 35: 1389-1398 (2002).
239. Vlugt-Wensink, K. D. F., Vlugt, T.J. H., Jiskoot, W., Crommelin, D. J. A., Verrijck, R., and Hennink, W. E., Modeling the release of proteins from degrading crosslinked dextran microspheres using kinetic Monte Carlo simulations, *Journal of Controlled Release*. 111: 117-127 (2006).
240. Vogelhuber, W., Magni, E., Gazzaniga, A., and Goepferich, A., Monolithic glyceryl trimyristate matrices for parenteral drug release applications, *European Journal of Pharmaceutics and Biopharmaceutics*. 55: 133-138 (2003).
241. Vogelhuber, W., Magni, E., Mouro, M., Spruss, T., Guse, C., Gazzaniga, A., and Gopferich, A., Monolithic triglyceride matrixes: A controlled-release system for proteins, *Pharmaceutical development and technology*. 8: 71-79 (2003).
242. Volkin, D. B., Staubli, A., Langer, R., and Klibanov, A. M., Enzyme thermoinactivation in anhydrous organic solvents, *Biotechnology and Bioengineering*. 37: 843-853 (1991).

243. Walduck, A. K., Opdebeeck, J. P., Benson, H. E., and Pranker, R., Biodegradable implants for the delivery of veterinary vaccines: design, manufacture and antibody responses in sheep, *Journal of controlled release*. 51: 269-280 (1998).
244. Walsh, G., Biopharmaceutical benchmarks 2006, *Nature Biotechnology*. 24: 769-776 (2006).
245. Walsh, G., Second-generation biopharmaceuticals, *European Journal of Pharmaceutics and Biopharmaceutics*. 58: 185-196 (2004).
246. Wang, P. Y., Lipids as excipient in sustained release insulin implants, *International Journal of Pharmaceutics*. 54: 223-230 (1989).
247. Wang, Paul Y., Sustained-release bioerodible lipid implants for delivery of bioactive macromolecules, especially insulin and somatotropin. (Can.). 87-106859 [246540], 23. EP. 12-5-1987.
248. Wang, P. Y., Palmitic acid as an excipient in implants for sustained release of insulin, *Biomaterials*. 12: 57-62 (1991).
249. Wang, W., Lyophilization and development of solid protein pharmaceuticals, *International Journal of Pharmaceutics*. 203: 1-60 (2000).
250. Wang, W., Instability, stabilization, and formulation of liquid protein pharmaceuticals, *International Journal of Pharmaceutics*. 185: 129-188 (1999).
251. Wang, W., Protein aggregation and its inhibition in biopharmaceutics, *International Journal of Pharmaceutics*. 289: 1-30 (2005).
252. Westrin, B. A., Axelsson, A., and Zacchi, G., Diffusion measurement in gels, *Journal of Controlled Release*. 30: 189-199 (1994).
253. Witschi, C. and Doelker, E., Residual solvents in pharmaceutical products. Acceptable limits, influences on physicochemical properties, analytical methods, and documented values, *European Journal of Pharmaceutics and Biopharmaceutics*. 43: 215-242 (1997).
254. Wright, J. C., Tao Leonard, S., Stevenson, C. L., Beck, J. C., Chen, G., Jao, R. M., Johnson, P. A., Leonard, J., and Skowronski, R. J., An in vivo/in vitro comparison with a leuprolide osmotic implant for the treatment of prostate cancer, *Journal of Controlled Release*. 75: 1-10 (2001).
255. Yamagata, Y., Iga, K., and Ogawa, Y., Novel sustained-release dosage forms of proteins using polyglycerol esters of fatty acids, *Journal of Controlled Release*. 63: 319-329 (2000).
256. Yang, T. H., Dong, A., Meyer, J., Johnson, O. L., Cleland, J. L., and Carpenter, J. F., Use of infrared spectroscopy to assess secondary structure of human growth hormone within biodegradable microspheres, *Journal of Pharmaceutical Sciences*. 88: 161-165 (1999).

257. Ye, Q., Asherman, J., Stevenson, M., Brownson, E., and Katre, N. V., DepoFoam technology: a vehicle for controlled delivery of protein and peptide drugs, *Journal of Controlled Release*. 64: 155-166 (2000).
258. Yeo, Y., Baek, N., and Park, K., Microencapsulation methods for delivery of protein drugs, *Biotechnology and Bioprocess Engineering*. 6: 213-230 (2001).
259. Yoo, H. S., Choi, H. K., and Park, T. G., Protein-fatty acid complex for enhanced loading and stability within biodegradable nanoparticles, *Journal of Pharmaceutical Sciences*. 90: 194-201 (2001).
260. Zheng, C., Gao, J., Liang, W., Yu, H., and Zhang, Y., Effects of additives and processing parameters on the initial burst release of protein from poly(lactic-co-glycolic acid) microspheres, *PDA J Pharm Sci Technol*. 60: 54-59 (2006).
261. Zhu, G., Mallery, S. R., and Schwendeman, S. P., Stabilization of proteins encapsulated in injectable poly (lactide- co-glycolide), *Nature Biotechnology*. 18: 52-57 (2000).
262. Zhu, G. and Schwendeman, S. P., Stabilization of proteins encapsulated in cylindrical poly(lactide-co-glycolide) implants: mechanism of stabilization by basic additives, *Pharm Res*. 17: 351-357 (2000).
263. Zilberman, M., Schwade, N. D., Meidell, R. S., and Eberhart, R. C., Structured drug-loaded bioresorbable films for support structures, *Journal of Biomaterials Science, Polymer Edition*. 12: 875-892 (2001).
264. Zygourakis, K., Development and temporal evolution of erosion fronts in bioerodible controlled release devices, *Chemical Engineering Science*. 45: 2359-2366 (1990).

## PRESENTATIONS AND PUBLICATIONS ASSOCIATED WITH THIS THESIS

### ARTICLES

Herrmann, S., Mohl, S., Siepmann, F., Siepmann, J., and Winter, G., New insight into the role of polyethylene glycol acting as protein release modifier in lipidic implants, *Pharmaceutical Research*. 27: in press (2007).

Herrmann, S., Winter, G., Mohl, S., Siepmann, F. and Siepmann, J., Mechanisms controlling protein release from lipidic implants: Effects of PEG addition, *Journal of Controlled Release*. 118: 161-168 (2007).

### POSTER PRESENTATIONS

Herrmann, S., Mohl, S., and Winter, G., Strategies to circumvent polymorphism in sustained release systems based on lipids. 5th World Meeting on Pharmaceutics, Biopharmaceutics and Pharmaceutical Technology, Geneva, 2006.

Herrmann, S., Mohl, S., and Winter, G., Enhanced stability of Interferon  $\alpha$ -2a in non aqueous solutions by using highly hydrophobic solvents. BioPerspectives 2005, Wiesbaden, Germany 2005.

Herrmann, S., Mohl, S., and Winter, G., Influence of the lipid modification on the release behaviour of a cytokine from lipid implants, Controlled Release Society German Chapter Annual Meeting, Marburg, Germany, 2005.

Lecomte, F., Mohl, S., Herrmann, S., Winter, G., and Siepmann, J., Rh-interferon  $\alpha$ -2a release from triglycerides-based matrices: Experiment and theory, 32nd Annual Meeting & Exposition of the Controlled Release Society, Miami Beach, Florida, 2005.

## CURRICULUM VITAE

### SANDRA HERRMANN

#### Personal Details

Date of birth: 26.02.1979

Place of birth: Bernburg

Nationality: German

#### Education

11/2003-07/2007 PhD-Thesis at the Department of Pharmacy, Pharmaceutical Technology and Biopharmaceutics, Ludwig-Maximilians-University, Munich

Supervision: Prof. Dr. Gerhard Winter

03/2006-04/2006 Research stay at the College of Pharmacy, University of Lille, France

Supervision: Prof. Dr. J. Siepmann

02/2003 License to practice as pharmacist

06/2002-06/2003 Diploma thesis "Der Nachweis der Glutathion-Abhängigkeit von Phospholipase  $A_2$  in *Escholzia californica* durch fluoreszenzmikroskopische Untersuchungen." Institute for Pharmaceutical Biology and Pharmacology, Department of Molecular Cell Biology, Martin-Luther-University Halle-Wittenberg  
Supervision: Prof. Dr. W. Roos

11/2001-04/2002 Practical education in public pharmacy, Paulus Apotheke, Halle/Saale

07/2000-10/2000 Research stay at the Department of Pharmacy, Federal University of Ouro Preto, Brasil

10/1997-09/2001 Study of Pharmacy at the Martin-Luther-University Halle-Wittenberg

09/1991-06/1997 High school, Friederiken Gymnasium, Bernburg, Graduation with Abitur

09/1985-07/1991 Elementary school, Oberschule Wilhelm von Humboldt, Bernburg

